THE DESIGN AND IMPLEMENTATION OF A BOTTOM UNIT OF AN UNDERWATER ACOUSTIC TELEMETRY SYSTEM

Cedric K. Cole

A Thesis
in
The Department
of
Electrical Engineering

Presented in Partial Fulfillment of the Requirements
for the degree of Master of Engineering at
Concordia University
Montreal, Quebec, Canada

March 1983

ACKNOWLEDGEMENT

I wish to express my indebtedness to Dr. Salvatore Morgera, my supervisor, whose support, guidance, knowledge and expertise were instrumental in the completion of this research project.

I want to thank Keith Rueben for his advice, assistance and encouragement during the many hours we worked together in the laboratory. Thanks also to Pierre Chevrier and Henry Kovalcik of Concordia University Electronics Laboratories for their assistance.

Special thanks to Don Dinn, David DeWolfe and the staff at the Bedford Institute of Oceanography for their co-operation and for providing the facilities (i.e., boats, instruments etc) used during the testing of the project. Thanks to my typist, Marie Berryman for her patience and for an excellent job.

Last but not least, thanks to Kathleen Pinder for her encouragement and understanding during the course of this work.

ABSTRACT

THE DESIGN AND IMPLEMENTATION OF
A BOTTOM UNIT OF AN UNDERWATER
ACOUSTIC TELEMETRY SYSTEM

by

Cedric K. Cole

This thesis described the design, implementation and testing of the bottom unit of an undersea acoustic telemetry system.

The problems of oceanic tidal data gathering are reviewed and the objectives of the acoustic telemetry system designed to address these problems, are stated.

A shallow water environmental model was developed. This model was used to make accurate estimates of such parameters as propagation loss, band level noise, frequency dispersion and time dispersion. The results of the environmental study were used as the guidelines for the design of the system.

The bottom unit is divided into three major subsystems. The functions, design and implementation of each of these subsystems are described.

System performance predictions are outlined. The results of sea tests conducted on June 12 and 13, 1982 in the Bedford Basin, Dartmouth, Nova Scotia are summarized. Ways to improve the system are suggested and other possible applications in which the system could be used are mentioned.

TABLE OF CONTENTS

PAGE

CHAPTER VII
CONCLUSION AND RECOMMENDATIONS

APPENDICES

LIST OF FIGURES

PAGE

CHAPTER III

CHAPTER IV

CHAPTER IV

CHAPTER IV

CHAPTER V

CHAPTER VI

LIST OF TABLES

LIST OF ABBREVIATIONS

A/D	Analogue to digital converter
A.G.C.	Automatic gain control
BIO	Bedford Institue of Oceanography
CPU	Central processing unit
D/A	Digital to analogue converter
FFT	Fast Fourier Transform
HEX	Hexadecimal
Im	Imaginary
I/O	Input/output
kts	Knots
LTA	Long term average,
LPF	Lowpass filter
MFSK	Multiple frequency shift keying
P_{CD}	Probability of correct decision
P_{FA}	Probability of false alarm
PROM	Program read only memory
RAM	Random access memory
R_e	Real
S/N	Signal-to-noise ratio
SS	Sea state
STA	Short term average
SVP	Sound velocity profile

CHAPTER I

INTRODUCTION

A. BACKGROUND

This thesis describes the design and operation of the ocean bottom unit of an underwater acoustic telemetry system developed at Concordia University for the Canadian Department of Fisheries and Oceans, Bedford Institute of Oceanography (BIO), Dartmouth, Nova Scotia. The primary function of the system is to collect oceanic tidal data over prolonged periods at specific mooring sites.

Tidal measurement is an integral part of the process of charting the ocean. Traditionally, the tide has been measured along the shore with simple recording instruments and the data obtained has been used to correct the measured water depth to the low-water datum. In practice, this method does not provide reliable data when the shoreline is gently sloping or when the tidal range is large. Moreover, the collection of good tidal data in harsh environments is difficult because of problems created by the weather, ice and surf. Such problems plague shore-mounted recording instruments. However development of an ocean bottom-mounted tide gauge by BIO about 6 years ago partially solved the problems. The gauge provided greater accuracy in depth measurements and could be moored at any location in the ocean, making it possible to obtain information about tides in off-shore areas. The major disadvantage of measuring tides with a bottom-mounted tide gauge was that

the tidal data became available only on recovery of the instrument. This problem could be solved if an electronic telemetering device could be used to transmit the tidal data gathered by the gauge to a ship within the vicinity of the mooring. However, doing this may create another problem. The tidal data could become corrupted due to the fading dispersive nature of the acoustic communications channel. This problem can be particularly severe in shallow water areas.

The acoustic telemetry system developed at Concordia University was tailored to address these problems. Its design was carried out with the following general requirements in mind:

(1) To access data produced by moored instruments.

(2) To operate in shallow water environments where severe multipath conditions exist.

(3) To transmit encoded data at a rate of at least 32 bits/sec.

(4) To achieve bit error rates of between 10^{-4} and 10^{-5} or better.

(5) To communicate effectively over ranges of 1 km or more during sea state 5 (SS5) weather conditions.

(6) To consume little standby power so that ordinary batteries could be used as the power source for the bottom unit for deployment periods in excess of 3 months.

B. OVERVIEW OF THE ACOUSTIC TELEMETRY SYSTEM

The telemetry system consists of an ocean-bottom unit shown in Figure I-1 and a deck unit placed on board a survey ship. The arrangement is illustrated in Figure I-2. The bottom unit and the tide gauge are moored on the ocean floor and left to collect the tidal data for a predetermined period of time. The bottom unit provides an interrupt-driven interface to the tide gauge. The data it receives is conditioned and stored in a microcomputer memory. At present the memory can accommodate 512 16-bit words. A time tag is affixed to every third data word to enable the correct time sequence to be reconstructed on receipt of the data.

The survey ship carrying the deck unit comes within the vicinity of the mooring site and signals the bottom unit by transmitting an interrogation command which is recognized by the bottom unit's command receiver. The interrogation command consists of a 250 ms tone burst which contains 5 tones spaced 400 Hz apart in a 2048 Hz bandwidth centred on 8192 Hz. A down-converter in the command receiver translates the 5 tones to the frequency range 0-2048 Hz. Each tone is captured by a narrow 40 Hz bandpass filter centred at the appropriate down-converted frequency. The tones are then envelope detected, A/D converted and processed by the microcomputer to form a detection statistic. The microcomputer forms a 64s sliding-window average of the ocean's background noise. Whenever the signal energy exceeds this noise energy by 20 dB or more, the bottom unit assumes that an interrogation command was received

Figure I-1. Photograph of the bottom unit of the acoustic telemetry system

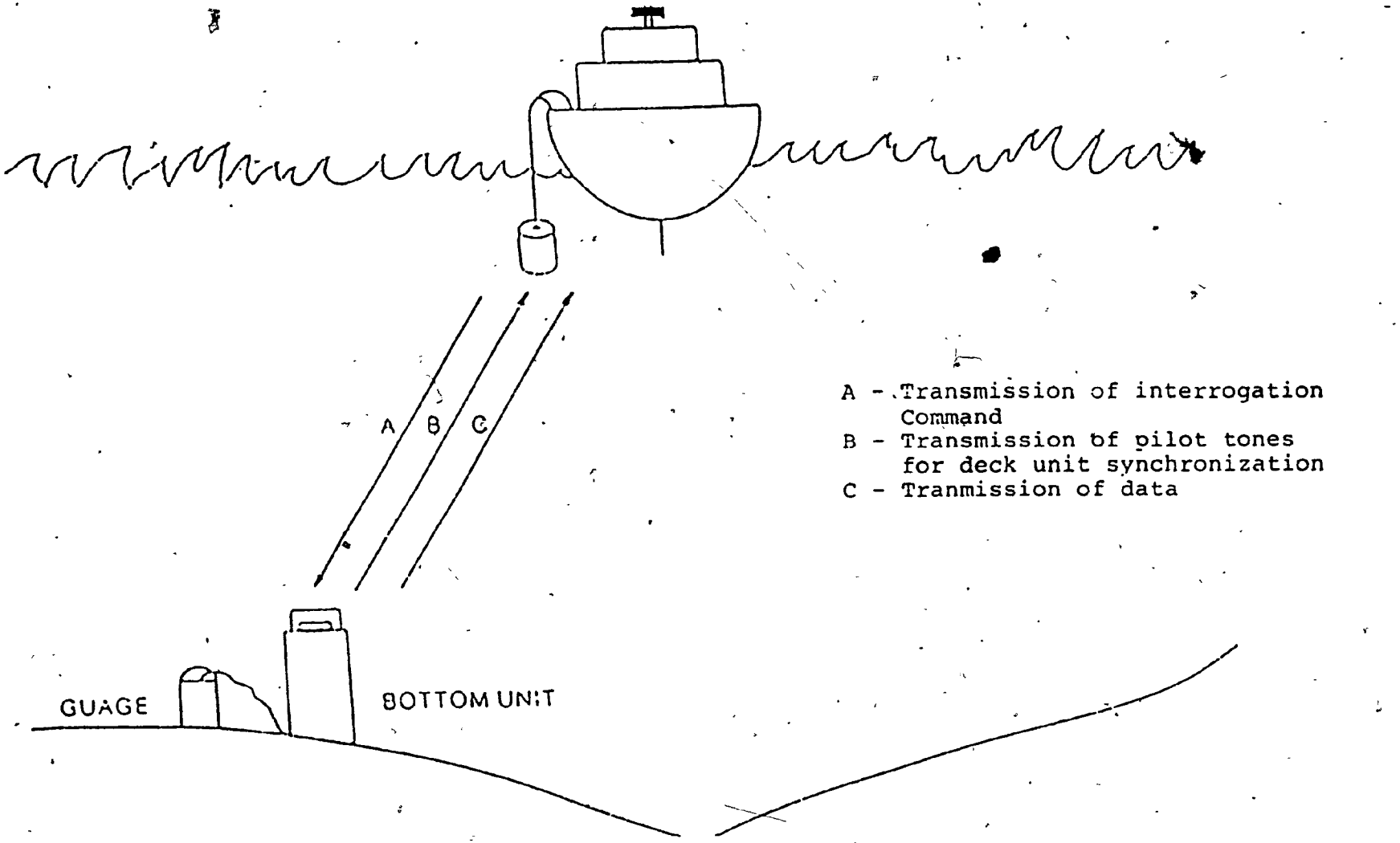

A - Transmission of interrogation Command
B - Transmission of pilot tones for deck unit synchronization
C - Tranmission of data

Figure I-2 Interrogation arrangement between the deck and bottom units

and initiates data transmission. First a preamble is sent to allow the deck unit to acquire synchronization and then the encoded data is transmitted.

The command receiver is designed to operate with a probability of false alarm, $P_{FA}=10^{-8}$ and a probability of correct detection, $P_{CD}=.99$. The tidal data to be transmitted is encoded via a software-based (32,16) quasi-cyclic code which enables all 3-error and some 4-error patterns to be corrected. The encoding offers protection against data corruption, but it also reduces the transmission rate from 64 bits/s to 32 bits/s.

The encoded data is fed to a dense MFSK modulator where each 16-bit data word is converted into a subset of 40 tones out of a possible 160 in the frequency range $\pm$1024 Hz. The MFSK scheme best suited to the environmental and implementation studies was the one in which there are M=4 frequencies, N=8 bit-pairs, and D=5-fold frequency diversity. The overall transmission bandwidth used by this scheme is 2048 Hz. The diversity bands are placed 408 Hz apart and each contains 32 tones spaced 12 Hz apart. In addition there are 4 pilot tones interleaved between diversity banches and used for doppler correction by the deck unit. All 164 tones are synthesized digitally using the accumulator overflow technique of frequency synthesis. The heart of the synthesizer is a sine/cosine lookup table which is addressed by a computed phase angle. The initial phases and the phase increments used to generate the tones are stored in a lookup table addressed by the bit-pairs obtained from the data words to be transmitted.

Each 16-bit data-words produces 44 sampled sinusoids which are added sample by sample to form an in-phase and a quadrature phase composite waveform channels. The output of each channel is D/A converted, lowpass filtered and fed to a single sideband (SSB) modulator which up-converts the baseband from ±1024 Hz to the frequency range 7168-9216 Hz. The output of the modulator is weighted by a triangular window to further reduce the peak-to-average ratio of the waveform and to reduce sidelobe spillover into adjacent FFT bins during deck unit signal processing. The tones are then power-amplified and transmitted. The block schematic diagram of the bottom unit is shown in Figure I-3.

C. THE STRUCTURE OF THE THESIS

The thesis contains 7 Chapters. In the first part of Chapter I, some of the problems of obtaining reliable tidal data are discussed and an overview of the bottom unit of the acoustic telemetry system designed to address these problems is provided.

Chapter II discusses the principles of undersea communications and their application to the design of the acoustic telemetry system. In this chapter a shallow water environmental model is described and used to deduce propagation, dispersion, and noise estimates. These estimates are developed from calculations made at two frequencies, 7 kHz and 16 kHz, six sea states SS0-SS5, and three different temperatures,

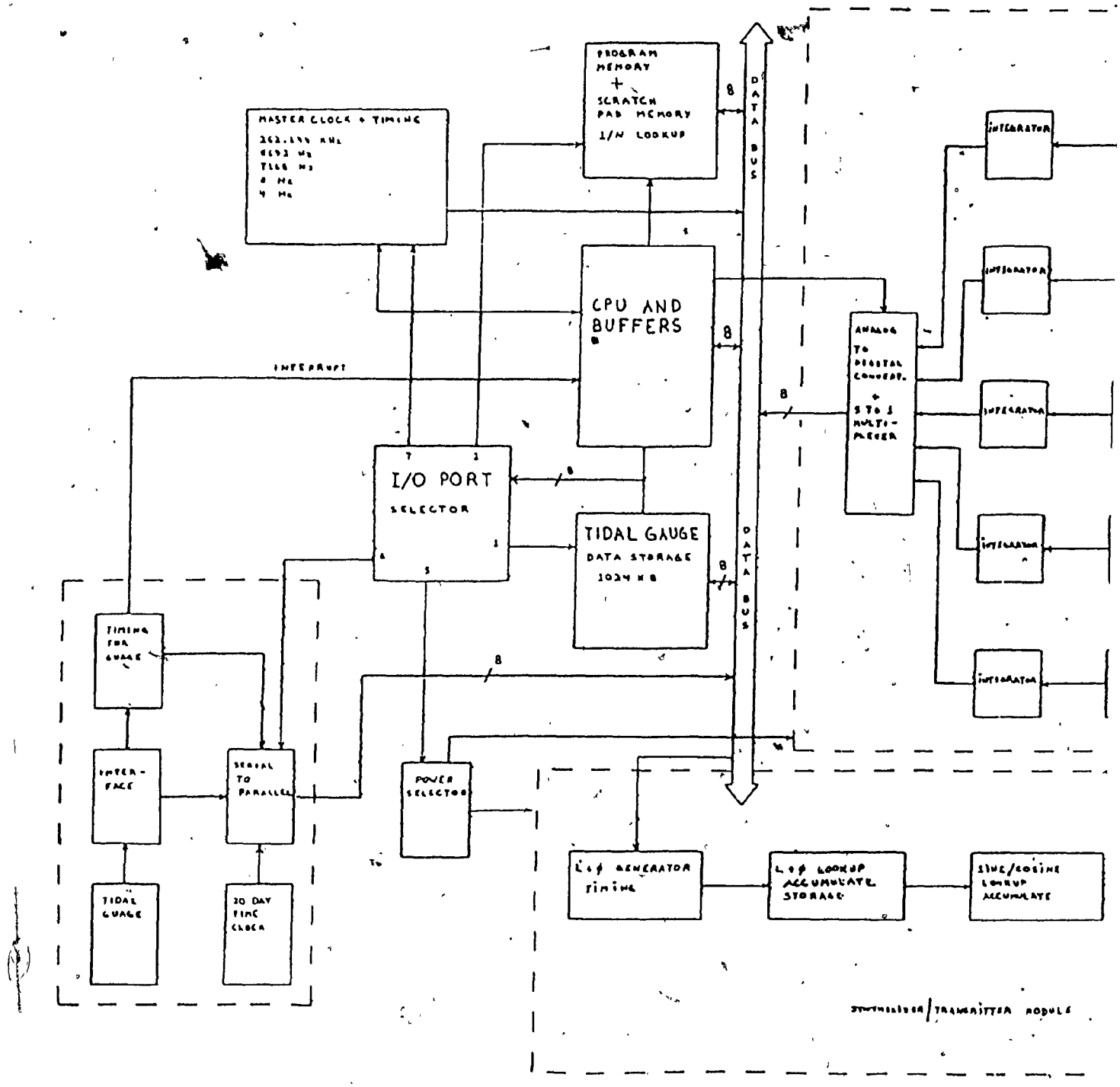

Figure I-3 Block schematic diagram o

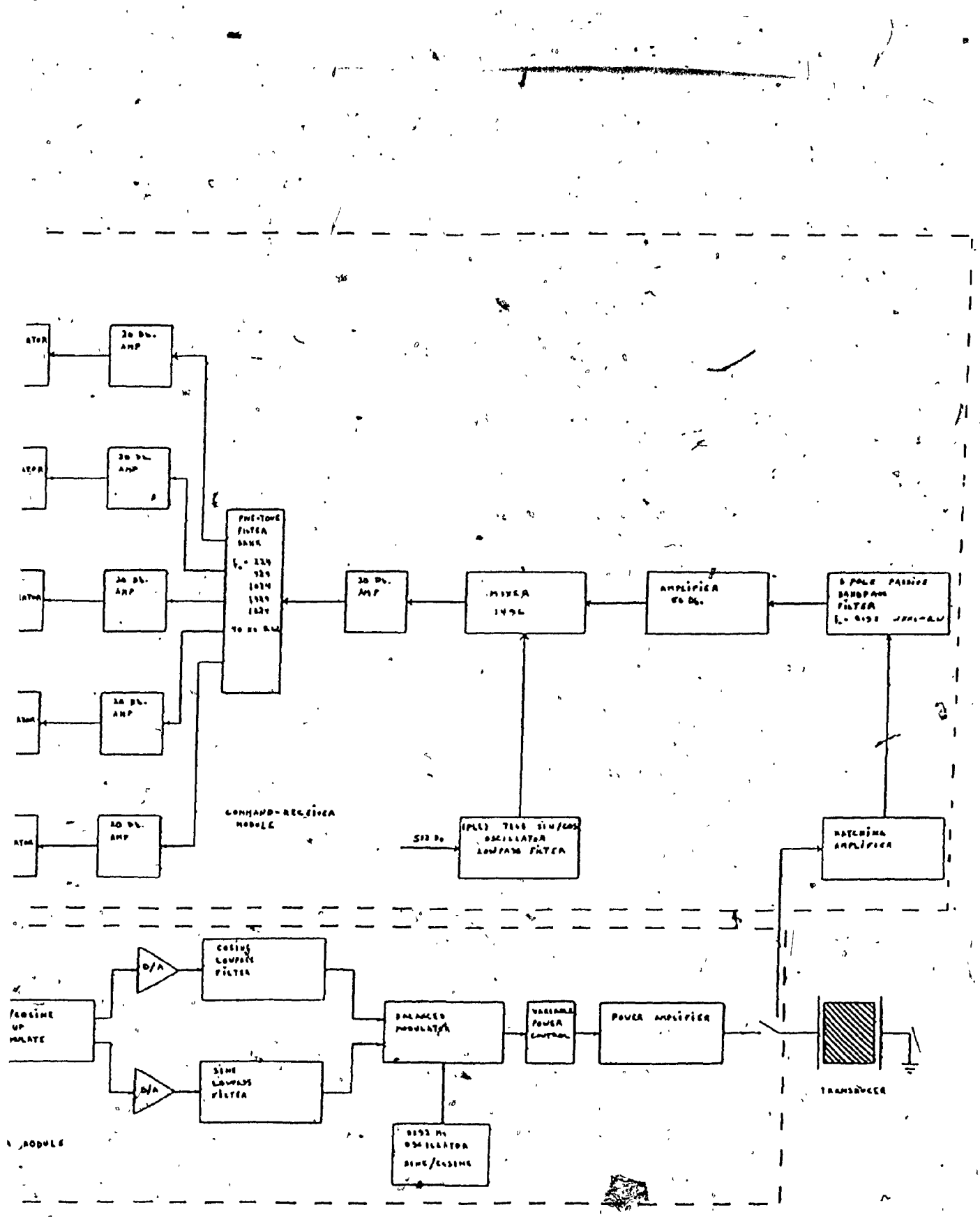

agram of bottom unit

-10°C, 0°C and 10°C. The results of the environmental study provide the guidelines for the design of the acoustic telemetry system.

Chapter III examines the signal processing functions of the command receiver, a subsystem of the bottom unit. It describes the mixture of hardware and software required to ensure a system performance level specified by a probability of false alarm $P_{FA}=10^{-8}$ and a probability of correct decision $P_{CD}=.99$. A detailed design of the command receiver is given in this chapter.

Chapter IV outlines the signal processing techniques employed in the collection of tidal data and its preparation for transmission. The functions and design of the gauge interface and the MFSK modulator, two other subsystems of the bottom unit are discussed. The chapter also contains an analysis of typical results of the signal processing performed by these two subsystems.

Chapter V looks at the design and operation of the microcomputer subsystem, the heart of the acoustic telemetry system. It explains the rationale behind the choice of the RCA CDP 1802 microprocessor. It outlines the functions of the microcomputer subsystem and it provides a flowchart describing the manner in which these functions are executed.

In Chapter VI, the performance predictions of the system are given. The discussion is treated in two areas:

(i) The performance prediction of the bottom units command receiver.

(ii) The performance predictions of the deck unit receiver.

These performance predictions provide the signal-to-noise ratios required to ensure reliable communications between the deck and bottom units. They combine with the recommendations of Chapter II, to establish that a maximum of 6 watts of electrical power is required to maintain effective communications between the deck and bottom units over a range of 1 km during SS5 weather conditions.

Finally Chapter VII reviews the design parameters of the system and discusses its actual performance during field tests conducted on July 12 and 13, 1982 in the Bedford Basin, Nova Scotia. The chapter concludes with suggestions for system improvement and a listing of the many other possible applications of the telemetry system such as its potential for use in water pollution monitoring, in water level monitoring, in ocean bottom resource mining and in military surveillence.

REFERENCES

1. Rossiter, J.R. "Sea Level Recording: The Need for New Instrumentation". Processings of the Symposium on Tidal Instrumentation and Prediction of Tides, Paris, May 3-7, 1965.

2. Dinn, D.F., "Underwater Data Telemetry System", unpublished memorandum, BIO, Dartmouth, Nova Scotia, 1980.

CHAPTER II

STUDY OF THE UNDERSEA ENVIRONMENT

A. INTRODUCTION

The sea together with its boundaries form a complex medium for the transmission of sound which is virtually the only form of energy that propagates effectively underwater.

This chapter discusses the principles of undersea communications and their application to the design of an acoustic telemetry system. It describes a shallow water environmental model from which propagation, dispersion, and noise estimates, essential for an analysis of the performance of the telemetry system, are deduced. These estimates are developed from calculations made at two frequencies, 7 kHz and 16 kHz; six sea states, SS0-SS5; and three different temperatues, -10°C, 0°C and +10°C.

B. THE SHALLOW WATER CHANNEL MODEL

The shallow water channel can be acoustically described as a medium in which propagation of sound energy from one point to another is supported by means of repeated reflections from the surface and bottom of the medium. Propagation in shallow sea water is therefore dependent on the properties of the sea surface and its bottom. As a result its study is characterized by great theoretical complexities because of the variability of surface and/or bottom properties with geographical locations, time of year, and weather conditions.

In general, there are two theoretical approaches for describing shallow water sound fields. They are ray theory and normal mode theory [4]. Ray theory describes the sound field as a summation of rays emanating from a source or its image in the surface or bottom of the medium. It specifies the sound pressure at a field point x located a distance r away from the source by the expression,

$$P = P_o \sum_{m=0}^{\infty} \frac{R_m e^{ikr_m}}{r_m} \qquad \text{II-1}$$

where P_o = source pressure

r_m = distance of mth image from x

k = $2\pi/\lambda$, wave number

R_m = amplitude reflection coefficient appropriate for mth image

e^{ikr_m} = phase factor for waves of wavelength λ propagating over distance r_m

An alternative solution using normal mode theory with the assumption of a pressure release surface and a perfectly rigid bottom, is given by,

$$\psi = \frac{2\pi i}{h} \sum_{L=0}^{\infty} \cosh b_L z_o \cosh b_L z H_o^{(1)}(x_L r) \qquad \text{II-2}$$

where

$$b_L = \frac{i(L+\frac{1}{2})\pi}{h}$$

$$hx_L = h(b_L^2 + k^2)^{\frac{1}{2}} = [(kh)^2 - (L + \tfrac{1}{2})^2 \pi^2]^{\frac{1}{2}}$$

$k = 2\pi/\lambda$

h = water depth

z_o = source depth

z = receiver depth

$H_o^{(1)}$ = Hankel function of the first kind

Ray theory is normally used for short range propagation where high order modes decay rapidly because of reflection losses and attenuation due to the greater distance they have to travel to reach the field point x. On the other hand, normal mode theory is used for long range propagation because of the greater attenuation of the high order modes with distance. In both cases the infinite summations of equations II-1 and II-2 are reduced to finite summations. Although the solutions offered by equations II-1 and II-2 appear quite different they are compatible [3,11]. The cross-over range where neither approach is superior to the other is defined as,

$$r = \frac{d^2}{\lambda} \qquad \text{II-3}$$

where

d = the water depth

λ = wave length

C. SONAR EQUATIONS

The efficiency of any communication system depends on the ability of the receiver to distinguish between the desired portion of a received signal and the undesired portion, which is often referred to as noise. The ratio of the desired to the undesired portion of a signal is known as the signal-to-noise ratio (S/N) and it can be related to a detection threshold in communication systems.

The sonar equations are based on the equality between signal level and noise level when some sonar function such as a detection decision is being performed. The equations vary slightly, depending on the system but essentially they provide the necessary relationships among the system parameters and the major environmental paramters such as transmission loss and ambient noise. In the case of a one way communication link the sonar equation of interest is given by,

$$(S/N)_{receiver} = L_s + (N_{DI})_R - (T_L + L_N) \qquad \text{II-4}$$

where $(S/N)_{receiver}$ is the signal-to-noise ratio at the receiver, L_s is the source level, $(N_{DI})_R$ is the directivity index of the receiver, T_L is the transmission loss and L_N is the band level noise. Each of these quantities are functions of other variables. They will be discussed briefly.

1. Source Level L_s

Source level L_s, is the sound pressure level in decibels relative to 1 microbar generated at a reference position one meter away from the source. For an omnidirectional source of spherical waves, the intensity I in watts/m^2 at a distance one meter from the source is $I=W/4\pi$, where W has units of watts. The corresponding r.m.s. acoustic pressure in Newtons/m^2 is,

$$P = \left(\frac{\rho_o C \beta w}{4\pi}\right)\frac{1}{2} \qquad \text{II-5}$$

where

w = the input power to the transmitting element in watts

β = the electro acoustic conversion efficiency of the transducer

ρ_o = medium density in kg/m^3

C = velocity of sound in water in m/sec

The quantity $\rho_o C$ is known as the characteristic impedance of the medium. It is a function of temperature and salinity for sea water. An average value for $\rho_o C$ is 1.54×10^6 $kg./m^2 sec$. Substituting for $\rho_o C$ in equation II-5 gives,

$$P = \left\{\left(\frac{1.54\times10^6}{4\pi}\right)(\beta w)\right\}^{\frac{1}{2}} = 350.07\ (\beta w)^{\frac{1}{2}} \qquad \text{II-6}$$

Thus, the source level L_S given in dB relative to 1 μbar, is,

$$S_L = 20\log(10P) = 10\log(\beta w) + 20\log(3500.7)\,dB$$
$$= 10\log(\beta w) + 71\ dB \qquad \text{II-7}$$

If the sound source is directional, then L_S is increased by the directivity index of the transmitter $(N_{DI})_T$. Source level is then given, in general, as,

$$L_S = 10\log(\beta w) + 71 + (N_{DI})_T\ dB \qquad \text{II-8}$$

2. Transmission Loss T_L

Transmission loss is the reduction of signal intensity measured some distance r away from the source. It is defined as,

$$T_L = 10\log\left(\frac{I_o}{I_1}\right)\ dB \qquad \text{II-9}$$

where I_o = the sound intensity a unit distance from the source

I_1 = the sound intensity a distance r from the source

It includes losses due to geometric spreading, attenuation by absorption and scattering, and a loss or gain due to refraction, reflection or diffraction. Refraction,

reflection and diffraction are phenomena resulting from the nature of the sound velocity profile of the medium [7,3].

a. Geometric Spreading

Geometric spreading loss represents the natural divergence of energy as the wave front expands outwards from the source. If it is assumed that the medium is homogeneous, boundless, and lossless, the power generated by a source would be evenly distributed over the surface of any sphere surrounding that source. Since power is defined as intensity times area, it follows that

$$\text{Power} = 4\pi r_1^2 I_1 = 4\pi r_2^2 I_2 = \ldots = 4\pi r^2 I \qquad \text{II-10}$$

If r_1 is considered a unit distance, then the transmission loss at any distance r, is proportional to the inverse square of the distance and is given by,

$$T_L = 20\log(r) \text{ dB} \qquad \text{II-11}$$

This type of loss is called spherical spreading loss and applies at distances near to the source.

Further away from the source, spreading is affected by refraction, reflection, and diffraction, as a result of the variation of sound velocity in the sea with depth, range, and the distance between the transmitting source and the

receiver. Generally we employ an average sound velocity profile which describes resonably well the variation of the sound velocity for all depths and ranges of interest.

i. Sound Velocity Effects

The variation of sound velocity in the sea has been extensively studied and is best expressed through empirical equations. One such equation is given as,

$$C = 1449+4.6t-0.055t^2+0.0003t^3+(1.39-0.012t)(s-35)+0.017d \qquad \text{II-12}$$

where C is the velocity of sound in m/sec, t is the temperature of the water in °C, and s is its salinity, expressed in ppt., and d is the depth in meters below the surface of the water [3]. Equations II-12 indicates that the velocity of sound in the sea increases with temperature, pressure (due to increasing depth), and salinity. Of these three factors the one that has the most pronounced effect on velocity variation is temperature. This is because the temperature of the ocean varies with the time of the day, season, weather conditions, effects of currents, and geographical location.

Because of the variation of temperature and ocean depths around the world, sound velocity profiles differ greatly. Typical average sound velocity profiles for shallow water

regions that are likely candidates for the deployment of the acoustic telemetry system are shown in Figures II-1 to II-6. The SVP data labelled SVP A to SVP G corresponds to the following geographical locations:

SVP A. Typical winter profile

SVP B. Centre of Hudson Bay (summer)

SVP C. Hudson Bay near Churchill (summer)

SVP D. Nain Bank 57°-17.0'N, 60°-0.18'W

SVP E. Nain Bank 57°-9.5'N, 60°-31.6'W

SVP F. Off Nova Scotia 43°-0.6'N, 63°-30.5'W

SVP G. Lancaster Sound 74°-36.6'N, 94°-20.4'W

These SVP's have also been used in the study and determination of the multipath spread estimates employed in the design of the telemetry system.

b. Attenuation

The third factor affecting transmission loss is attenuation due to absorption and scattering. Absorption results from a loss of acoustic energy in the form of heat to the medium in which propagation takes place. In sea water absorption is caused by three major effects: shear viscosity, volume viscosity and chemical relaxation.

The relationship between the intensities I_1 at a distance r_1, and I at a distance r, is expressed as,

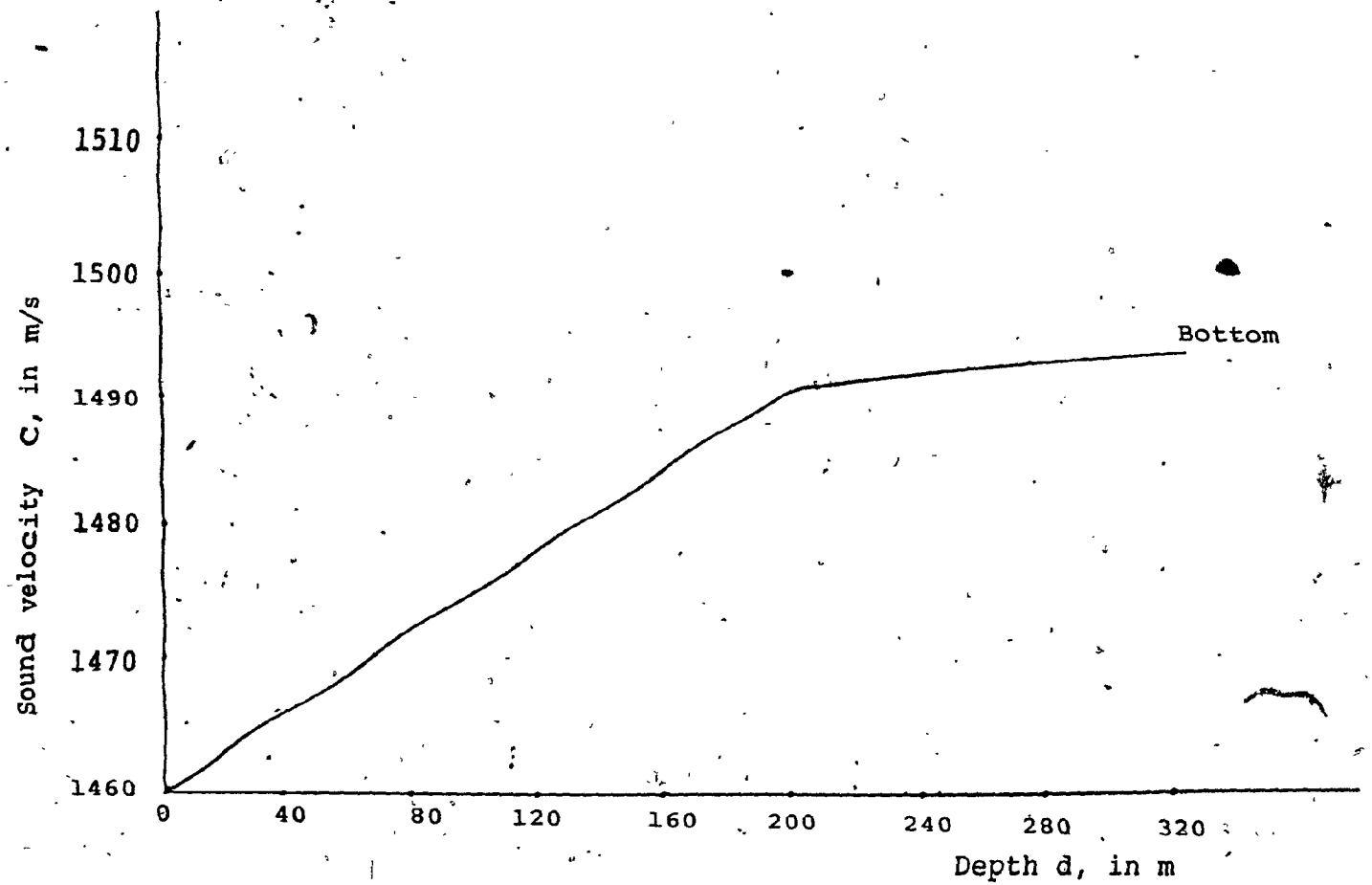

Figure II-1 SVP A

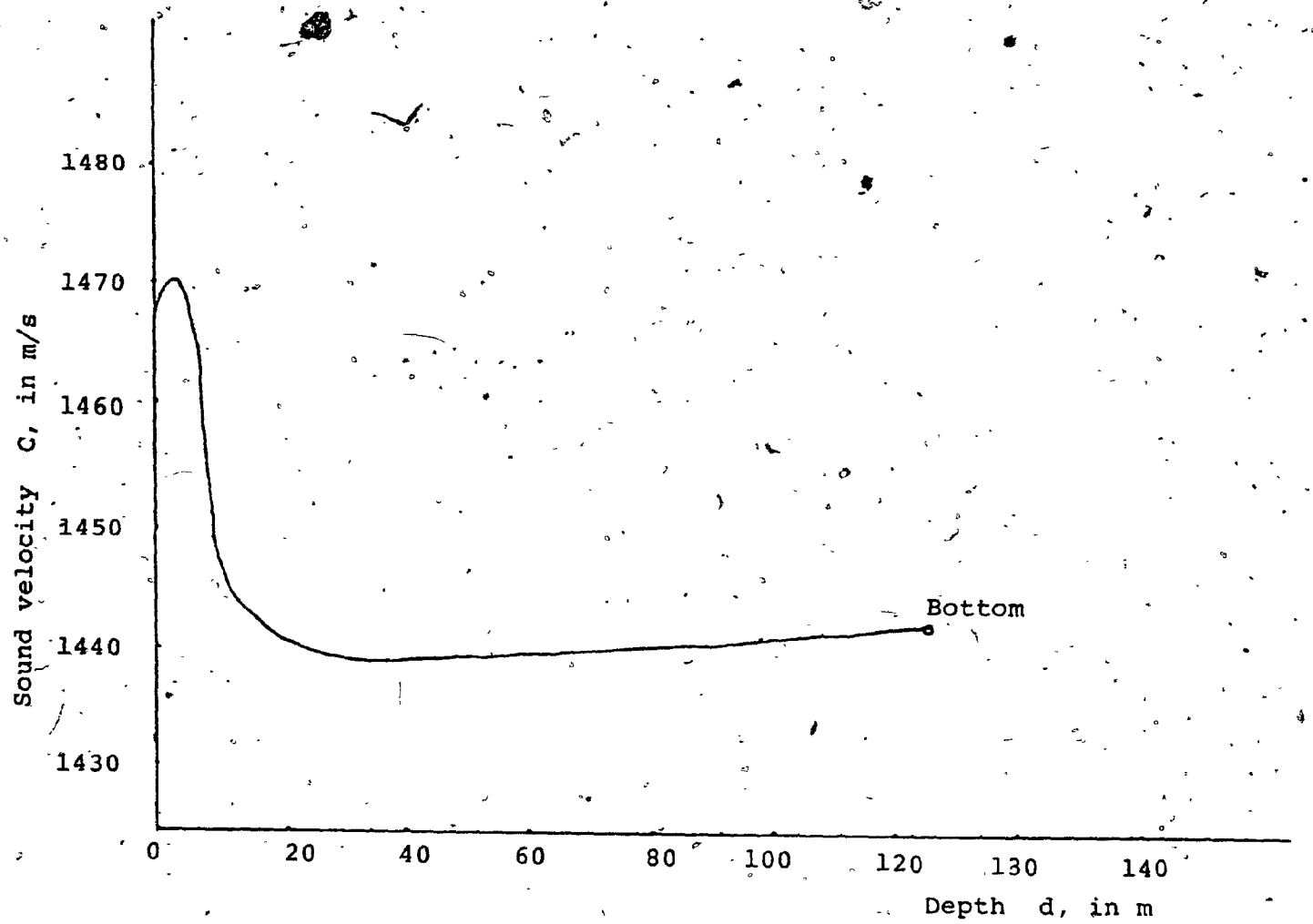

Figure II-2 SVP B

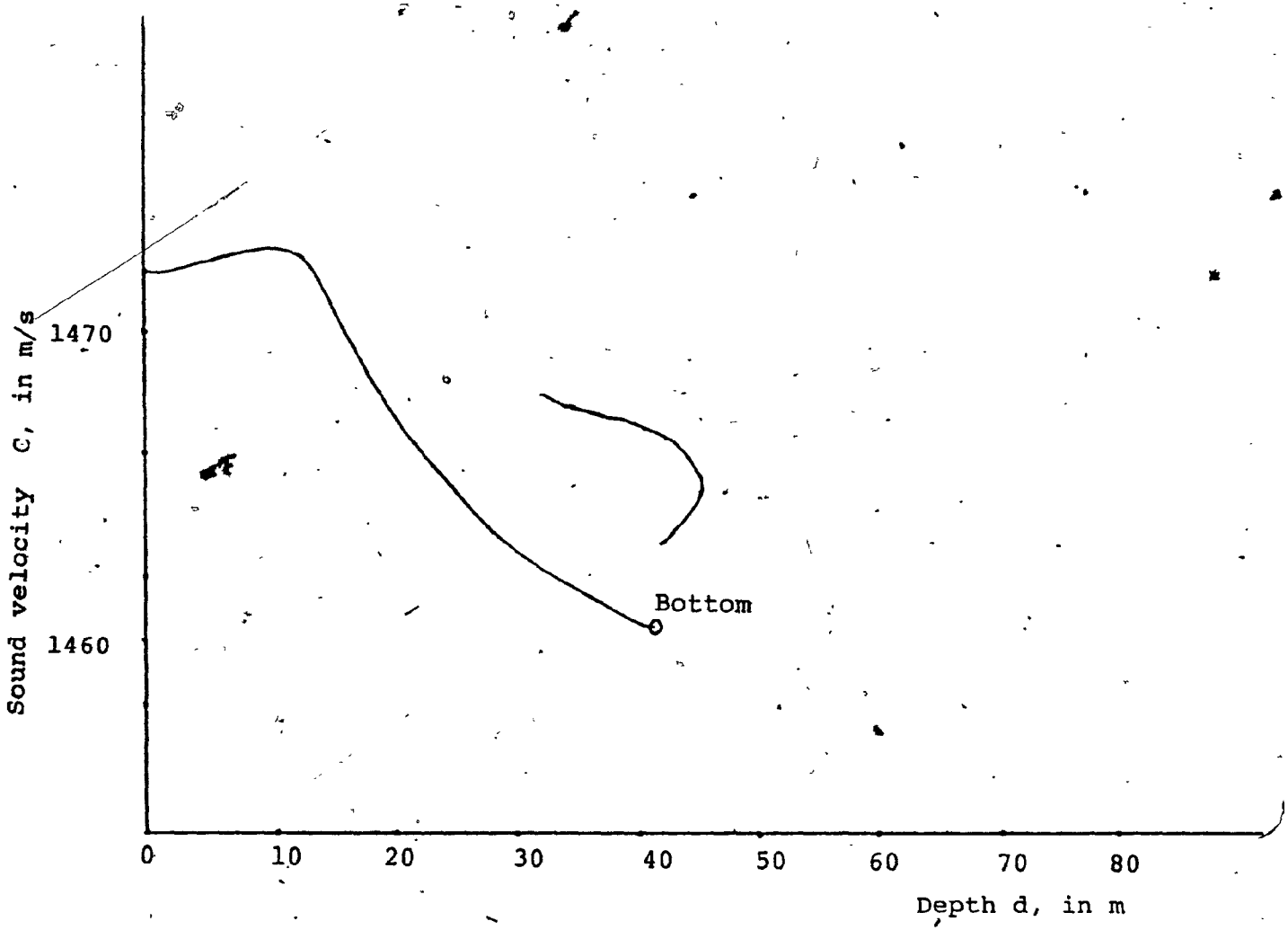

Figure II-3 SVP C

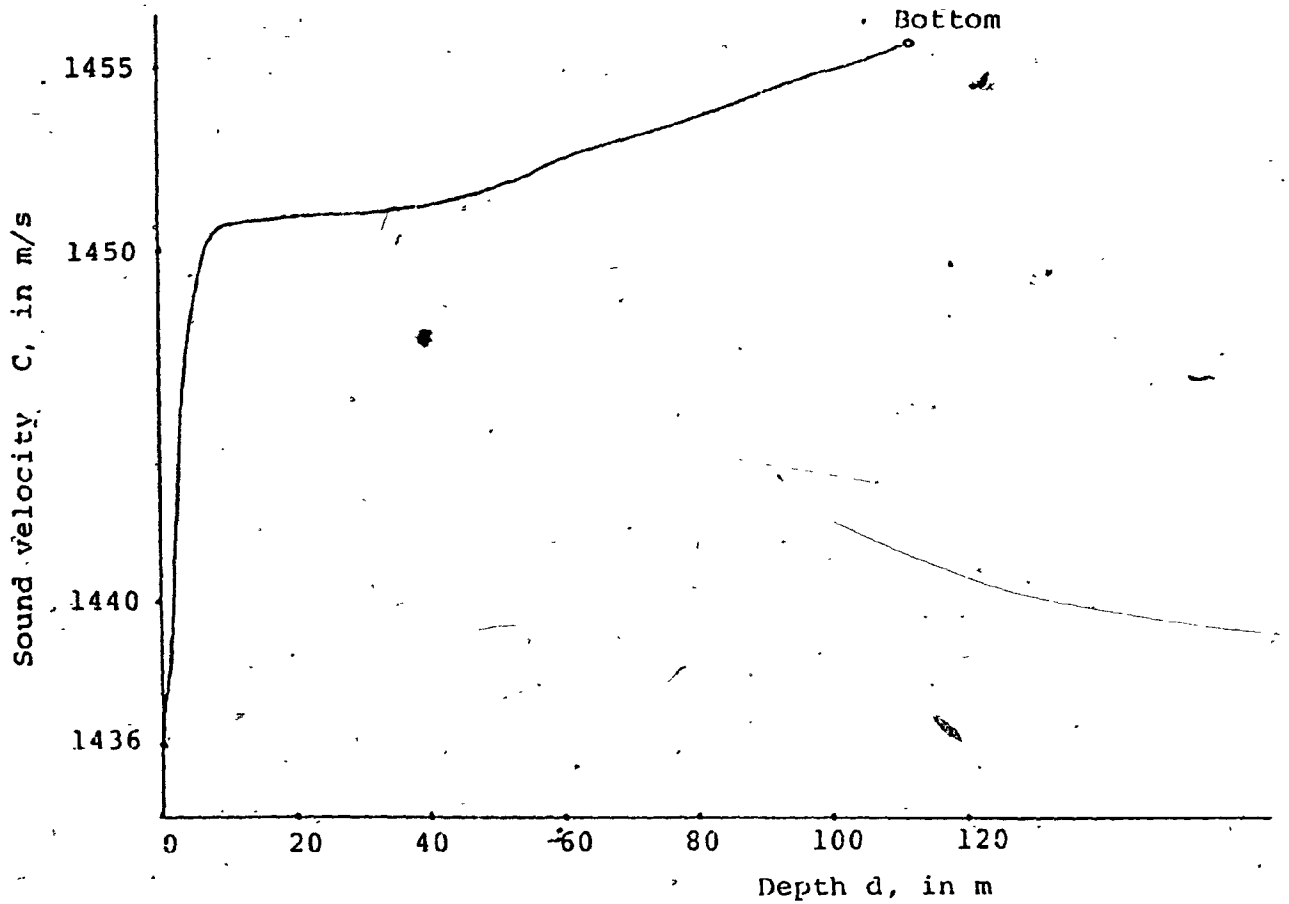

Figure II-4 SVP D

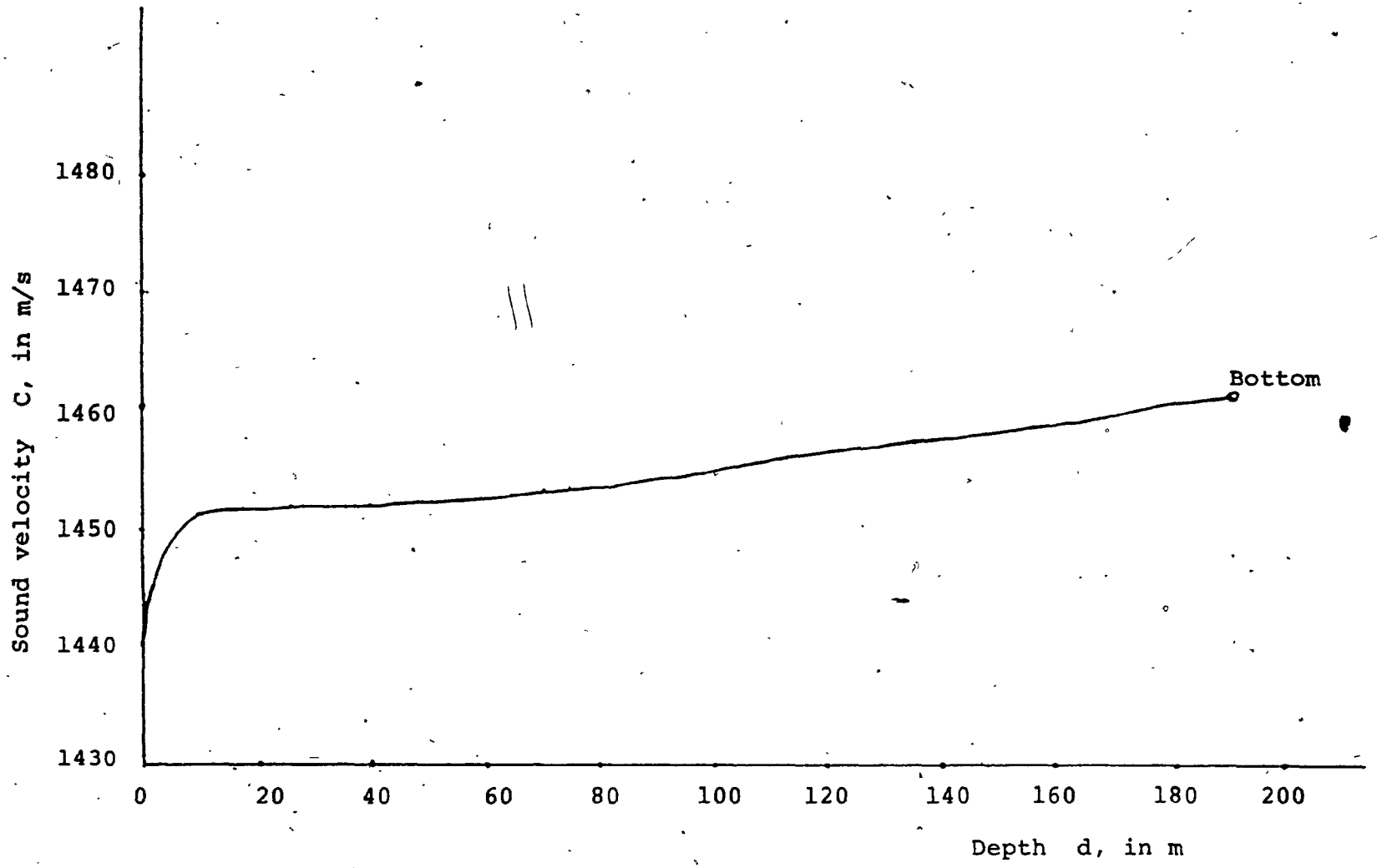

Figure II-5 SVP E

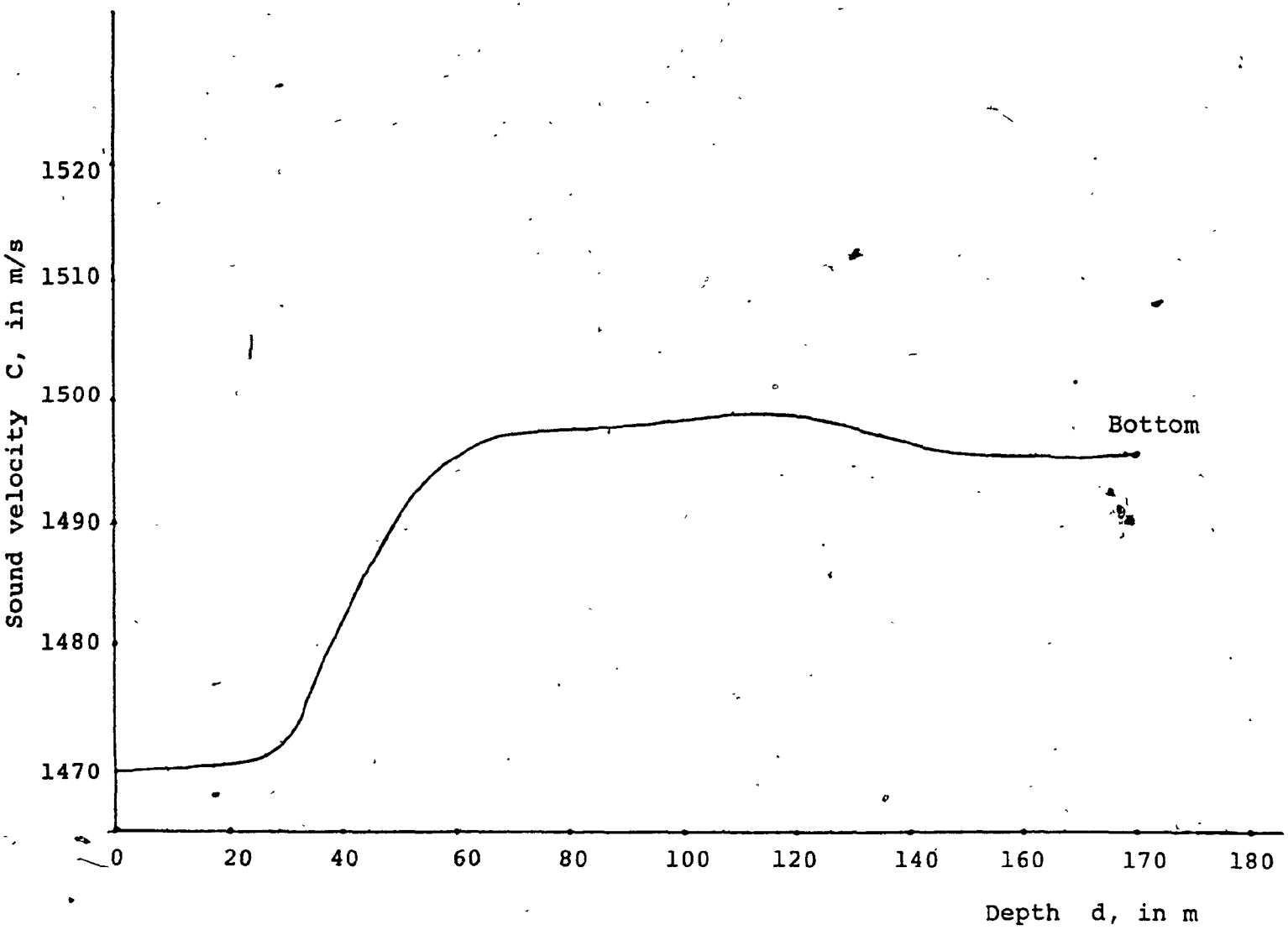

Figure II-6 SVP F

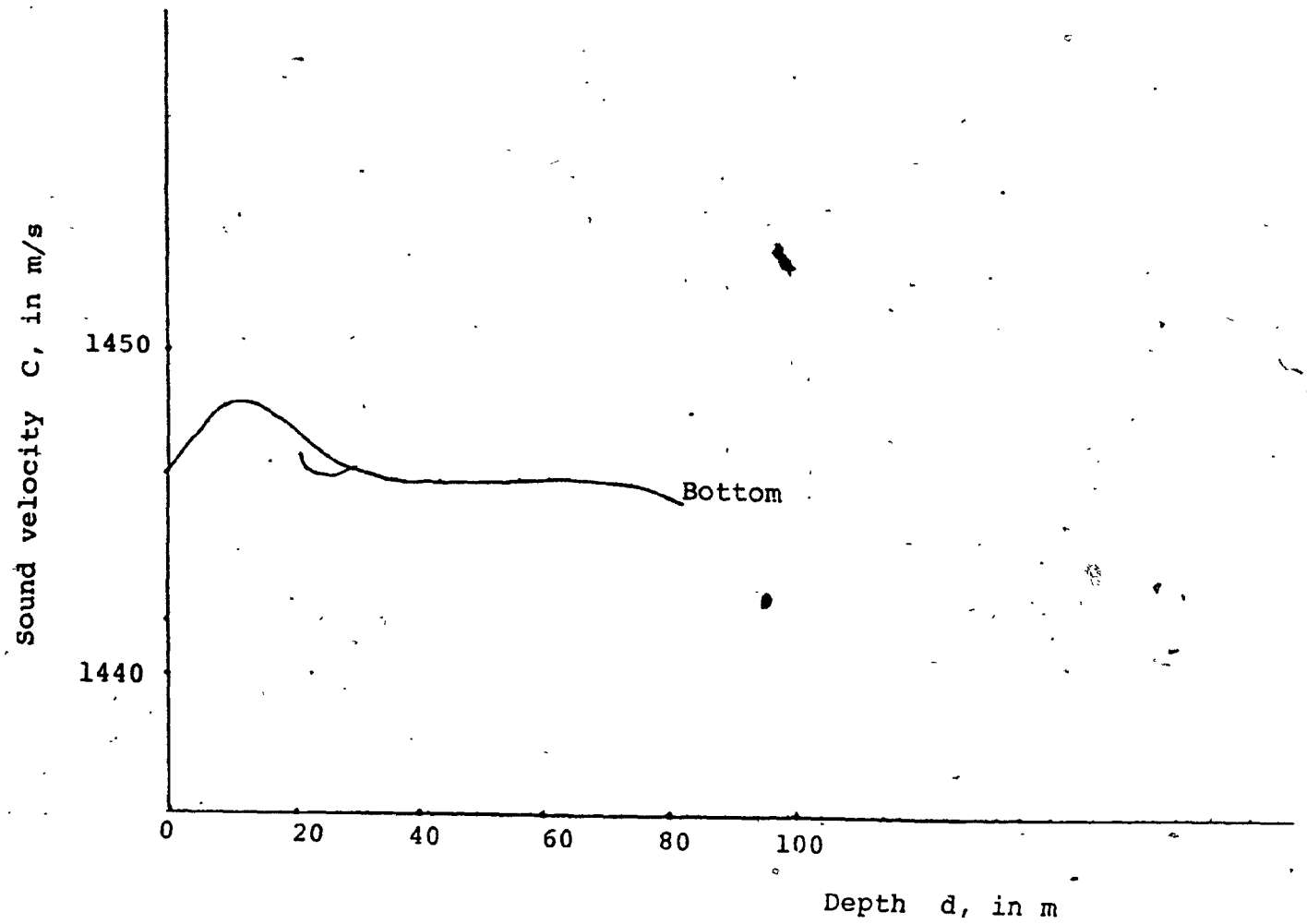

Figure II-7 SVP G

$$I = I_1 e^{-n(r-r_1)} \qquad \text{II-3}$$

Taking the logarithm of both sides of equation II-13, writing (10 nloge) as α, and rearranging the expression, gives,

$$\alpha = \frac{10\log I_1 - 10\log I}{r-r_1} \qquad \text{II-14}$$

The quantity α is known as the attenuation coefficient and it can be expressed as a function of frequency, temperature, salinity and pressure. Schulkin et al [13] have expressed α in terms of these variables. If the pressure dependent term is disregarded, α can be written as,

$$\alpha = \left(\frac{A.s.f_t.f^2}{f_t^2 + f^2}\right) + \left(\frac{Bf^2}{f_t}\right) \qquad \text{II-15}$$

where s is the salinity in ppt, t is the temperature in degrees centigrade, f is the frequency in kHz, $A = 1.86\times10^{-2}$, $B = 2.68\times10^{-2}$ and $f_t = 21.9\times10^{[6-1520/(t+273)]}$.

An overall expression for transmission loss due to spherical spreading and absorption can thus be written as,

$$T_L = 20\log(r) + \alpha r \text{ dB} \qquad \text{II-16}$$

where r is the distance away from the source and α is given in decibels per unit distance.

Equation II-16 must, however, be further modified to take into account surface and bottom reflections. The complicated time dependence of surface and bottom reflection coefficients makes it often necessary for these coefficients to be determined empirically. They can then be adapted to the ray theory model to form semi-empirical models for transmission loss. One such model is due to Marsh and Schulkin [10] and is employed in the design of the telemetry system. The model defines a quantity H, known as the skip distance, as, $H = \{\frac{(d+L)}{8}\}\frac{1}{2}$, where d and L are the water depth and layer depth respectively, given in feet. It expresses transmission loss for three different ranges r, in terms of H. For the short range, i.e. (r<H), transmission loss is defined as,

$$T_L = 20\log(r) + \alpha r + 60 - k_L \quad dB \qquad \text{II-17}$$

where

r = distance in kyds.

α = absorption coefficient of sea water in dB/kyd.

K_L = near field anomaly which depends on the sea state and bottom type and is expressed in dB.

In order to compute T_L as a function of distance from equation II-17, the value of K_L, the near field anomaly, must be known. Marsh et.al [13] have determined the near field anomaly for six sea states, SS0-SS5, and two bottom

types, mud and sand, as a function of frequency in the range 0.1 kHz to 10 kHz. These results have been extrapolated to determine the near field anomaly at 16 kHz by Morgera and are presented in Table II-1 for the two frequencies of 7 kHz and 16 kHz [11].

SEA STATE	f = 7 kHz		f = 16 kHz	
	Sand bottom	Mud bottom	Sand bottom	Mud bottom
0	4.7	4.2	3.5	3.0
1	3.4	2.9	2.5	2.1
2	3.1	2.6	2.3	1.8
3	2.7	2.0	2.0	1.7
4	2.4	2.0	1.8	1.4
5	2.2	1.8	1.6	1.3

Table II-1. Near-field anomaly k_L dB

Computer program TLOSS given in Appendix II-1 can be used to determine partial transmission loss figures (i.e. TPL = 20log(r) + αr), as a function of temperature, frequency and range. The data produced then has to be modified by the near-field anomaly figures k_L, to give the transmission loss estimates. By using TLOSS and the data

presented in Table II-1, transmission loss estimates for three different temperatures, six sea states, two bottom types, two frequencies, and two different ranges, have been computed and are recorded in Tables II-2 to II-5. From these tables the worst case estimates of transmission loss at the two frequencies of 7 and 16 kHz are determined and tabulated in Table II-6.

	SEA STATES AND BOTTOM TYPES											
	0		1		2		3		4		5	
t(°C)	SAND	MUD	SAND	MUD	SAND	MUD	SAND	MUD	SAND	MUD	SAND	MUD
-10	57.04	57.54	58.34	58.84	58.64	59.14	59.04	59.74	59.34	59.74	59.54	59.94
0	56.68	57.18	57.98	58.48	58.28	58.78	58.68	59.38	58.98	59.38	59.18	59.58
10	56.46	56.96	57.76	58.26	58.06	58.56	58.46	59.16	58.76	59.16	58.96	59.36

Table II-2 Shallow water transmission loss for f=7 kHz and r=1 km

	SEA STATES AND BOTTOM TYPES											
	0		1		2		3		4		5	
t(°C)	SAND	MUD	SAND	MUD	SAND	MUD	SAND	MUD	SAND	MUD	SAND	MUD
-10	64.03	64.53	65.33	65.83	65.63	66.13	66.03	66.73	66.33	66.73	66.53	55.93
0	63.31	63.81	64.61	65.11	64.91	65.41	65.31	66.01	65.61	66.01	65.81	66.21
10	62.87	63.37	64.17	64.67	64.47	64.97	64.87	65.57	65.17	65.57	65.37	65.77

Table II-3 Shallow water transmission loss for f=7 kHz and r=2 km

t(°C)	SEA STATES AND BOTTOM TYPES											
	0		1		2		3		4		5	
	SAND	MUD	SAND	MUD	SAND	MUD	SAND	MUD	SAND	MUD	SAND	MUD
-10	61.68	62.18	62.68	63.08	62.88	63.38	63.18	63.48	63.38	63.78	63.58	63.88
0	60.27	60.77	61.27	61.67	61.47	61.97	61.77	62.07	61.97	62.37	62.17	62.47
10	59.26	59.76	60.26	60.66	60.46	60.96	60.76	61.06	60.96	61.36	61.16	61.46

Table II-4 Shallow water transmission loss for f=16 kHz and r=1 km

t(°C)	SEA STATES AND BOTTOM TYPES											
	0		1		2		3		4		5	
	SAND	MUD	SAND	MUD	SAND	MUD	SAND	MUD	SAND	MUD	SAND	MUD
-10	72.1	72.6	73.1	73.5	73.3	73.8	73.6	73.9	73.8	74.2	74.0	74.3
0	69.29	69.79	70.29	70.69	70.49	70.99	70.79	71.09	70.99	71.39	71.19	71.49
10	67.26	67.76	68.26	68.66	68.46	68.96	68.76	69.06	68.96	69.36	69.16	69.46

Table II-5 Shallow water transmission loss for f=16 kHz and r=2 km

RANGE	Freq.	SEA STATE					
		0	1	2	3	4	5
r=1 km	7 kHz	57.54	58.84	59.14	59.74	59.74	59.94
	16 kHz	62.18	63.08	63.38	63.48	63.78	63.88
r=2 km	7 kHz	64.53	65.83	66.13	66.73	66.73	66.93
	16 kHz	72.6	73.5	73.8	73.9	74.2	74.3

Table II-6 Shallow water transmission loss for r=1 and 2 km, t=-10°C and mud botton

3. Band Level Noise L_N

The band level noise can be defined as the total field of noise which obscures the signal. It includes ambient noise due to the sea itself, "self-noise" due to the hydrophone, and its manner of mounting, and localized forms of noise such as thermal noise and noise radiated into the water by machinery. In terms of spectrum level, the band level noise L_N, is given as,

$$L_N = L_{NO} + 10\log(\omega) \qquad \text{II-18}$$

where L_{NO} is the spectrum level of noise in dB/μbar/Hz and ω is the receiver bandwidth in Hz. The telemetry system bandwidth has been selected to be 2.048 kHz, as described in Chapter IV, Section D1. According to Urich [4] the spectrum level of noise in shallow water can be described in terms of the ambient noise level of deep water in the frequency range above 500 Hz. It is defined as,

$$L_{NO} = N_{amb} + (5\text{-}10) \qquad \text{II-19}$$

where N_{amb} is the spectrum level of deep water ambient noise.

a. Sources of Ambient Noise in Deep and Shallow Water

Ambient noise measurements in the ocean have been made over a wide band of frequencies from below 1 Hz to approximately 100 kHz. The data indicates that the noise spectrum has different characteristics in different frequency regions and assumes that the noise is produced by a variety of different sources.

In the deep ocean the main causes of ambient noise are believed to be [4],

(a) Waves and tides and/or seismic activity in the earth in the frequency band 0 to 1 Hz.

(b) Large scale oceanic turbulences in the frequency range 1 to 20 Hz.

(c) Distant shipping traffic in the frequency range 20 to 500 Hz.

(d) Sea surface roughness (breaking whitecaps etc.) near to the point of measurement in the frequency range 500 to 50,000 Hz.

(e) Thermal noise originating in molecular motion of the sea in the frequency range above 50 kHz.

The level of deep sea noise can be estimated fairly well through the use of a composite spectrum deduced from a consideration of the different sources just described.

By contrast, the magnitude of shallow water ambient noise is not so easily predicted. Shallow water ambient noise at any given frequency results from a mixture of three types of noise. These are shipping and industrial noise, wind noise, and biological noise emanating from marine life. The variability of this mixture with time and geographical location prevents the prediction of shallow water noise magnitude to any great degree of accuracy.

b. Knudsen Curves

The Knudsen curves shown in Figure II-8 are graphical representations of empirically derived relationships among deep water ambient noise N_{amb}, sea state and frequency. From the curves, estimates of N_{amb} at 7 and 16 kHz for SS0 to SS5 can be deduced and modified by the worst case adjustment of 10 dB as indicated in equation II-19, to produce estimates for L_{NO}. These values are shown in Table II-7.

	SEA STATE					
Frequency	0	1	2	3	4	5
7 kHz	-58.4	-49.3	-44.1	-40.3	-37.4	-35
16 kHz	-64.5	-55.4	-50.2	-46.4	-43.5	-41.1

Table II-7. Spectrum level of shallow water ambient noise (dB/μbar/Hz)

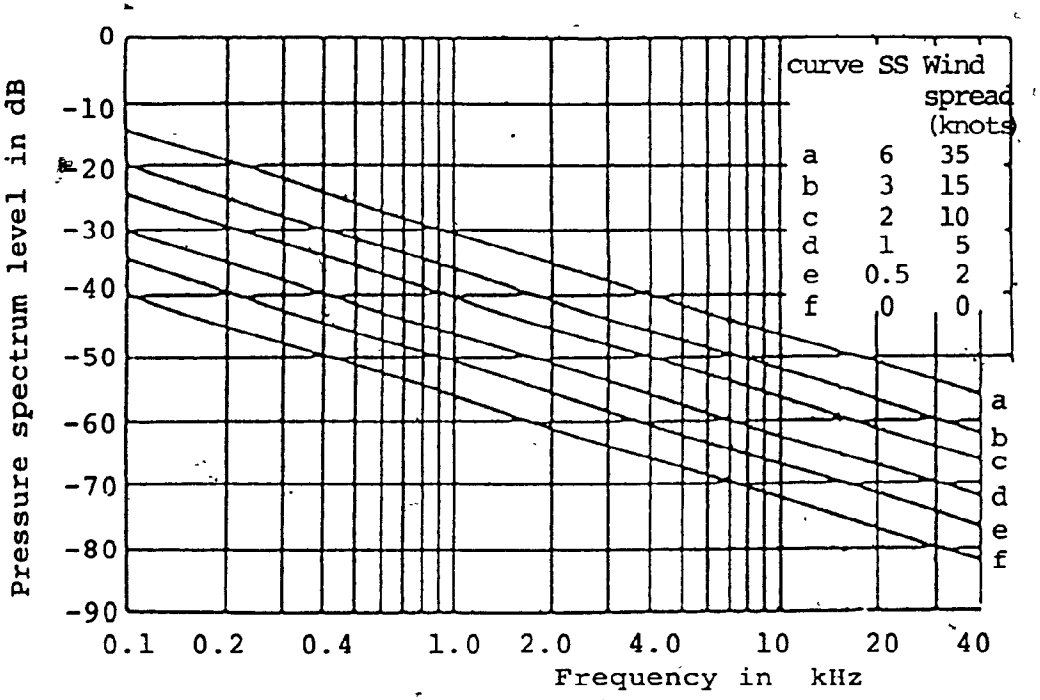

Figure II-8 Pressure spectrum level of ambient noise for various sea states and wind speed expressed in decibels relative to 1 μbar.

The data of Table II-7 is adjusted by the receiver bandwidth of 2.048 kHz to produce, the band level noise L_N described in equation II-18 and given in Table II-8.

	SEA STATE					
Frequency	0	1	2	3	4	5
7 kHz	-25.39	-16.29	-11.09	-7.29	-4.39	-1.99
16 kHz	-31.49	-22.39	-17.19	-13.39	-10.49	-8.09

Table II-8. Band level noise for receiver bandwidth of 2 kHz in shallow water (dB/μbar).

Morgera [12] has agreed that the ambient noise figure of -35 dB/μbar/Hz for a frequency of 7 kHz in shallow water as given in Table II-7, is a good estimate for sub-arctic regions. These are the regions in which the telemetry system is likely to be deployed. He suggested that an ambient noise figure 10 dB lower be used as an estimate for Arctic regions, due to the reduction in certain areas of the wind-driven ocean surface noise component.

4. Receiver S/N Ratio Computation

The transmission loss T_L and band level noise L_N estimates given in Tables II-6 and II-8 respectively are combined to form a loss figure (T_L+L_N) which is a partial indicator of the receiver signal-to-noise ratio. The loss

figure is shown in Table II-9.

	Frequency in kHz	SEA STATE					
		0	1	2	3	4	5
r=1 km	7	32.15	42.55	48.05	52.45	55.35	57.95
	16	30.69	40.69	46.19	50.09	53.29	55.79
r=2 km	7	39.14	49.54	55.04	59.44	62.34	64.94
	16	41.11	51.11	56.61	60.51	63.71	66.21

Table II-9. Loss figure (T_L+L_N) dB

The data of Table II-9 indicates that there is not much difference in the loss figures at 7 and 16 kHz. However since the band level noise L_N, at both frequencies is fixed and the transmission loss increases more rapidly with range at 16 kHz than at 7 kHz, it was decided that 7 kHz would be chosen as the lower edge of the frequency band used for communication between the top and bottom units of the telemetry system.

In order to guarantee effective communication, the source level L_s plus the directivity index of the receiver must exceed the figures of Table II-9 by an amount equal to the desired signal-to-noise ratio of the receiver. This amount depends on the desired communications probability of

error, and will be discussed in the sequel.

D. Dispersion

The ocean is a medium that is characterized by dispersion both in frequency and time. The frequency dispersion is known as the doppler spread B and the time dispersion is referred to as the multipath spread L. In part, these two parameters, B and L, determine the communication tonal transmit time duration and the receiver frequency resolution.

Thus if a tonal of length T_p, and bandwidth ω_p were transmitted in such a medium, it would be received as a signal of length (T_p+L), and bandwidth (ω_p+B). It is therefore, pointless for a transmitted pulse to possess finer frequency and time resolution properties that those imposed by the medium.

The BL product is used to classify a time-warying medium into three categories:

(1) Underspread : $BL < 1$

(2) Critically Spread: $BL = 1$

(3) Overspread : $BL > 1$

This classification is useful in establishing the fading properties of a signal. This is demonstrated pictorially in Figure II-9. The figure represents a plot of the

time-frequency plane. The abscissa represents time and is divided into increments of 1/B s. While the ordinate represents frequency and is divided into increments of 1/L Hz. Each rectangle of the plane has an area equal to 1/BL and represents a piece of a transmitted signal with constant fading properties. Thus, if a transmitted signal of length T_p and bandwidth ω_p, falls within one rectangle of the grid, as shown in Figure II-9, it will fade coherently, and is said to possess one diversity element. It is obvious therefore that, in order not to exceed one diversity element the product, $T_p\omega_p$, which in this design is equal to 1, must be less than 1/BL.

Morgera [12] has produced multipath and doppler spread estimates for the geographical area whose SVP's are labelled SVP A to SVP G. These results are reviewed and data relevant to the design of the telemetry system are extracted and reproduced in sub-sections a and b.

a. Multipath Spread L.

The multipath spread L is a measure of the time delay between rays arriving at the receiver via the direct path and those arriving after undergoing multiple reflections from the surface and bottom of the sea.

In general the received waveform can be expressed as,

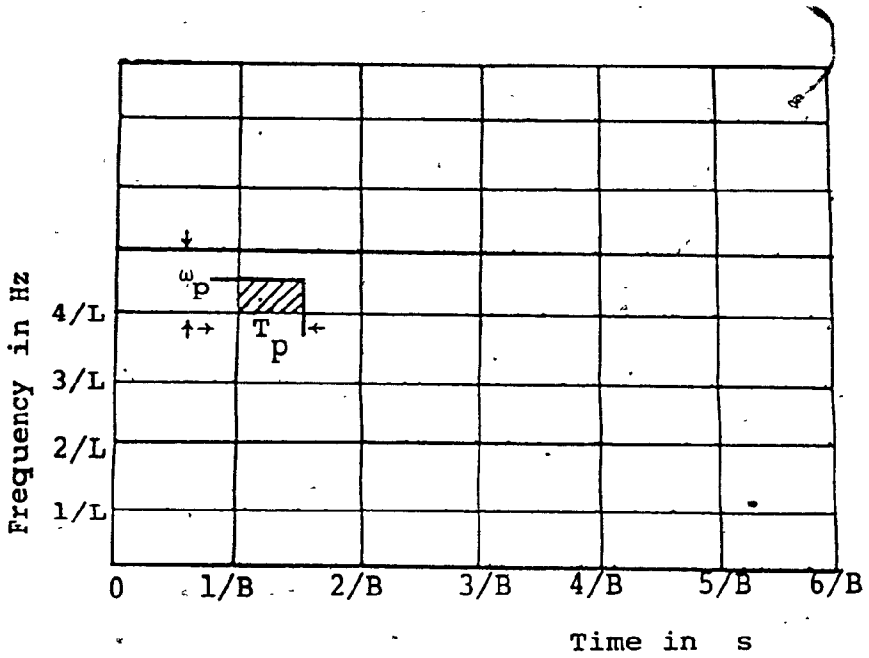

Figure II-9 A diversity model for signal structure

$$y(t) = \sum_{n=1}^{N} a_n \, x(t-\tau_n(t)) \qquad \text{II-20}$$

where $x(t)$ is the transmitted waveform, $\{\tau_n(t)\}$ is the set of propagation path delays and, $\{a_n\}$ is the set of respective path amplitudes. It can be assumed that these path amplitudes are ordered (i.e. $a_n < a_{n-1} \ldots < a_1$) because higher order rays suffer more energy loss due to greater bottom absorption, greater surface scattering and higher attenuation as a result spherical spreading and absorption over the longer paths. Thus it is reasonable to assume that multipaths higher than third order can be neglected in the estimation of the multipath spread.

Morgera expressed the multipath spread L as

$$L = \left[\sum_{n=1}^{N} a_n^2 (\tau_n - \bar{\tau})^2 \Big/ \sum_{n=1}^{N} a_n^2 \right]^{\frac{1}{2}} \qquad \text{II-21}$$

where

$$\bar{\tau} = \sum_{n=1}^{N} a_n^2 \tau_n \Big/ \sum_{n=1}^{N} a_n^2 \qquad \text{II-22}$$

He utilized these expressions together with the data presented in Figures II-1 to II-7, to determine the multipath spread estimates over a horizonal range of [0.55-2.187] kyds in small range increments. For these calculations the transmitting hydrophone was located at the ocean bottom while the receiving hydrophone was located at a minimum

depth d' at which the propagation loss was consistent with that obtained by the semi-empirical models and given in Tables II-2 to II-5. The multipath spread estimates for SVP A to SVP G, over two different ranges, for two sea states, and for optimum receiver depth are given in Table II-10.

SVP	d'	r = 1.094 kyds		r = 2.187 kyd	
		SS0	SS4	SS0	SS4
A	33' (10.1m)	109	105	60	60
B	54' (16.5m)	47	22	24	10
C	105' (32.0m)	6	1	1	1
D	23' (7.0m)	49	1	22	18
E	33' (10.1m)	99	50	27	27
F	33' (10.1m)	85	43	24	23
G	46' (14.1,)	SS3	15	13	

Table II-10. Multipath spread L(ms) for two communication ranges, optimum receiver depth d', and SS0 and SS4

Estimates of multipath spread for intermediate ranges can be obtained from graphs presented in [12].

b. Doppler Spread. B

Doppler spread B is the frequency dispersion observed in the received signal due to reflections from the ocean surface and the relative motion of the vehicle, on which the top unit is placed, with respect to the bottom unit. It is defined as the r.m.s. sum of B_s, doppler spread due to surface roughness effects and, B_v, the doppler spread due to vehicle-current motion.

i. Frequency Effects due to Ocean Surface Roughness. B_s

When the surface of the ocean is moving, the vertical motion of the waves interacts with the signals incident upon it, producing amplitude and angle modulation of these signals. The nature of the spectrum of the reflected signals is dependent on the roughness of the surface. This roughness is measured by the Rayleigh parameter which is defined as,

$$R_n = KH \sin\theta \qquad \text{II-23}$$

where K is the wave number $2\pi/\lambda$, H is the r.m.s. wave height and θ is the surface grazing angle. The Rayleigh numbers $R_n < 1$, ≈ 1, and > 1 describe a smooth, moderate and rough surface respectively. The relationship between the roughness of the surface and the spectrum of the reflected signal for a single incident tone, is shown in Figure II-10

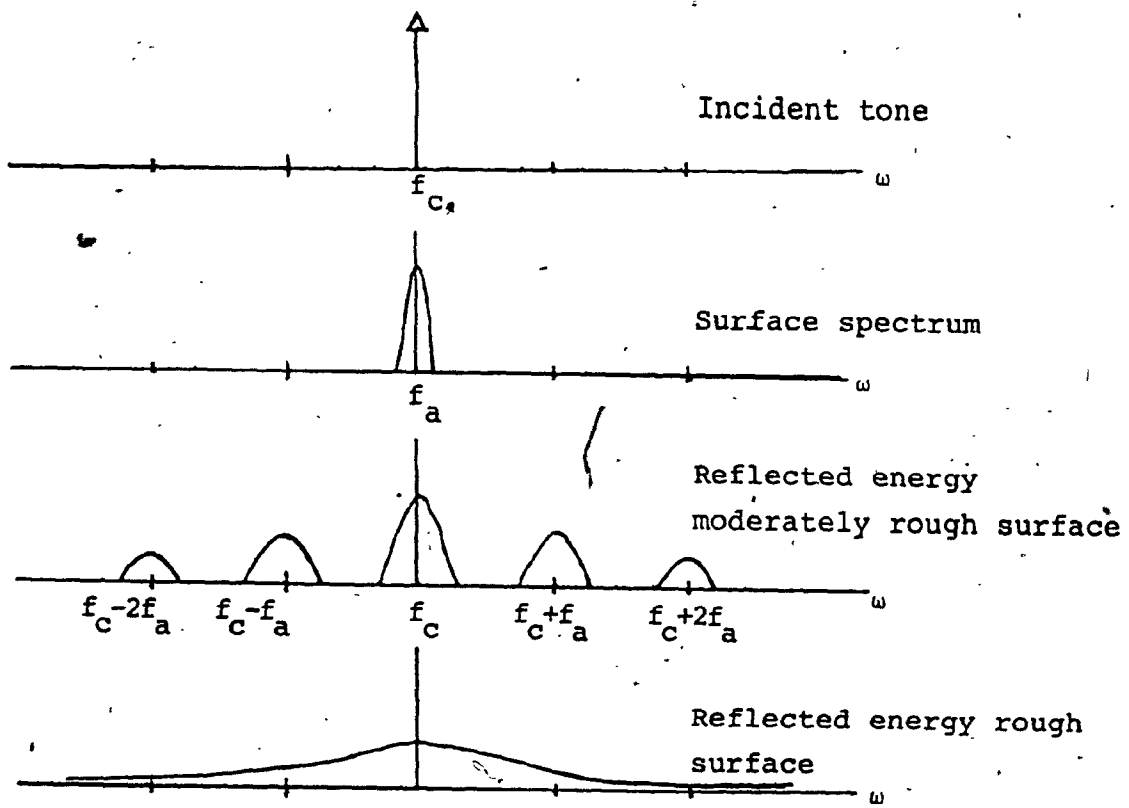

Figure II-10 Surface reflected spectrum, Dependence on Rayleigh number

where f_c is the frequency of the incident tone and f_a is the central frequency due to surface motion. A smooth surface acts as a perfect reflector, while, as indicated in Figure II-10, a moderate surface produces angle modulation giving rise to discrete sidebands and a rough surface introduces amplitude as well as angle modulation resulting in smeared sidebands.

Calculations of the frequency effects due to ocean roughness at frequencies of 7 and 16 kHz, grazing angles θ, of 3° and 6°, and r.m.s. wave heights of 1m (SS2-3) and 2m (SS4), have been made using the bifrequency function. The results are given in Table II-11.

freq (kHz)	SS 2-3, θ=3°	SS4, θ=6°
7	.9 Hz	3 Hz
16	1.9 Hz	6.8 Hz

Table II-11. Frequency dispersion due to ocean roughness B_s.

ii. Frequency Effects due to Vehicular Motion, B_v

The vertical and axial motion of the vehicle on which the receiving unit is placed, create an additional frequency dispersion effect, B_v. An analysis of the effect is lengthy and complex. It involves many assumptions and approximations

and may be followed in reference [12]. The computation of B_v depends on parameters relating to the multipath structure of the medium such as the amplitude, a_n, of the nth ray and the angle, θ_n it makes with the receiving hydrophone relative to the horizontal. It also depends on vehicle-current motion parameters such as, the axial speed of the vehicle resolved with the ocean current, and the vertical oscillation amplitude of the vehicle.

Computations of the doppler spread due to vehicle motion, B_v, over a range [0.55 kyds - 2.187 kyds] for geographical locations represented by SVP A to SVP G, and different axial vehicle motion, have been done by Morgera. An excerpt from his results for two communication ranges of interest is given in Table II-12.

SVP	V = 0.1 kt		1 kts		2 kts		5 kts	
	r=1.094 kys,	2.187 kyds						
A	.14	.18	1.38	1.79	2.70	3.60	6.70	9.00
B	.19	.15	1.88	1.50	3.75	3.00	9.40	7.40
C	.17	.16	1.65	1.63	3.26	3.26	8.20	8.15
D	.15	.23	1.45	2.25	2.95	4.58	7.40	11.30
E	.17	.14	1.70	1.4	3.40	2.84	8.60	7.00
F	.14	.14	1.43	1.38	2.85	2.80	7.10	7.00
G	.19	.14	1.9	1.46	3.80	2.74	9.50	6.70

Table II-12. Doppler spread due to vehicle motion, B_v (Hz), for two communication ranges and optimum receiver depth d'.

The Table indicates that the doppler spread due to vehicle motion does not change appreciably with range at any given location once the axial velocity is kept constant. From the estimates of B_s and B_v, values of B for SS0 and SS4, at the lower axial velocity range (i.e. V<3 kTs), and the higher axial velocity range (V = 5-6 kts), have been made and are presented in Table II-13.

Axial velocity kts.	SEA STATE	
	SS0	SS4
Lower speed range V<3 kts	3.41	4.45
Higher speed range V=5-6 kts.	8.3	8.8

Table II-13. Estimates for overall doppler spread B (Hz) as a function of sea state and vehicle-current motion.

c. Summary of Dispersion Results

The dispersion estimates for L and B are summarized by the contents of Tables II-10 and II-13 respectively. An average of 100 ms for L is chosen, based on the data presented in Table II-10. Table II-13 indicates that for axial vehicular velocities less than 3 kts, a doppler spread of approximately 4 Hz is to be expected.

d. Determination of Optimum Pulse Length

The resolution properties of the transmitted pulse should be consistent with the time and frequency uncertainties of the medium. Thus the pulse duration T_p and bandwidth ω_p are respectively given as,

$$T_p = \frac{1}{B} \qquad \text{II-24}$$

$$\omega_p = 1/L \qquad \text{II-25}$$

Thus

$$T_p \omega_p = 1/BL \qquad \text{II-26}$$

Since for the chosen tonals, $\omega_p = 1/T_p$. the pulse length that gives maximum coherence is given by [8],

$$T_p = \sqrt{L/B} \qquad \text{II-27}$$

Table II-14 provides estimates of T_p, over several communications ranges for SS0 and SS4, for each of the SVP's graphed in Figures II-1 to II-7.

SVP	r=.273 kyds		r=.820 kyds		r=1.094 kyds		r=2.187 kyds	
	SS0	SS4	SS0	SS4	SS0	SS4	SS0	SS4
A	270	200	210	170	190	160	130	110
B	175	104	136	82	110	68	88	49
C	72	45	46	25	42	15	17	15
D	212	139	157	108	114	87	68	57
E	220	164	175	114	169	105	95	83
F	212	146	173	110	168	102	90	75
G(SS3)	107		64		56		57	

Table II-14. Optimum pulse length T_p(ms) as a function of geographical location for several intermediate ranges and sea states

From scrutiny of Table II-14, and practical considerations from a system implementation point-of-view, it was felt that a pulse length T_p = 125 ms. would be reasonable for the telemetry system design.

E. Design Recommendations

The preceeding study dictated the guidelines that were used in the design of the telemetry system. Transmission loss and band level noise estimates indicate, that for a given transmitter power and directivity index, the signal-to-noise ratio is better at 7 kHz than at 16 kHz. Thus

7168 Hz was assigned as the lower edge of the system communication band. Since the system bandwidth is 2048 Hz, the midband frequency is 8192 Hz.

The estimates of doppler spread B and multipath spread L at 7 kHz are taken to be 4 Hz and 100 ms respectively. The optimum pulse duration T_p is set at 125 ms. Thus the receiver frequency resolution is $(B + 1/T_p)$ Hz or 12 Hz while the received tonal duration is $(T_p + L)$s or approximately 225 ms. The system transmit tonals are therefore spaced 12 Hz apart and a 125 ms dead time is used between transmissions.

To combat the problems of fading, 5-fold frequency diversity is used. The value 5 was arrived at as a result of the modulation format to be used by the system and the fact that each tonal has to be spaced at least 1/L Hz apart. The modulation format is discussed in Chapter IV.

Finally, the estimates of B and L as given in Tables II-13 and II-10 respectively, indicate that in order for the telemetry system to operate, at or close to one diversity element per tone, a vehicle-current axial velocity of $V \leq 3$ kts and a range approximation of about 820 yds between the bottom unit and the vehicle, should be observed. Such an operational constraint is realistic in any acoustic communication system operating between end points, one or both of which may be moving. This allows a certain performance predictability and reliability. However, a system

should have enough robustness to operate at a lower but acceptable performance level when some of the specified operational constraints are not fully satisfied.

REFERENCES

1. Schwartz, N., Information, Transmission, Modulation and Noise, McGraw Hill, New York, 1970.

2. Kennedy, R.S., Fading Dispersive Communication Channels, J. Wiley, New York, 1969.

3. Kinsler, L.W., and A.R. Frey, Fundamentals of Acoustics, J. Wiley, New York.

4. Urick, R.J., Principles of Underwater Sound, McGraw Hill, New York.

5. Browning, D.G., and R.H. Mellen, "Environmental Factors Affecting Sonar Performance", Eascon '75, pp. 69A-69C.

6. Costa, J.P., "Medium Constraints on Sonar Design and Performance", Eascon '75, pp. 68A-68L.

7. Deavenport, R.L., "The Influence of the Ocean on Sonar System Design", Eascon '75, pp. 66A-66E.

8. Kennedy, R.S., and I.L. Lebow, "Signal Design for Dispersive Channels", IEEE Spectrum, 1, pp. 231-237, March 1964.

9. Kennedy, R.S., and I.R. Lebow, "Signal Design for Dispersive Channels", IEEE Spectrum, March 1964, pp. 231-237.

10. Marsh, H.W. and M. Schulkin, "Shallow Water Transmission,"J. Acoust. Soc. Am.," 34:863 (1962).

11. Morgera, S.D., "Optimum Underwater Acoustical Telemetry Techniques", prepared for Canadian Department of Environment, Oceans and Fisheries, Contract 07SC.KF806-8-E330, 28th February 1979.

12. Morgera, S.D., "A Conceptual Design of an Underwater Acoustic Telemetry System, Phase II Study", prepared for Canadian Department of Environment, Oceans and Fisheries, Contract 20th February 1980.

13. Schulkin, M., and H.W. Marsh, "Sound Absorption in Sea Water", J. Acoust. Soc. Am., 34, pp. 864-865, 1967.

14. Thiele, R., "Measurement of the Weighting Function of the Time Variant Shallow Water Channel", in Aspects of Signal Processing, Part 1, edited by G. Tacconi, pp. 109-122, 1977.

15. Thomas, R.S., J.C. Molden and J.M. Ross, "Shallow Water Acoustics Related to Signal Processing", in Signal Processing, proceedings of the NATO advanced Study Institute on Signal Processing, edited by J.W.R. Griffiths and P.L. Stocklin, Academic Press, pp. 281-298, 1973.

16. Tufts, D.W., "Data Transmission for Undersea, Acoustic Channels", IEEE International Conf. on Comm., Philadephia 1968.

CHAPTER III

SIGNAL PROCESSING: THE COMMAND RECEIVER

A. INTRODUCTION

This chapter examines the signal processing functions of the command receiver and explains the rationale behind its design. It describes the mix of hardware/software functions required to implement the signal processing techniques needed to ensure the desired system performance.

The performance criteria, as specified by the probability of false alarm, P_{FA}, and the probability of correct detection, P_{CD}, are given. Methods to reduce the time and frequency uncertainties resulting from the fading dispersive nature of the medium are discussed.

It is shown that the dynamic range and structure of the command receiver are determined by the required signal-to-noise ratio per diversity channel S/N_{req} and a sub-optimum detection technique which produces results within 1 dB of the optimum detection rule.

A description of the block schematic diagram of the command receiver is given and the hardware implementation is discussed. Finally the switched power supplies used by the command receiver are analysed.

B. DESCRIPTION AND FUNCTION OF COMMAND RECEIVER

A block schematic diagram of the command receiver is given in Figure III-1. It consists of three circuit boards whose design will be discussed later in this chapter. These boards are:

(a) The pre-amplifier and bandpass filter board

(b) The command receiver filter bank and mixer board

(c) The precision rectifier and A/D converter board

The command receiver is that portion of the telemetry system bottom unit which deals with the recognition and processing of an interrogation command issued by the system top unit, located on board a ship.

The top unit concurrently transmits five tonals, four of which are symmetrically placed around the band centre frequency of 8192 Hz. The frequencies of the five tonals are 7392 Hz, 7792 Hz, 8192 Hz, 8592 Hz and 8992 Hz. The tonals are spaced a distance of b=400 Hz ($b \geq (\omega_p + 1/Lmin)$) apart so as to ensure statistically independent fading, thus giving the system D-fold diversity where D is equal to 5. Upon receipt of the tonals, the command receiver processes them and forms a decision statistic which is tested against a threshold level. If the threshold level is exceeded, the microcomputer, which

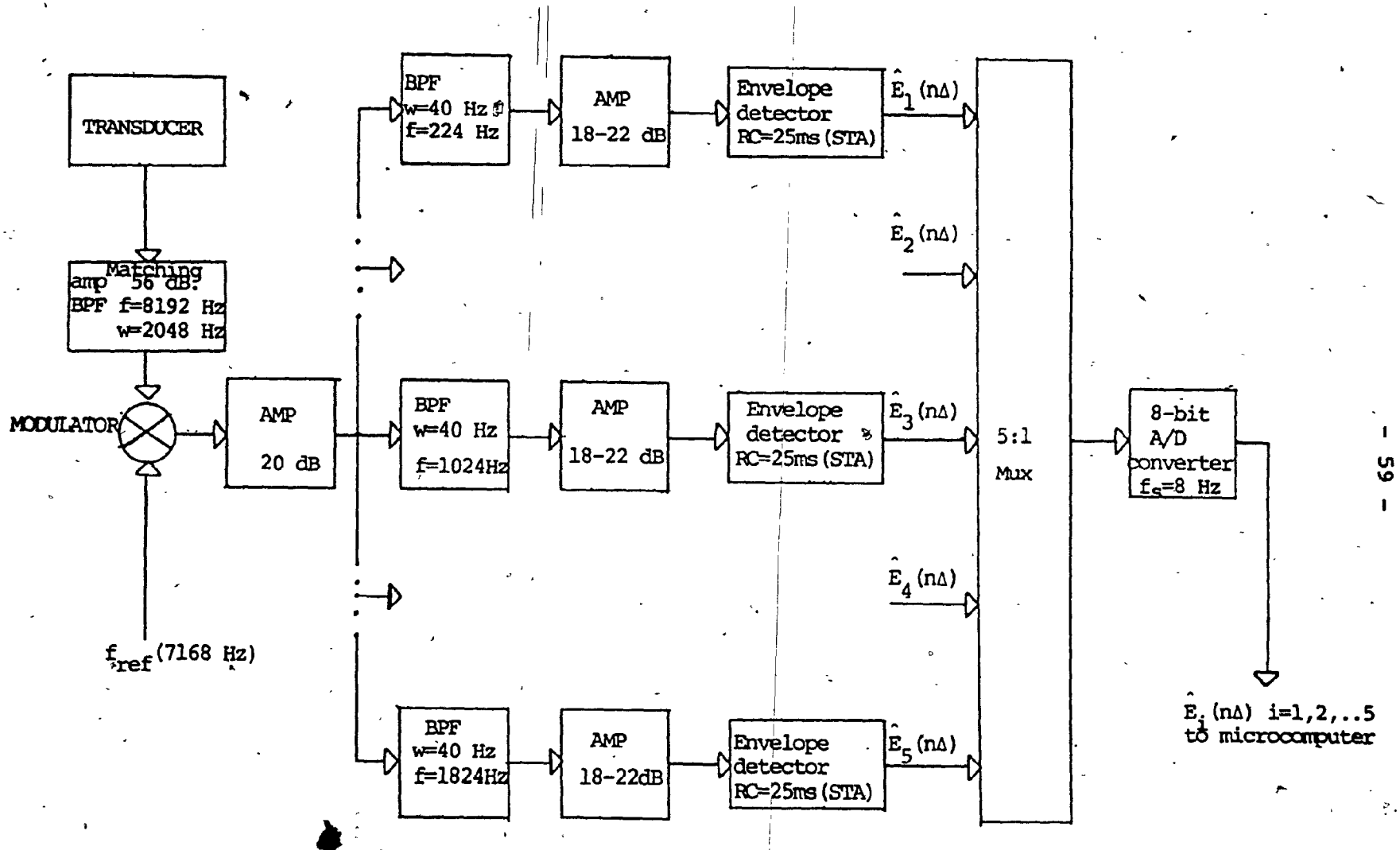

Figure III-1 Block diagram of command receiver

controls the entire functioning of the bottom unit, activates the transmitter and the data stored in memory is encoded and transmitted after the transmission of a preamble which is intended for the synchronization of the top unit.

C. PERFORMANCE CRITERIA

The location of the bottom unit on the ocean floor introduces a severe power constraint in its design. Thus, it is essential that the bottom unit transmit when and only when it has been properly interrogated in order to conserve its power source. Two performance criteria, therefore, are that the probability of false alarm P_{FA}, should be very low and that the probability of correct decision P_{CD}, given a fixed signal-to-noise ratio, should be as high as possible.

The realization of these performance criteria is complicated by the fading dispersive nature of the medium. Dispersion results in there being an uncertainty in both the time and the frequency of the tonals arriving at the command receiver. This means that there are a total of $M=M_t+M_f$ alternative locations in which the received tonals may fall, where M_t and M_f are the time and frequency uncertainties respectively.

The width of any of the five tonal arriving at the command receiver should be 8 Hz (i.e., $\frac{1}{2T_p}$ + 4). If in addition, a relative top-to-bottom unit doppler shift of $\pm$16 Hz is assumed, the uncertainty in frequency would be

M_f=5. This uncertainty is eliminated by receiving each tonal with a filter that is 40 Hz wide.

The time uncertainty M_t can be minimized by using the integration scheme shown in Figure III-2. The command receiver has a 50% duty cycle with an on-time of 125 ms. The integration scheme ensures that regardless of the time of arrival of the tonals, the integrators will always capture 125 ms of signal energy. The signal energies of two adjacent integration periods are summed to form the detection statistic. The integration scheme reduces the time uncertainty to M_t=2. The total uncertainty, therefore, is $M=M_f+M_t=2$. This results in a system performance degradation which will be discussed in Chapter VI.

Since M and D are known, if the P_{FA} and P_{CD} are given, the signal-to-noise ratio per diversity channel, R_o, required to ensure a specific system performance, can be computed using equations III-1 and III-2, which are given respectively, as, [11],

$$P_{FA} = 1 - [1-e^{-\Lambda} \sum_{k=0}^{D-1} \Lambda^k/K!]^M \qquad \text{III-1}$$

$$P_{CD} = \int_{\Lambda}^{\infty} \frac{X^{D-1} e^{-(\frac{X}{1+R_o})}}{(D-1)!\,(1+R_o)^D} [1-e^{-x} \sum_{k=0}^{D-1} X^k/k!]^{M-1} dx \qquad \text{III-2}$$

where Λ is the detection threshold level and the signal-to-

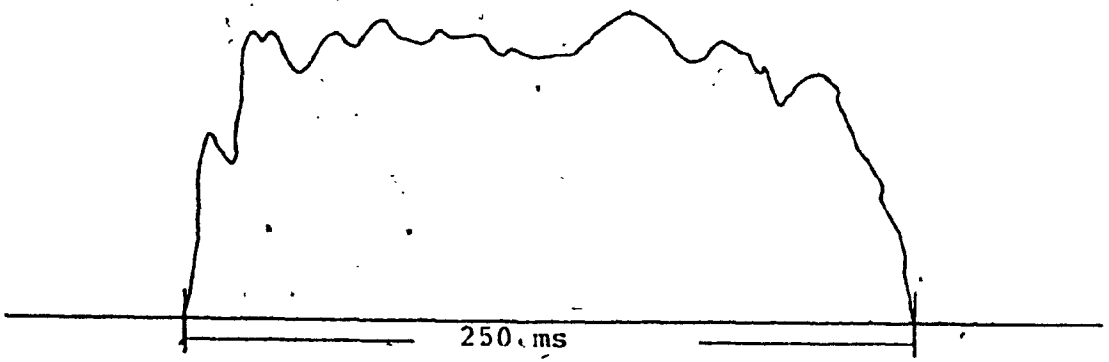

Top unit transmission interval

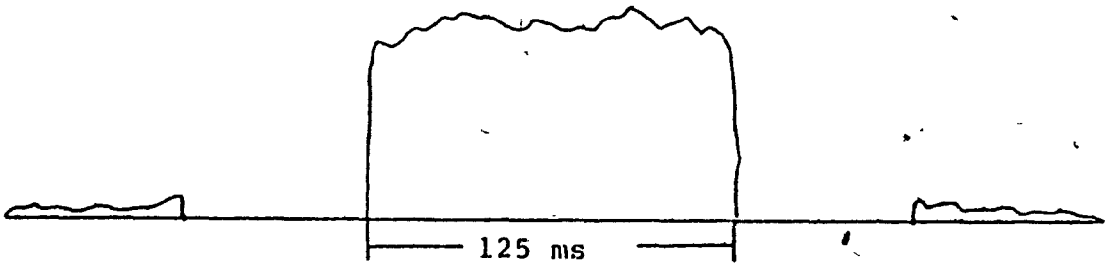

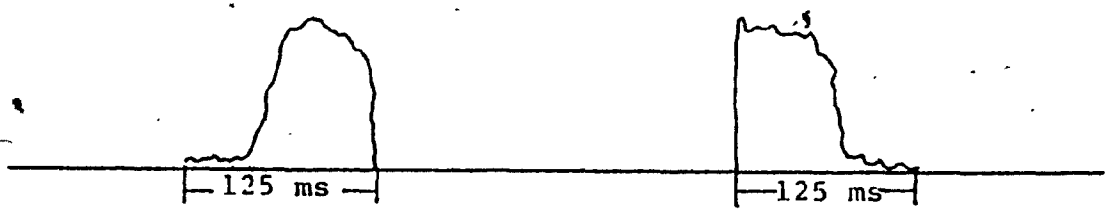

Typical reception intervals

Figure III-2 Command receiver duty cycle/integration scheme

noise ratio per diversity channel is R_o, which is defined for slow Rayleigh fading as,

$$R_o = \frac{\bar{E}_1}{N_o} = \frac{\bar{E}_t}{DN_o} \qquad \text{III-3}$$

where $\bar{E}_1$ is the average signal energy per diversity channel, $\bar{E}_t$ is the total signal energy for all D diversity channels and N_o is the single sided noise power spectral density. The graph of Figure III-3 is plotted from equations III-1 and III-2. It gives R_o as a function of D and E_T/N_o with M and P_{FA} held constant at values of 2 and 10^{-8} respectively.

It was felt that good system performance could easily be obtained by specifying $P_{FA}=10^{-8}$ and $P_{CD}=0.99$. These figures translate to mean that the probability of a missed detection, $(P_{MD}=1-P_{CD})$, is 1 in every 100 interrogations and the P_{FA} is 1 in every $\left(\frac{.250}{10^{-8}(24)(36000}\right) = 289$ days of operation.

Thus with $P_{FA}=10^{-8}$, $P_{CD}=0.99$, M=2, and D=5, R_o is obtained from the graph of Figure III-3, as,

$$R_o = \frac{\bar{E}_1}{N_o} = \frac{E_T}{DN_o} = 14 \text{ dB} \qquad \text{III-4}$$

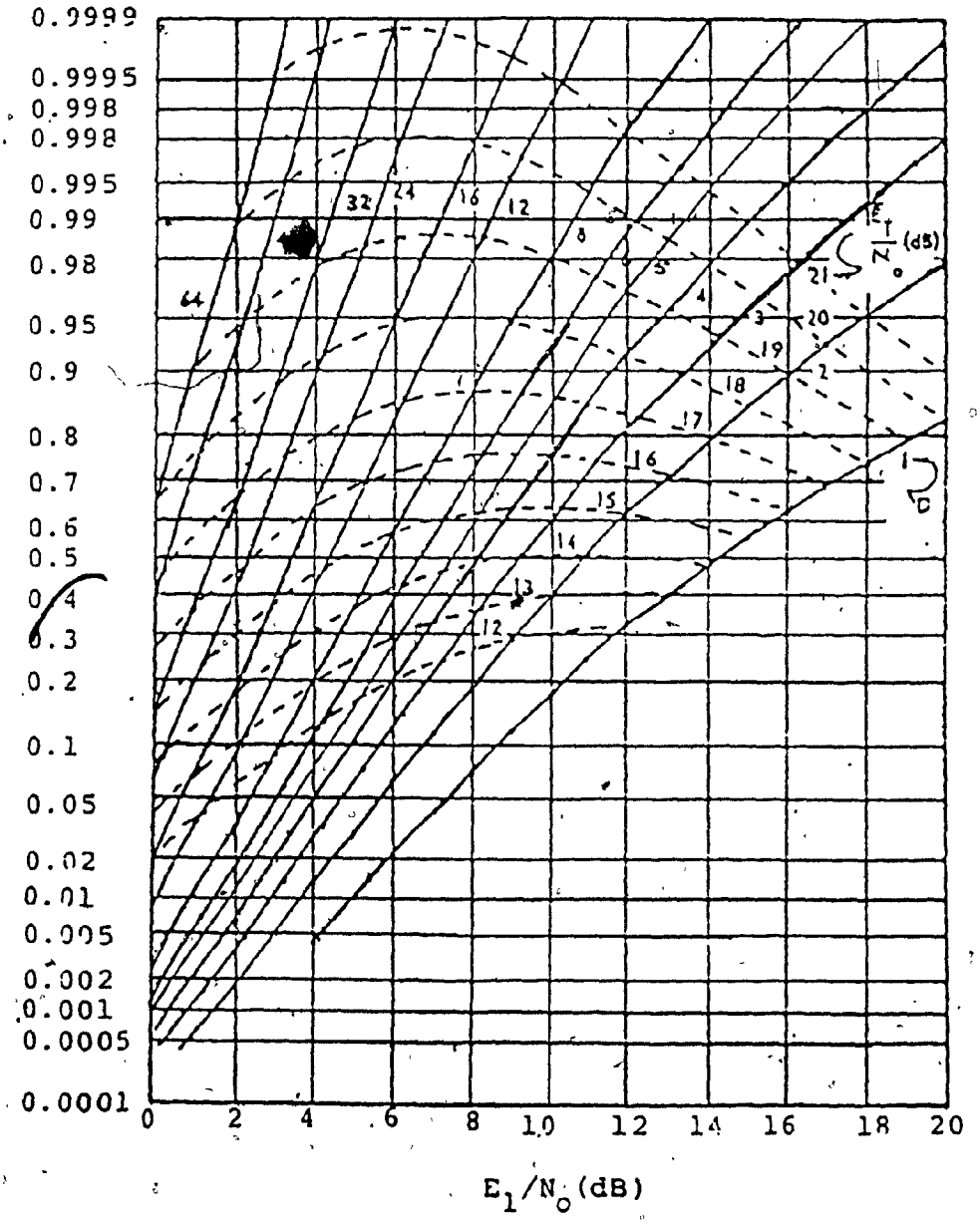

Figure III-3 Detection Characteristics for $P_{FA} = 10^{-8}$, M=2

D. STRUCTURE AND DYNAMIC RANGE OF THE COMMAND RECEIVER

The structure and dynamic range of the command receiver are determined by the statistical model used for system performance analysis. The reader is referred to Chapter VI for details of this. There it is shown that the optimum detection rule for each channel, as given by the log likelihood ratio ℓ_i, contains a signal-to-noise scaling factor which is difficult to compute. In order to overcome this problem a sub-optimum technique is adopted whereby, a short term average (STA) of the signal energy taken over a 125 ms period, on each channel, is normalized by a long term average (LTA) of the noise energy for that channel. The LTA is done over a period of K(125) ms, where K is a suitably large integer and it is intended to counteract implusive noise that may occur sporadically on the channels.

The noise normalization technique makes it mandatory that the command receiver has a minimum level of amplification so as to ensure that the noise level fills at least one step of the A/D converter. The amount of amplification needed is now investigated. For an 8 bit A/D converter having a 5 volt window, there are 19.5 mv/step. The transducer selected for use in the system is the ITC-3241 which has a sensitivity of -172 dBv/μP_a^2 at 8 kHz. If a noise level representative of quiet Artic sea conditions is assumed, that is 55 dB/μP_a^2/Hz, the output of the transducer would be -117.5 dBv which is approximately equal to 1.33 μV.

To determine the transducer output when both signal and noise are present, the required signal-to-noise ratio, S/N_{req}, of the system, must be known. This is the sum of the signal-to-noise ratio per diversity channel, R_o, and losses, L_f and L_t, due to the non-ideal detection schemes used to minimize the frequency and time uncertainties, respectively.

The required signal-to-noise ratio is, therefore given as

$$S/N_{req} = \bar{E}_1/N_o + L_f + L_t$$

$$= 14 + 10\log \frac{40}{4} + 10\log 2 = 27 \text{ dB} \qquad \text{III-5}$$

where L_f is a bandwidth loss due to the filter width being wider than the tonal width, and L_t is an integration loss resulting from the fact that there is always 125 ms of noise present at the output of the integrators. The nominal signal level at the input to the command receiver, will therefore, be $-(117.5+27)=99.5$ dBv which is approximately 10.59 μv and the signal plus noise level will be (10.59+1.33) = 11.92 μv. If transducer matching network and demodulation losses (see Figure 1) of 12 dB are consider, the output of the integrators would be:

-129.5 dBv ≈ 0.335 μv quite noise only

-111.15 dBv ≈ 2.7 μv nominal signal plus quiet noise

These calculations indicate that the command receiver must have a minimum of 96 dB of amplification in order that the quiet noise level occupy at least one step of the A/D converter.

The structure of the command receiver is shown in Figure III-1. Its operation is as follows. The five incoming tonals are received by the transducer and then passed to the pre-amplifier which consists of a matching network amplifier and a bandpass filter centred at 8192 Hz and having a bandwidth of 2048 Hz. The tonals are then mixed with a 7168 Hz reference signal and the difference frequencies amplified and passed through a bank of five bandpass filters each 40 Hz wide and centred at one of the five difference frequencies ($f_i - f_{ref}$ i=1,...5). Further amplification is applied at the output of each of the five bandpass filters and envelope detection follows. The RC time constant of the envelope detectors is 25 ms. This ensures that the integrators are at a maximum when they are sampled at the end of the 125 ms period. The samples from the five diversity channels are multiplexed into an 8 bit A/D converter operating at a sample rate of 8 Hz, then they are transferred to the microcomputer which continues the signal processing by performing the following functions:

(a) It forms the LTA of the noise energy on each of the diversity channels over K(125)ms periods.

The LTA noise estimate of the ith channel is given as,

$$\hat{N}_i(n\Delta) = \frac{1}{k} \sum_{\ell=n-k}^{n} \hat{E}_i(\ell\Delta) \qquad \text{III-6}$$

The quantity Δ, is the sampling period and is equal to 125 ms. The LTA is done as a "sliding-window" average as indicated by equation III-6.

(b) It produces a weighting rule $\gamma_i(n\Delta)$ for each channel by normalizing the STA estimate of signal energy on that channel by its corresponding LTA noise estimate. The weighting rule is given as,

$$\gamma_i(n\Delta) = \hat{E}_i(n\Delta)/\hat{N}_i(n\Delta) \qquad \text{III-7}$$

The weighting rule has an effect similar to a.g. c. and is used instead of it.

(c) It does frequency diversity combining by summing the outputs of all five diversity channels every 125 ms to partially form the detection statistic. The summation $\gamma(n\Delta)$ is written as,

$$\gamma(n\Delta) = \sum_{i=1}^{5} \gamma_i(n\Delta) \qquad \text{III-8}$$

(d) It does temporal combining by summing two consecutive values produced through frequency

combining to form the detection statistic which is denoted by,

$$\gamma = \gamma(n\Delta) + \gamma((n-1)\Delta) \qquad \text{III-9}$$

(e) Finally, it makes a decision as to whether or not the bottom unit has received an interrogation command by comparing γ against a fixed threshold level, Λ . If the threshold is exceeded, the microcomputer instructs the bottom unit to commence transmission.

E. COMMAND RECEIVER HARDWARE

The design of the three cards comprising the command receiver will now be discussed. The design has been principally influenced by the desire to conserve power. As a result the hardware consists of a mixture of CMOS and special low power chips.

1. Pre-Amplifier Unit

A photograph of the pre-amplifier unit is shown in Figure III-4. Its schematic diagram is given in Figure III-5. The unit is encased in a metal box for shielding so as to minimize noise pick-up. It consists of an impedance matching transistor amplifier which interfaces the transducer to a passive fourth order Butterworth filter centered at 8192 Hz

and having a bandwidth of 2048 Hz. This filter is followed by a three stage transistor amplifier. The maximum gain of the pre-amplifier unit is 58 dB and it can be varied by adjusting potentiometer R1.

The bandpass filter was chosen to be a passive filter in order to conserve power, inspite of the fact that at 8 kHz the coils are rather large.

A design specification for the bandpass filter was that it should have 40 dB of attenuation at 12 kHz. The following steps were taken to effect the design [1,6]:

(1) The normalization of the lower cut-off frequency, the centre frequency, and bandwidth to the upper cut-off frequency which is 9216 Hz.

(2) The transformation of all bandpass specifications into lowpass specifications by means of the low-pass-to-bandpass transformation.

(3) The determination of the order, n, of the low-pass Butterworth prototype. The order needed was found to be 4.

(4) Determination of the values of the components of the lowpass prototype from Tables [6].

(5) Application of frequency transformation and impedance scaling to the prototype to produce the desired bandpass filter.

Figure III-4 Photograph of pre-amplifier unit

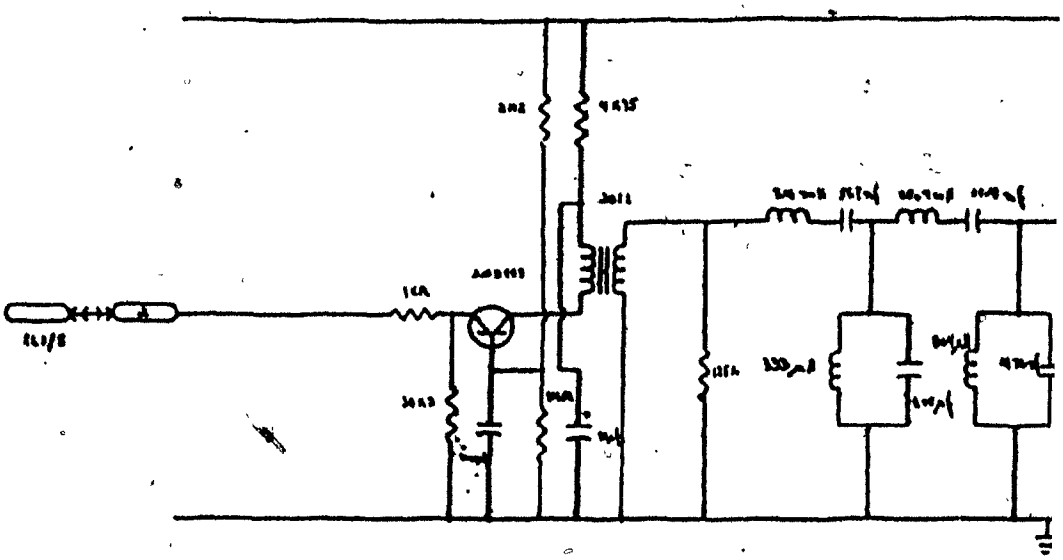

Figure III-5 Schematic diagram of p

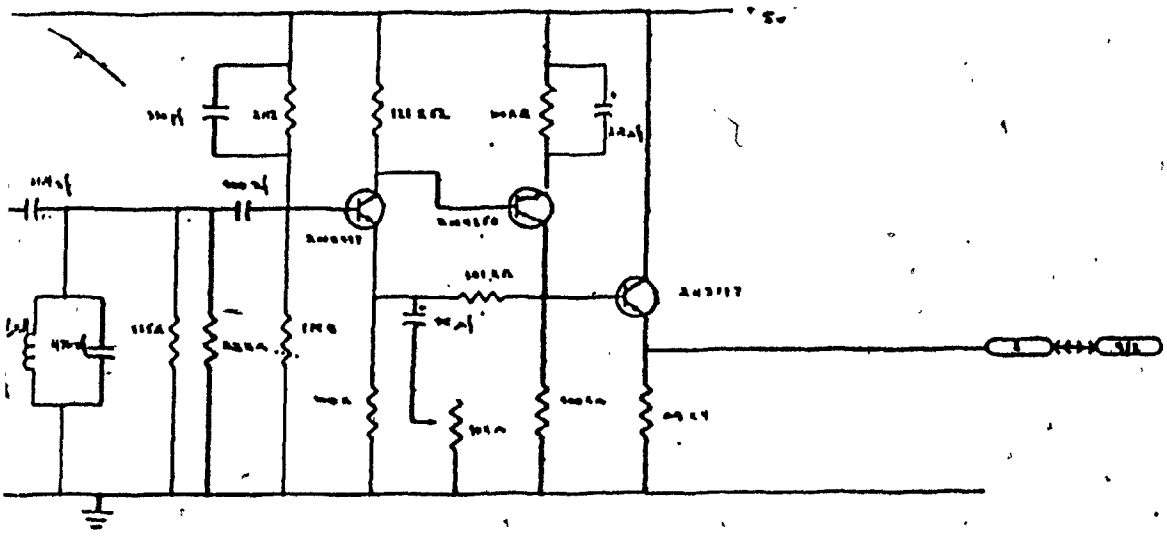

n of pre-amplifier unit

Measurement of the frequency response of the filter is given in Table III-1 and plotted in Figure III-6. It should be noted that the phase response is not given, because it is not important since the command receiver uses an incoherent detection scheme.

Frequency in Hz	Attenuation in dB
4000	-44
5000	-42
6000	-28
6500	-18
7192	-4
8192	0
9192	-3
9500	-7
10000	-16
10500	-24
11000	-29.5
11500	-34
12000	-38
13000	-43

Table III-1 Frequency response of pre-amplifier

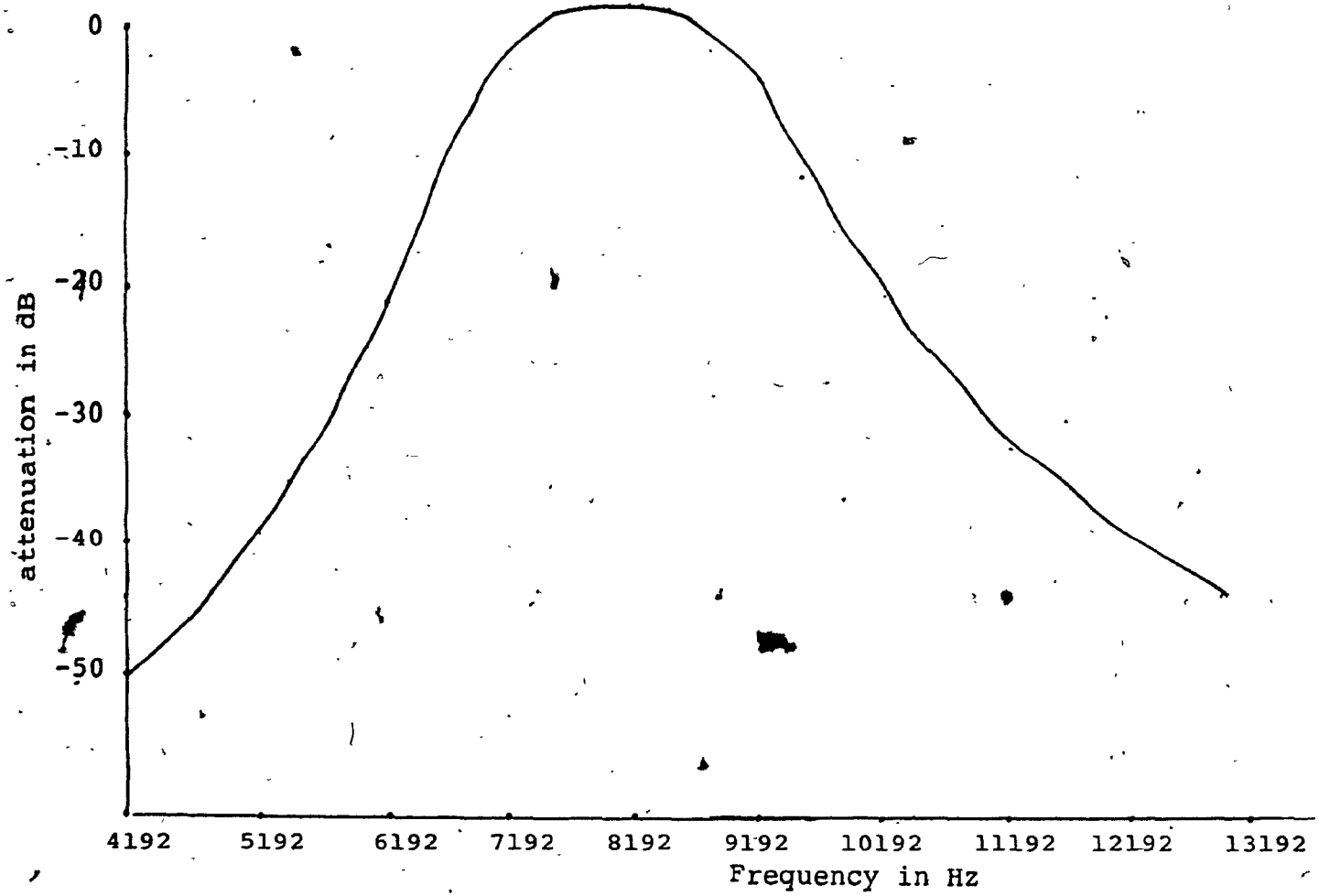

Figure III-6 Frequency response of pre-amplifier unit

2. Receiver Filter Bank and Mixer Board

Figure III-7 shows a photograph of the receiver filter bank and mixer board. Its schematic diagram is given in Figure III-8.

The board contains a balanced modulator (MC 1496), followed by an inverting amplifier having a variable gain between 20 dB and 26 dB. This amplifier feeds a bank of fourth order Deliyannis bandpass filters.

One input to the mixer comes from the output of the pre-amplifier. The other input is fed by a 7168 Hz reference signal. Since 7168 is not a sub-multiple of the telemetry system master clock, whose frequency is 262144 Hz, it has to be synthesized using a phase lock loop (CD 4046) as a frequency multiplier. A 512 Hz square wave is multiplied by 14, the number to which the programmable counter (CD 4516) is set, to produce a 7168 Hz square wave. This is then filtered by an RC lowpass filter to provide a low level 7168 Hz sinusoid for use as the reference signal.

When the five tonals from the top unit are present at the input to the command receiver they mix with the reference to form sum and difference frequencies. The frequency spectrum at the output of the modulator is shown in Figure III-9, for tonals of infinitely narrow width. The 2 dB "scalloping" seen in the figure, is due to the response of the pre-amplifier BPF (Figure III-6), and is within specifications.

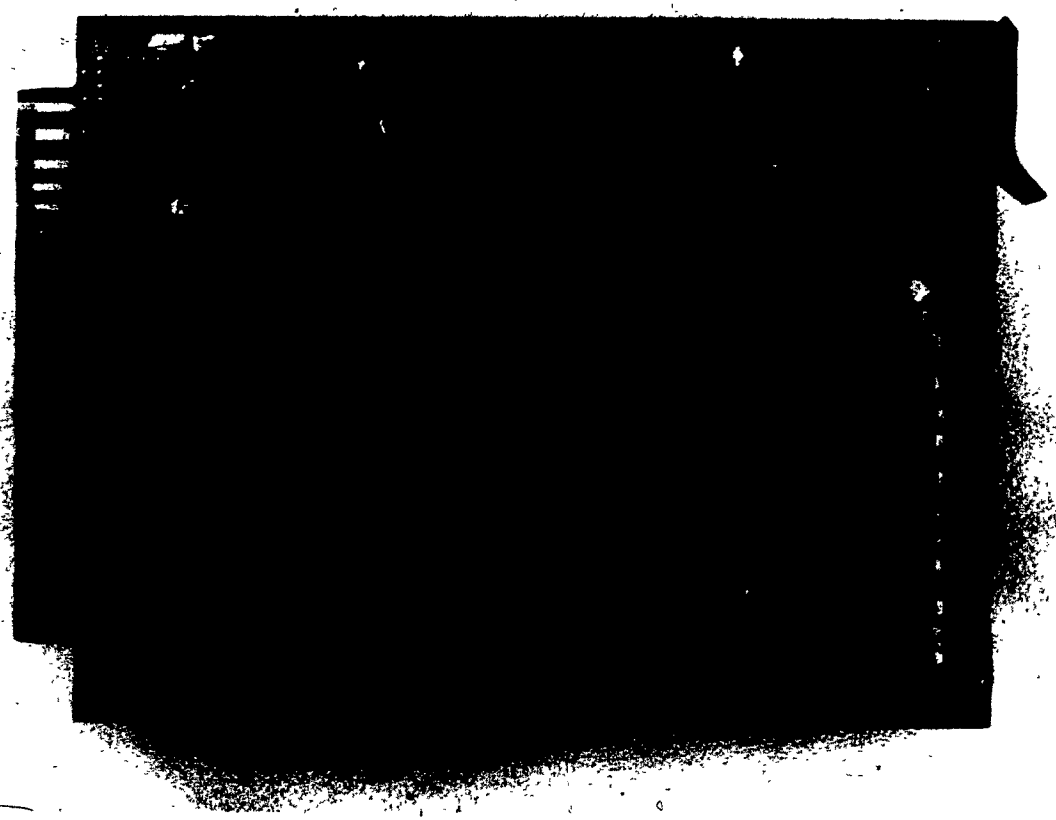

Figure III-7 Photograph of the Receiver Filter Bank and Mixer Board

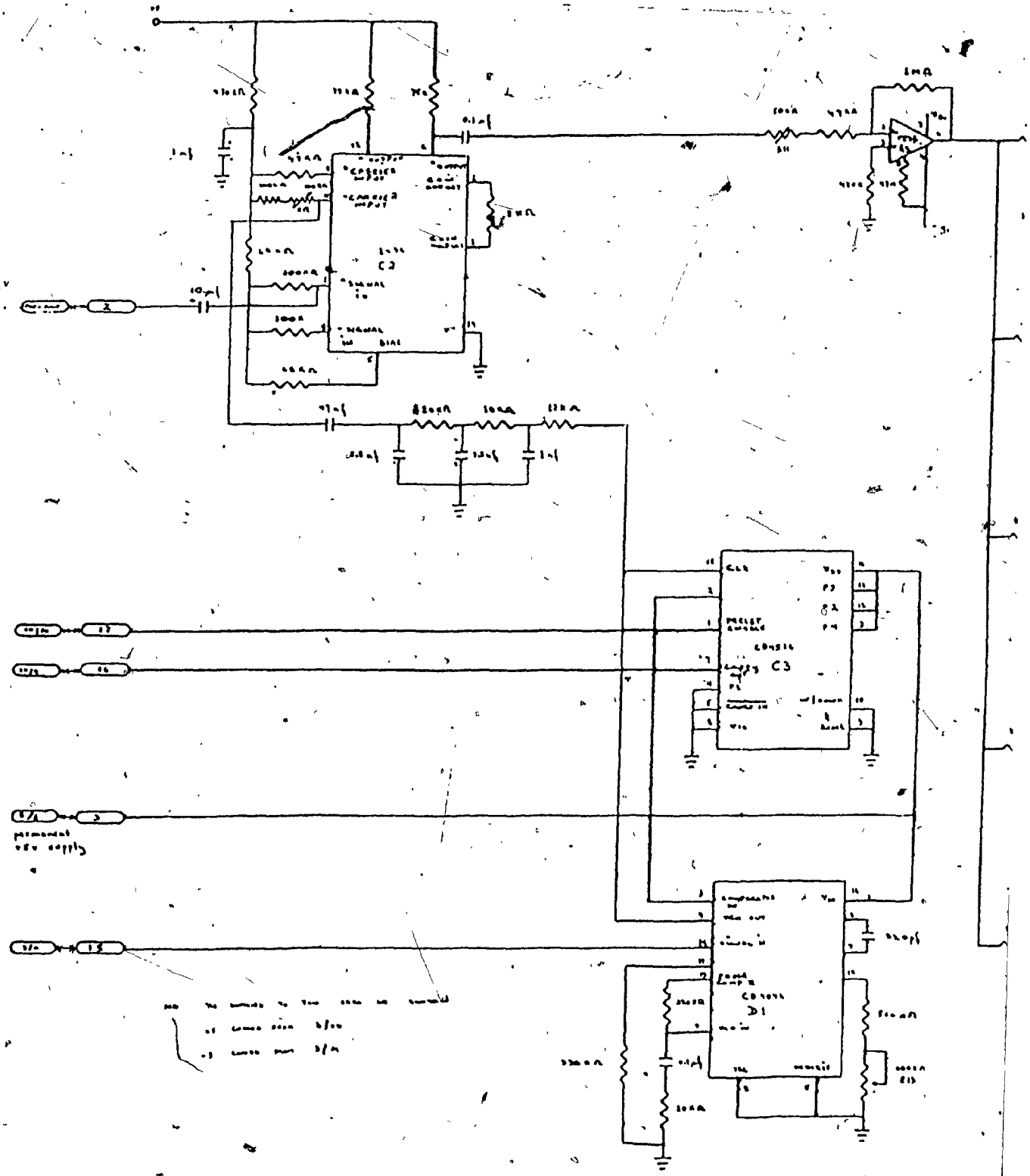

Figure III-8 Schematic diagram of rece
bank and mixer board

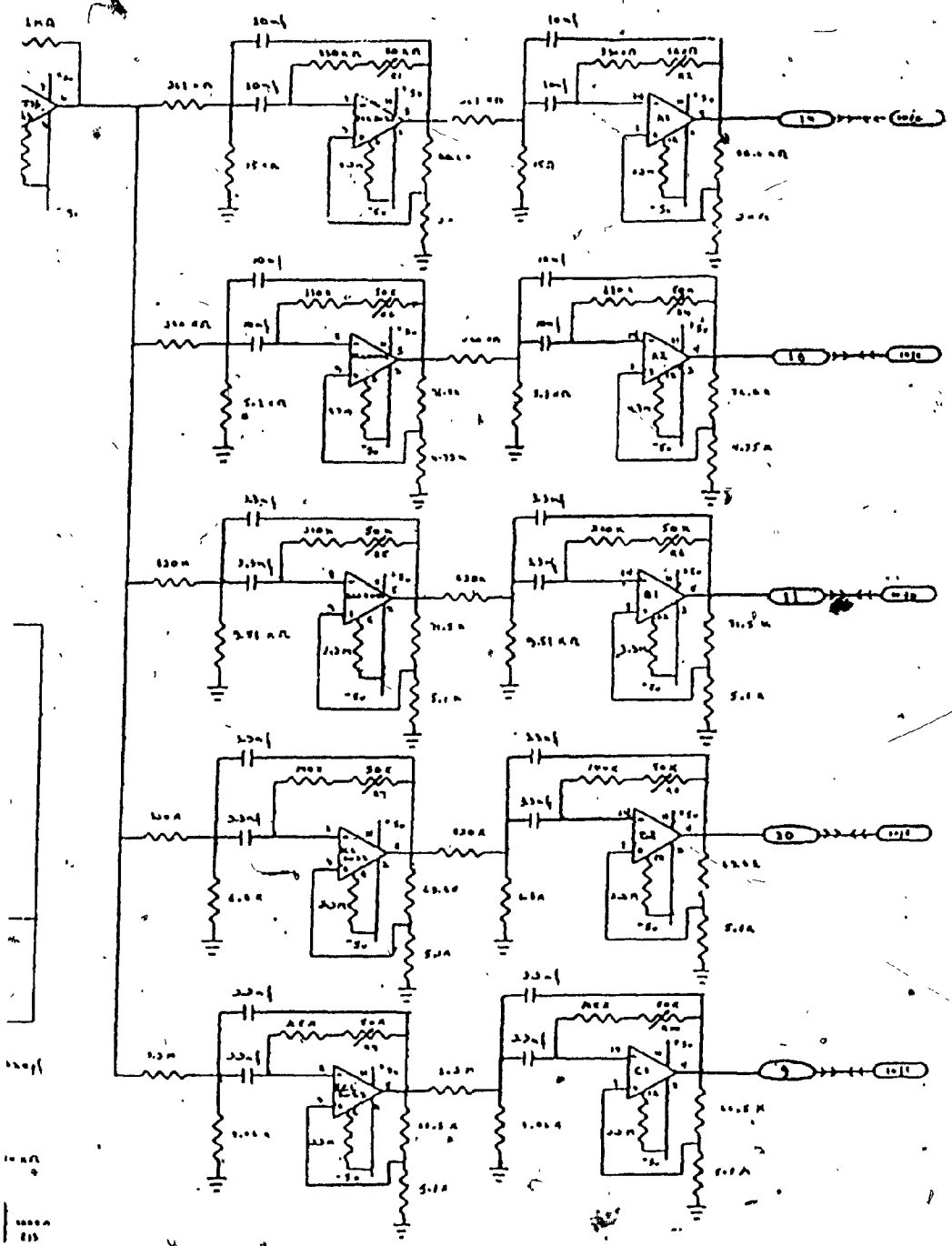

m of receiver filter
oard

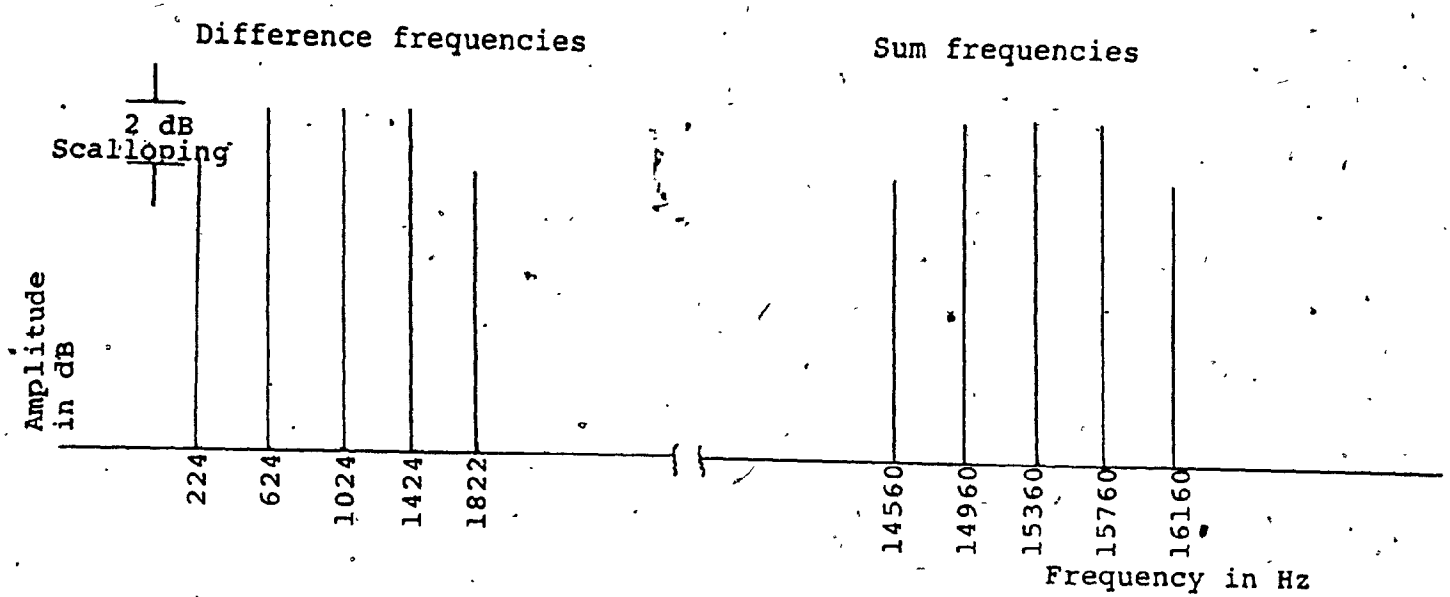

Figure III-9 Frequency spectrum at the output of the mixer

Each of the Deliyannis bandpass filters is centred on one of the difference frequencies.

There are several reasons for choosing the Deliyannis filter over any other type. First, the low frequencies to which the five tonals are translated render the design of passive filters impractical. Second, of the different types of active filters, the Deliyannis filter offers the most flexibility in light of the severe power constraint imposed on the command receiver design. It is a simple, inexpensive circuit, capable of a high yet stable Q factor. Moreover, it is relatively simple to design and easy to adjust.

A second order Deliyannis bandpass filter is shown in Figure III-10. Essentially, it is identical to a second order infinite-gain multiple feedback bandpass filter except that it has positive feedback provided by the voltage divider formed by R_b and R_a. The relevant equations needed for the design of this type of filter are given as, [5]

$$M = \frac{BQ}{2\theta - \sqrt{B}} \qquad \text{III-10}$$

$$R = \frac{1}{2\pi f_o c\sqrt{B}} \qquad \text{III-10}$$

$$G = \frac{Q(M+1)\sqrt{B}}{M} \qquad \text{III-12}$$

$$R_{11} = \frac{GR}{x} \qquad \text{III-13}$$

$$R_{22} = \frac{GR}{(G-x)} \qquad \text{III-14}$$

where B is a number arbitrarily chosen to be a perfect square for ease of calculations, Q is the quality factor, f_o is the centre frequency, and x is the desired gain at the centre frequency.. The design procedure can then be carried out according to the following steps:

(a) Select f_o and Q

(b) Choose a convenient value for C

(c) Choose B equal to a number that is a perfect square

(d) Calculate R from equation III-11

(e) Calculate M from equation III-10

(f) Select R_a=r and R_b=Mr such that their sum is greater than 20,000 ohms, but less than 200,000 ohms.

(g) Calculate G from equation III-12

(h) Calculate R_{11} and R_{22} from equations III-13 and III-14 respectively.

All five filters were designed by Dely, a computer program which follows the above algorithm. This program is given in Appendix III-1.

Filter adjustment is done in two stages. First, the Q is set by fixing R_a and R_b and then potentiometer R_x is adjusted to obtain the correct centre frequency. The gain remains very much constant and does not need to be adjusted.

The fourth order Deliyannis bandpass filters are designed by cascading two identical second order sections, each having a Q factor related to the overall Q factor of the filter by the expression,

$$Q_s = Q_f/(n\sqrt{2} - 1)^{\frac{1}{2}} \qquad \text{III-15}$$

where Q_s is the Q-factor of each second order section, Q_f is the Q-factor of the overall filter, and n is the number of second order sections.

Measurement of the frequency response of the Deliyannis BPF centred at 1024 Hz is given in Table III-2 and graphed in Figure III-11. The results are representative of all the filters. Each filter has at least 24 dB of attenuation at the geometric mean between the centre frequencies of adjacent filters.

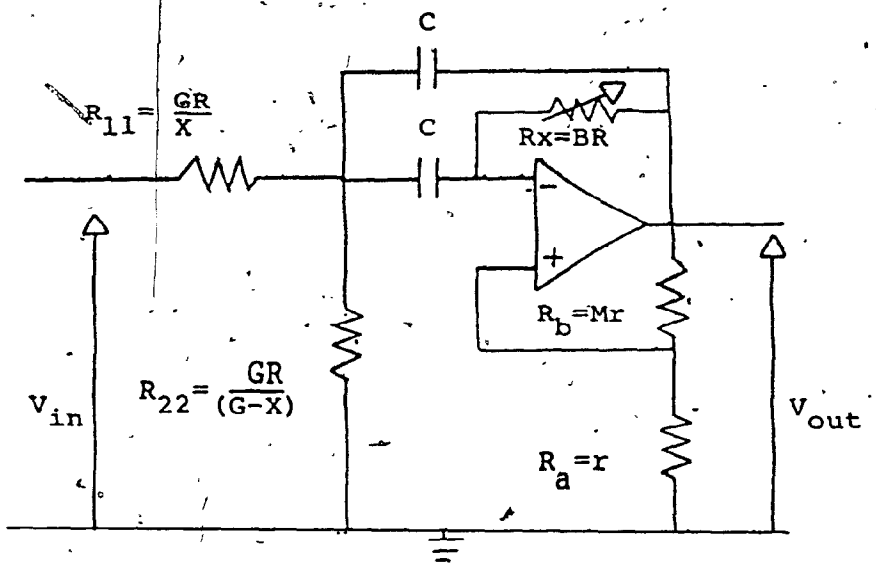

Figure III-10 Second order Deliyannis bandpass filter

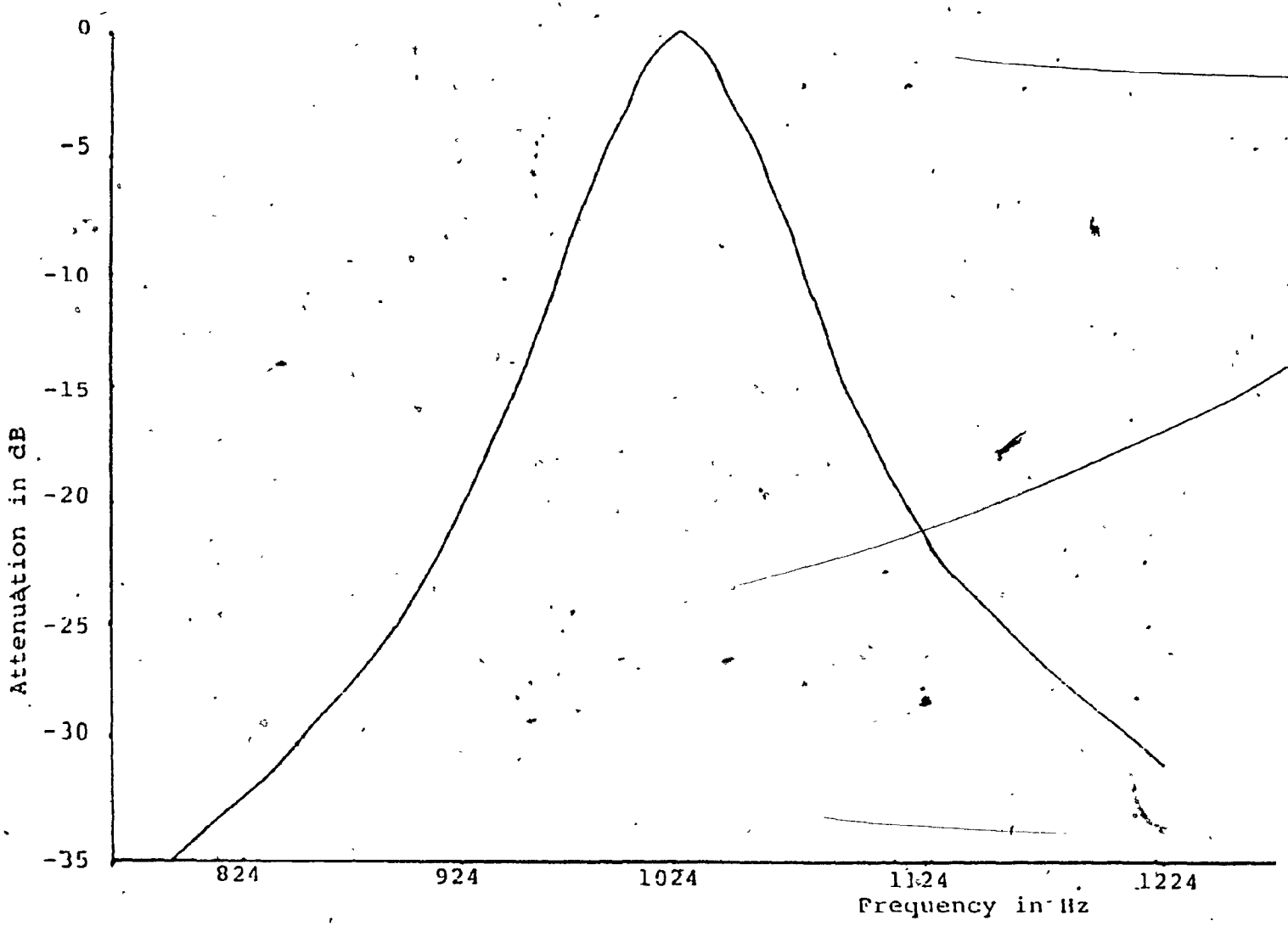

Figure III-11 Frequency response of Deliyannis bandpass filter centred on 1024 Hz

Frequency in Hz	Attenuation in dB
600	-45
700	-43
800	-36
900	-25
1003	-3
1024	0
1044	-3
1100	-17
1207	-29
1300	-34.5
1400	-40

Table III-2 Frequency response of fourth order Deliyannis bandpass filter centred on 1024 Hz

3. Precision Rectifiers and A/D Converter Board

A photograph of the board is shown in Figure III-12 while the schematic diagram is shown in Figure III-13. The board contains five amplifiers each feeding a precision rectifier-filter which is connected to an A/D converter that has a built-in multiplexer. The board also has combinational logic to provide timing control signals for the A/D converter.

The amplifiers are all identical. They are each capable

of giving a variable gain from 18 dB to 22.5 dB. The individual gains are adjusted by potentiometers R1 through R5.

The precision rectifier-filters are also identical. A typical one is shown in Figure III-14 and the output waveforms at various points of that circuit are given in Figure III-15. Amplifier A1 is an inverting rectifier. If capacitor C is removed from the circuit, A2 will act as an inverting summing mixer, adding together signals E_1 and E_{in} in the ratio of 2:1. During the negative half cycle of E_{in}, E_1 is zero volts and therefore E_o is equal to $-E_{in}$. When the positive half cycle of E_{in} occurs $E_o=E_1-E_{in}=E_{in}$ Thus E_o is a full wave rectified sinusoid. The inclusion of capacitor C in Figure III-14, results in the rectified sinusoid being smoothed, producing a dc signal.

The outputs of the five rectifiers are multiplexed and digitized by the A/D converter. The relationship among some timing pulses used by the A/D converter and produced by the combinational logic circuitry is shown in Figure III-16.

V_{cc} is 125 ms long and V_{ref} occupies the last 15.625 ms time slot of V_{cc}. During this period, 8192 clock pulses are available for the microcomputer to carry out the instructions necessary to read the A/D converter channels and store the data. The microcomputer requires 8 clock pulses to do an instruction. The three address lines needed to multiplex the five A/D converter channels are connected to the three least significant bits of the microcomputer bus. During the time when the reference voltage, V_{ref}, is high, the

microcomputer selects the A/D converter which it treats as an I/O device. It then latches the channel address and the A/D converter begins conversion. The microcomputer, then, monitors flag $\overline{EF4}$. When this flag goes high the microcomputer enables the A/D converter and reads the data on the relevant channels. Eight channels are processed in this way but three of them are inactive and so their outputs are always zero.

Command Receiver Power Supplies

Since the command receiver operates with a 50% duty cycle to conserve power, its positive and negative supplies are switched on and off at the same rate. The circuitry used to provide this switching for the positive and negative supplies is shown in Figure III-17 and III-18 respectively. The input pulse for both circuits are 125 ms long and they are related to the output pulses as indicated in the figures.

If it is necessary to return to a steady supply for the command receiver, inverter D_3 may be removed without affecting circuit operation. P_{in} 2 of the edge connector can then be connected directly to D1/1.

It should be mentioned that the phase lock loop on the filter bank and mixer board, is run off steady supplies because switching results in frequency instability of the 7168 Hz reference signal, that it produces.

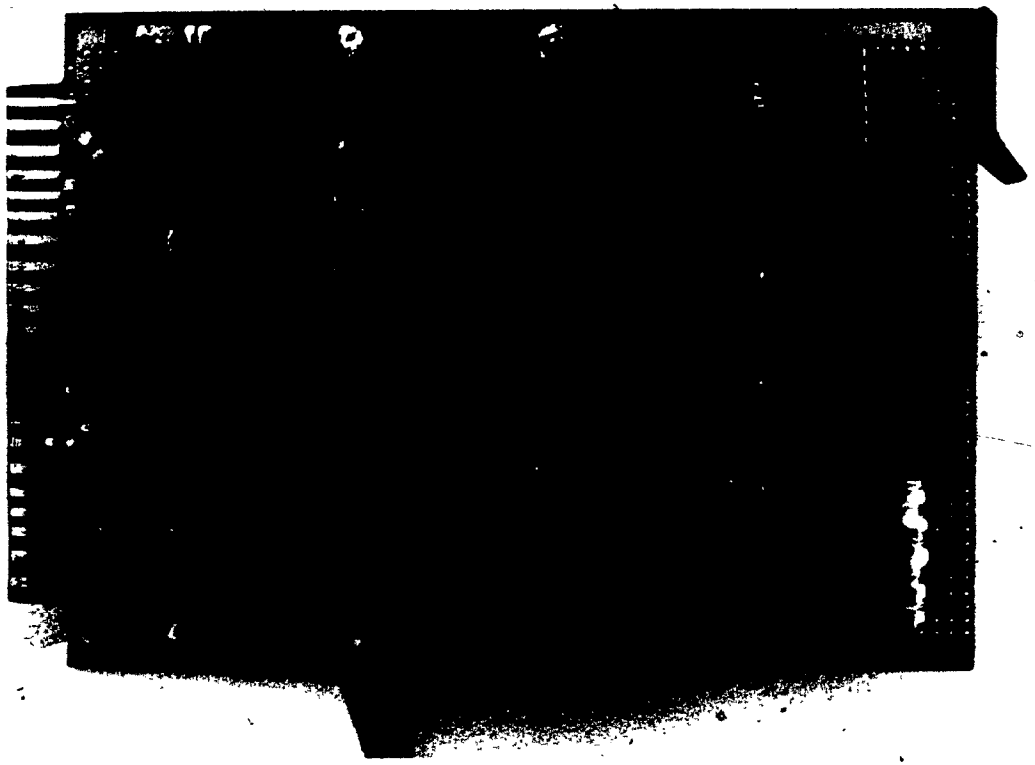

Figure III-12 Photograph of precision rectifier and A/D converter board

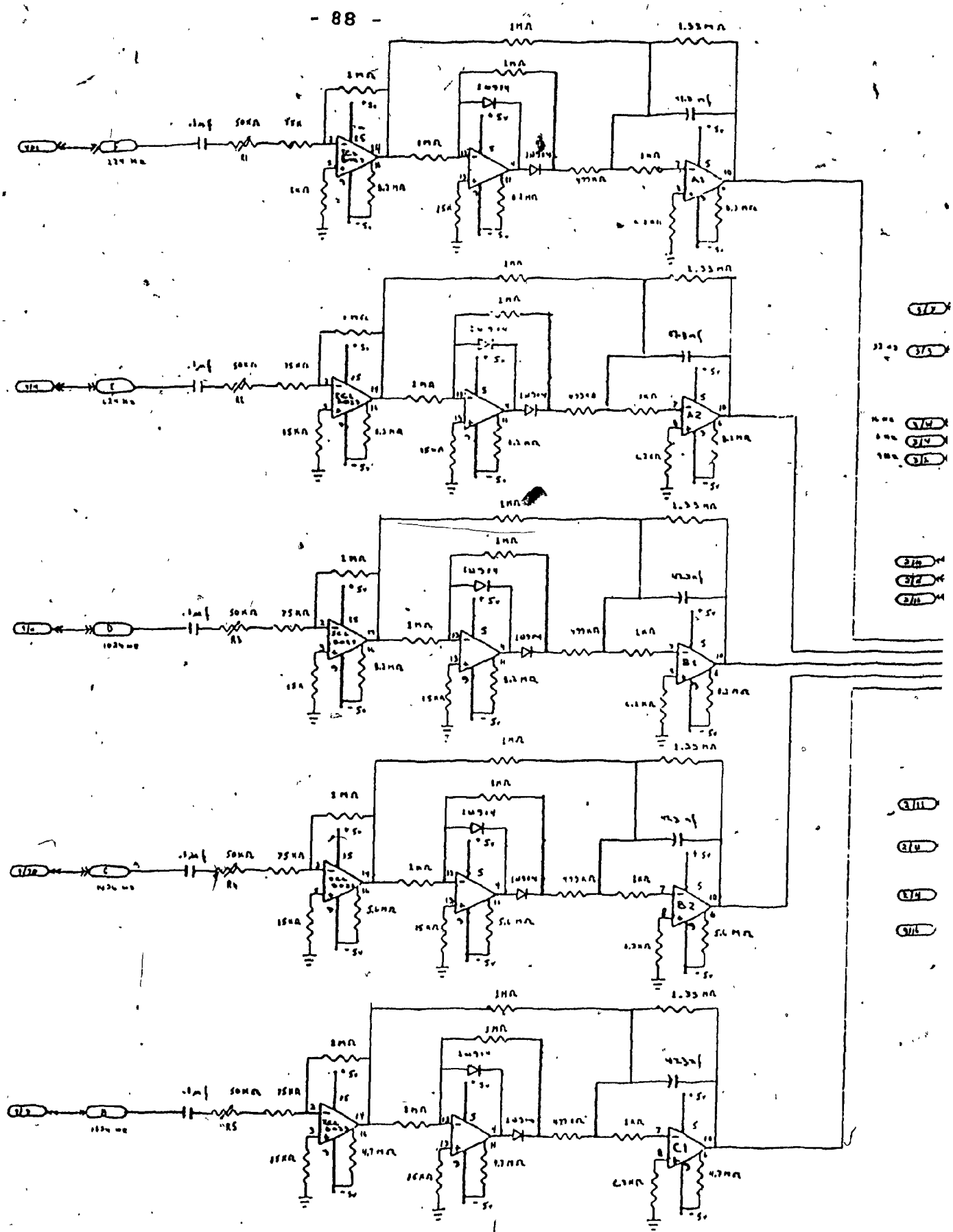

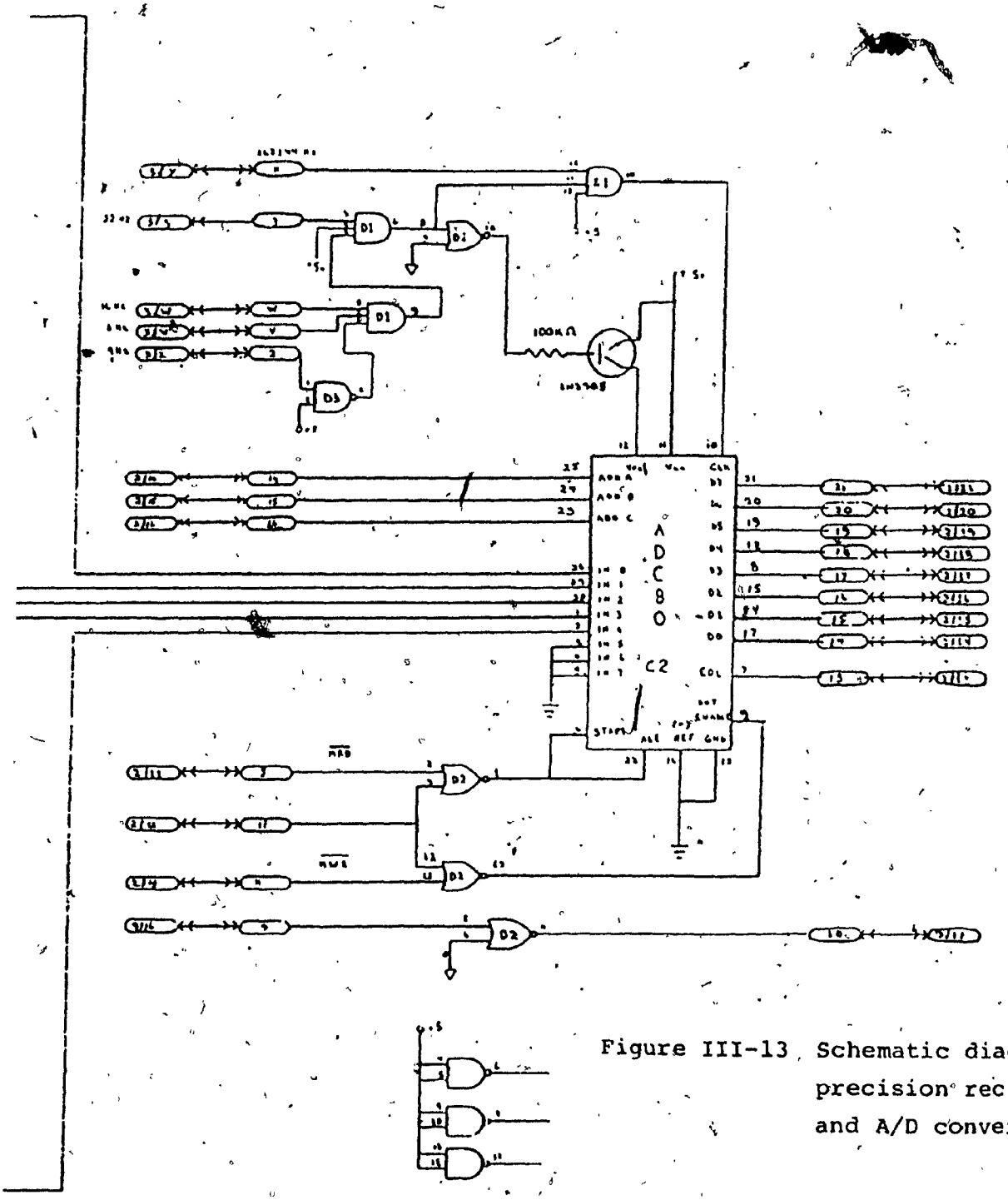

Figure III-13 Schematic diagram of precision rectifier and A/D converter board

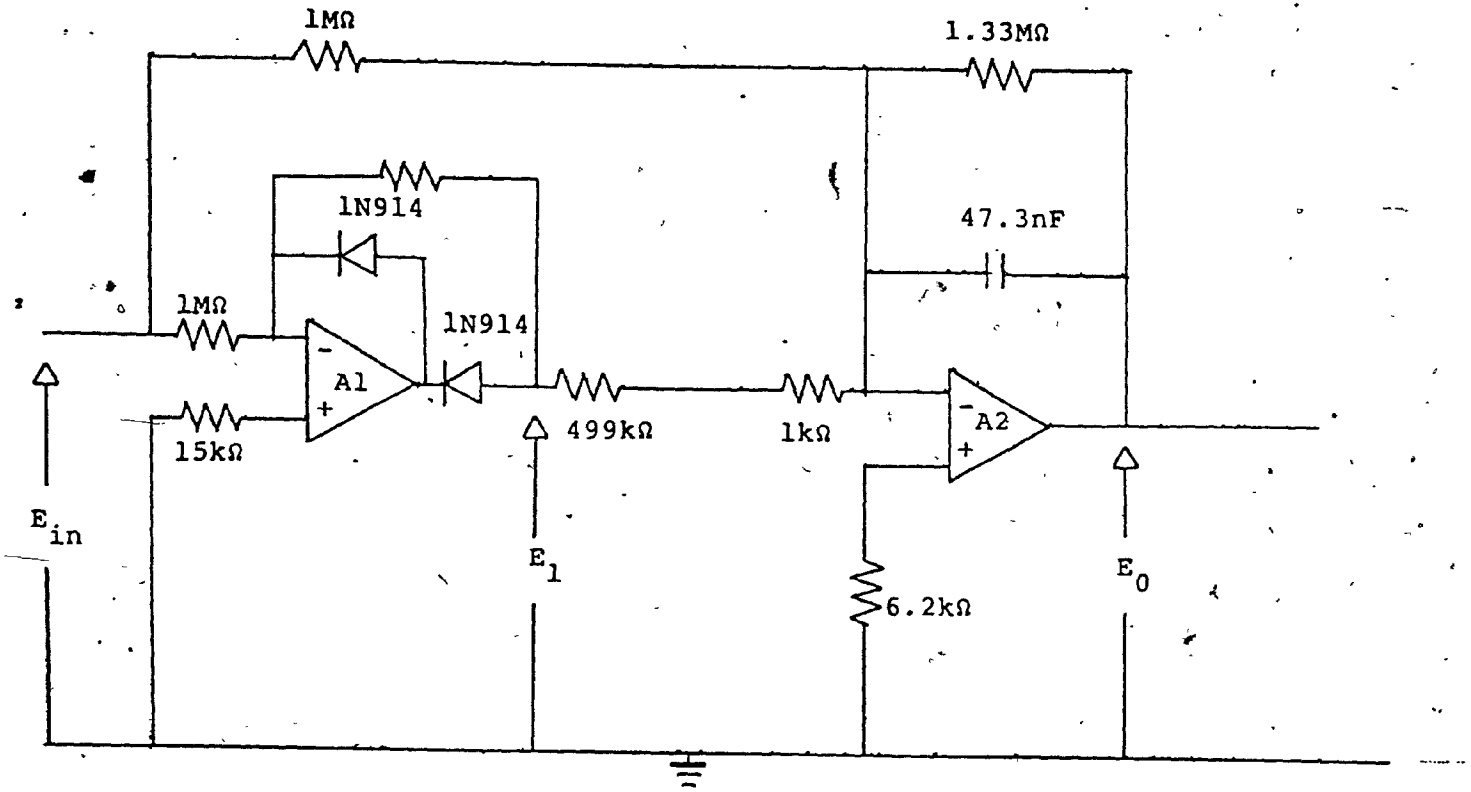

Figure III-14 Full wave rectifier-filter

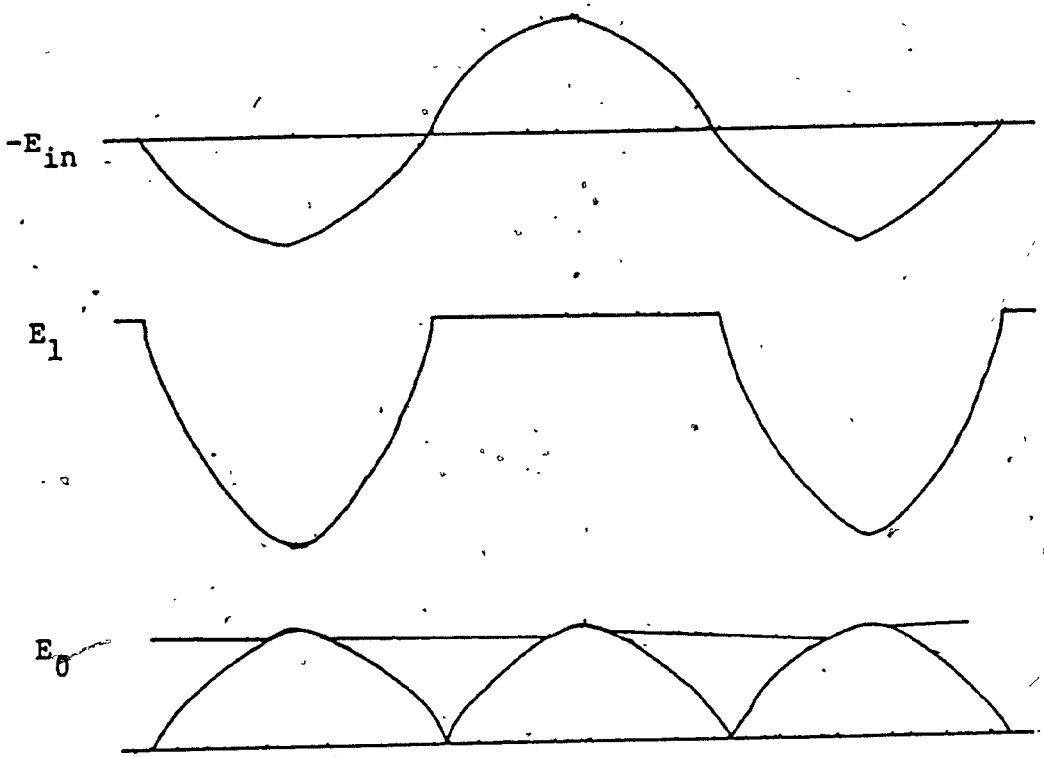

Figure III-15 Waveforms at various points in precision rectifier-filter circuit

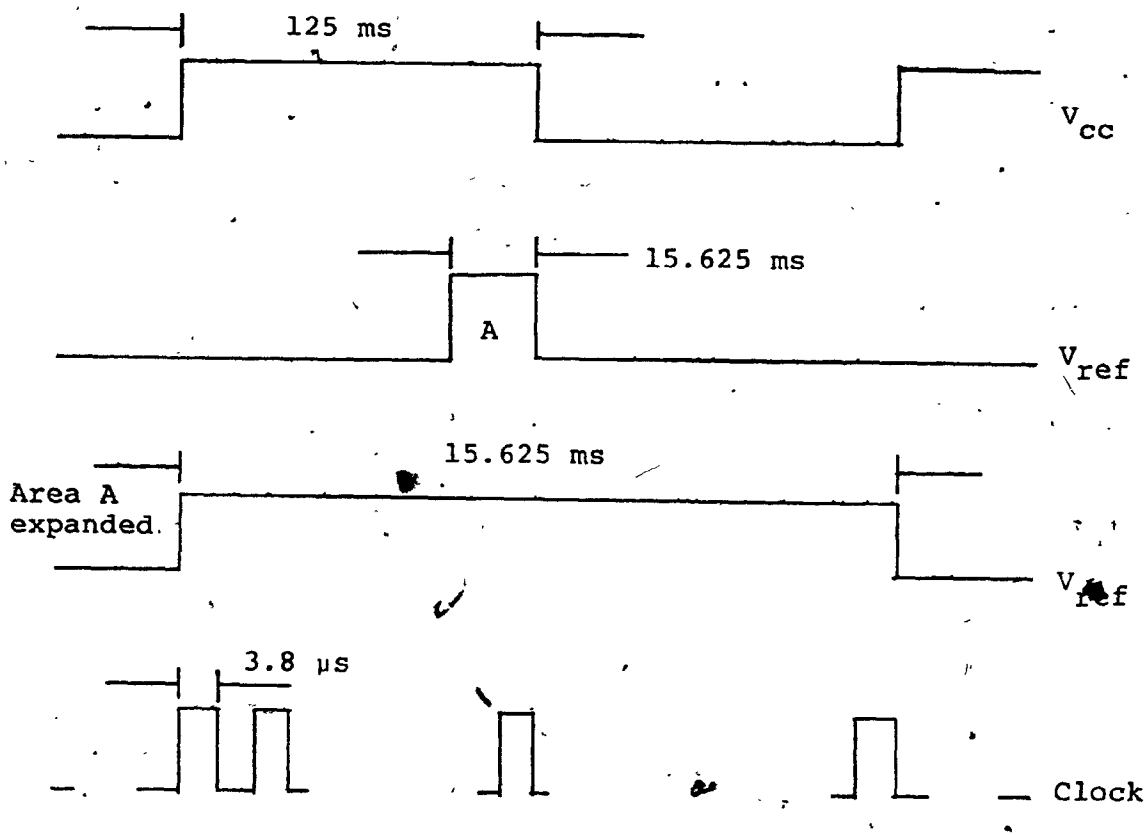

Figure III-16 Partial timing diagram of A/D converter

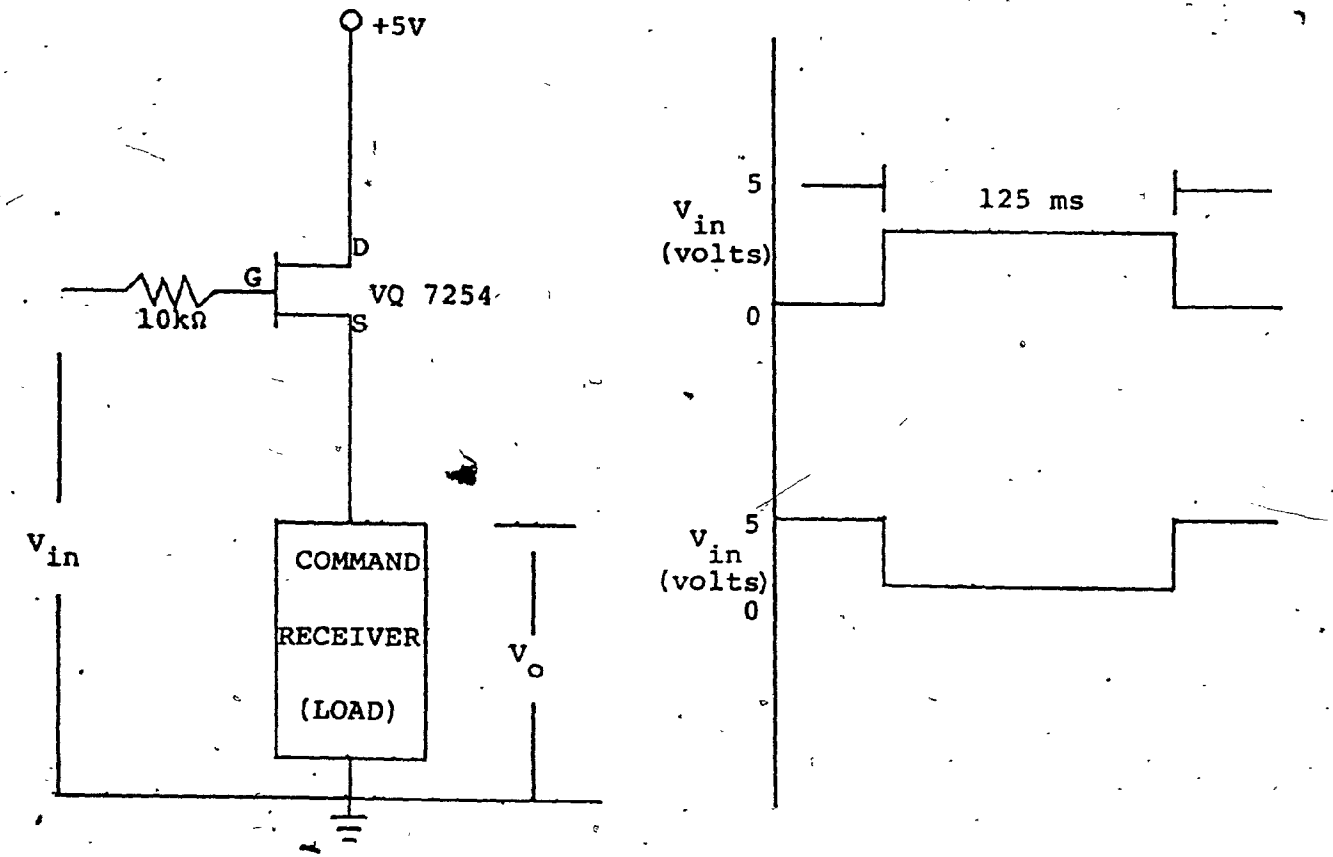

Figure III-17 Circuitry to provide 50% duty cycle positive supply for comnand receiver

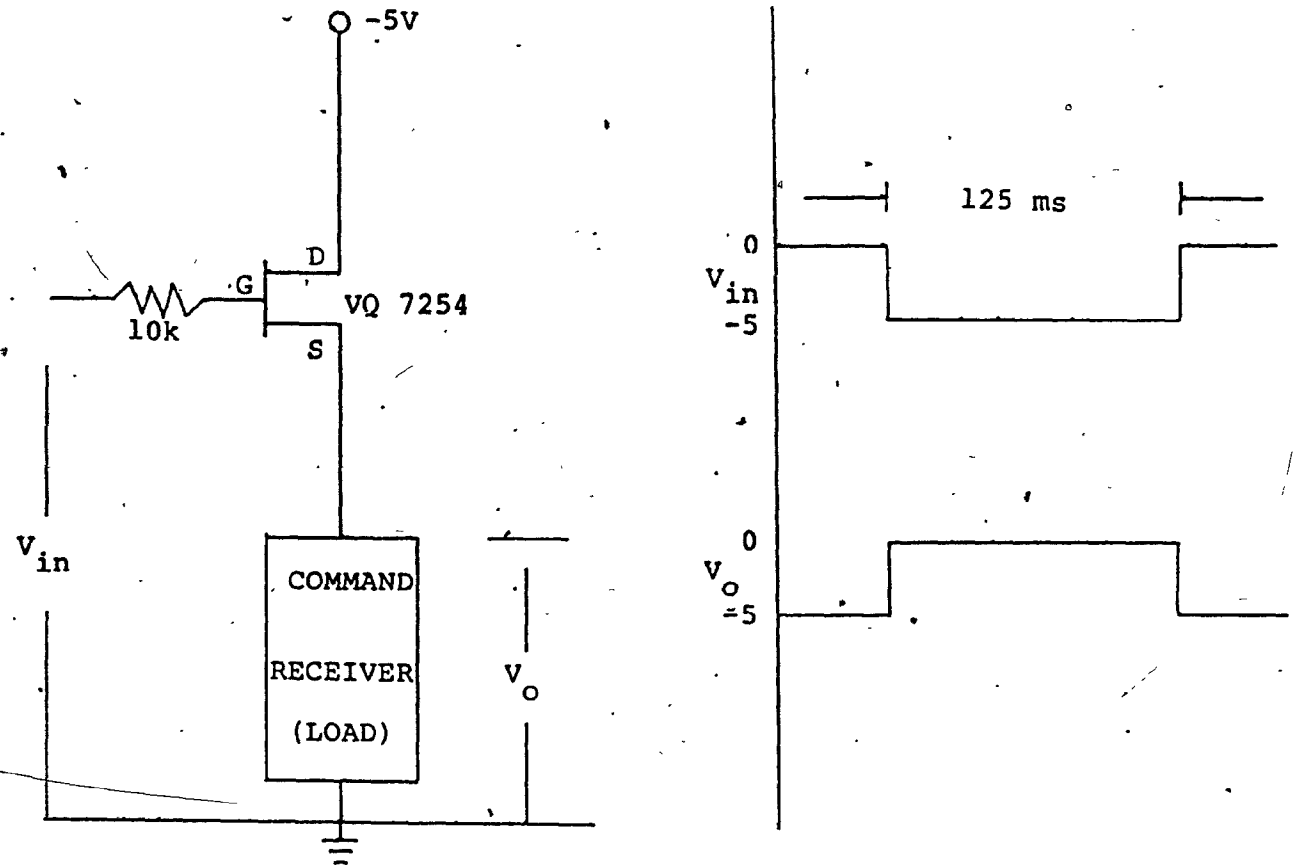

Figure III-18 Circuitry to provide 50% duty cycle negative supply for command receiver

REFERENCES

1. Johnson, D.E., Introduction to Filter Theory, Prentice Hall, Englewood Cliffs, New Jersey, 1976.

2. Jung, W.G., I.C. Op-amp Cookbook, H.W. Sams, Indianapolis, 1977.

3. Lancaster, Donald E., CMOS Cookbook, H.W. Sams, Indianapolis, 1977.

4. Schwartz, M., W.R. Bennett, S. Stein, Communication Systems and Techniques, McGraw Hill, New York, 1966.

5. Tedeschi, Frank P., The Active Filter Handbook, Tab Books, Pennsylvania, 1977.

6. Weinberg, L., Network Analysis and Synthesis, McGraw Hill, New York, 1962.

7. Wozencraft, John M. and I.M. Jacobs, Principles of Communication Engineering, John Wiley, New York, 1965.

8. Morgera, S.D., "Optimum Underwater Acoustic Techniques", prepared for Canadian Department of Environment, Oceans and Fisheries, Contract 07SC.kF806-8.E330, 28th Feb. 1979.

9. Morgera, S.D., "A Conceptual Design of an Underwater Acoustic Telemetry System, Phase II Study", prepared for Canadian Environment, Oceans and Fisheries, February 20th, 1980.

10. Morgera, S.D., "Command Receiver Noise Normalization Technique", prepared for Canadian Department of Environment, Oceans and Fisheries, contract OSC79-00268, October 21st, 1980.

11. Nuttall, A.H., "Operating Characteristics for Detection of Fading Signal in M Alternative Locations with D-fold Divserity", NUSC/NLL TR4793, 20th August 1974.

CHAPTER IV

SIGNAL PROCESSING: GAUGE INTERFACE, FREQUENCY SYNTHESIZER AND TRANSMITTER SUBSYSTEMS

A. INTRODUCTION

This chapter describes the manner in which tidal data is collected, stored and recalled for transmission following the recognition of an interrogation request by the command receiver. The subsystems responsible for performing these functions are the guage interface unit, the frequency synthesizer, and the transmitter. A block schematic diagram showing their interconnection is discussed.

The functions and design of the guage interface unit are outlined. The design and operation of the frequency synthesizer are discussed. The synthesizer, based on the accumulator-overflow technique of frequency synthesis, is examined, first as a single tone synthesizer and then as a multi-tone synthesizer. Next the transmitter, consisting of a balanced modulator, a triangular windowing unit and a power amplifier, is discussed. Finally, some typical results of the signal processing performed by the frequency synthesizer and the transmitter are highlighted and analysed.

B. OPERATION OF GUAGE INTERFACE, FREQUENCY SYNTHESIZER AND TRANSMITTER SUBSYSTEMS

Figure IV-1 is a block schematic diagram of the guage interface, frequency synthesizer and transmitter subsystems.

Serial data from the tide gauge is conditioned and stored as 16-bit words in the data storage memory of the microcomputer. When the threshold of the command receiver is exceeded, the microcomputer fetches the data from memory, starting with the most recent word, encodes it, and passes it on to the frequency synthesizer. The synthesizer converts each 16-bit word into forty four tones in the frequency range [-1024, +1024] Hz. The tones then modulates a 8192 Hz carrier and the resulting band of frequencies extending from 7168 Hz to 9212 Hz, is amplified and used to excite an electro-mechanical transducer.

C. GAUGE INTERFACE UNIT

The gauge interface unit consists of one card, the gauge interface card. It is a specialized digital hardware module which works in conjunction with Aanderaa tide guages, TG1A, TG2A and a modified version of TG3A. It is under the control of the microcomputer. It is important to note that with a suitable change of interface, many other types of oceanographic parameter sensing instruments may serve as input to the acoustic telemetry system.

A functional block schematic diagram of the gauge

interface card is shown in Figure IV-2 and a detailed schematic is given in Figure IV-3.

1. Functions of Gauge Interface Unit

The functions of the gauge interface unit are:

(i) To extract data from the tide gauge at the appropriate time.

(ii) To condition and amplify the pressure estimates from the tide gauge.

(iii) To perform parallel to serial conversion of the data.

(iv) To inform the microcomputer when the data is ready for storage in memory.

2. Operation of Gauge Interface Unit

The data produced by the Aanderaa tide gauge is a 41 bit serial word, of which the least significant 20 bits (A_{19}-A_0), reflect a pressure measurement. The gauge interface unit selects bits A_{17} through A_2 as a representative 16-bit data word and stores it in data memory. The truncation of the two LSB's results in a small loss of resolution in the data word. Bit A_{19} is always zero and the omission of A_{18} causes a range folding which, however, does not introduce any ambiguity for this application.

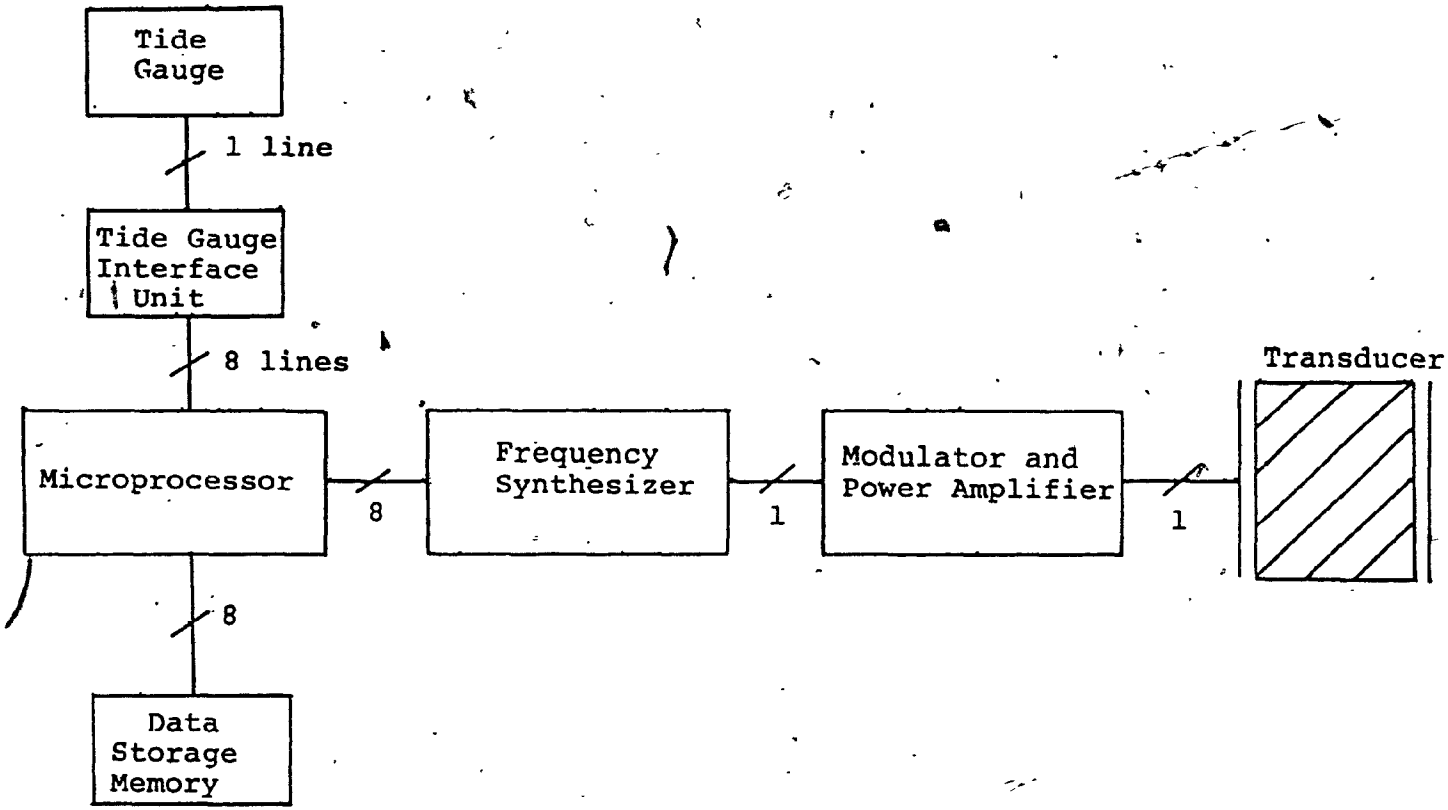

Figure IV-1 Block schematic diagram of gauge interface, frequency synthesizer and transmitter subsystems

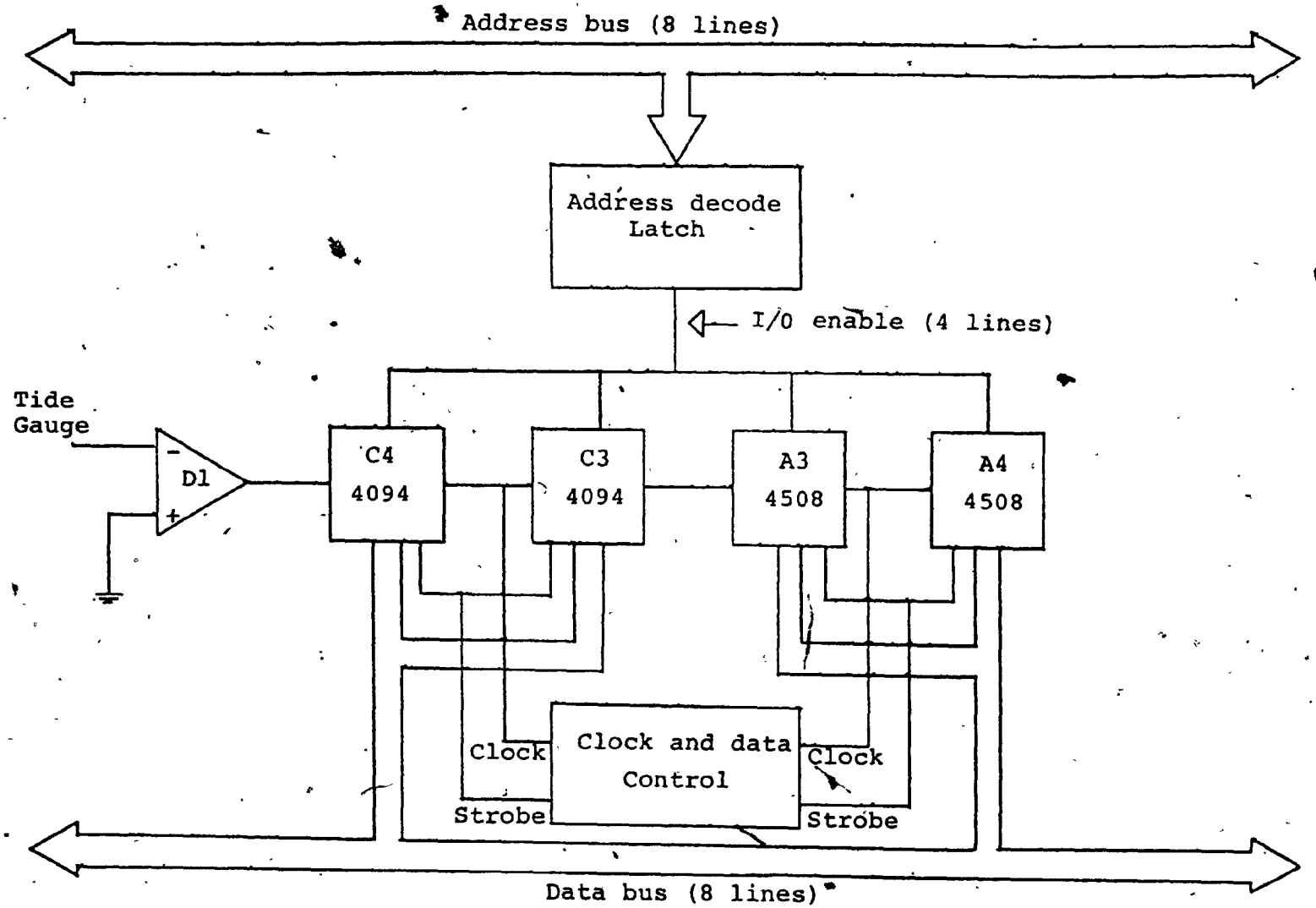

Figure IV-2 Functional block diagram of Aanderaa tide gauge interface

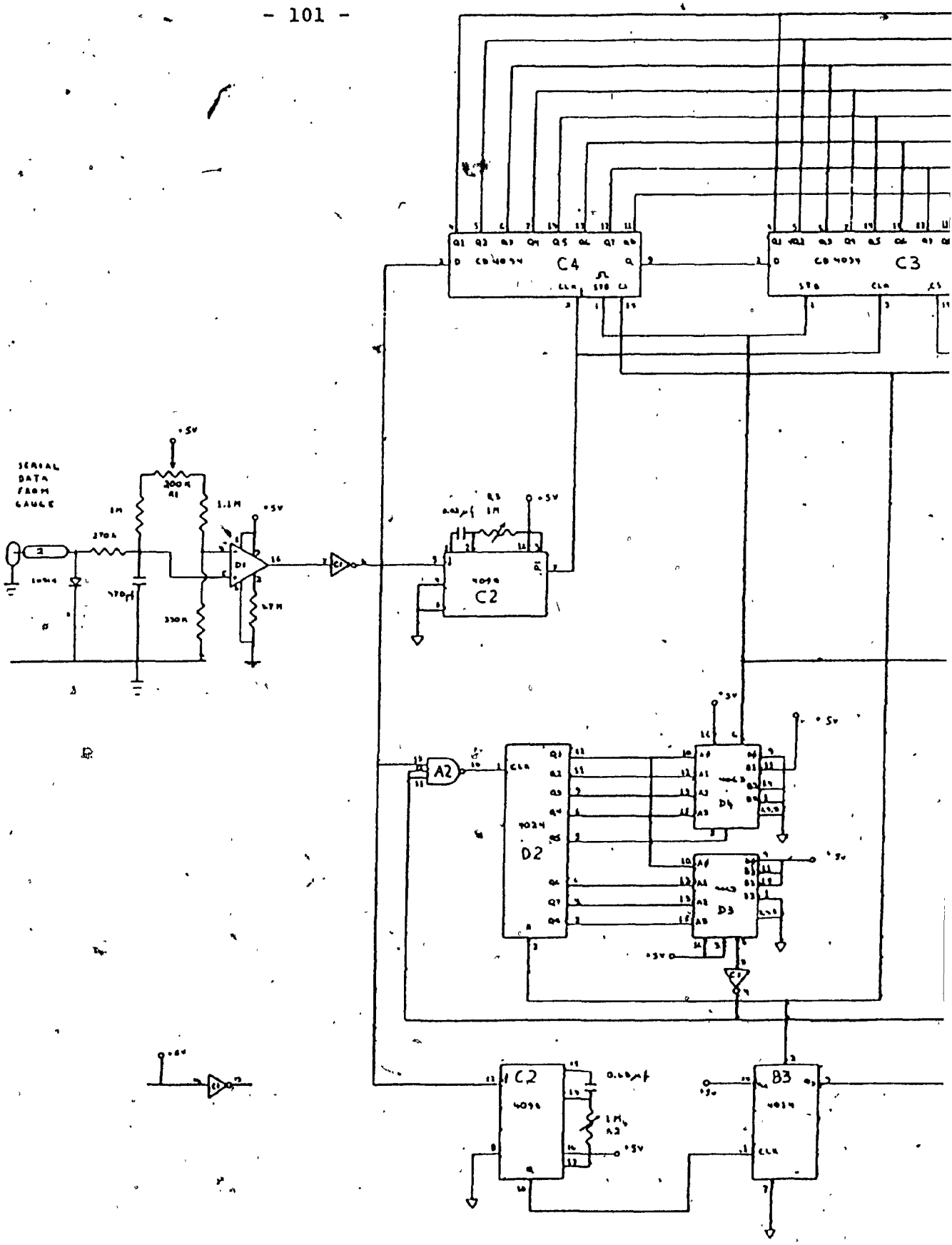
SERIAL DATA FROM GAUGE
+5V
300K
1M
1.1M
270Ω
330Ω
4.7K
C4
C3
C2
A2
D2
D4
D3
B3
1M

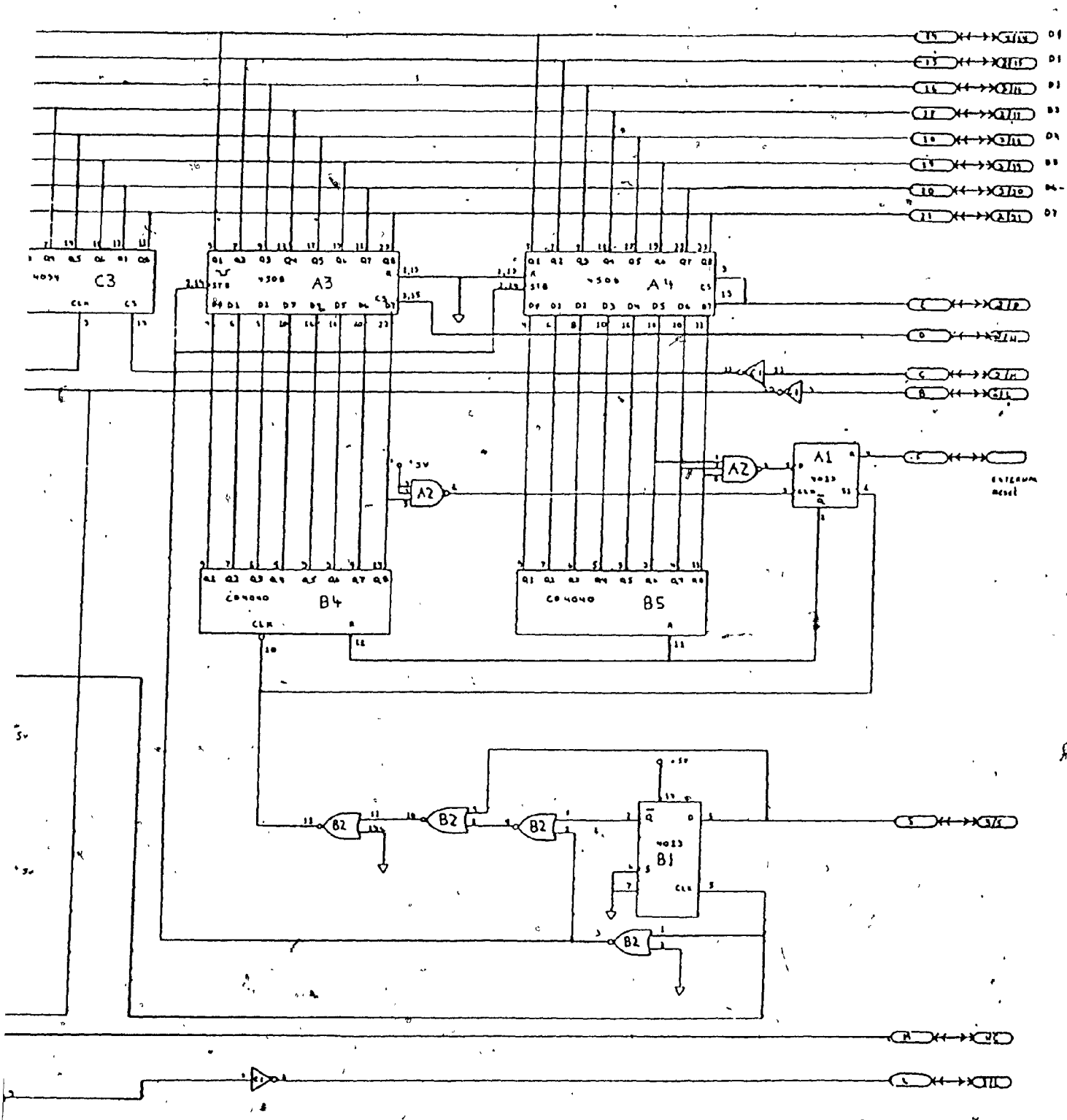

Figure IV-3 Schematic diagram of tide gauge interface card

The gauge interface has its own relative time clock which can be reset to zero at some reference time. Time from this clock is used to tag every third data word from the Aanderaa gauge. The time is represented as a 16-bit natural number indicative of the time that has elapsed since the clock was reset.

The operation of the gauge interface unit can be explained with reference to Figure IV-3. A low power operational amplifier, D1, is used to condition and amplify the pressure data from the gauge. The input to the op-amp is a series of pulses of amplitude 0 to 0.5 volts. The output is a series of pulses having amplitude 0 to 5 volts, in which a digital 1 is represented by a pulse 30 ms long and a 0 by a pulse 90 ms long. The period of each pulse is 160 ms.

Figure IV-4 shows how the 30 ms and 90 ms pulses are stored as digital 1's and 0's, respectively, in shift register A, formed by two 4094's connected in series. The negative edge of each bit of data triggers monostable, C2/5, to produce a pulse 60 ms long. The positive edge of this pulse then clocks the gauge data, available at C1/6, into shift register A.

Figure IV-5 illustrates how the data stored in the shift register is transferred to the microcomputer data memory. The incoming bits of data are counted by counter D2 which feds a comparator D4. The comparator produces a high output when the 18th bit of data is received. It is

reset on the 19th bit and the narrow pulse then produced is used to strobe bits A_{18} through A_2 into shift register A.

When the 41st bit of data is received, a comparator C3 produces a high output which is used to disable the clock to the counter, D2. The positive edge of each data bit triggers a monostable, C2/10, which has a period longer than 160 ms. This monostable gives four pulses for each 41 data bits received as shown in Figure IV-5. Counter B3, counts these pulses and on the fourth pulse produces a high level which is inverted at C1/2, and tied to the microcompressor flag $\overline{EF1}$. When this flag goes low, the microcomputer enables shift register A and reads the data stored there. It then resets counters D2 and B3.

If the data requires a time tag, the microcomputer will enable shift register B, formed by chips A3 and A4, and will read the appropriate time data. The time data is advanced by a count of 1 every 30 s, but is only written into shift register B, after every third data word from the gauge is written into shift register A. The time data is produced by the gauge interface relative time clock which is formed by chips A1, A2, B1, B2, B4 and B5. The time clock has an external reset so that it can be stopped and restarted at any desired time.

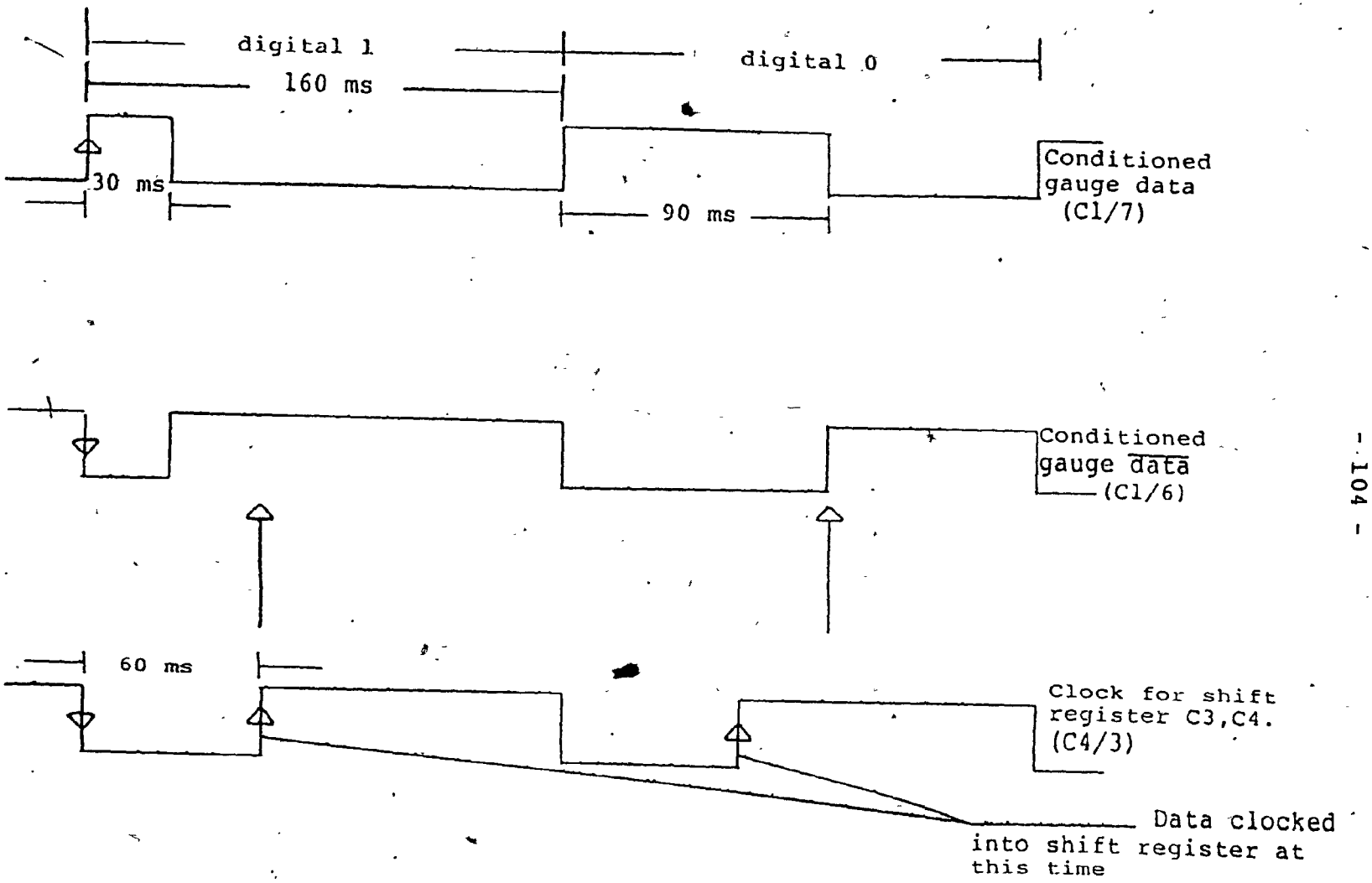

Figure IV-4 Timing diagram to illustrate how Aanderaa gauge data is processed into digital words for microcomputer storage

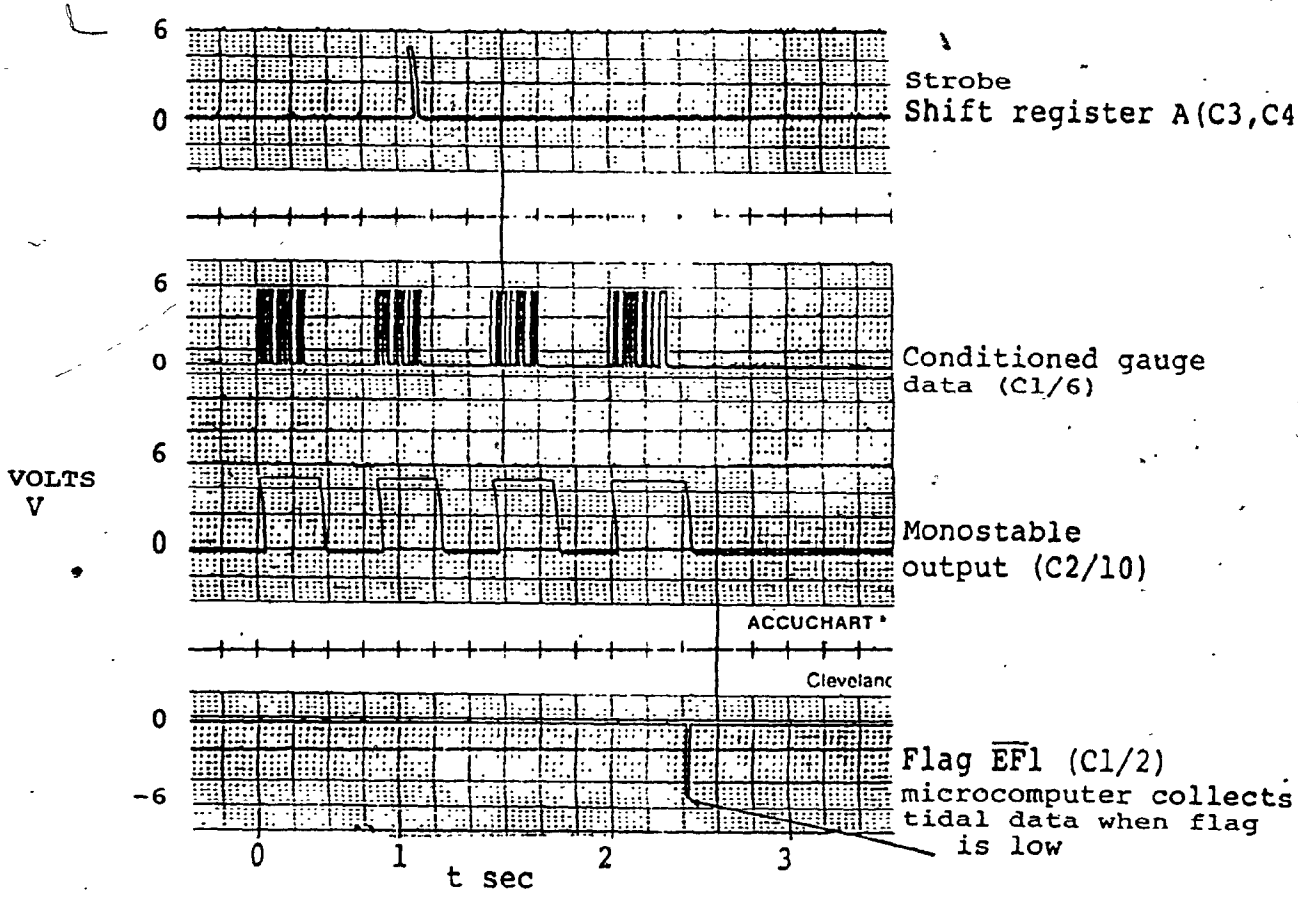

Figure IV-5 Timing relationship to illustrate how Aandera tide gauge data is collected for microcomputer storage

D. FREQUENCY SYNTHESIZER

The frequency synthesizer consists of the following cards:

(a) Tone address generator card

(b) L and ϕ look-up accumulate card

(c) Sine look-up accumulate card

(d) Cosine lookup accumulate card

It is that portion of the telemetry system bottom unit responsible for converting the digital data collected from the gauge into tones. The design of the synthesizer was based on the type of modulation scheme chosen and also on the method of frequency synthesis selected. These will be discussed.

1. Modulation Parameters

Morgera [10] has examined several modulation schemes for underwater acoustic telemetry system design and has concluded that MFSK with D-fold diversity is a cheap efficient and reliable modulation scheme for effective underwater communication. In MFSK modulation, one of M equiprobable equal strength alternatives is transmitted via explicit D-fold diversity, each diversity channel being subject to independent Rayleigh fading.

The time duration and frequency bandwidth of each

signaling element are denoted by T_p and ω_p respectively. In order that the received pulse (signaling element) not be distorted,

$$T_p < \frac{1}{B}, \quad \omega_p < \frac{1}{L} \qquad \text{IV-1}$$

where B and L are the frequency spread and the multipath spread of the medium, respectively.

To prevent time and frequency overlap between pulses at the receiver, the following inequalities must be observed,

$$\Delta t > L \qquad \text{IV-2}$$

$$\Delta f > B \qquad \text{IV-3}$$

where Δt is the transmitted time separation between pulses (i.e. the transmitter dead time), and Δf is the frequency separation between a pair of pulses. All intersymbol interference between the MD possible pulses that can be transmitted in an MFSK scheme will be avoided if either IV-2 or IV-3 is satisfied for all the pairing of the MD pulses possible. When two pulses are transmitted statistical dependence in time and frequency can be avoided if,

$$\Delta t > \frac{1}{B_{min}} \qquad \text{IV-4}$$

$$\Delta f > \frac{1}{L_{min}} \qquad \text{IV-5}$$

where B_{min} and L_{min} are the minimum frequency spread and the minimum time spread of the scattered paths of significant strength, respectively.

The choice of M and D in an M-ary modulation scheme can be optimized if the signal-to-noise ratio $\bar{E}_T/N_o$ and the probability of error, P_e, are specified [11]. The bandwidth needed at the receiver for the reception of a subset of the MD possible pulses can be determined from a consideration of Figure IV.6. Suppose the transmission of one M-ary character is accomplished by sending D pulses simultaneously. Let the centre frequencies of the D pulses be such that

$$f_{m2}-f_{m1}=f_{m3}-f_{m2} = \ldots f_{MD}-f_{M,D-1}=b, \quad 1\leq m\leq M \qquad \text{IV-6}$$

Also, let the separation of frequencies in any diversity group be equal:

$$f_{2d}-f_{1d}=f_{3d}-f_{2d} = \ldots f_{MD}-f_{M,D-1} = a \quad 1\leq d\leq D \qquad \text{IV-7}$$

Define the overall bandwidth of the MD possible pulses as ω_1. Now, in order to satisfy IV-2,

$$b-\omega_p > \frac{1}{L_{min}} . \qquad \text{IV-8}$$

And to satisfy IV-3

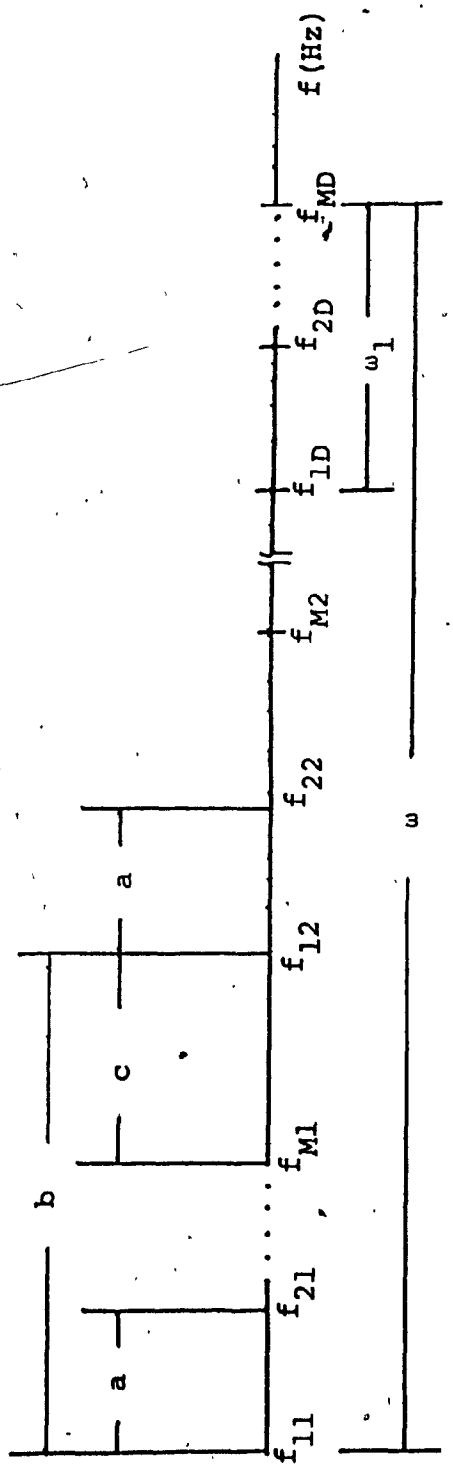

Figure IV-6 Transmission of frequency in M-ary FSK

$$a - \omega_p > B \quad \text{and} \quad c - \omega_p > B \qquad \text{IV-9}$$

However, since $b=(M-1)a+c$, equations IV-8 and IV-9 can be combined to give,

$$b \geq \max \{(\omega_p + \frac{1}{L_{min}}), M(\omega_p+B)\} \qquad \text{IV-10}$$

The overall bandwidth of the pulses at the receiver is

$$\omega' = (f_{MD}-f_{11})+\omega_p+ B = (D-1)b+(M-1)a+\omega_p+B$$

$$\geq \max\{((D-1)(\omega_p+\frac{1}{L_{min}})+M(\omega_p+B)), DM(\omega_p+B)\} \qquad \text{IV-11}$$

The actual frequency extent used is given by,

$$\omega = DM(\omega_p+B) \qquad \text{IV-12}$$

ω and ω' may vary considerably if L_{min} is small because then the diversities must be placed far apart and the unoccupied spectral regions between them cannot be used since frequencies in these regions are statistically dependent.

From the detailed environmental study undertaken in Chapter II, it was decided that a pulse duration time, T_p=125 ms should be used. During this time a 16 bit message word is to be transmitted with an error probability,

P_e, of 10^{-4}. The transmission bandwidth is limited to 2048 Hz and L_{min} is taken as 50 ms.

Such a transmission can be accomplished in many ways, a number of which has been examined by Morgera [6]. A summary of the results is given in Table IV-1.

CHARACTERS	M	D	No. of Tones Trans.	Freq. extent Hz.	Mess. error Prob.	Total SNR per mess. required dB.
1. 16 bits	65,536	1	1	>2048	10^{-4}	>40 dB
2. 8 bits	256	1	2	>2048	10^{-4}	>40 dB
3. 4 bits	16	2	8	1584	10^{-4}	37.8
4. 2 bits	4	5	40	2032	10^{-4}	30.0
5. 1 bit	2	4	64	1968	10^{-4}	34.6

Table IV-1 Comparison of Several MFSK Modulation Formats

From the Table it is seen that the MFSK scheme in which M=4 and D=5 is best suited for this design. Using this scheme, 40 tones (8x5) are selected for transmission, from a set of (32x5)=160. Four pilot tones are added to the forty to make a total of forty-four and the overall bandwidth used is 2032 Hz. The placement of the 164 tones across the frequency band is shown in Fig. IV-7. Each diversity has 32 tones which are spaced 12 Hz apart.

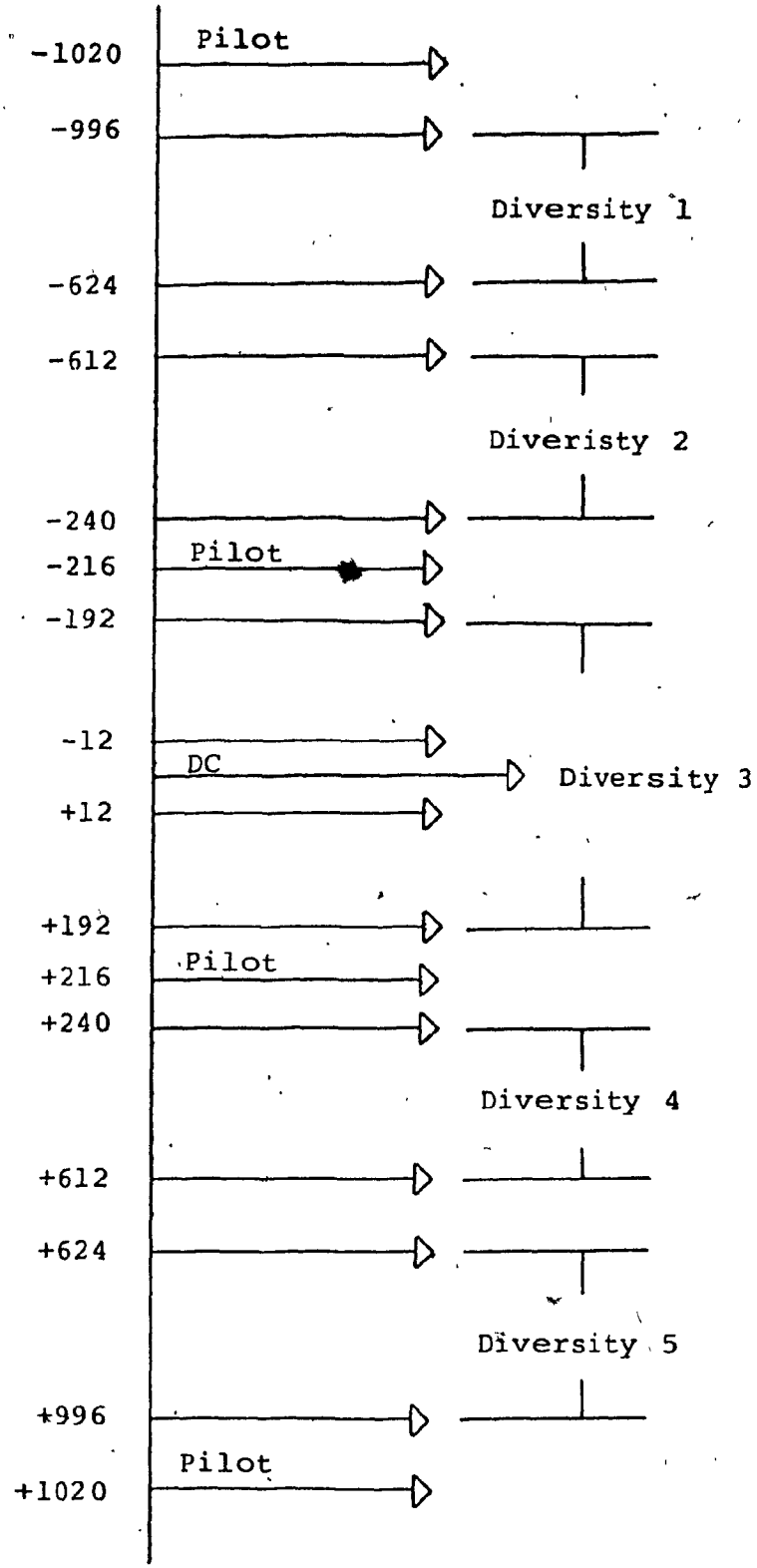

Figure IV-7 Synthesizer tone placement in the 2032 Hz transmission band

2. The Synthesis Technique

Frequency synthesis can be achieved by analog as well as digital means [5]. The digital method of frequency synthesis is the one used in this design. In this approach a stable source frequency is used to define sampling times at which digital sinusoidal values are produced. These samples are then D/A converted and smoothed by a filter to produce analog frequency signals. Digital synthesis consists of computing, in some real-time interval, T, values of a desired phase angle $\omega t=\omega nT$, where ω is the desired synthesizer output frequency, and using this value of phase angle to look up sinusoidal output samples, sin ωnT and cos ωnT in real-time. Since the phase angle is a linear function of time and is treated modulo 2π, an accumulator of phase increments ωnT, with overflow at 2π, solves the angle computation problem. This is the accumulator-overflow technique of frequency synthesis.

There are many methods of determining the sine and cosine of an arguement ωnT, the most straight-forward of which is that of a direct table look-up.

Consider the computation of values of:

$$\cos 2\pi fnT = \text{Re } e^{j2\pi fnT} \qquad \text{IV-13}$$

and

$$\sin 2\pi fnT = \text{Im } e^{j2\pi fnT} \qquad \text{IV-14}$$

where $f = Lf_o$, f_o = lowest frequency, n = time index and T = sample interval. If the lowest frequency f_o is defined as

$$f_o = 1/NT \qquad \text{IV-15}$$

where N is a design parameter, then the exponential in IV-13 and IV-14, can be written as

$$e^{j[(2\pi fnT)]} = e^{j[(2\pi/N)nL]} \qquad \text{IV-16}$$

Computing samples of this exponential, indexed by a frequency index L and a time index n, is equivalent to computing co-ordinates of N equi-spaced points on the unit circle in the complex plane.

For any particular index L, the argument of the exponential varies in increments of $(\frac{2\pi}{N})L$ in successive time indices. The product nL is treated modulo N since $e^{j[(2\pi/N)(X)]} = e^{j[(2\pi/N)(X+N)]}$. The generation of samples of a complex sinusoid therefore consists of accumulating multiples of L [i.e. nL at time n, (n+1)L at time (n+1) etc.] and using the accumulated values to look up $e^{j[(2\pi/N)(nL)]}$. These samples can be stored as a look-up Table in a PROM. Negative frequencies can be generated by negating L. If in accumulating L, the initial content of the accumulator is not zero, but some constant ϕ, the

argument of the exponential becomes $[(j(2\pi/N)\cdot(nL+\phi)]$ which affects the phase of the result but not the frequency. This is useful in applications where phase control is necessary. The frequency can be altered by changing the magnitude of L, thus causing the accumulator to overflow after a differing number of accumulations.

3. Single Tone Synthesizer

A block schematic diagram of a quadrature-output, single-tone frequency synthesizer based on the accumulator-overflow technique of frequency synthesis, is shown in Figure IV-8.

A frequency control word L is stored in a register and used to update an accumulator every T sec. to produce a new value $(nL+\phi)$, which acts as an address to read the real and imaginary parts of $e^{j[(2\pi/N)\cdot(nL+\phi)]}$. The digital samples obtained are then D/A converted to create analog signals.

4. Multi-tone Synthesizer

The multi-tone synthesizer used in the design to generate the 44 tones from each 16-bit word, is an extension of the single-tone synthesizer of Figure IV-8. A block schematic diagram of the multi-tone synthesizer is shown in Figure IV-9. The L and ϕ look-up tables are each 256 words long. However since it is necessary only to generate

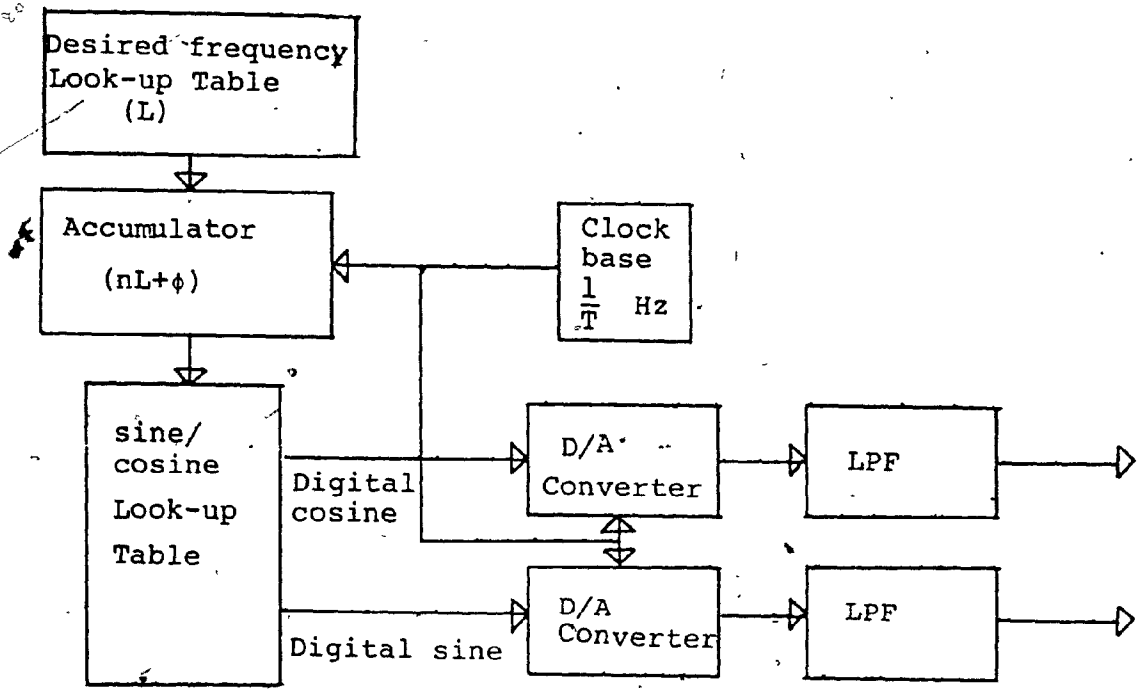

Figure IV-8 Digital synthesizer producing quadrature outputs

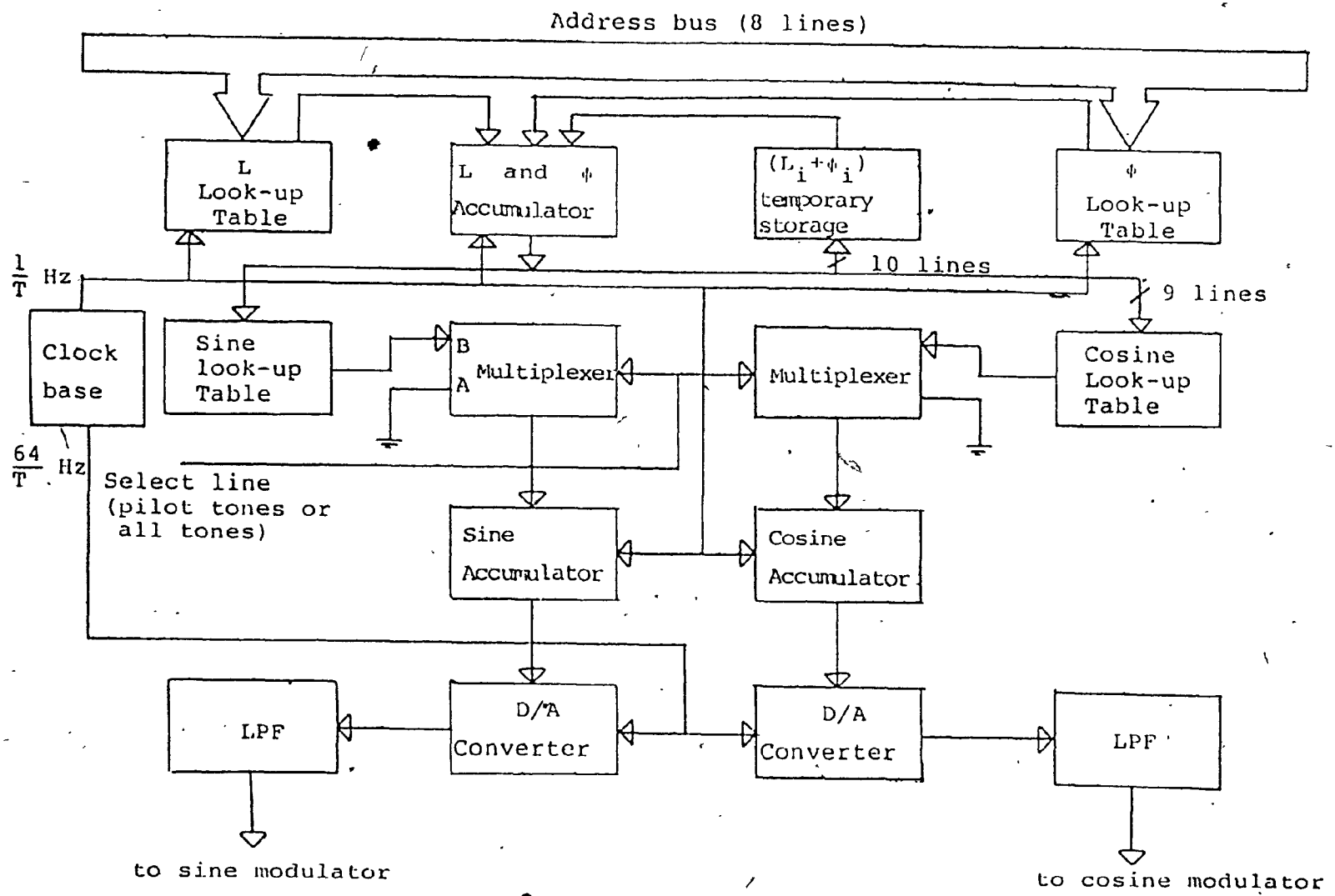

Figure IV-9 Block schematic diagram of multi-tone frequency synthesizer

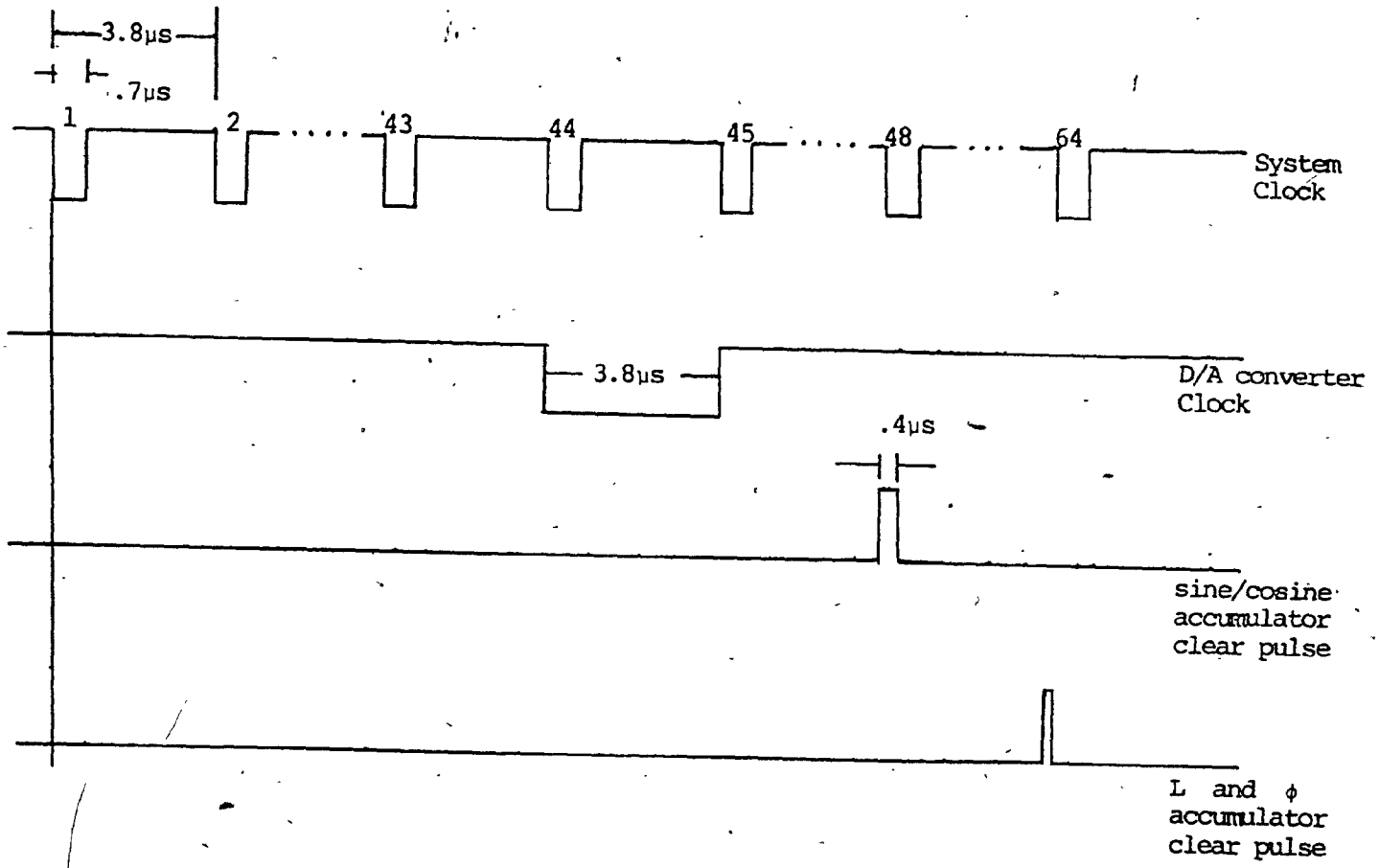

Figure IV-10 Relationship among clock pulses and clear pulses of the multi-tone synthesizer

164 tones, only 164 values of L and ϕ are stored in the upper portion of each table, respectively. The other locations beyond 163 are filled with zeros.

Because each 16-bit word produces 44 tones, the L and ϕ accumulator is multiplexed in the ratio of 64:1, thus making it necessary to store intermediate values of the 44 tones (i.e., $(nL_i+\phi_i)$ $i=1,\ldots44$) in temporary storage.

A 16-bit word provides 40 addresses which, together with the 4 addresses specified for the 4 pilot tones, look-up 44 values of L and ϕ. Each value of L is added to its corresponding value of ϕ in the L and ϕ accumulator, and the results $(L_i+\phi_i)$ $i=1\ldots44$, are placed in temporary storage. After the first 64 clock pulses the ϕ look-up table is disabled. Thus, after (64xn) clock pulses, the results in temporary storage are samples $(nL_i+\phi_i)$ $i=1\ldots64$. However, the samples for $44<i\leq64$, are all zeros.

Each $(nL_i+\phi_i)$ looks up a sample of the sine and cosine tables. These samples are added in the sine and cosine accumulators so that after (64xn) clock pulses the outputs of the sine and cosine accumulators are respectively,
$\sum_{i=1}^{64} \sin(2\pi f_i nT+\phi_i)$ and $\sum_{i=1}^{64} \cos(2\pi f_i nT+\phi_i)$.

The D/A converters are written into on each 44th clock pulse, therefore their outputs represent samples having instantaneous values of $\sum_{i=1}^{44} \sin(2\pi f_i nT+\phi_i)$ and $\sum_{i=1}^{44} \cos(2\pi f_i nT+\phi_i)$ accordingly.

In every 64 clock pulses, the sine/cosine and L and ϕ accumulators are cleared once. The sine/cosine accumulators are cleared on the 48th pulse while the L and ϕ accumulator is cleared on the 64th pulse. The relationship among the clock pulses, and the clear pulses of the accumulators is shown in Figure IV-10.

5. Design of the Dense MFSK Modulator

The design of the dense MFSK modulator was carried out in accordance with the following specifications:

1) ω = 2048 Hz bandwidth
2) $f_s = \frac{1}{T}$ = 4096 Hz sample rate
3) f_o = 4 Hz frequency resolution
4) 40 dB spectral purity

The frequency resolution of 4 Hz provides for ω/f_o=512 tonal locations within the bandwidth. Only 164 of these positions are used by the modulator and of the 164, only 44 are synthesized and transmitted per 16-bit word.

From IV-15, it is seen that the design parameter N and the integer L must be as follows:

$$N = \frac{1}{Tf_o} = 2^{10} = 2^b$$

$$L \in [1,256] \text{ (in increments of 1)} \qquad \text{IV-17}$$

Thus the L and ϕ accumulator of Figure IV-9 must be 10 bits long. This means that the sine and cosine look-up tables should contain $2^{10} = 1024$ entries. However if the LSB of the accumulator output is dropped, the sine and cosine look-up tables will be reduced to 512 entries. The amplitude error resulting from this will be negligible.

To meet the specification of 40 dB spectral purity, the sine and cosine samples should consist of a sign bit and 7 bits [10].

In order to satisfy all the required specifications, the multi-tone synthesizer of Figure IV-9 should have the following:

(1) 8×256 L and ϕ look-up tables

(2) 10 bit L and ϕ accumulator

(3) 8×512 sine and cosine look-up tables

The content of the sine and cosine look-up tables are given in Appendices IV-1 and IV-2, respectively. The data is present in Hex format. Appendix IV-3 gives the data, in binary format, that is stored in the L and ϕ PROMS. It also gives the frequencies that each L produces, at baseband and after mixing with the 8192 Hz carrier.

6. Phase Control

Since the outputs of the sine and cosine D/A's represent the summation of 44 sinusoids, it is necessary to randomize their phases, so as to minimize the peak-to-average ratio of the resulting waveform. This must be done in order to utilize the power amplifier efficiently.

An analytic solution for the "best" phases, does not seem possible, however "good" phase selections may be found using computer search techniques. If the tones are irregularly spaced, the problem of "good" phase selection is made even harder.

One phase set $\{\phi_k\}$ which has proven to work well in many applications is the quadratic phase set which is defined as,

$$\pm\phi_k = \pm\pi k^2/N \pmod{2\pi} \quad 0 \leq k \leq N-1 \qquad \text{IV-18}$$

This phase set is chosen for the telemetry system design.

E. SYNTHESIZER HARDWARE

The implementation of the design of the synthesizer will now be examined. Each of the 4 cards comprising it will be discussed separately.

1. Tone Address Generator Card

The schematic diagram of the tone address generator card is shown in Figure IV-11. Figure IV-12 is a photograph of the card.

The functions of the card are:

(i) To convert a 16-bit data word into an address for reading the L and ϕ PROM.

(ii) To provide the control signals for specifying the status of the synthesizer (i.e., reset, pilot tones only or all-tones modes).

(iii) To create the timing pulses necessary for the operation of the synthesizer.

Each 16-bit data word is broken down into odd and even bits. The even bits are routed to the single 8 channel multiplexer A2 while the odd bits are fed to the other single 8 channel multiplexer B2. The even and odd bits constitute the least significant bits of the L and ϕ address. The other address bits A_7 to A_2, are obtained from outputs Q_6 through Q_1 of counter C4.

The control words that determine the status of the synthesizer come from the microcomputer and are latched by C3.

Monostable vibrators D1, D2 and D3 provide the timing pulses used for the operation of the synthesizer. The relationship among these pulses is shown in Figure IV-13.

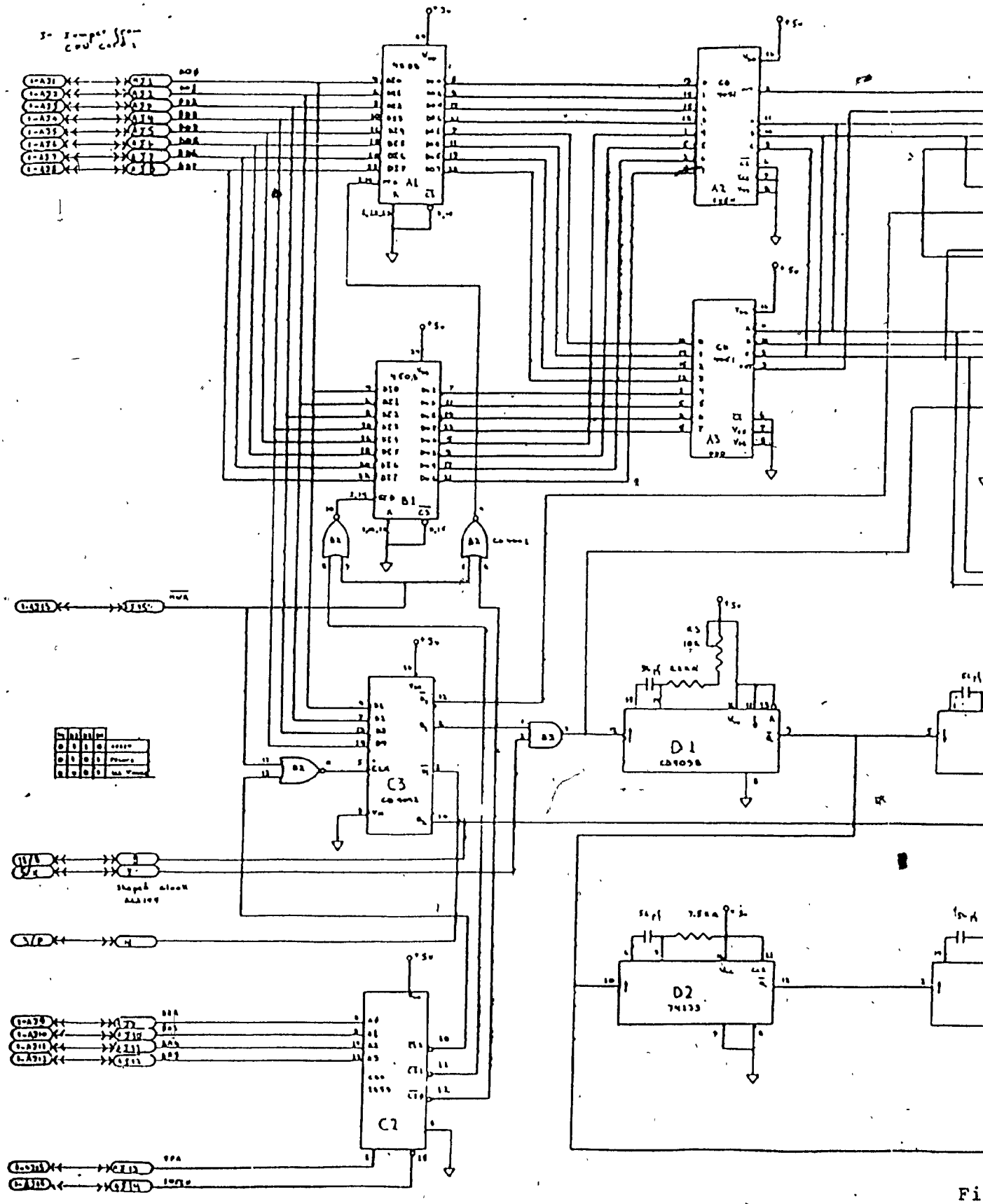

Fi

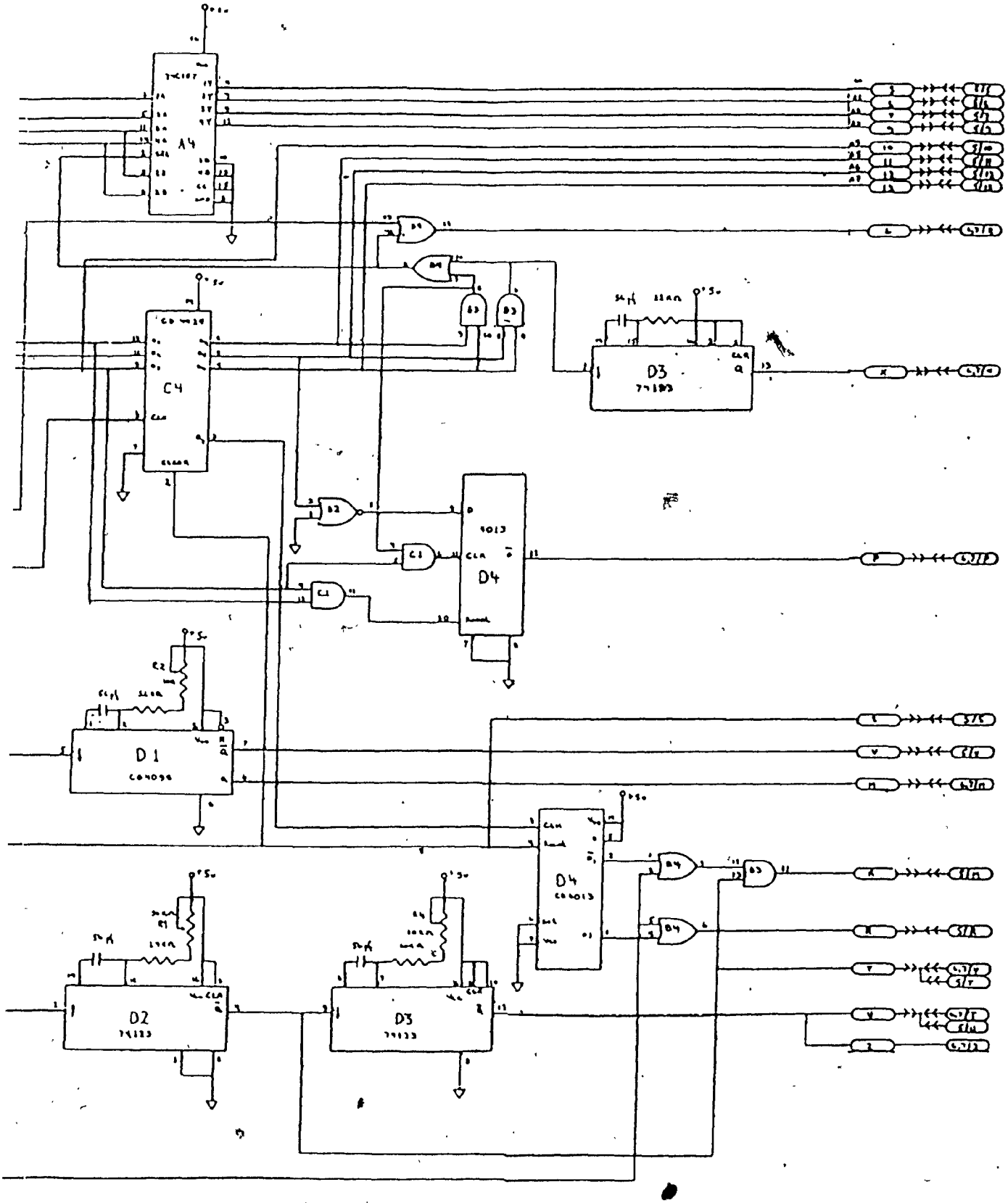

Figure IV-11 Schematic diagram of the tone address generator card.

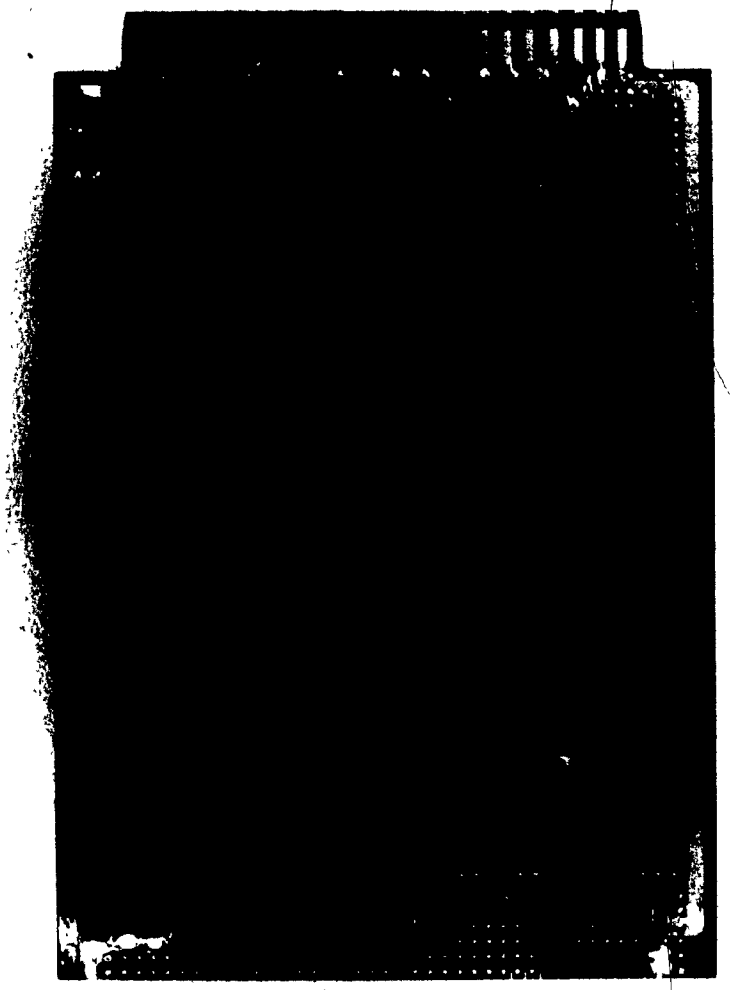

Figure IV-12 Photograph of tone address generator card

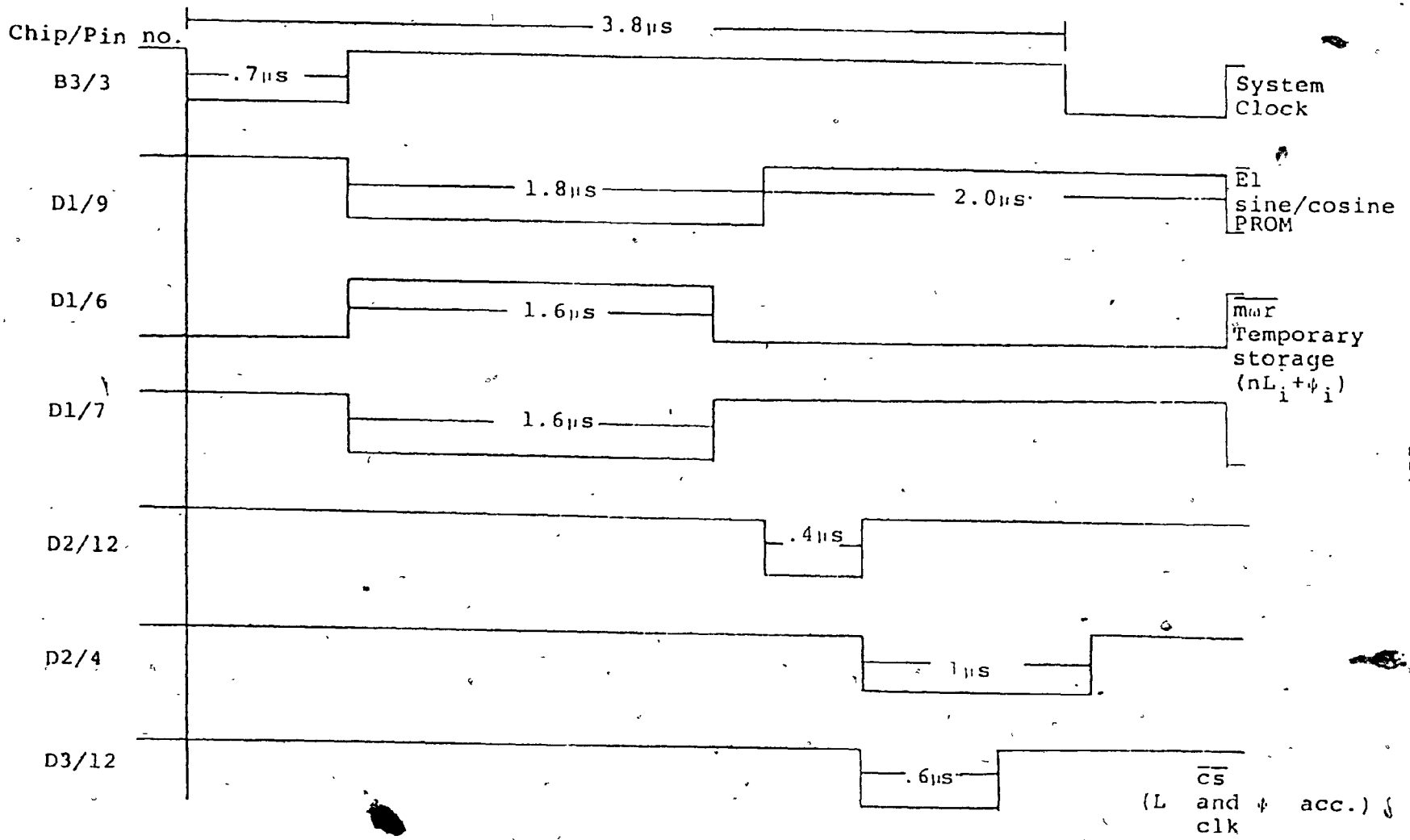

Figure IV-13 Timing relationship among pulses for the operation of the multi-tone synthesizer

2. The L and ϕ Accumulator Card

The schematic diagram of the L and ϕ accumulator card is shown in Figure IV-14. A photograph of the card is shown in Figure IV-15. The card consists of the L PROM (B1, B2, B3), the ϕ PROM (A1, A2, A3), the $(L+\phi)$ temporary storage (D1, D2, D3) and $(L+\phi)$ accumulator (C1, C2, C3). A block schematic diagram of the card is given in FigureIV-16 and the timing diagram for its operation is illustrated in Figure IV-17.

When n=1 44 values of L and ϕ are read from the L and ϕ PROMS and each value of L is added to its corresponding ϕ value to form $(L_i+\phi_i)$ i=1,...44. These results are clocked into the buffer and then written into storage. For n>1, the ϕ look-up table is disabled and the information in storage (i.e., $(n-1)L_i+\phi_i$) i=1,...44, is recalled and added to L_i to form $(nL_i+\phi_i)$ i=1,...44. This is the output of the 10-bit accumulator. The LSB is dropped and the remaining 9 bits are used as the address to read samples from the sine and cosine PROMS on the sine and cosine look-up accumulate cards.

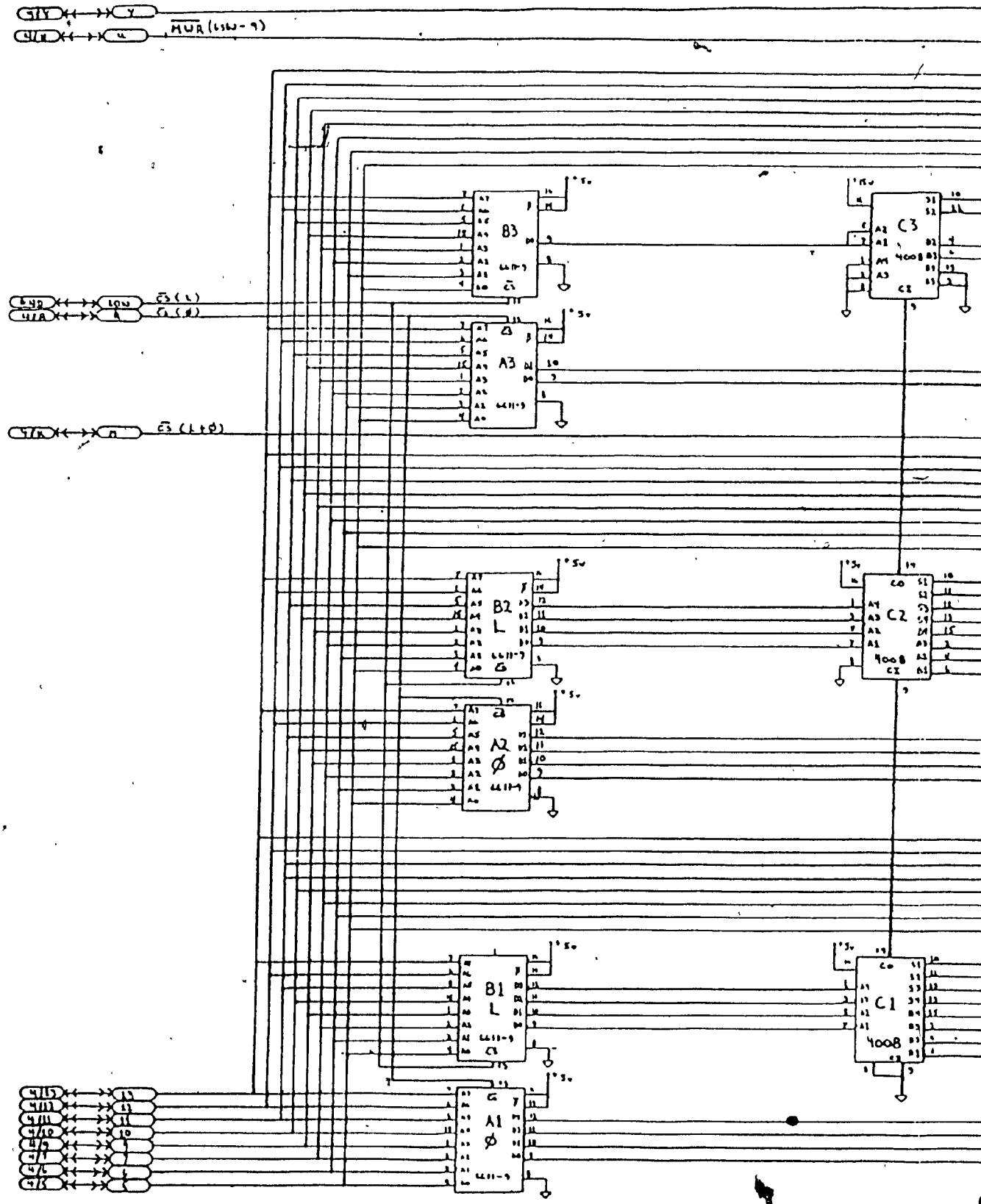

Figure IV-14 Schematic diagram of L and ϕ accumulator card

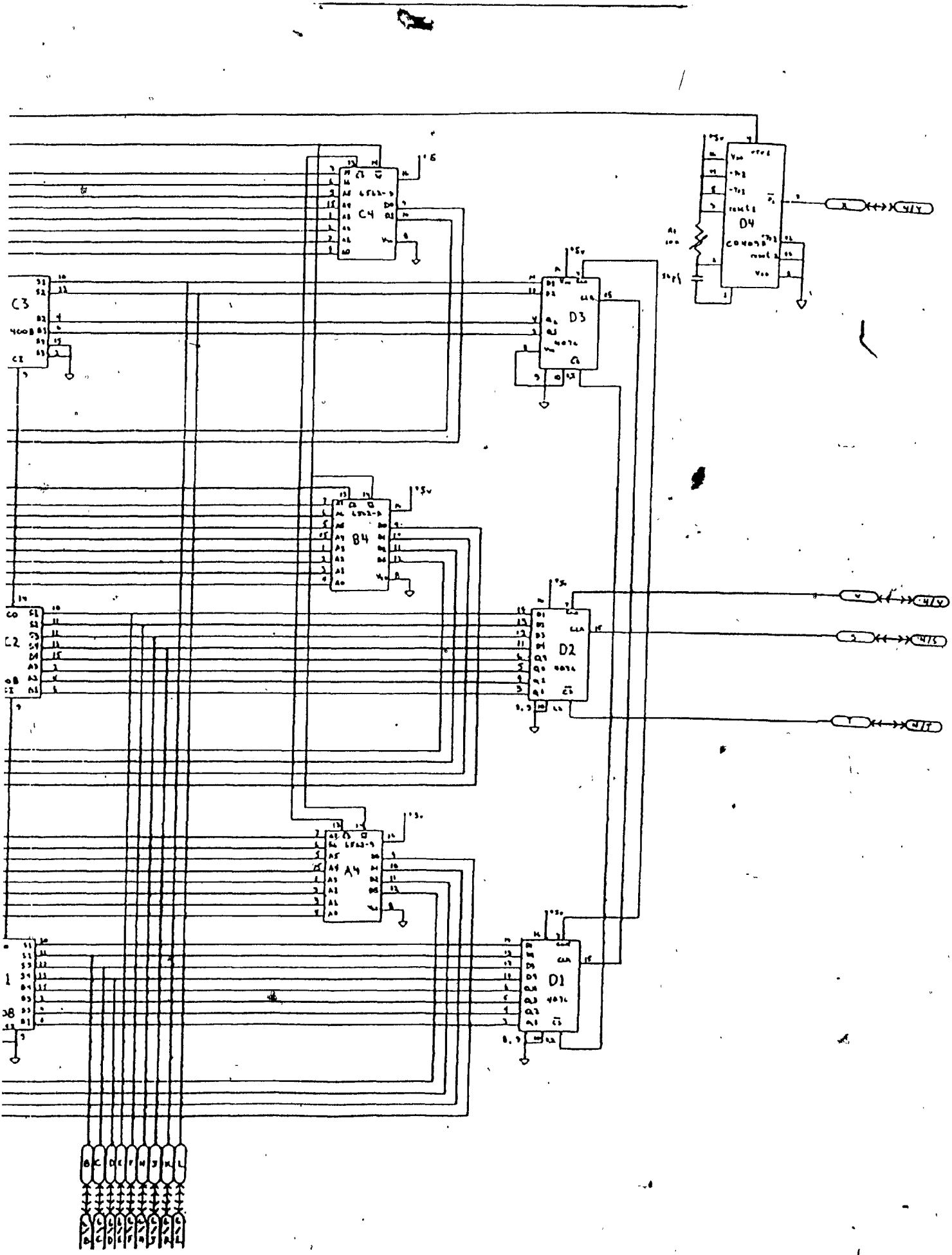
C4
D4
C3
D3
B4
D2
A4
D1

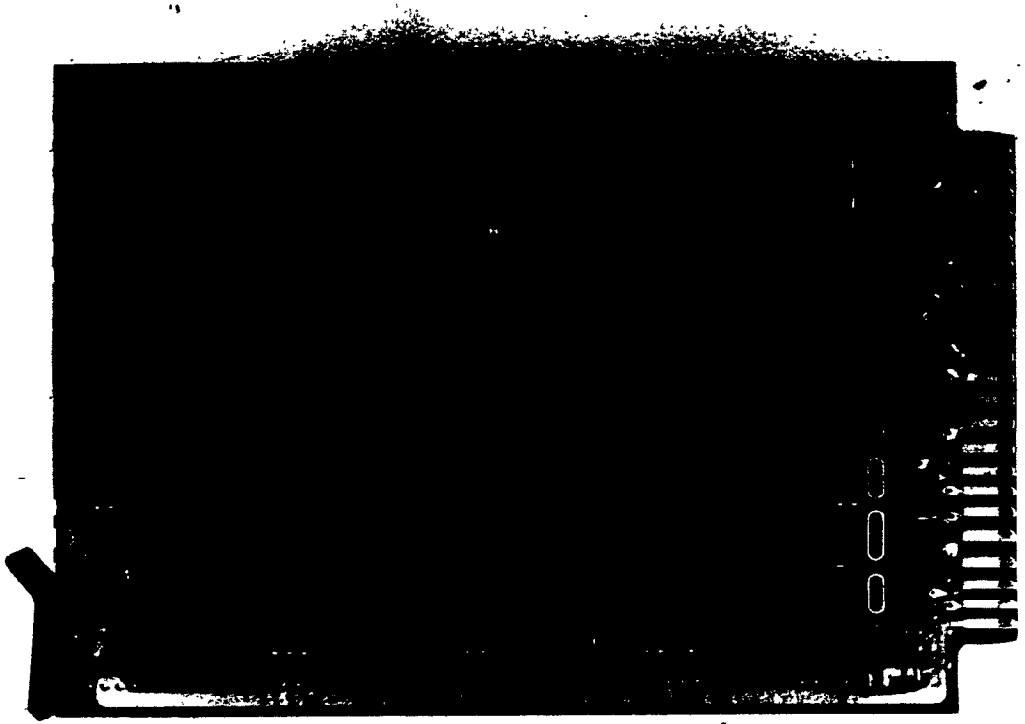

Figure IV-15 Photograph of L and ϕ accumulator card

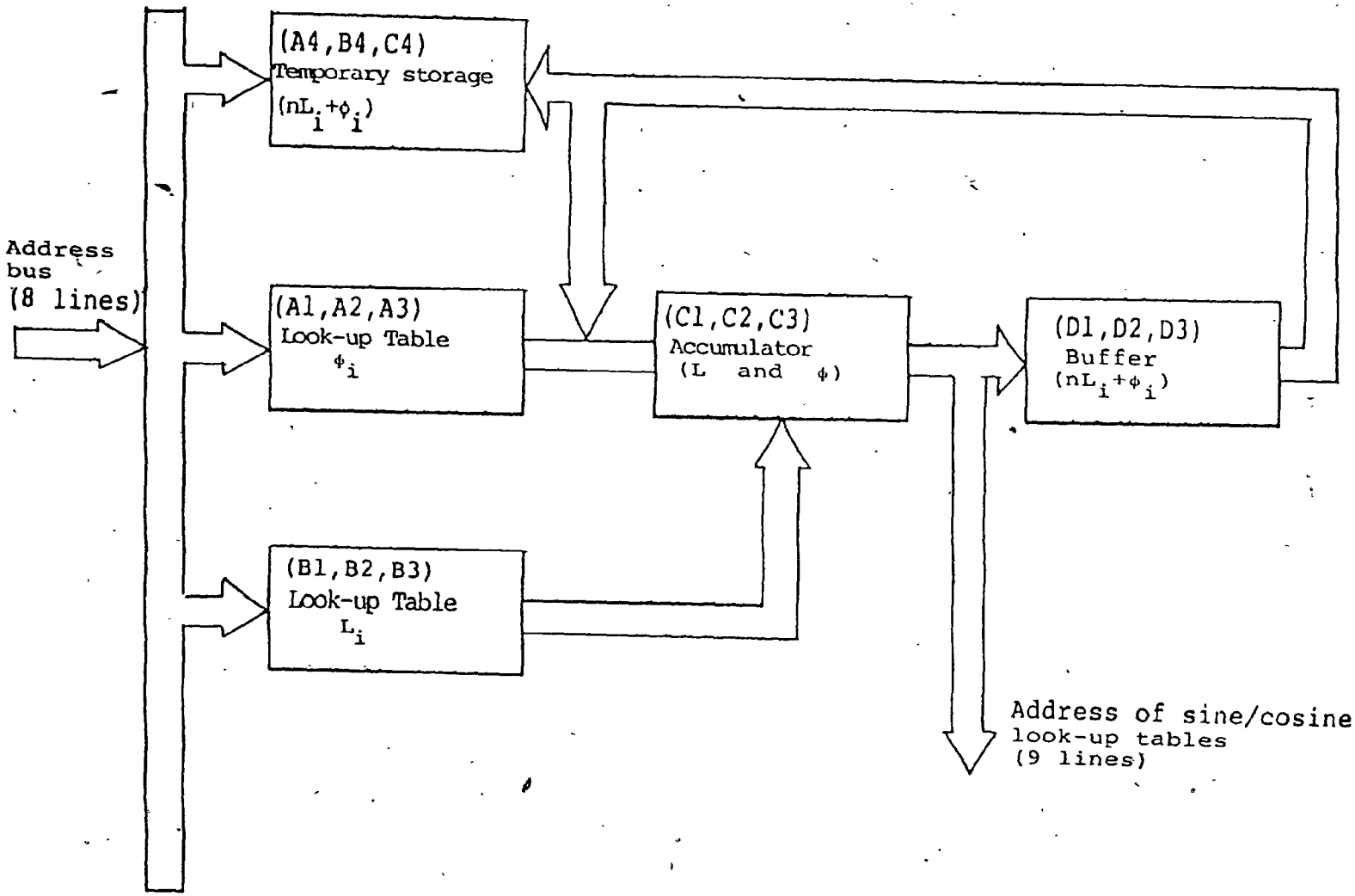

Figure IV-16 Block schematic diagram of L and ϕ accumulator card

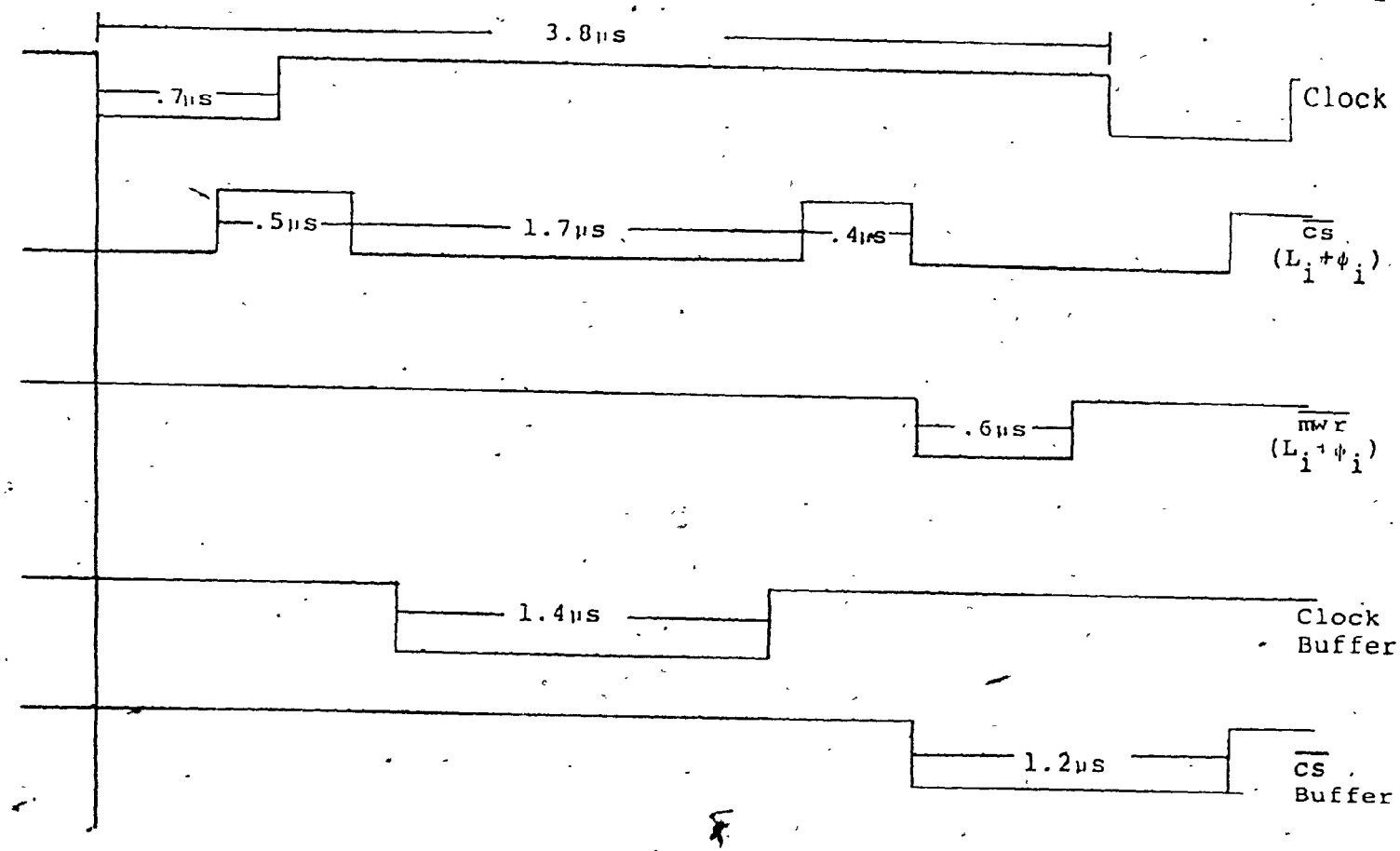

Figure IV-17 Timing diagram for L and φ accumulator card

3. Sine and Cosine Look-up Accumulate Cards

The sine and cosine look-up accumulate cards are identical except for the fact that one card has a sine look-up table stored in PROM A1 while the other has a cosine table. Photographs of the cards are shown in Figures IV-18 and IV-19.

A block schematic diagram of one of the cards is shown in Figure IV-20, while a detailed schematic diagram is presented in Figure IV-21. Figure IV-22 is a timing diagram for the operation of the card.

The sine/cosine look-up table is a 512x8 bit table in which the data is stored in 2's complement form. The output of the table feeds a multiplexer that is used to distinguish between the transmission of the pilot tones alone, or all 44 tones.

If all the tones are being transmitted, 44 samples out of the sine/cosine look-up table are routed to the accumulator. On the other hand, when the pilots alone are transmitted during the preamble or receiver synchronization phase, the multiplexer input is forced to zero for the first 40 samples and only samples 41 to 44, representing the four pilot tones are allowed through to the accumulator.

The sine/cosine accumulator is 16 bits long. Its A input is sign extended so that bits 8 through 16 are identical. A shift register (C1, C2, C3, C4), acts as a buffer that delays the partial sum of the accumulation and feeds it back as the second input to the accumulator.

Bits 14 through 6, from the output of the shift register constitute the digital data that the D/A converts to an analog signal. This signal passes through a 4-pole bandpass Butterworth filter for smoothing and is then directed to the signal input of a modulator in the transmitter.

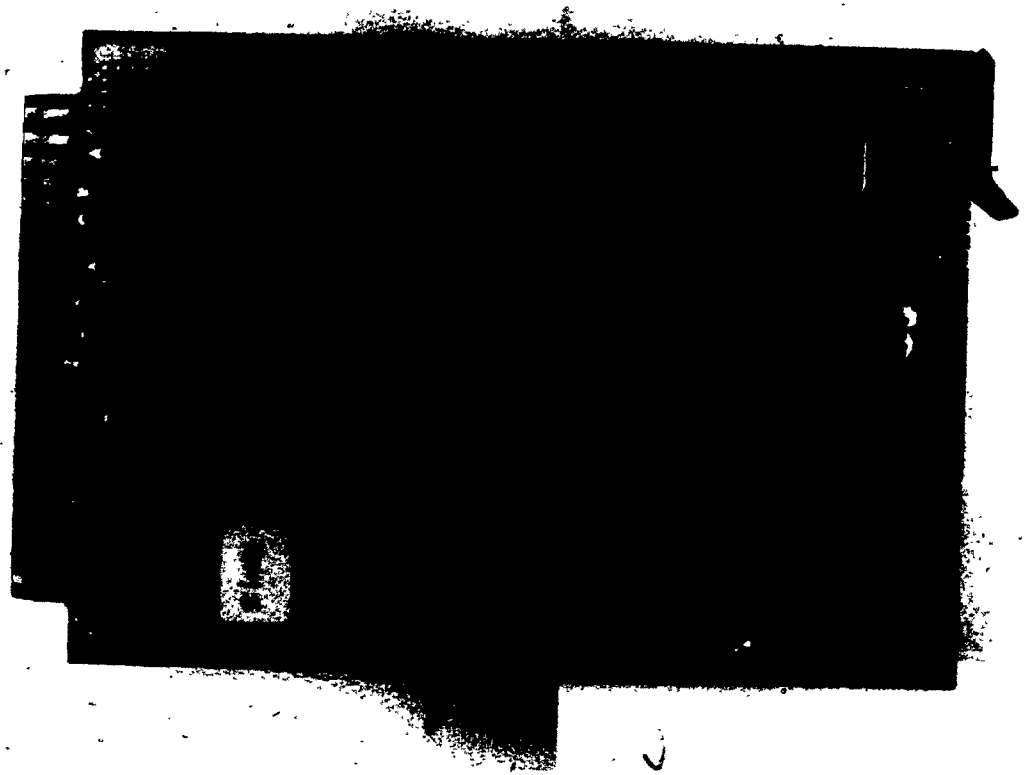

Figure IV-18 Photograph of the sine look-up accumulate card

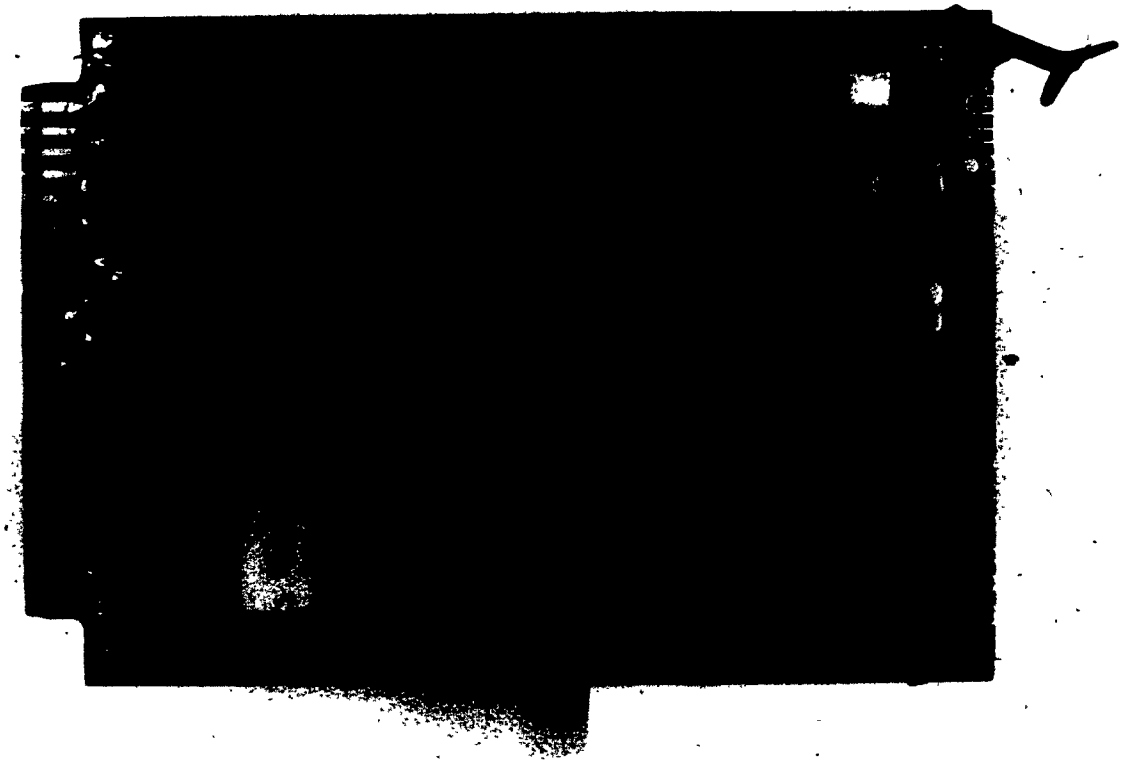

Figure IV-19 Photograph of the cosine look-up accumulate card

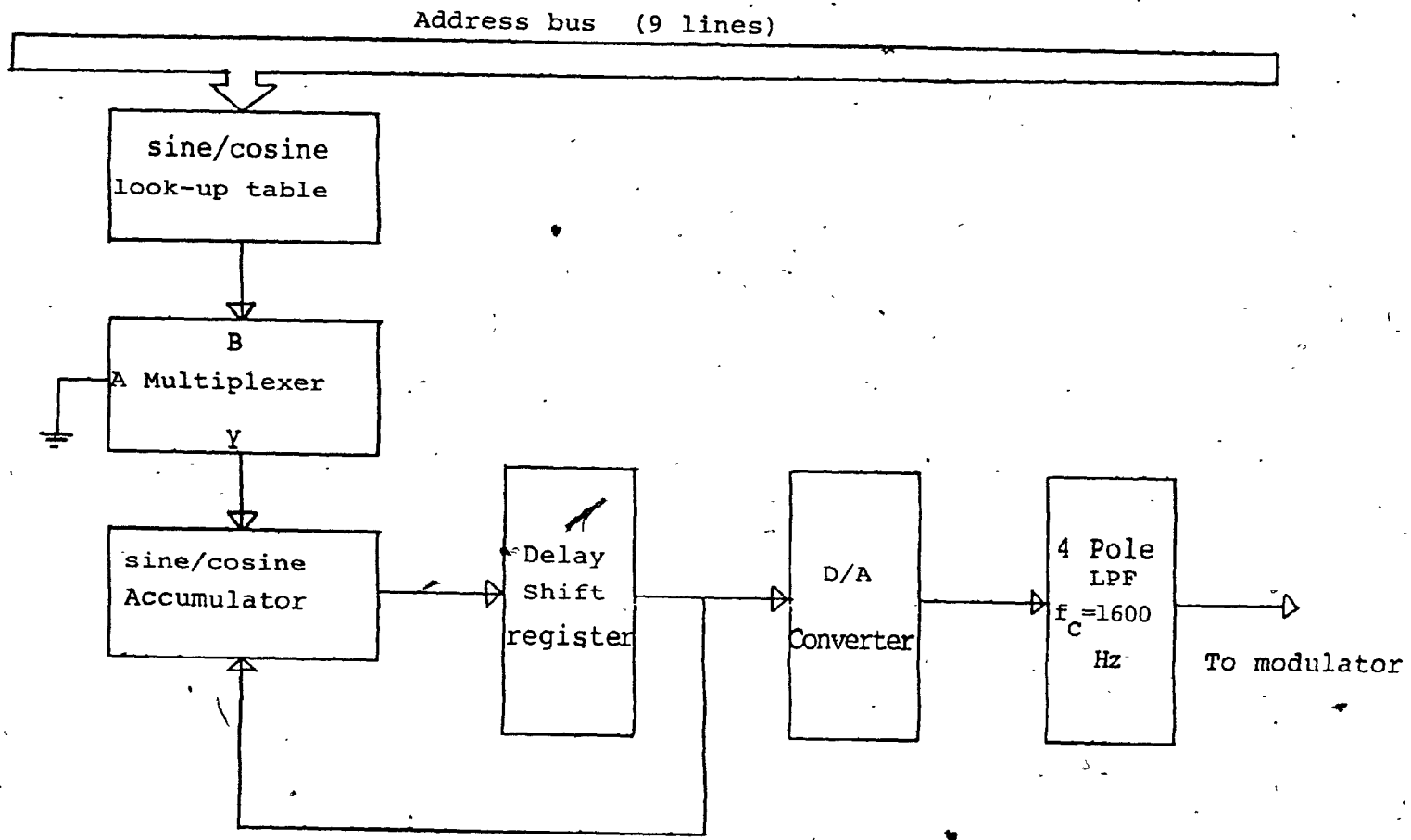

Figure IV-20 Block schematic diagram of sine/cosine accumulator

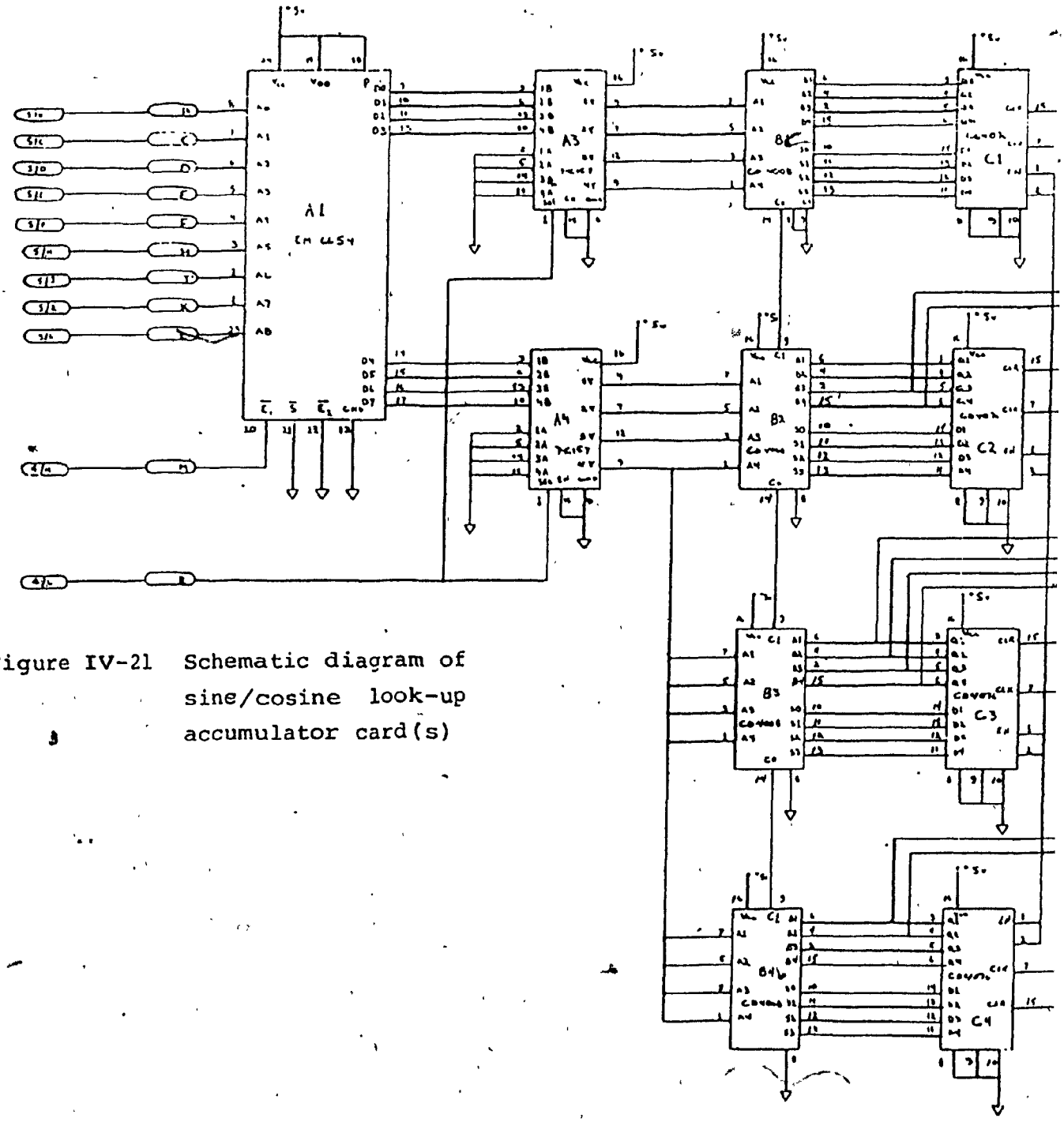

Figure IV-21 Schematic diagram of sine/cosine look-up accumulator card(s)

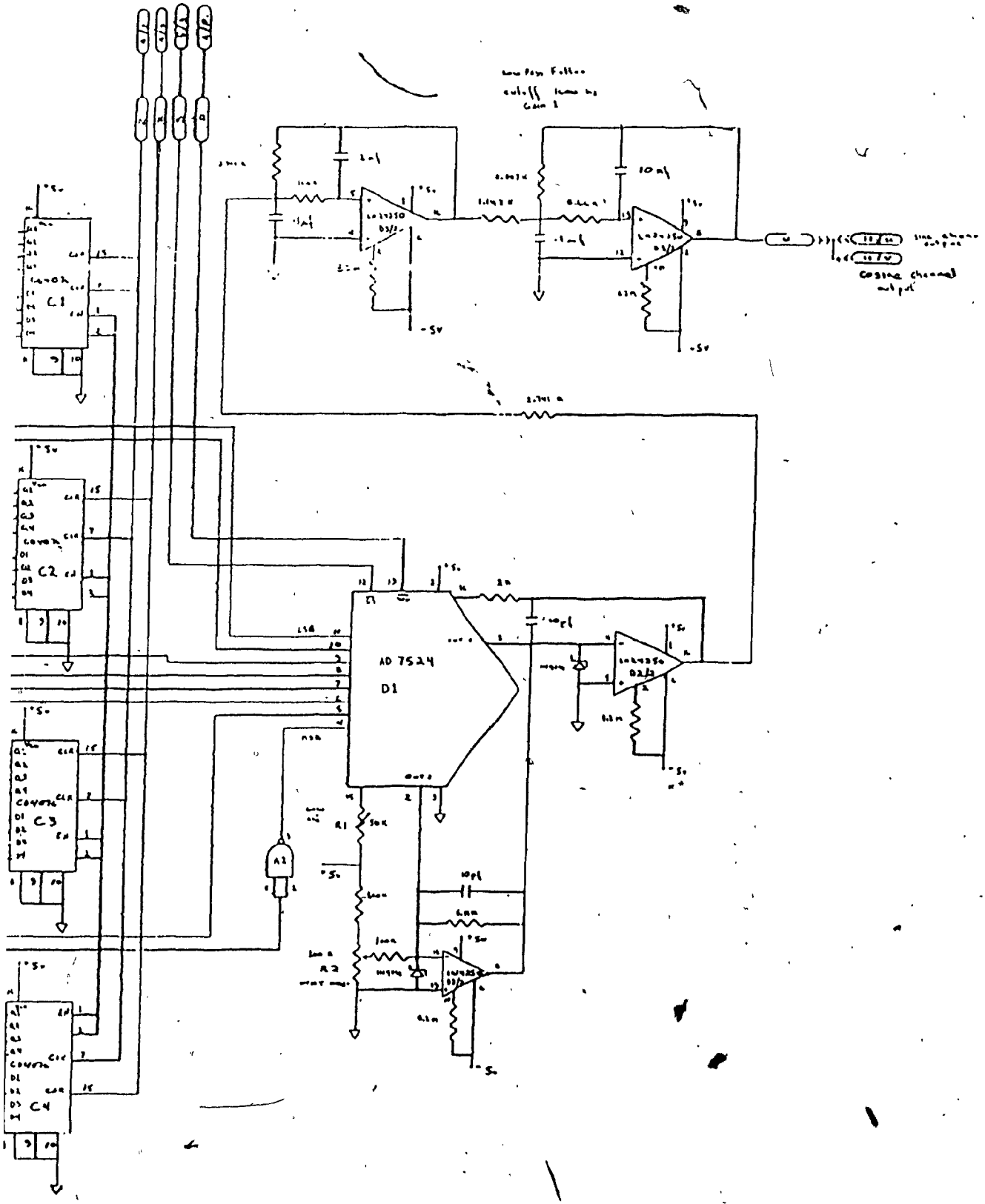
AD 7524
D1
C1
C2
C3
C4
R1
R2
A1
A2
-5v
+5v
cosine channel output

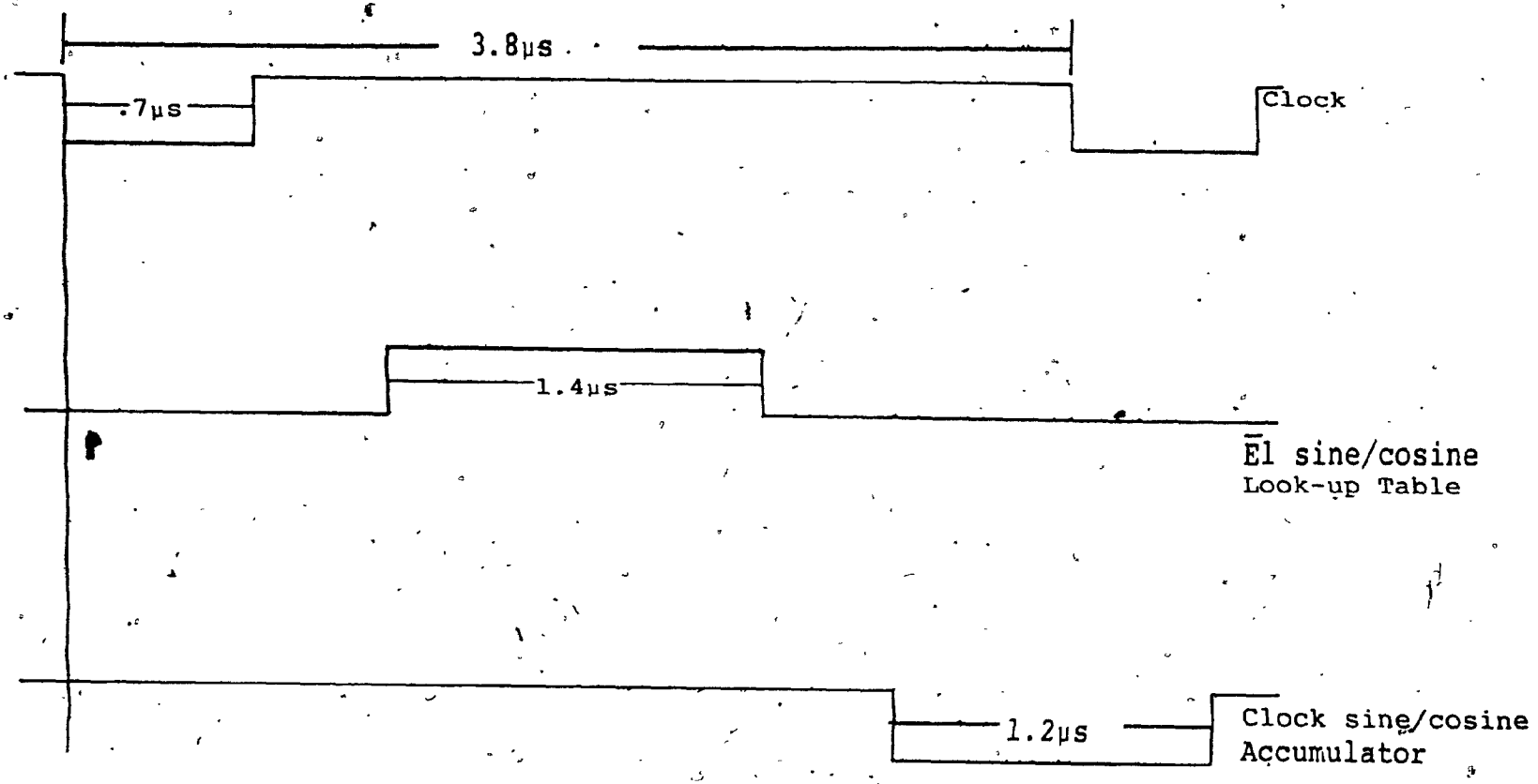

Figure IV-22 Timing diagram of sine/cosine accumulate card

F. TRANSMITTER

The transmitter is that portion of the bottom unit that conditions the output of the synthesizer for transmission. It consists of one card which is referred to as the balanced modulator and power amplifier card.

1. Balanced Modulator and Power Amplifier Card

The schematic diagram of the balanced modulator and power amplifier card is shown in Figure IV-23 and a photograph of the card is shown in Figure IV-24. A block schematic diagram of the card is given in Figure IV-25.

The baseband input to the sine and cosine modulators are $\sum_{i=1}^{44} \sin(2\pi f_i t+\phi_i)$ and $\sum_{i=1}^{44} \cos(2\pi f_i t+\phi_i)$, respectively. The carriers are two 8192 square waves in quadrature.

If the phases ϕ_i, are disregarded, the output of the sine and cosine modulators would be

$$\sum_{i=1}^{44} \sin(2\pi f_i t)\sin(2\pi f_c t) \quad \text{and} \quad \sum_{i=1}^{44} \cos(2\pi f_i t)\cos(2\pi f_c t),$$

respectively. Now

$$\sum_{i=1}^{44} \sin(2\pi f_i t)\sin(2\pi f_c t) = \frac{1}{2}\left[\sum_{i=1}^{44} \cos(2\pi(f_c+f_i)t - \sum_{i=1}^{44} \cos(2\pi(f_c-f_i)t\right] \quad \text{IV-19}$$

and

$$\sum_{i=1}^{44} \cos(2\pi f_c t)\cos(2\pi f_i t) = \frac{1}{2}\left[\sum_{i=1}^{44} \cos(2\pi(f_c+f_i)t + \sum_{i=1}^{44} \cos(2\pi(f_c-f_i)t\right] \quad \text{IV-20}$$

Adding IV-19 and IV-20 gives,

$$\sum_{i=1}^{44} \cos(2\pi f_c t)\cos(2\pi f_i t) - \sin(2\pi f_c t)\sin(2\pi f_i t) = \sum_{i=1}^{44} \cos(2\pi(f_c+f_i)t \quad \text{IV-21}$$

Thus the output of the summer consists of 44 sinusoids in the frequency range 7168 Hz to 9216 Hz.

The variable amplifier following the sine modulator is to ensure that the outputs of the two modulators are equal so that the lower sidebands of IV-19 and IV-20 completely cancel each other after summation. The output of the summer is passed through a 125 ms triangular window so as to reduce the amplitude of the side lobes when the tones are demodulated by the top unit receiver. Also the triangular window reduces the peak-to-average ratio of the signal from the summer, allowing the power amplifier to be more efficiently used.

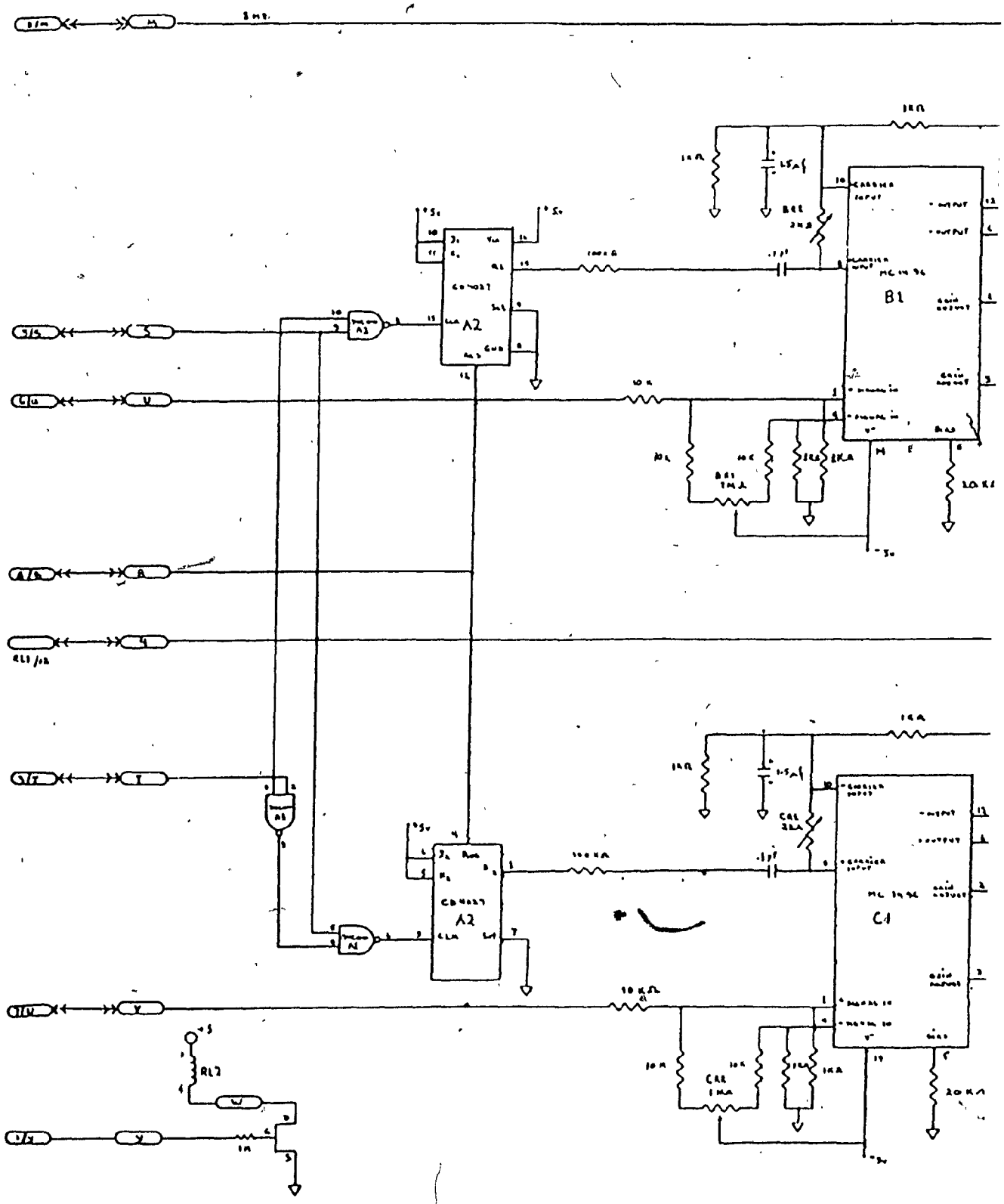

Figure IV-23 Schematic diagram of balanced modulat power amplifier card

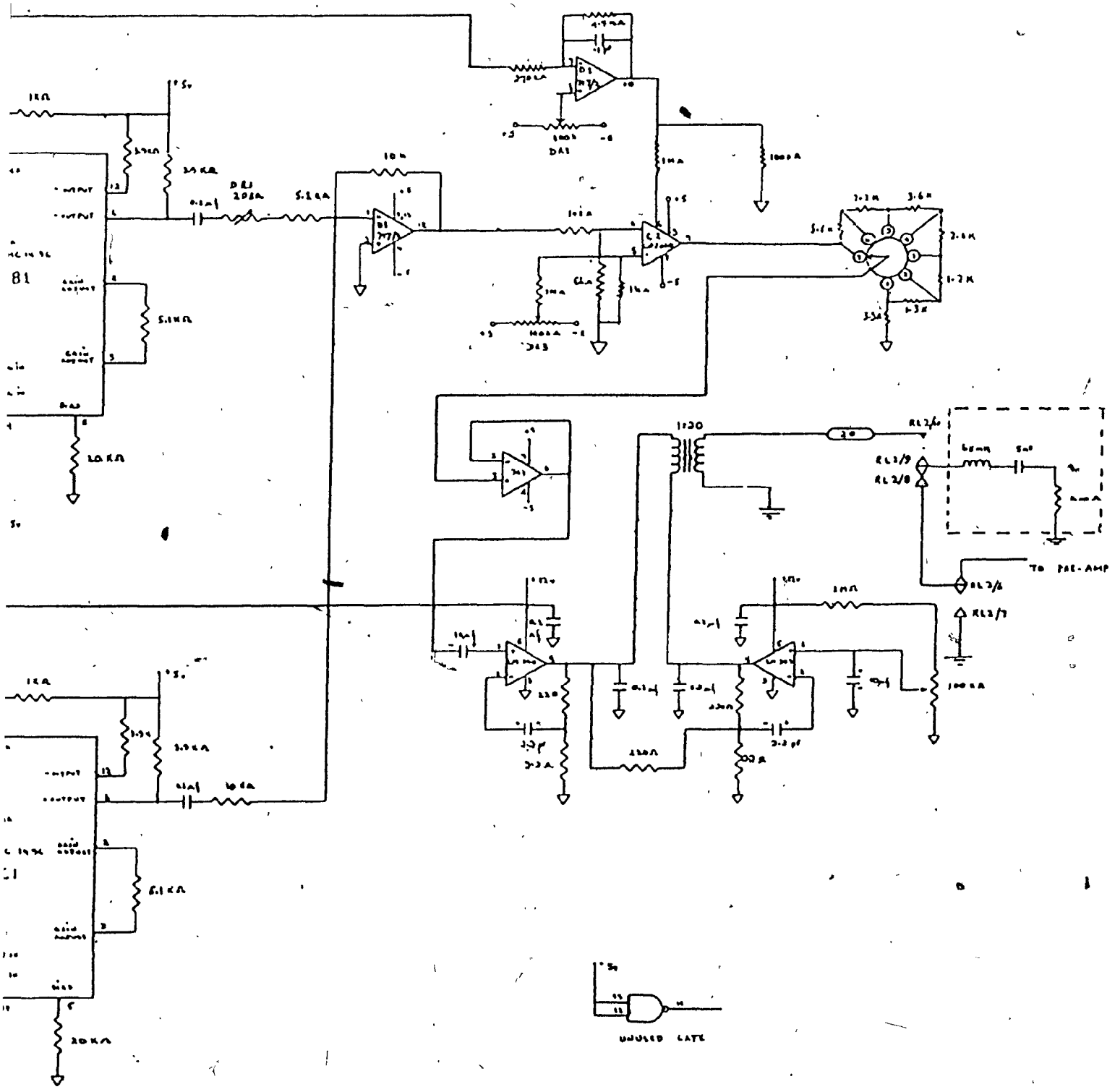

d modulator and

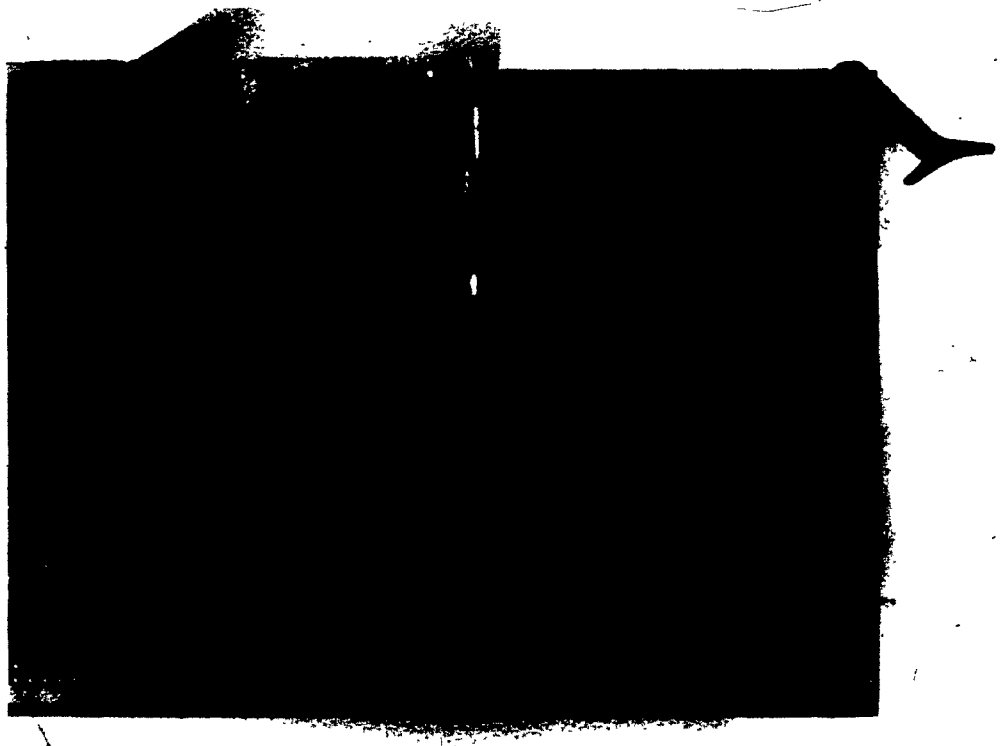

Figure IV-24 Photograph of balance modulator and power amplifier card

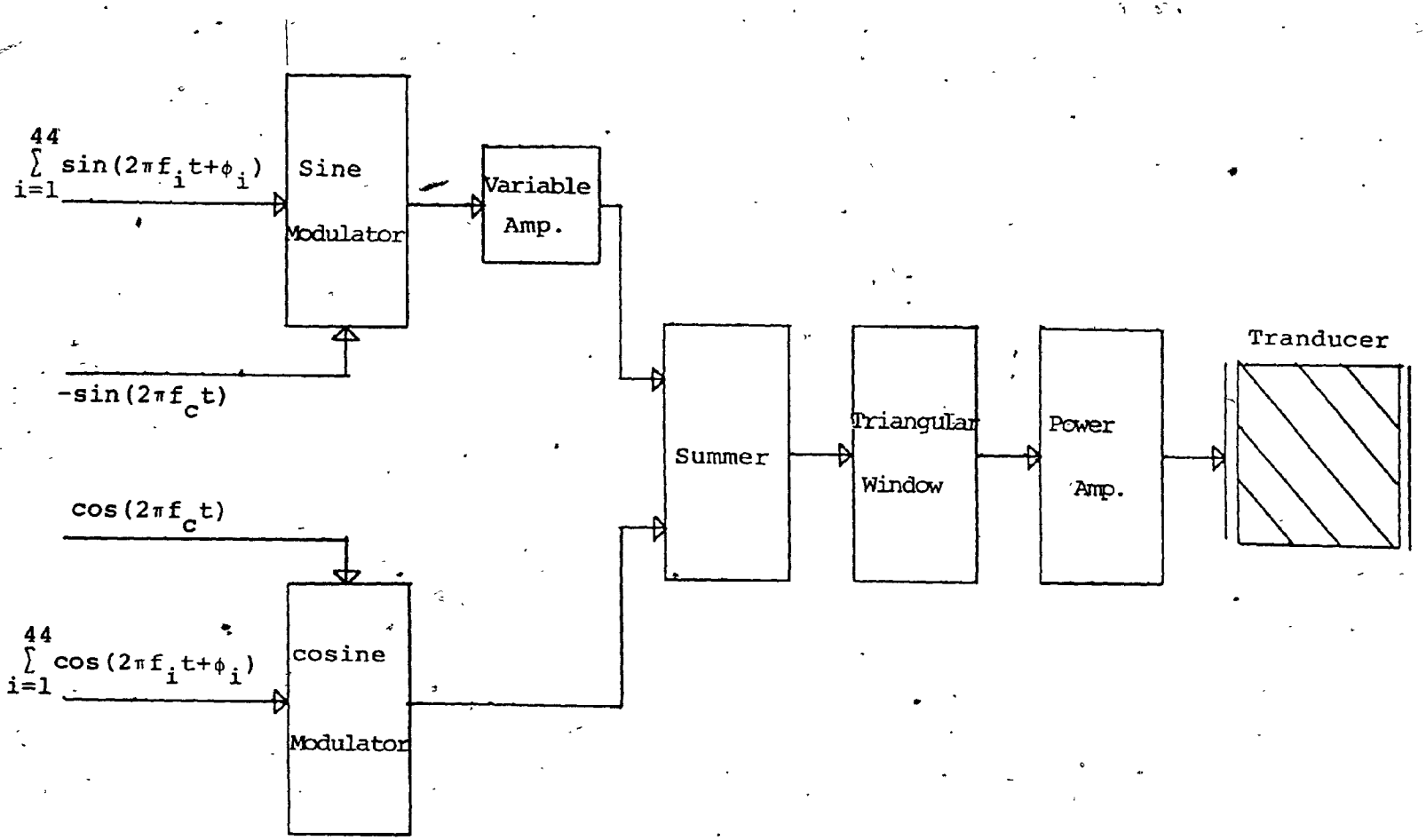

Figure IV-25 Block schematic diagram of the balanced modulator and power amplifier card

The power amplifier is a class B amplifier using two LM383's connected in a bridge configuration. It is capable of dissipating 16 watts of peak power into a 4Ω load with 10% total harmonic distortion if the supply voltage is set at 14.4 volts. The amplifier has a very high gain, therefore its printed circuit board layout is critical and has to be custom-made.

For this application the amplifier is run on a 12v supply and its output power is delivered in seven steps depending on the position of a rotary switch which controls the level of the input signal. This is indicated in Table IV-2.

SWITCH POSITION	R.M.S. OUTPUT POWER IN WATTS
1	.25
2	.50
3	.75
4	1.50
5	3.0
6	4.0
7	6.0

Table IV-2 Power amplifier r.m.s. output power as a function of rotary switch position

The amplifier's output power was measured with a steady input from which windowing was removed. It is expected that the application of the triangular window to the input signal, will cause a 50% reduction in the output power.

In order to achieve the higher power outputs indicated in Table IV-2, the amplifier has to be driven so that the output is clipped. The output therefore is distorted with intermodulation products causing the signal to "noise" ratio to deteriorate. Photographs of the amplifier's output for different power settings, ranging from 6.0 watts r.m.s. to 0.5 watt r.m.s., are shown in Figures IV-26 to IV-31.

There is a loss of some energy resulting from clipping. Also, because the 8192 Hz carrier is a square wave, there is again some energy loss in every 2 kHz band around the odd harmonics of the carrier. However, in the latter case, the wasted power is but a small disadvantage when compared to the difficulty of having to produce sinusoids in quadrature at exactly 8192 Hz. Moreover, this excess energy is transparent to the top unit receiver because the receiver has a 6-pole bandpass elliptic filter centred on 8192 Hz in its front end.

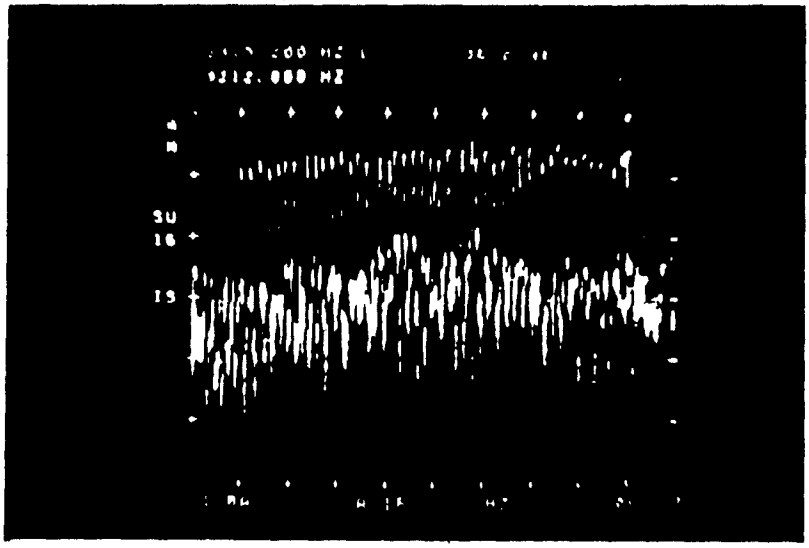

Figure IV-26 Power amplifier output
6 watts r.m.s.

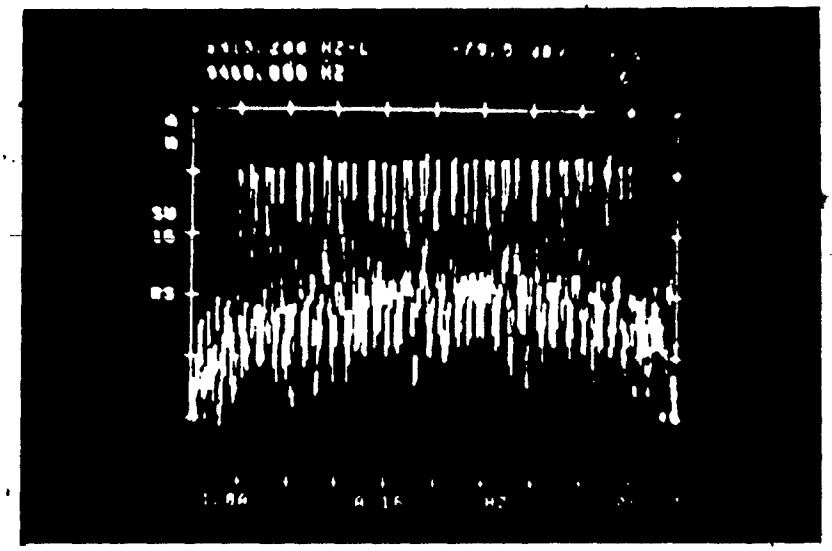

Figure IV-27 Power amplifier output
4 watts r.m.s.

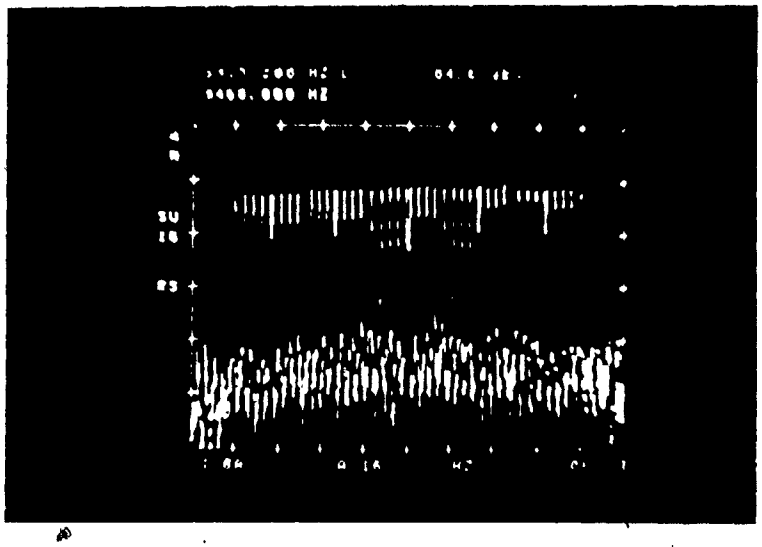

Figure IV-28 Power amplifier output
3 watts r.m.s.

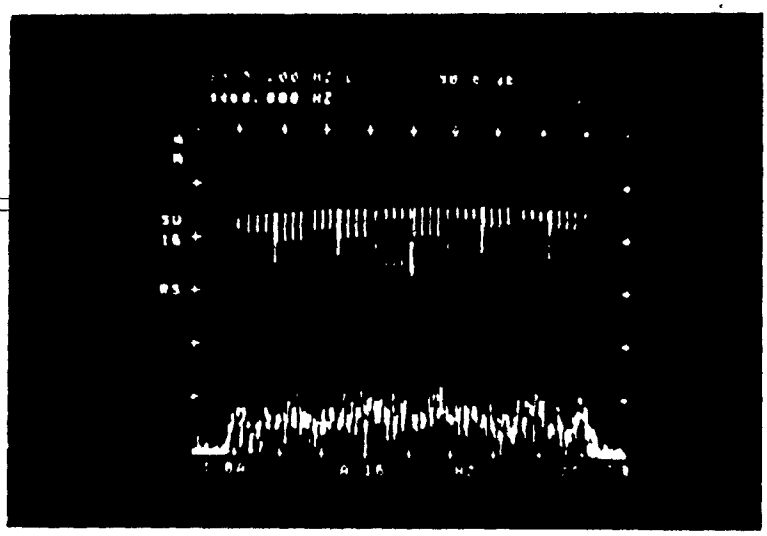

Figure IV-29 Power amplifier output
1.5 watts r.m.s.

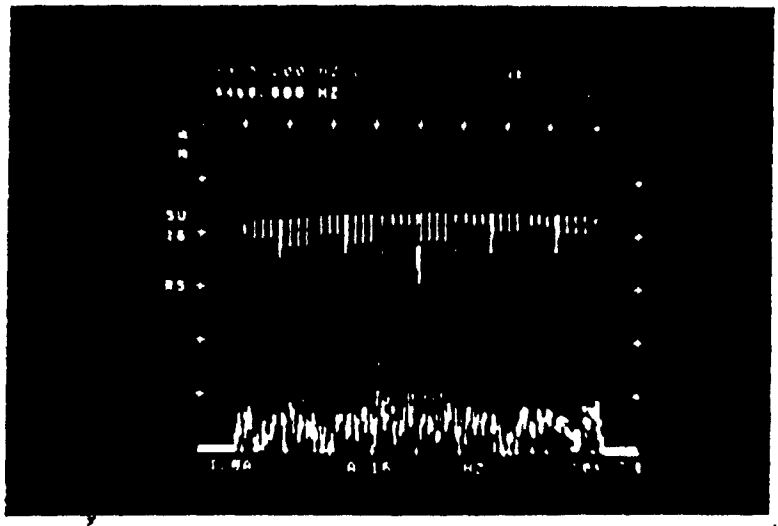

Figure IV-30 Power amplifier output .75 watts r.m.s.

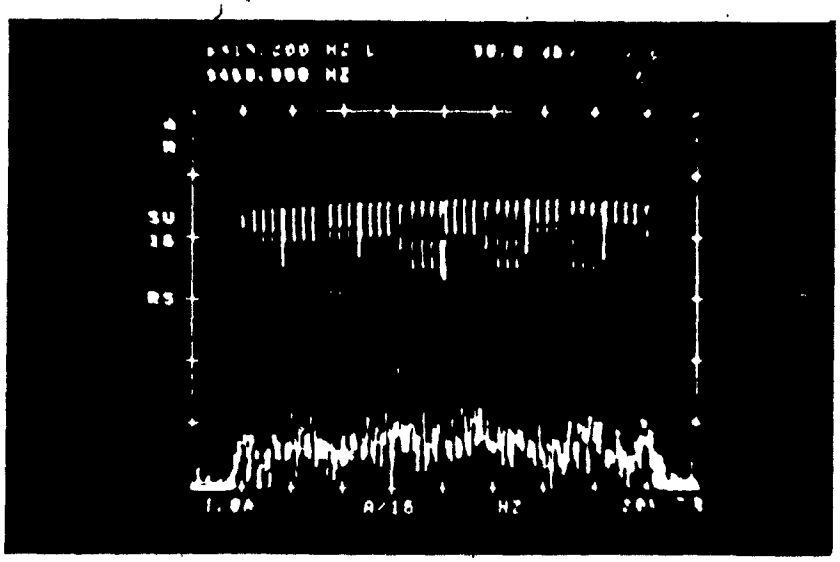

Figure IV-31 Power amplifier output .5 watts r.m.s.

G. RESULTS

Some typical results of the signal processing performed by the frequency synthesizer and transmitter will now be highlighted. Two 16-bit data words shown in Table IV-3 will be examined because they represent the two extreme cases of tone placement across the frequency band of ± 1024 Hz.

16-bit data word in binary format	16-bit data word in HEX format
0 0 0 0 0 0 0 0 0 0 0 0 0 0 0 0	0 0 0 0
1 1 0 0 1 1 0 0 1 1 0 0 1 1 0 0	c c c c

Table IV-3 Two different data words in binary and HEX formats

Data word 0000 results in tones being spaced furthest apart, that is 48 Hz. On the other hand, data word cccc, produces some tones which are only 12 Hz apart, the closest they can occur. The tone patterns at baseband and after modulation for the data words 0000 and cccc are given in Tables IV-4 and IV-5, respectively. These tables are complied from Appendix IV-3. Note that the pilot tones are fixed. They are not generated from the data words and as such they do not follow the same tone placement patterns as the tones that are synthesized. This accounts for the fact that the spacing between the pilot tones which are located at ±1020 and the adjacent tones in Figure IV-4, is not 48 Hz.

DATA WORD 0000			
f_i	f_c+f_i	f_i	f_c+f_i
-1020	7172	12	8204
-996	7196	60	8288
-948	7280	108	8300
-900	7292	156	8384
-852	7376	216	8408
-804	7388	240	8432
-756	7472	288	8516
-708	7484	336	8528
-660	7568	384	8612
-612	7580	432	8624
-564	7664	480	8708
-512	7676	528	8720
-468	7760	576	8804
-420	7772	624	8816
-372	7856	672	8900
-324	7868	720	8912
-276	8952	768	8996
-216	7976	816	9008
-192	8000	864	9092
-144	8084	912	9104
-96	8096	960	9188
-48	8180	1020	9212

Table IV-4 Tone patterns for data word 0000

DATA WORD cccc			
f_i	f_c+f_i	f_i	f_c+f_i
-1020	7172	12	8204
-996	7196	96	8288
-912	7280	108	8300
-900	7292	192	8384
-816	7376	216	8408
-804	7388	240	8432
-720	7472	324	8516
-708	7484	336	8528
-624	7568	420	8612
-612	7580	432	8624
-528	7664	516	8708
-516	7676	528	8720
-432	7760	612	8804
-420	7772	624	8816
-336	7856	708	8900
-324	7868	720	8912
-240	7952	804	8996
-216	7976	816	9008
-192	8000	900	9092
-108	8084	912	9104
-96	8096	996	9188
-12	8180	1020	9212

Table IV-5 Tone patterns for data word cccc

Figure IV-32 shows the time waveform representing the summation of the four pilot tones, at the output of the cosine channel of the frequency synthesizer. The sine channel is silent because the pilot tones are symmetrically placed around 0 Hz in the baseband. The frequency spectrum of the four pilot tones, centred around 8192 Hz, at the output of the summer, is shown in Figure IV-33.

Figure IV-34 represents the time spectrum of the output of the synthesizer on the cosine channel for data word 0000. For this pattern the sine channel, also, is active. The frequency spectrum at the output of the sine and cosine channels are shown in Figures IV-35 and IV-36, respectively. There are 40 tones at the output of the sine channel because the 4 pilot tones are absent. The output of the cosine channel, on the other hand has 42 tones, 40 generated by the data word 0000 and the other 2 representing the 4 pilot tones. This is so because the spectrum analyzer cannot distinguish between identical positive and negative frequencies. However, where two frequencies ($\pm f$) are superimposed, as in figure IV-36, there is 6 dB more energy in the spectral line representing the positive frequency (i.e. +f). Figure IV-37 shows 80 tones at the output of the sine modulator while Figure IV-38 shows 88 tones at the output of the cosine modulator. When these two spectra are combined the proper 44 tones result. This is demonstrated in Figure IV-39 which shows the frequency spectrum at the

output of the summer.

Figure IV-40 through IV-43 demonstrate the manner in which the 44 tones representing the data word cccc are created. From Table IV-5 it is seen that at baseband the 44 tones are symmetric around 0 Hz. Thus the sine channel and, consequently, the sine modulator are silent. On the cosine channel shown in Figure IV-40, there are 22 tones superimposed on another 22 tones (i.e. $\pm f_i$ i=1...22). These mix with the 8192 Hz carrier in the cosine modulator to produce the proper 44 tones, seen in Figure IV-42 and IV-43.

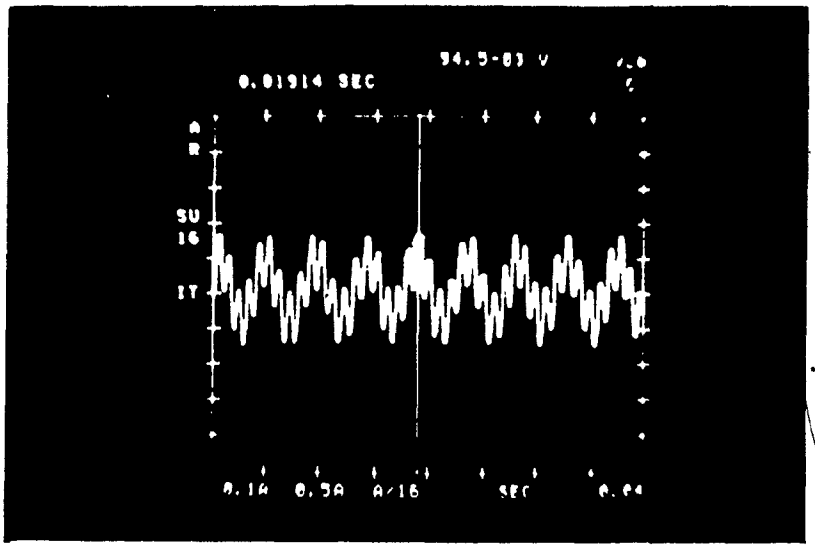

Figure IV-32 Summation of 4 pilot tones at the output of the cosine

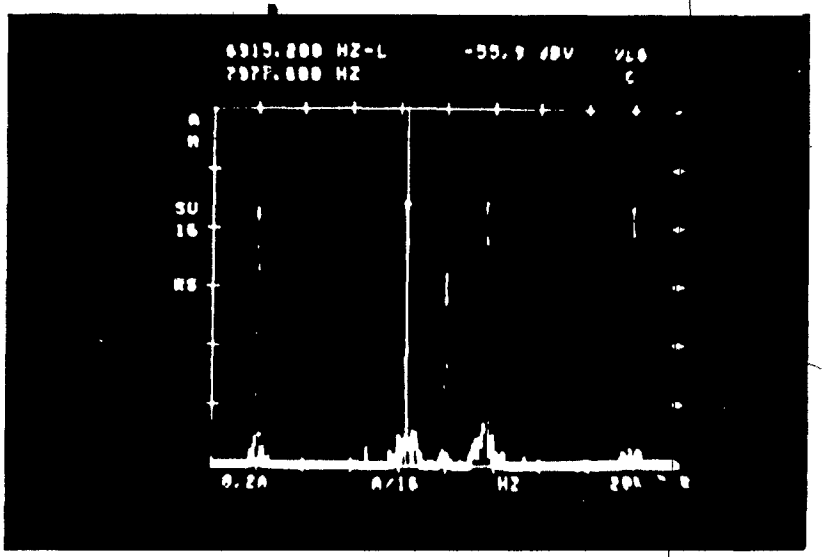

Figure IV-33 Frequency spectrum of pilot tones at the output of the summer

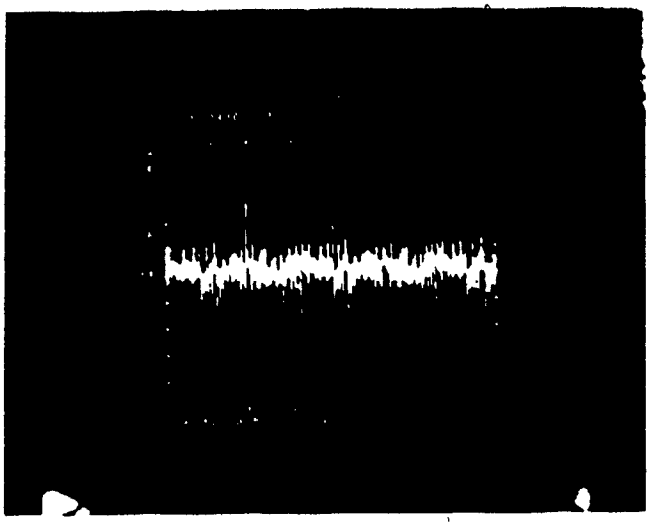

Figure IV-34 Synthesizer output on the cosine channel for data word 0000.

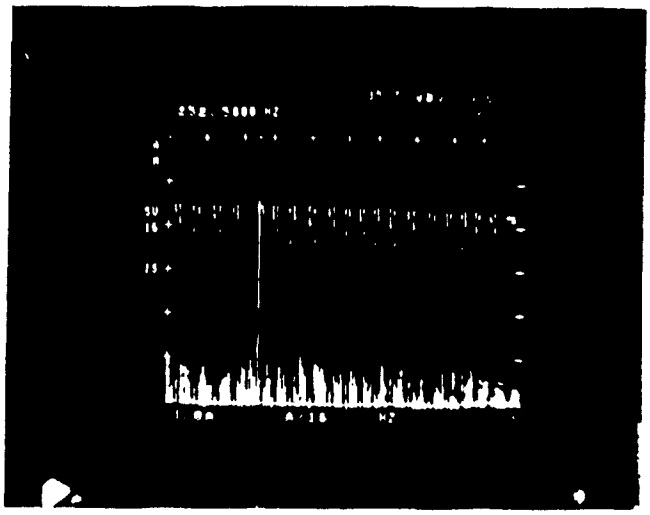

Figure IV-35 Frequency spectrum of sine channel for data word 0000

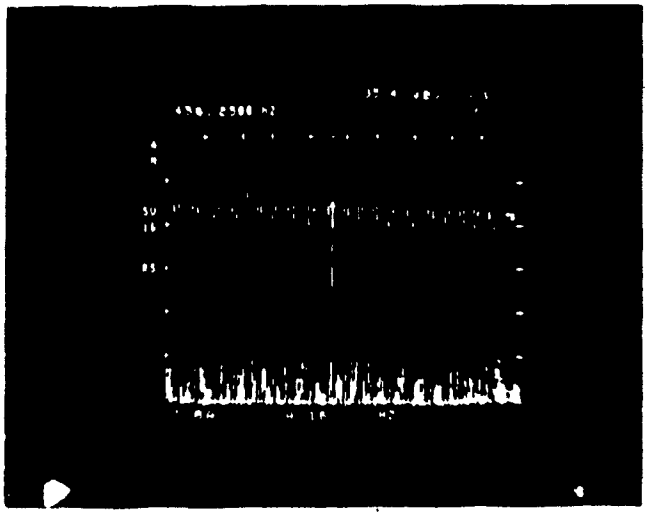

Figure IV-36 Frequency spectrum of cosine channel for data word 0000

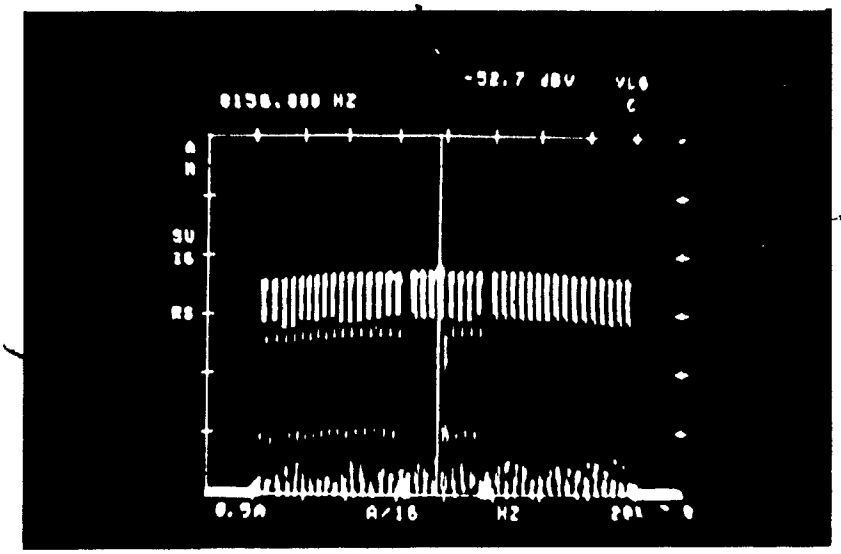

Figure IV-37 Frequency spectrum at the output of the sine modulator for data word 0000

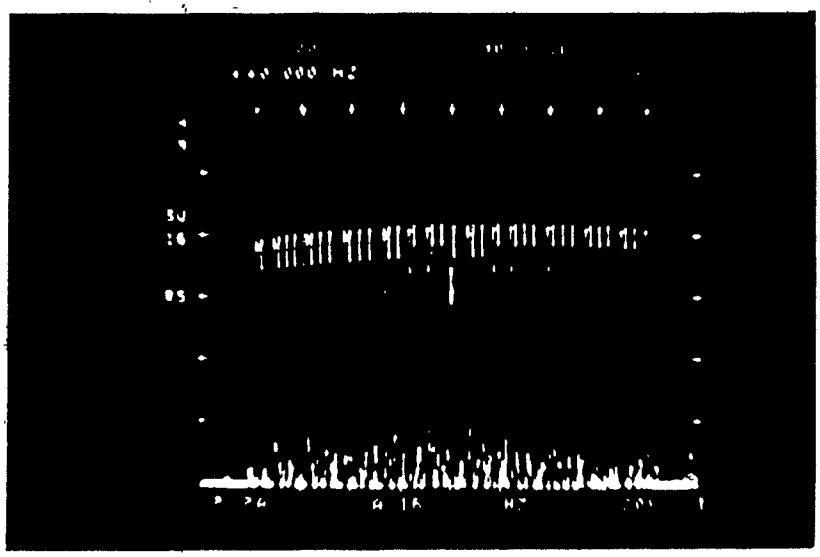

Figure IV-38 Frequency spectrum at the output of the cosine modulator for data word 0000

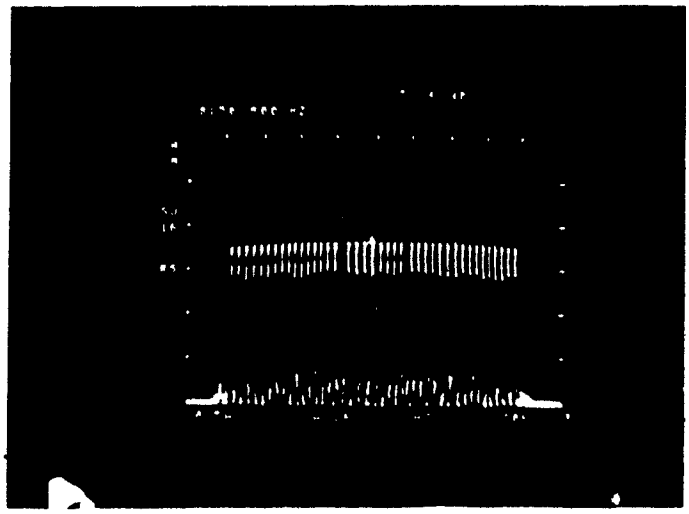

Figure IV-39 Frequency spectrum at the output of the summer for data word 0000

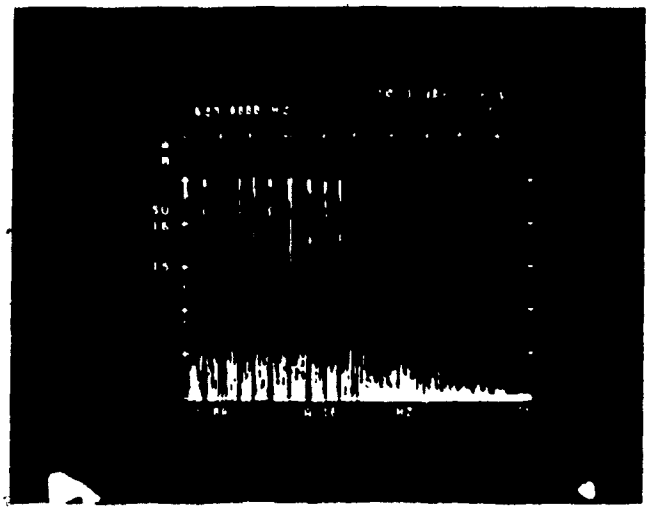

Figure IV-40 Frequency spectrum of cosine channel for data word cccc

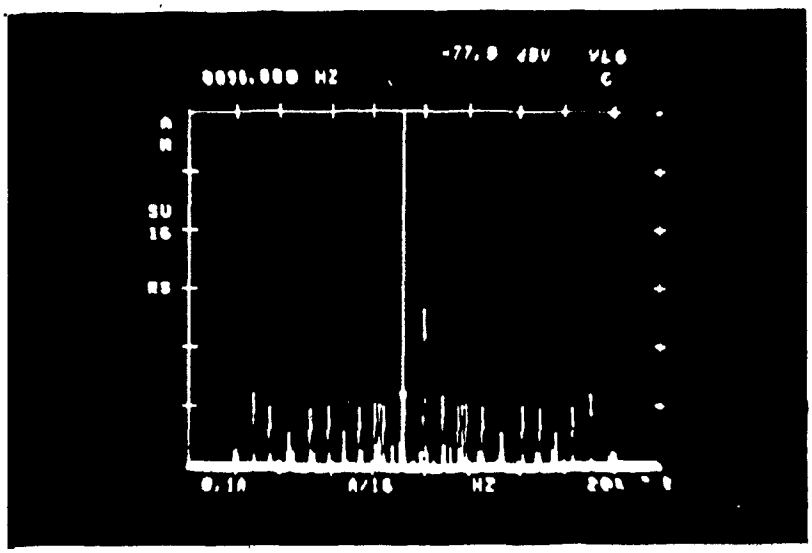

Figure IV-41 Frequency spectrum at the output of the sine modulator for data word cccc

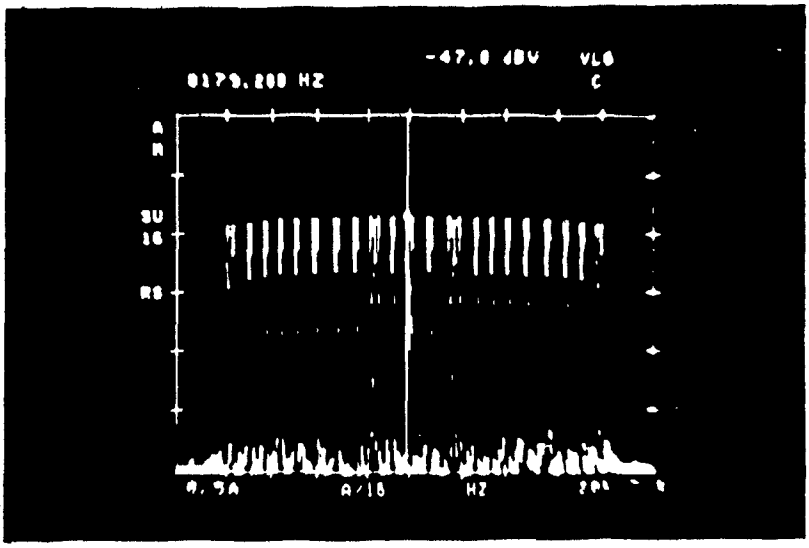

Figure IV-42 Frequency spectrum at the output of the cosine modulator for data word cccc

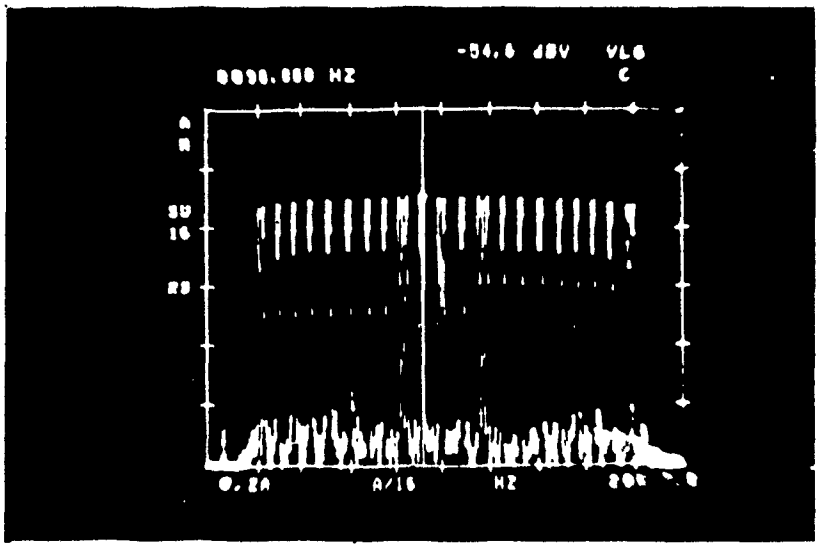

Figure IV-43 Frequency spectrum at the output of the summer for data word cccc

REFERENCES

1. Groski-Popiel, Jerzy, Frequency Synthesis: Techniques and Applications, IEEE Press, New York, 1975.

2. Schwartz, M., Information, Transmission, Modulation and Noise, McGraw Hill, New York, 1980.

3. Stein, S., et al., Communication Systems and Techniques, McGraw Hill, New York, 1966.

4. Buxton William, "Design Issues in Generation of a Computer-based Tool for Music Composition", Computer Systems Research Group Tech. Report CSRG-97, 10/78, University of Toronto.

5. Morgera, S.D., "A conceptual design of an underwater acoustic telemetry system, Phase II study", Prepared for Canadian Department of Environment, Oceans and Fisheries, 20th February 1980.

6. Morgera, S.D., "Multiple Terminal Acoustic Communications System Design", IEEE J. on Oceanic Engineering, Vol. OE5, No. 3, July 1980.

7. Morgera, S.D., "Optimum Underwater Acoustical Telemetry Techniques", prepared for Canadian Department of Environment, Oceans and Fisheries, contract 07SC.KF806-8-E330, 8th February 1979.

8. Nuttall, A.H., "Error Probability characteristics for Orthogonal Alternative Communication with D-fold

Diversity", NUCS TR4769, 19th June 1974.

CHAPTER V

THE MICROCOMPUTER SUBSYSTEM; ITS DESIGN AND OPERATION

A. INTRODUCTION

A microcomputer is a fully operational computer system built around a microprocessor. Included in a microcomputer are, memory, a clock and interfaces. A microcomputer subsystem, configured around the RCA CDP 1802 COSMAC microprocessor, forms the heart of the acoustic telemetry system. This Chapter discusses the design and functions of the microcomputer subsystem. It explains the choice of microprocessor and discusses the manner in which the microcomputer is interfaced with the remainder of the telemetry system to perform a number of specific functions. These functions are outlined and a flowchart explaining the manner in which they are executed, is described.

B. RCA CDP 1802 COSMAC MICROPROCESSOR

One of the initial steps in the development of a microcomputer system, is the establishment of a set of criteria for microprocessor selection. Some factors to be considered in this respect are:

(a) cost

(b) Reliability

(c) Peripheral compatability

(d) Performance

(e) Power consumption

(f) The availability of a good software support system.

The last two considerations were most important in establishing the RCA CDP 1802 COSMAC microprocessor as the choice of microprocessor for the microcomputer in the acoustic telemetry system. The placement of the bottom unit of the acoustic telemetry system on the ocean floor imposes a severe power constraint in its design. This, together with the fact that the microcomputer subsystem is always on, thus consuming power, meant that it was absolutely necessary to minimize power consumption. Since the 1802 microprocessor is one of the few available CMOS, single voltage supply, central processing units, it was a natural choice. Moreover, the Concordia University research laboratories have extensive PDP 11/45 - based support hardware and support software for the development of COSMAC-based microcomputer systems.

The CDP 1802 microprocessor includes all of the circuitry required to fetch, interpret, and execute instructions which can be stored in standard type memories. It also has extensive input/output (I/O) features to facilitate system design. Some of its special features and operating characteristics are [1]:

(a) Static CMOS circuitry, no minimum clock frequency.

(b) Full military temperature range (-55 to +125°C).

(c) High noise immunity, wide operating-voltage range.

(d) Simple control of reset, start, and pause.

(e) 8-bit parallel organization with bidirectional data bus.

(f) Direct memory addressing up to 65,536 bytes.

(g) Four I/O flags testable by branch instructions.

(h) 91 easy to use instructions.

The CDP 1802 can be operated from an external clock connected to the clock input or from an oscillator formed by connecting a crystal between the $\overline{\text{Xtal}}$ and clock inputs. The speed of the clock determines the operating speed of the microprocessor which requires 8 clock pulses to complete each machine cycle. Each instruction requires either 2 or 3 machine cycles for execution. A two bit state code (SC0, SC1), is provided to indicate which of the four states the machine is in (i.e. fetch, execute, DMA transfer or interrupt).

The CDP 1802 provides 8 memory address lines, supplying a 16 bit address word in the form of two consecutive

address bytes. The high order address byte (A_{15}-A_8) appears on the address lines first followed by the low order address byte (A_7-A_0). The timing signals, TPA and TPB, are used by the memory and I/O systems to latch memory address, to take memory data from the bus, and to set and reset the I/O controller flip flops. The relationship between TPA, TPB and the 8 address lines is shown in Figure V-1.

Bytes are transferred between I/O devices, memory, and the RCA 1802 microprocessor by means of a common bidirectional 8-bit data bus. The microprocessor provides two lines ($\overline{MRD}$, $\overline{MWR}$), to control the memory read/write cycles. During a memory write cycle, the byte to be written appears on the data bus, either from the CPU or an I/O device, and the CPU generates a memory write ($\overline{MWR}$) pulse at the appropriate time. During a memory read cycle ($\overline{MRD}$), a memory read level is generated by the system to gate the memory output byte onto the data bus for use by the CPU or an I/O device.

There are fifteen I/P control signal lines. These are SC0, SC1, TPA, TPB, $\overline{MRD}$, N0, N1, N2, $\overline{DMA-IN}$, $\overline{DMA-OUT}$, $\overline{INT}$, Q, $\overline{EF1}$, $\overline{EF2}$, $\overline{EF3}$, and $\overline{EF4}$. The Q line is under the control of the microprocessor and the four flag lines are directly testable by COSMAC instructions to determine whether or not they are active.

Finally, there are the $\overline{clear}$ and $\overline{wait}$ lines, which provide the microprocessor with one of four operating modes.

These modes together with a signal description of all the other lines mentioned above are outlined in Figure V-2.

C. MICROCOMPUTER DESIGN

The microcomputer subsystem consists of three circuit cards. They are:

(a) The CPU and buffer card

(b) The memory card

(c) The timing card

A block schematic diagram of the microcomputer is shown in Figure V-3.

1. The CPU and Buffer Card

The schematic diagram of the CPU and buffer card is shown in Figure V-4. A photograph of the card is shown in Figure V-5. The card contains the RCA CDP 1802 microprocessor, buffers, and the master clock which provides a frequency of 262144 Hz. Data lines D0 through D7 are buffered by IC chips A2. IC chips B2, B3, C3, and C4 buffer a number of lines which are routed to the synthesizer and are active only when an interrogation command has been recognized by the command receiver and transmission of the tidal data stored in memory is about to begin

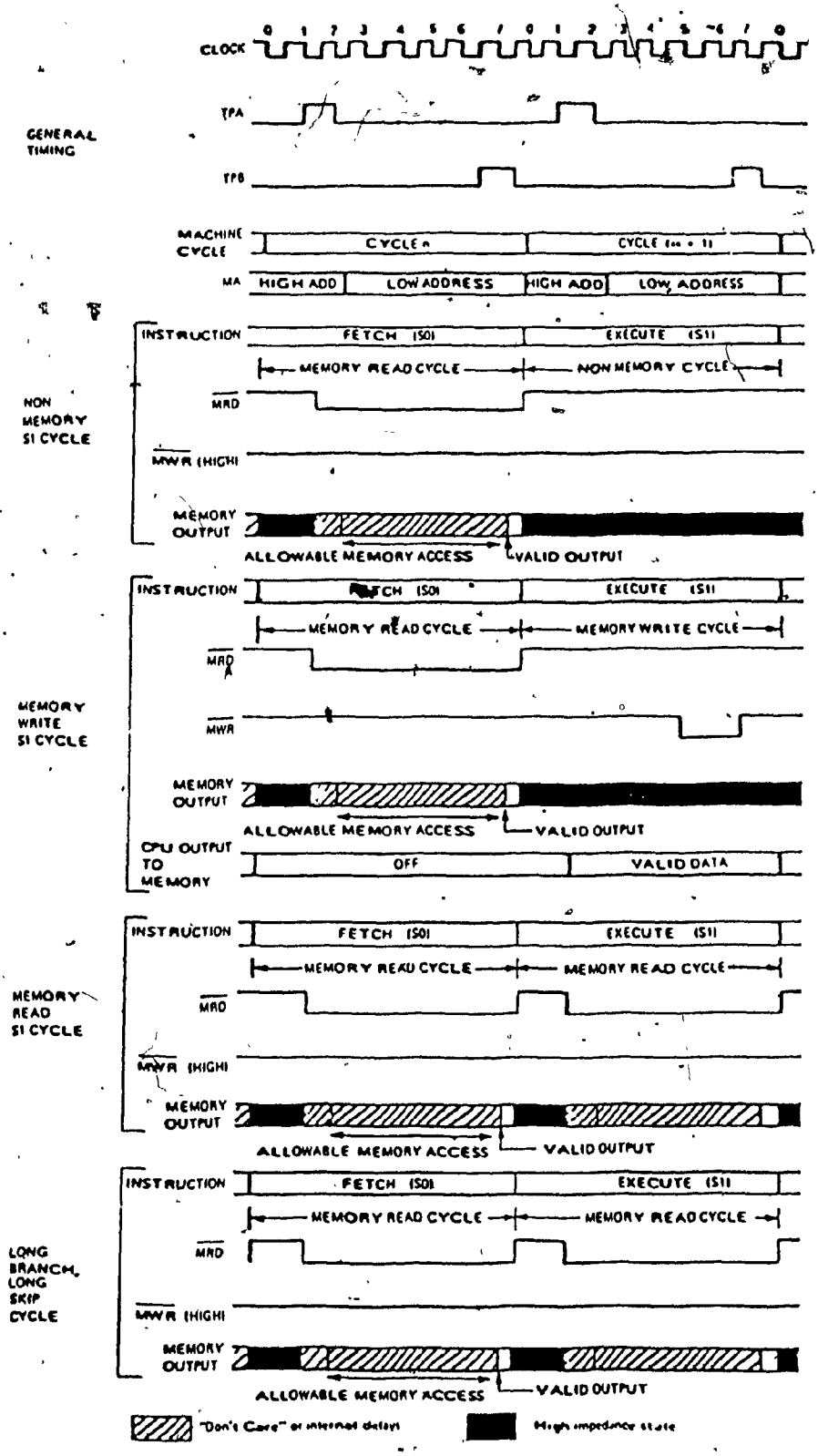

Figure V-1 RCA 1802 timing waveforms

Signal Descriptions

BUS_{0-7}
8-bit bidirectional data bus for CPU - memory - I/O transfers.

N_{0-2}
I/O selection lines. The 3 lowest-order bits of the N register appear on these lines when an input or output instruction is executed. They are used to uniquely select the desired I/O port. Different I/O instructions generate different signals on the N- lines (op codes 61–67 are outputs, 69–6F are inputs).

Q
Bit-serial output line that can be set or reset under program control via two dedicated instructions (7B, 7A).

INTERRUPT
Input to the CPU that initiates execution of the user's interrupt service program.

$\overline{DMA\ IN}$
$\overline{DMA\text{-}OUT}$
Direct Memory Access request lines. Initiates DMA data transfer action within the SCP1802.

$\overline{EF_{1-4}}$
Four External Flag lines. Conditionally tested by branch instructions to convey external information to the CPU, prioritize multiple interrupts, etc.

SC_0, SC_1
The State Code lines output the SCP1802's current machine state.

STATE		SC_0	SC_1
S0	Instruction Fetch	0	0
S1	Instruction Execute	0	1
S2	DMA Transfer	1	0
S3	Interrupt	1	1

MA_{0-7}
8-bit Memory Address bus carries the multiplexed 16-bit memory address, high-order byte first followed by the low-order byte.

$\overline{MWR}$
Memory Write. A pulse appearing after the memory address lines have stabilized.

$\overline{MRD}$
Memory Read signal. Can be used to control 3-state outputs from addressed memory if it has a common data in/out bus. Also used to indicate direction of data transfer during an I/O instruction.

CLOCK
Input for external one phase clock signal.

$\overline{XTAL}$
A crystal is connected between $\overline{XTAL}$ and CLOCK (typically with a 10 megohm resistor) when the on-chip oscillator is used.

$\overline{WAIT}$
$\overline{CLEAR}$
Control lines to determine the SCP1802's mode:

MODE	$\overline{CLEAR}$	$\overline{WAIT}$
Run	1	1
Pause	1	0
Reset	0	1
Load	0	0

Run: Normal CPU instruction execution.

Pause: Stops CPU operation at the next high-to-low clock input; only the oscillator continues to operate.

Reset: I, N, Q, X, P, R (0), BUS ↓ 0
IE ↓ 1 (interrupts enabled)

Load: Allows an I/O device to load memory from location 0000 without a "bootstrap loader".

V_{DD}, V_{CC}, V_{SS}
The I/O voltage supply level V_{CC} is isolated from the internal CPU voltage level V_{DD}. This allows for simple interfacing between the SCL1802 and TTL, NMOS, etc. V_{SS} is ground.

TPA
Timing Pulse for strobing high order memory address byte into external latch or ROM.

TPB
Timing Pulse used by external I/O devices to time interaction with CPU.

Figure V-2 RCA 1802 signal description

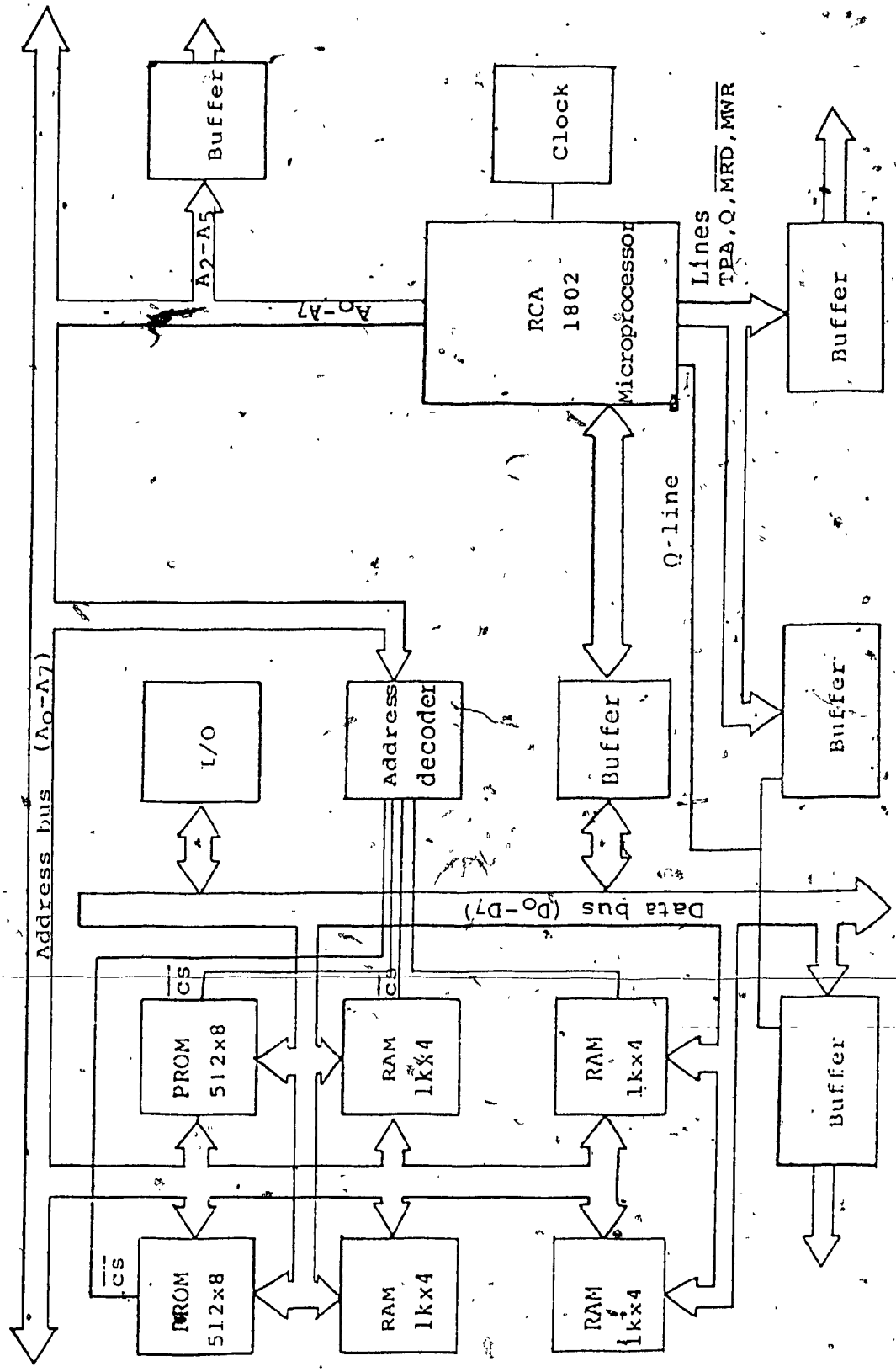

Figure V-3 Block schematic diagram of microcomputer subsystem

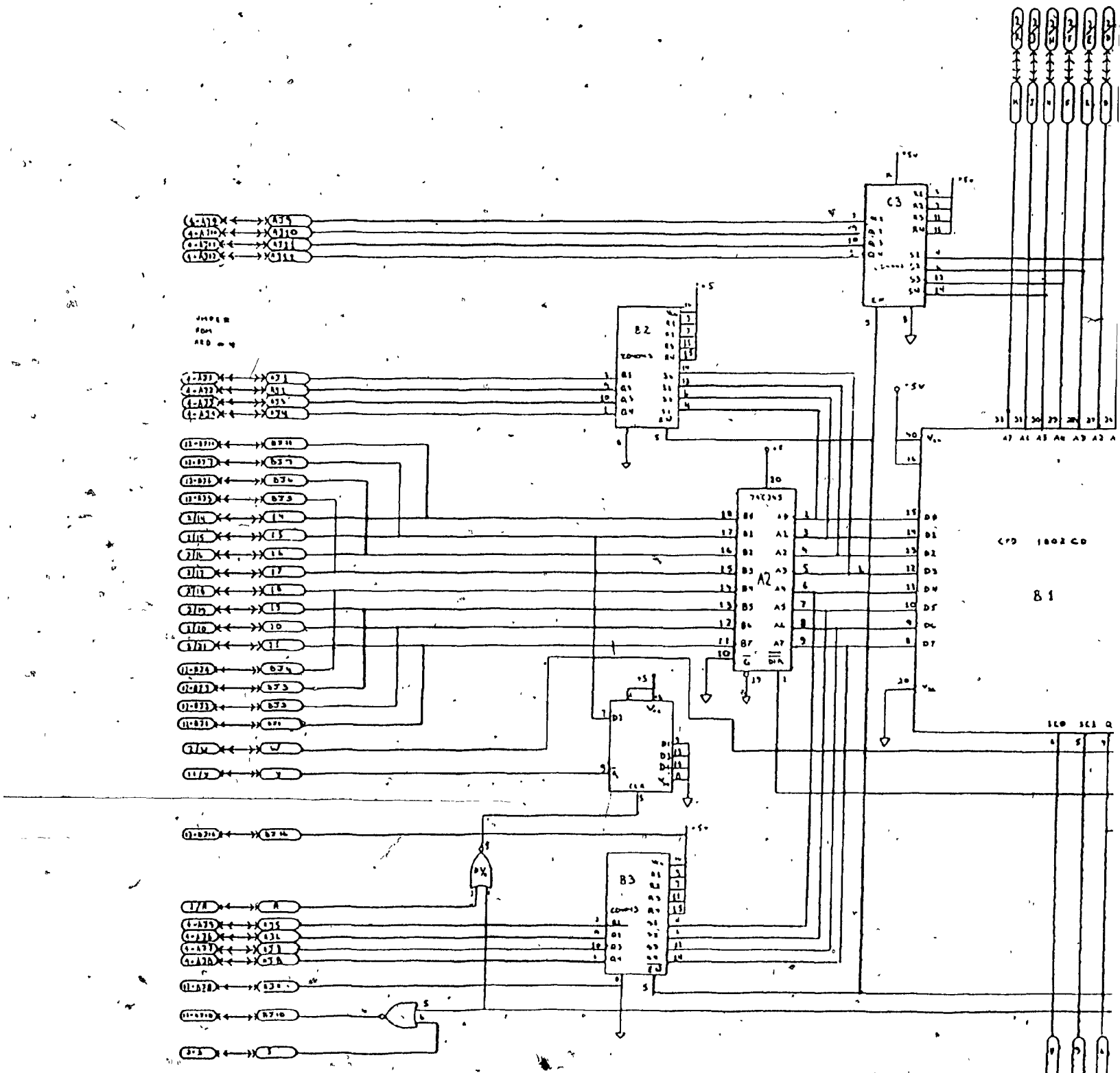

Figure V-4 Schematic diagram of CPU and buffer card

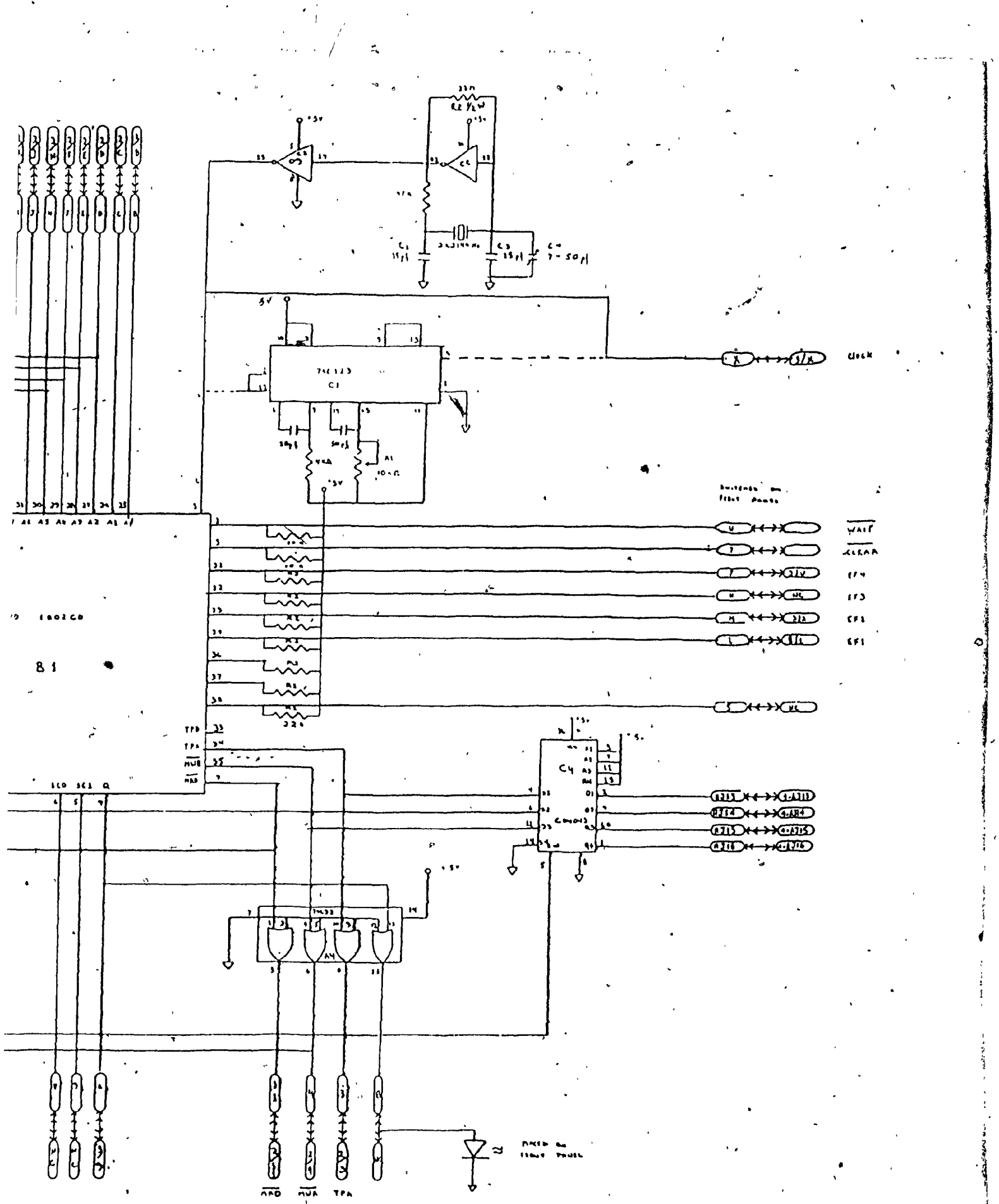

2 of 2

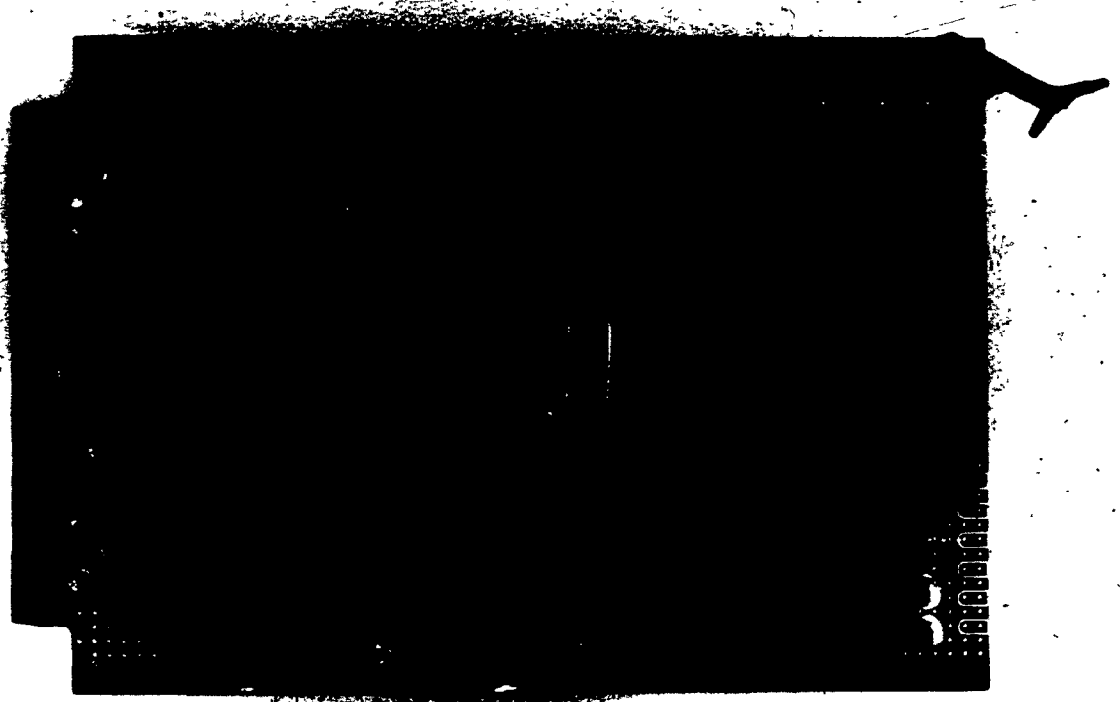

Figure V-5 Photograph of CPU and buffer card

2. Memory Card

The schematic diagram and photograph of the memory card are shown in Figure V-6 and V-7, respectively. The card consists of the microcomputer memory and an address decoder. The memory is made up of 1 kbyte of PROM and 2 kbytes of RAM. The PROM stores the system's executive program and two look-up tables, one containing the noise values used in the noise normalization routine, and the other holding a 16x1 matrix used for data encoding. The first kbyte of RAM is used as scratch pad memory for the storage of variables and intermediate results produced during the signal processing. The second kbyte of RAM is for the storage of tidal data from the Aandera tide guage. The organization of this 3 kbytes of memory is shown in Figure V-8.

Since the microprocessor is an 8-bit machine, address decoding is necessary in order to expand the memory to its full capacity. The microprocessor can address 2^{16}=65 kbytes of memory. The upper 32 kbytes is set aside for I/O selection. Each I/O device is assigned a unique address code. Figure V-9 illustrates how address bits A_{13} through A_{10} are decoded to provide 16 addresses in the upper 32 kbytes of memory for I/O selection.

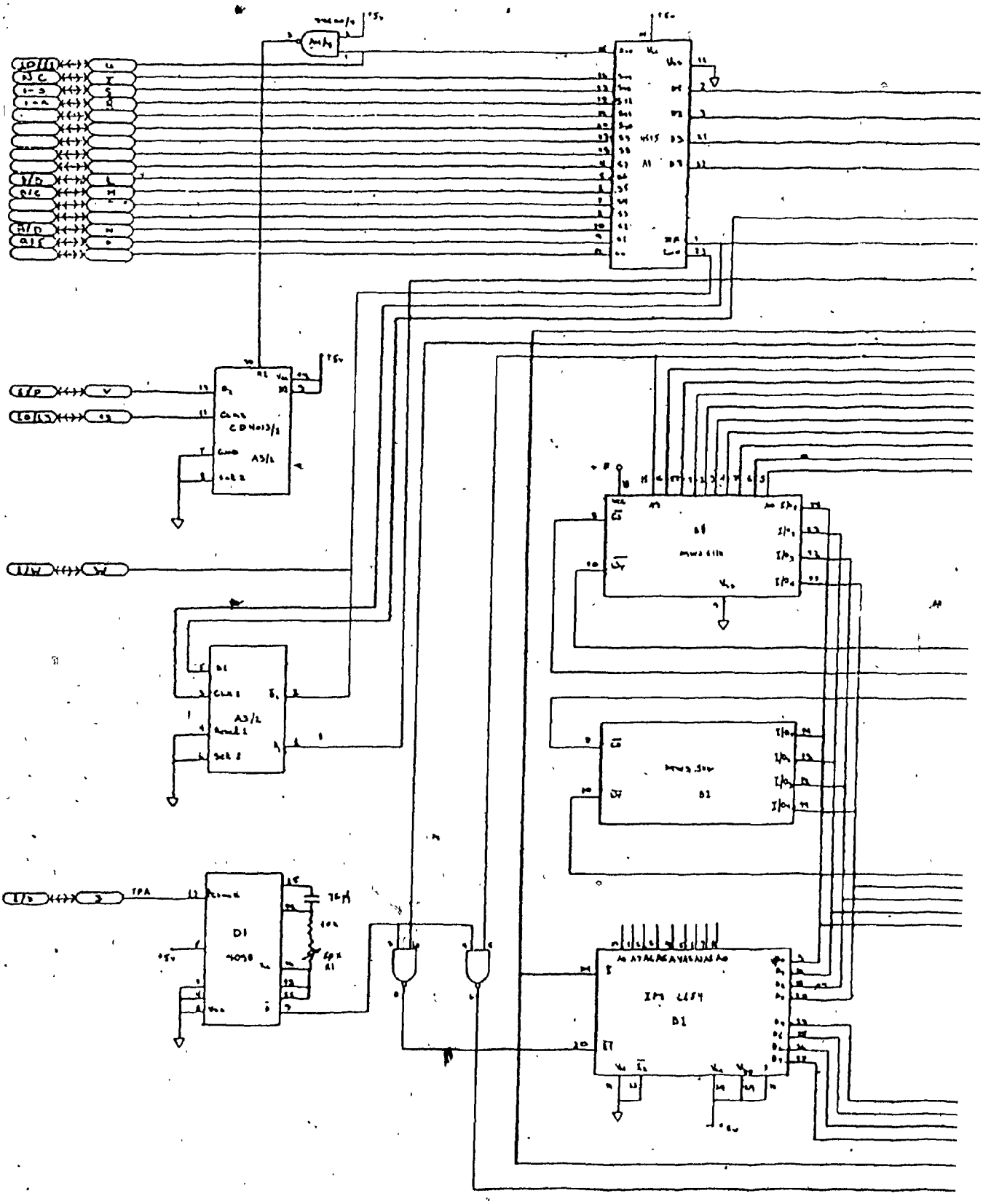

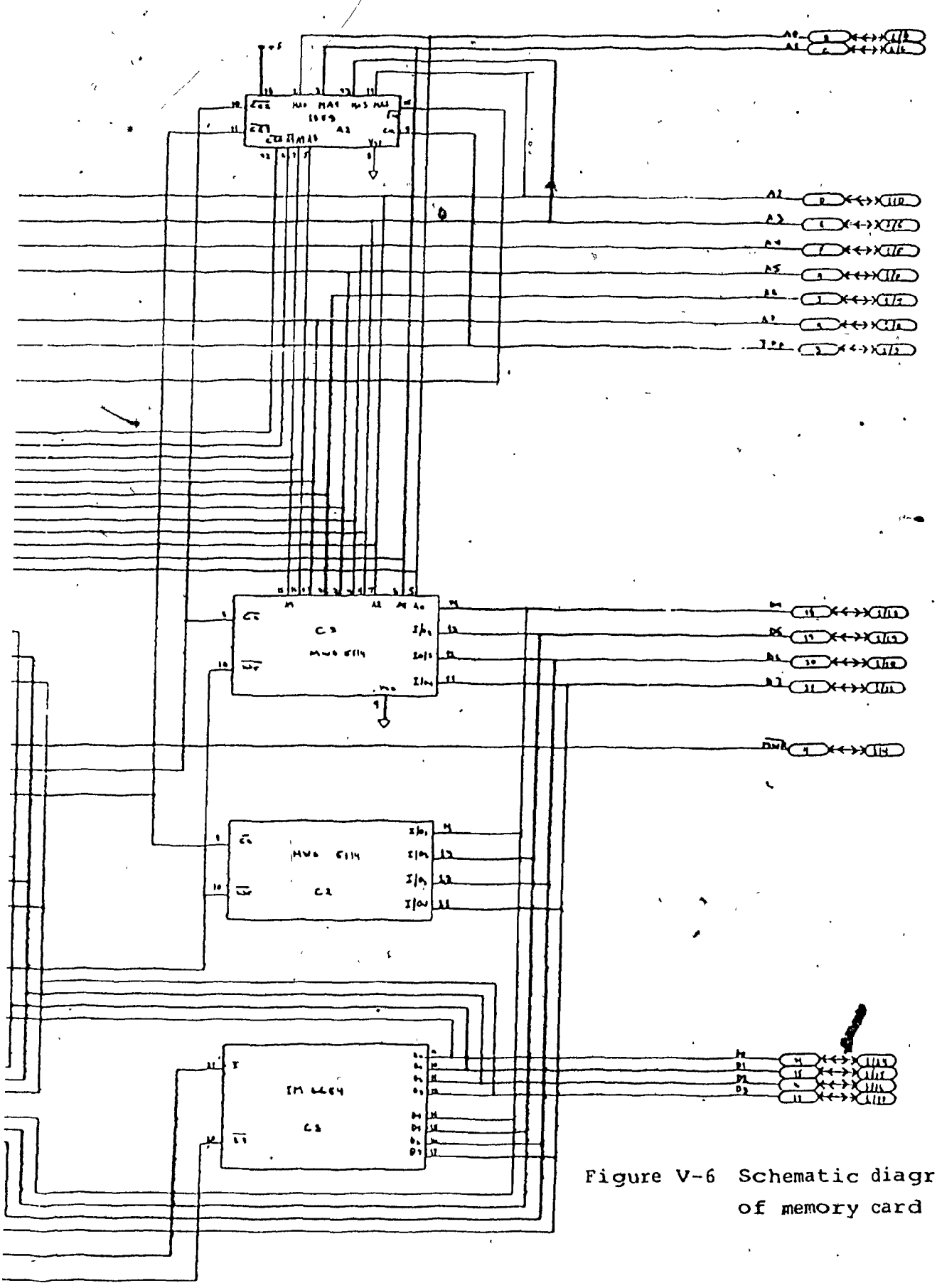

Figure V-6 Schematic diagram of memory card

Figure V-7 Photograph of memory card

Address in Hex	Chip selected (card-chip)	Content of memory
0000-01FF	2-B1	First half of system program
0200-03FF	2-C1	Remainder of system program, storage of first row of encoding matrix. Storage of noise lookup Table.
0400-07FF	2-(B2,C2)	Scratch pad memory
0800-0BFF	2-(B3,C3)	Storage of tide gauge data

Figure V-8 Organization of the lowest 3kbyte of memory

Address in Binary								Chip selected (card-chip)	Function of I/O Device
A_{15}	A_{14}	A_{13}	A_{12}	A_{11}	A_{10}	A_9	A_8		
1	0	0	0	0	0	0	0	4-A1	Seperates odd and even bits of high byte of tidal data
1	0	0	0	0	1	0	0	8-A4	Holds the low byte of tidal data
1	0	0	0	1	0	0	0	8-A3	Holds the high byte of tidal data
1	0	0	0	1	1	0	0		
1	0	0	1	0	0	0	0	4-A2	Separates odd and even bits of low byte of tidal data
1	0	0	1	0	1	0	0	8-C3	Holds the low byte of time data
1	0	0	1	1	0	0	0	8-C4	Holds the high byte of time data
1	0	0	1	1	1	0	0		
1	0	1	0	0	0	0	0	4-B3	Determines the modes of the synthesizer
1	0	1	0	0	1	0	0		
1	0	1	0	1	0	0	0		
1	0	1	0	1	1	0	0		
1	0	1	1	0	0	0	0	1-D1	Controls relay that connects power amp O/P to transducer
1	0	1	1	0	1	0	0	Front Panel	Latches data for noise display
1	0	1	1	1	0	0	0		
1	0	1	1	1	1	0	0	10-	D/A conversion of diveristy channel outputs

Figure V-9 I/O address assignment

3. The Timing Card

The schematic diagram of the timing card is shown in Figure V-10 and a photograph of the card is given in Figure V-11. The card is essentially comprised of counters which sub divides the clock frequency of 262144 Hz providing the base for all the timing pulses used in the command receiver and the synthesizer. It also has the circuitry that provides the 50% duty cycle power supply for the command receiver and the circuitry that turns the power to the frequency synthesizer on and off.

D. FUNCTIONS OF THE MICROCOMPUTER SUBSYSTEM

The microcomputer subsystem provides the storage for the tidal data collected by the gauge interface unit. The manner in which this is accomplished is described in Chapter IV, Section C. It also works in conjunction with the command receiver to perform the signal processing functions that are essential in determining whether or not the bottom unit has been interrogated by the top unit. These funtions are outlined and discussed in Chapter III, Section D. When the command receiver has been interrogated, the microcomputer turns on the power to the synthesizer and power amplifier and then recalls the tidal data stored in memory for transmission. Because of the fading dispersive nature of the acoustic medium, it is necessary to protect

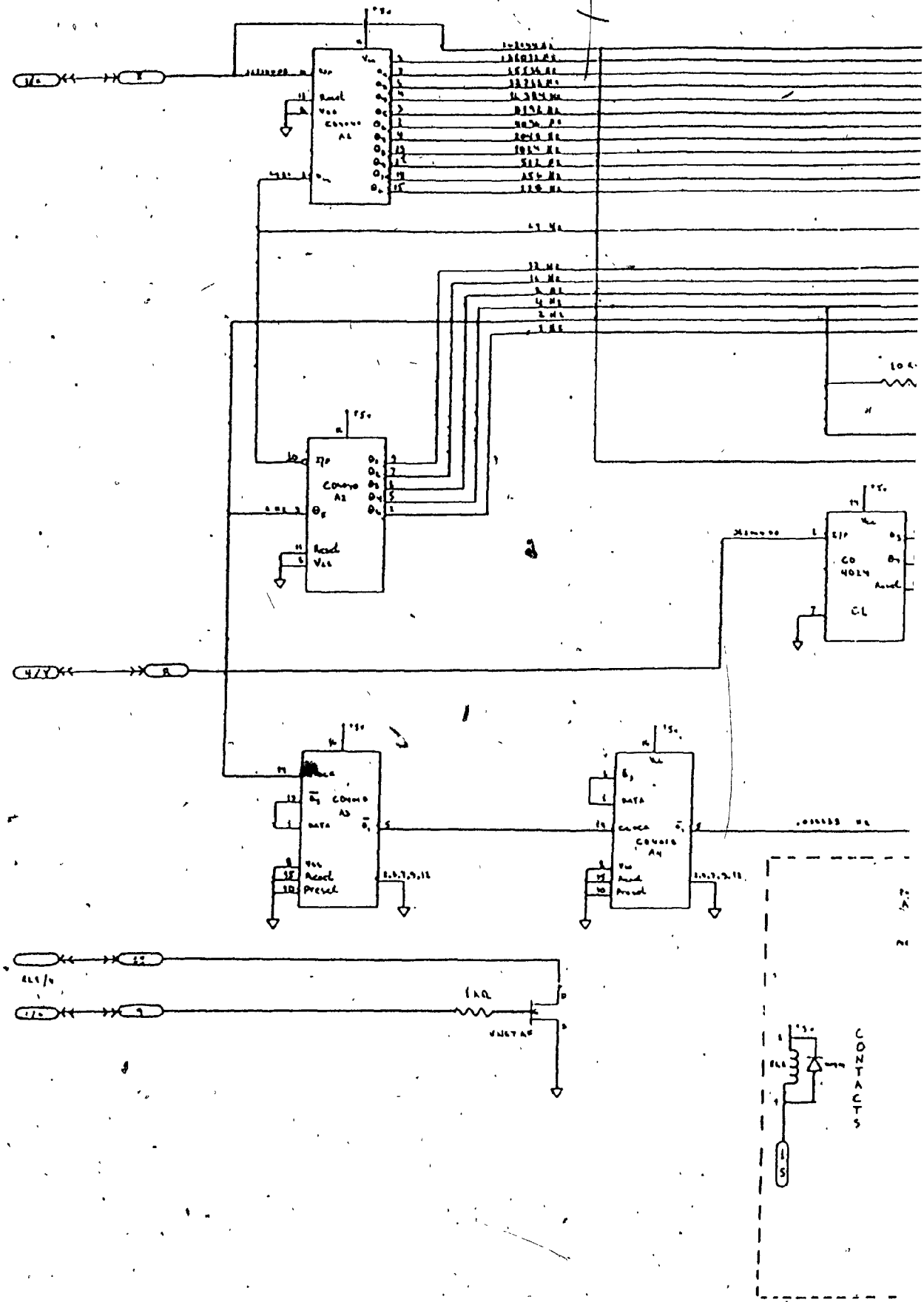
CONTACTS

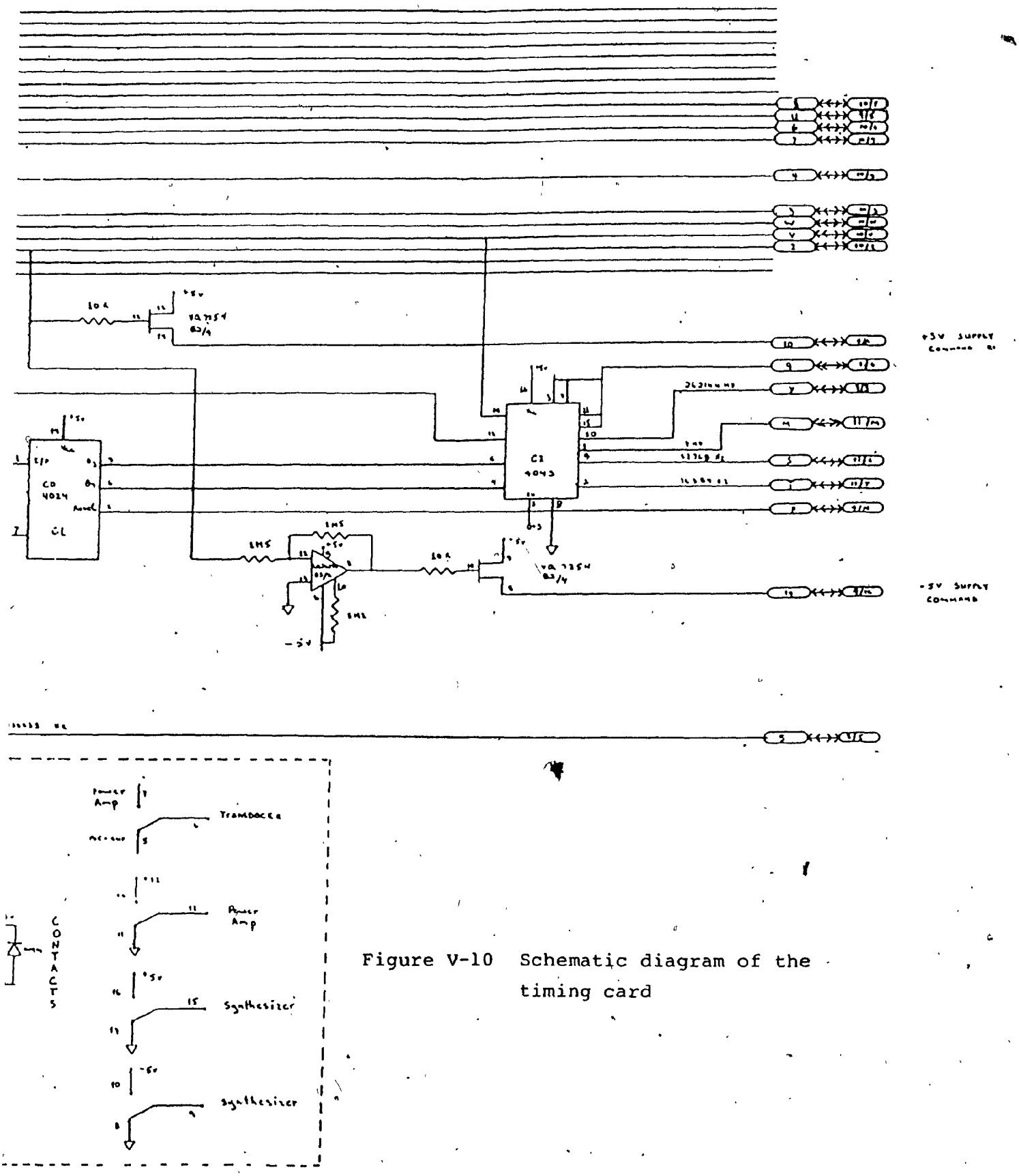

Figure V-10 Schematic diagram of the timing card

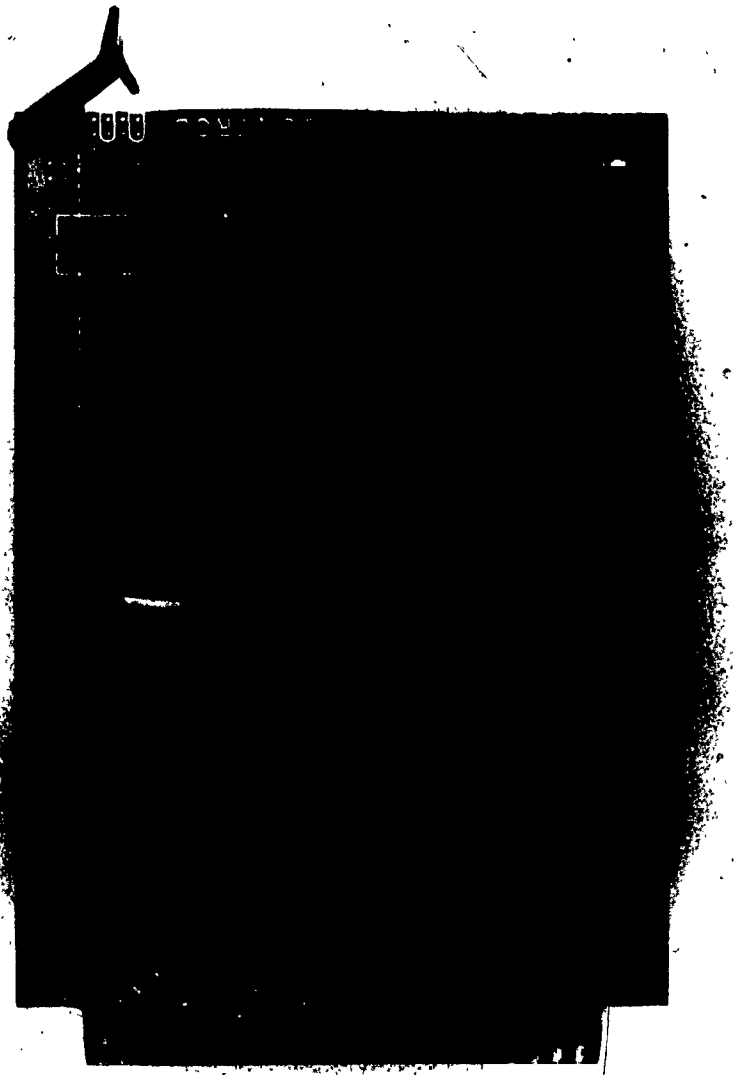

Figure V.11 Photograph of the timing card

against the possible corruption of the data that is transmitted. This protection takes two forms: first, the data is duplicated by means of 5-fold diversity transmission and second, it is encoded. Data encoding is one of the functions of the microcomputer that has not been previously discussed.

1. Encoding

A practical method of reducing the probability of incorrect data transfer is to employ error-correcting codes to encode the data. The implementation of encoding and decoding schemes is usually accomplished through the use of special purpose hardware. However, if time permits, it is possible to use software for the same purpose. The use of software for encoding presents certain advantages over the use of hardware. Some of these are:

(a) Occupation of less space due to less hardware.

(b) Reduced power consumption.

(c) Increased encoder flexibility resulting form the fact that it is much easier to change a computer program than to reconfigure and rewire hardware.

Advantages (a) and (b) above assume, of course, that the

microcomputer is required in the system to perform other tasks as well. The code used in this design is a (32,16) quasi-cyclic code capable of correcting all 3-error patterns and some 4-error patterns. Quasi-cyclic codes are a special case of binary cyclic codes which can be completely specified either by their parity check or generator polynomials. These polynomials are related by the expression,

$$h(x)\ g(x) = x^n - 1 \qquad \text{V-1}$$

where $h(x)$ is the parity check polynomial and $g(x)$ is the generator polynomial. Cyclic codes are invariant under a large group of permutations. The same is true of quasi-cyclic codes. A (mn_o, mk_o) linear code, C , is said to be cyclic if it has the following property. If an n-tuple,

$$\underline{V} = (V_o, V_1, \ldots, V_{n-1})$$

is a code vector in C, then

$$\underline{V}(n_o) = (V_{n-n_o}, V_{n-n_o+1}, \ldots, V_{n-n_o-1})$$

obtained by shifting $\underline{V}$ cyclically by n_o bits to the right, is also a code vector in C.

Thus, cyclic codes for which an integer $m \neq 1$, divides both n and k are said to be quasi-cyclic. Quasi cyclic codes are therefore invariant under the permutation

$i \rightarrow (i+n_o) \mod mn_o$ [3,4]. There are 396 (32,16) quasi-cyclic codes, four of which have been examined by Tavares, et al. [6]. The (32,16) quasi-cyclic code used for encoding is one of these four. It is chosen because it has the largest gap in its weight distribution and because the circulant matrix by which it is characterized has an inverse, a necessary condition for karlin-type decoding. The first row of the circulant matrix of the (32,16) quasi-cyclic code is given by,

$$C(x) = 1+x+x^2+x^3+x^4+x^6+x^9 \qquad \text{V-2}$$

The first row of the inverse circulant matrix is given by,

$$C^{-1}(x) = 1+x^7+x^{10}+x^{12}+x^{13}+x^{14}+x^{15} \qquad \text{V-3}$$

Any rate one-half systematic quasi-cyclic code can be written as,

$$\underline{V} = IG = [I, IC] \qquad \text{V-4}$$

where I is the information vector to be encoded, G is the generator matrix and C is the circulant matrix. From V-4, it is seen that the code vector $\underline{V}$ comprises the information vector followed by a parity check vector formed by multiplying the information vector by the circulant matrix.

The realization of V-4, can be accomplished in one of two ways:

(a) The information vector can be stored in a 16x1 array, the circulant matrix in a 16x16 array and the code vector generated by straight forward matrix multiplication with addition done modulo 2.

or

(b) The information vector and the first row of the circulant matrix can both be stored in 16x1 arrays and encoding can be accomplished by generating the circulant matrix row-by-row from the first row, and then multiplying it by the code vector, with addition again done modulo 2.

The first approach utilizes more storage than the second, but it is quicker. However, since the encoding can be done during the dead time between transmissions the second approach is better suited to this design and is in fact, the one used.

E. MICROCOMPUTER PROGRAM EXECUTION

The manner in which the system program is executed is illustrated in the flowchart of Figure V-12. The flowchart can be described in very general terms. Initially all registers to be used as pointers and counters are set-up. Also, memory locations in which data or vaiables are to be stored are assigned and initialized. The signal estimates $\{\hat{E}_i(n\Delta)\}$ at the output of the diversity channels are then formed. Each estimate is normalized by the long term noise estimates $\{\hat{N}_i(\Delta)\}$ on the appropriate diversity channel to form a weighting rule $\{\gamma_i(n\Delta) = \hat{E}_i(n\Delta)/N_i(n\Delta)\}$, similar to a "signal-to-noise" ratio for that channel. The summation of the "signal-to-noise" ratios of all the diversity channels form a partial detection statistic $\gamma(n\Delta)$, two consecutive values of which are added to form the final detection statistic, denoted by γ. This detection statistic is tested against a threshold Λ and a decision as to whether or not the bottom unit has been interrogated is reached. If the unit has not been interrogated, the program continues in a loop, collecting tidal data and continuously performing the signal processing functions, until the threshold has been exceeded. When this occurs, power is applied to the frequency synthesizer and the power amplifier. The power amplifier is allowed to stabilize and then a preamble

consisting of a specific sequence is transmitted. After this, the data in memory is sequentially encoded and transmitted. When the transmission is finished, the power to the synthesizer and the power amplifier is turned off and the program sequence begins again.

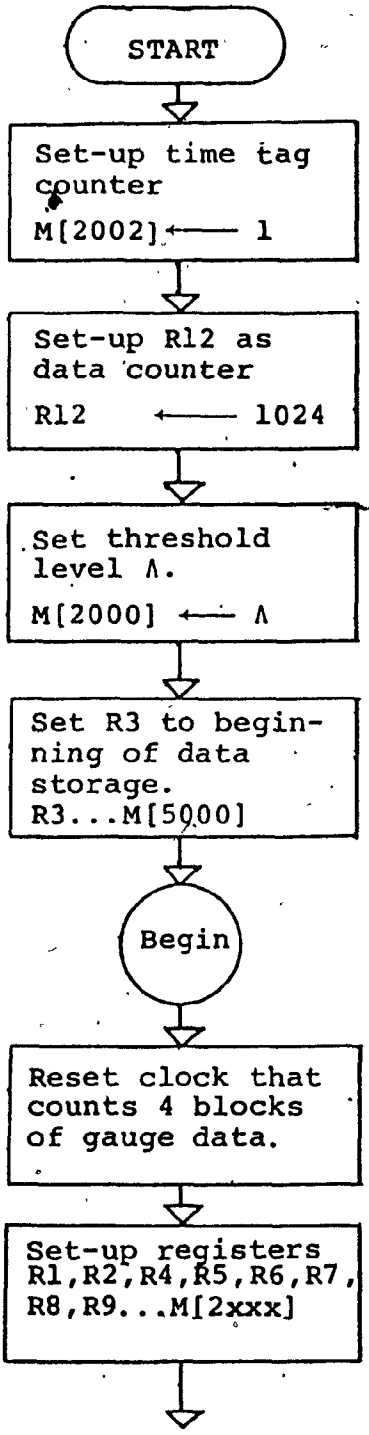

1. M[A]←B means that variable B is stored in memory location A

2. R0-R15 are sixteen general purpose registers.

   RX..M[A] means that register X is pointing to memory location A

Figure V-12 System program flowchart

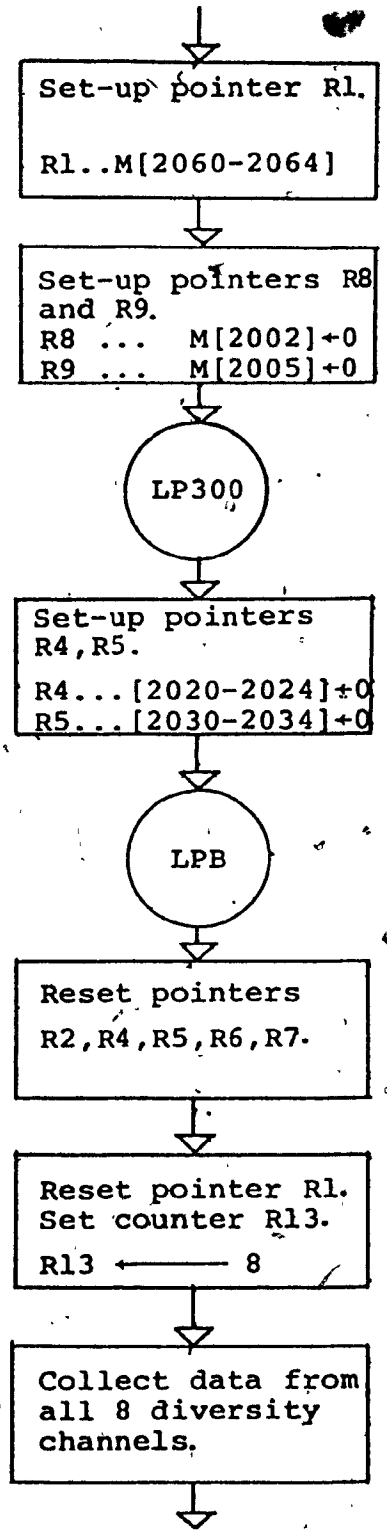
Set-up pointer R1.
R1..M[2060-2064]
Set-up pointers R8 and R9.
R8 ... M[2002]←0
R9 ... M[2005]←0
LP300
Set-up pointers R4,R5.
R4...[2020-2024]←0
R5...[2030-2034]←0
LPB
Reset pointers R2,R4,R5,R6,R7.
Reset pointer R1.
Set counter R13.
R13 ← 8
Collect data from all 8 diversity channels.

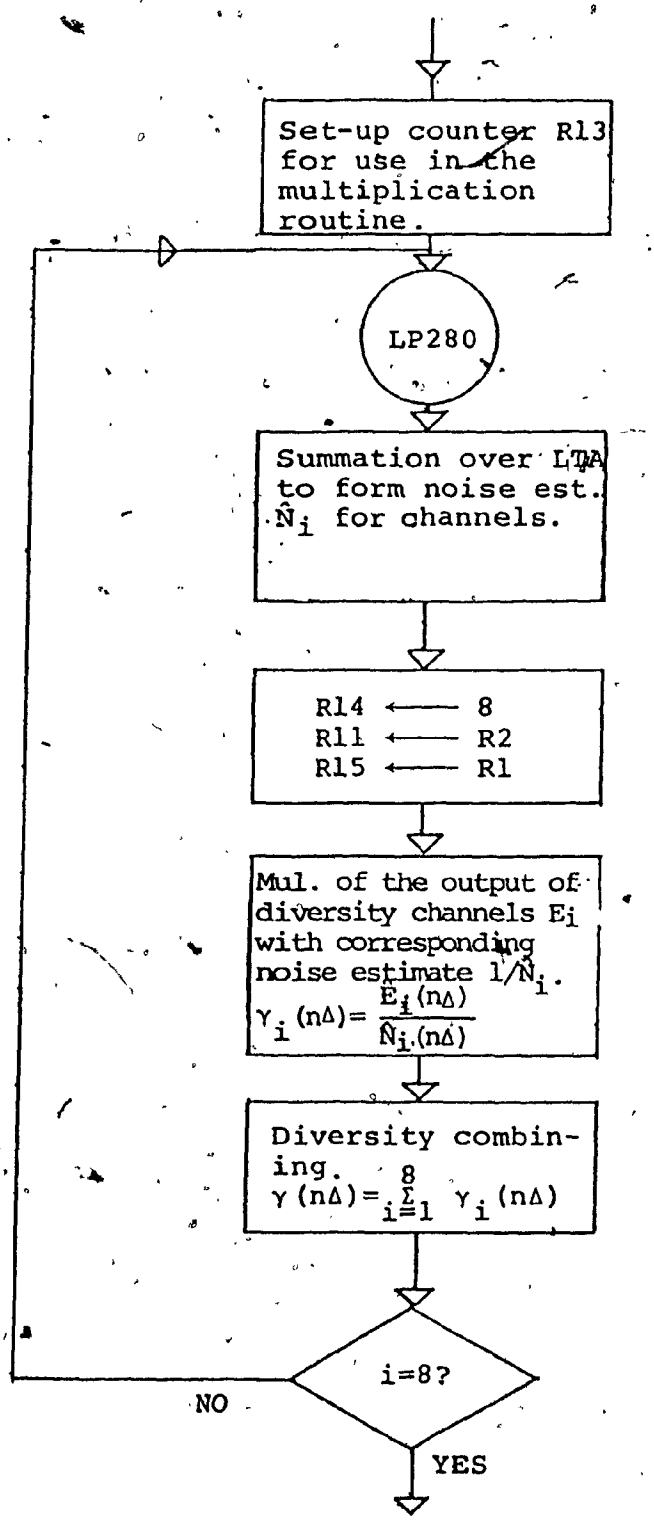
Set-up counter R13 for use in the multiplication routine.
LP280
Summation over LTA to form noise est. $\hat{N}_i$ for channels.
R14 ⟵ 8
R11 ⟵ R2
R15 ⟵ R1
Mul. of the output of diversity channels E_i with corresponding noise estimate $1/\hat{N}_i$.
$\gamma_i(n\Delta)=\frac{E_i(n\Delta)}{\hat{N}_i(n\Delta)}$
Diversity combining.
$\gamma(n\Delta)=\sum_{i=1}^{8}\gamma_i(n\Delta)$
i=8?
NO
YES

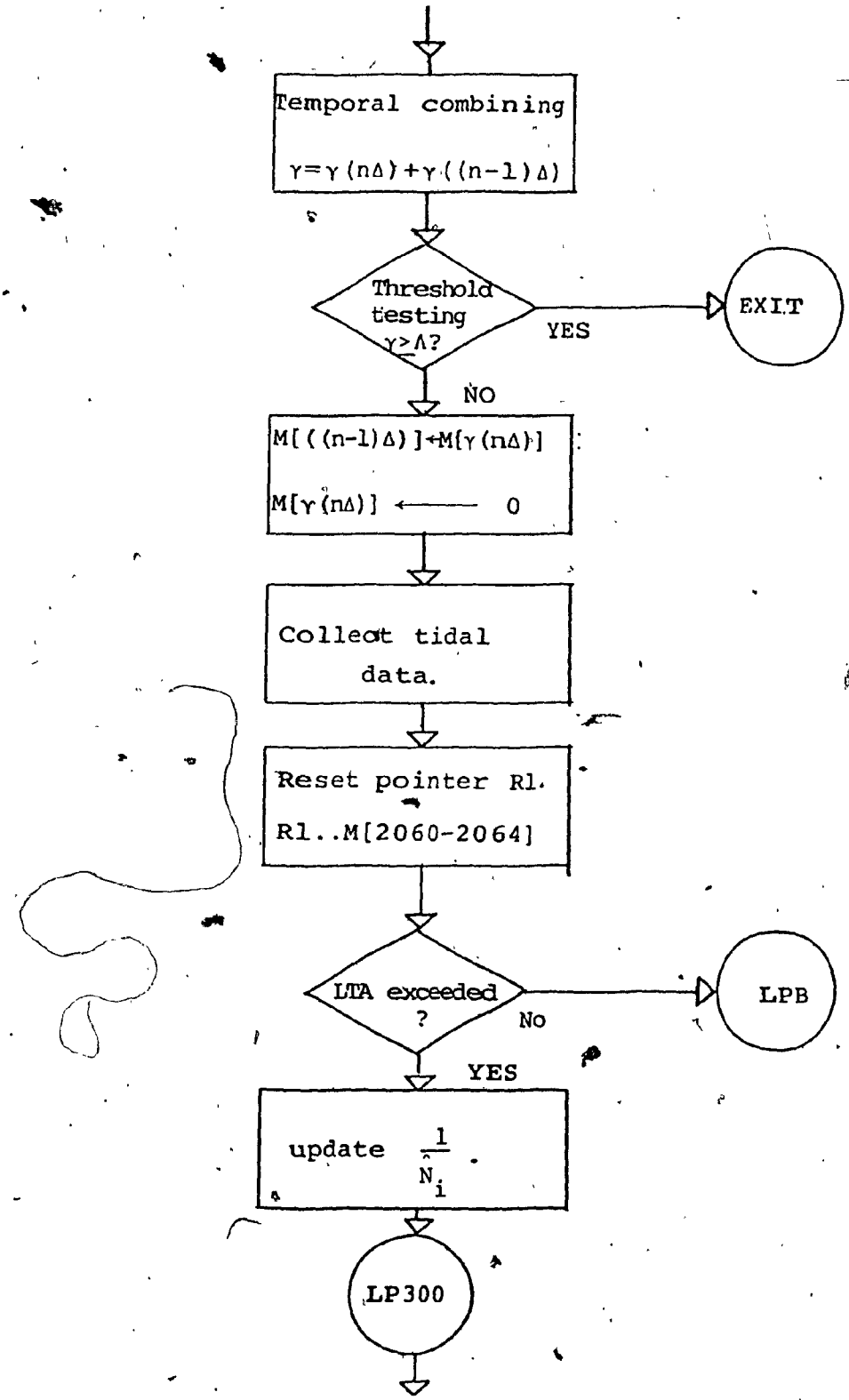
Temporal combining
$\gamma=\gamma(n\Delta)+\gamma((n-1)\Delta)$
Threshold testing
$\gamma \geq \Lambda$?
YES
EXIT
NO
$M[((n-1)\Delta)] \leftarrow M[\gamma(n\Delta)]$
$M[\gamma(n\Delta)] \leftarrow 0$
Collect tidal data.
Reset pointer R1.
R1..M[2060-2064]
LTA exceeded ?
No
LPB
YES
update $\frac{1}{N_i}$
LP300

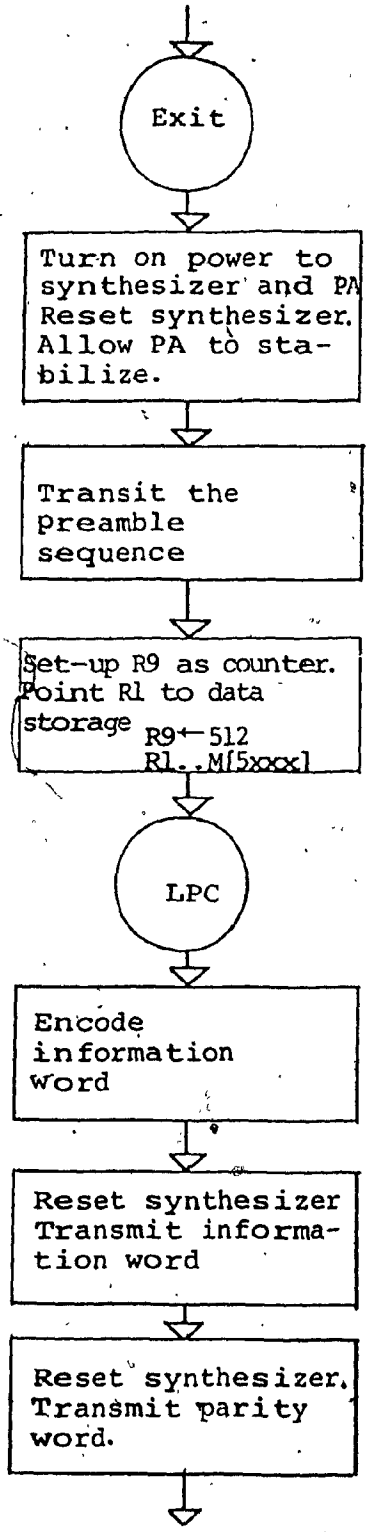
Exit
Turn on power to synthesizer and PA Reset synthesizer. Allow PA to stabilize.
Transit the preamble sequence
Set-up R9 as counter. Point R1 to data storage
R9←512
R1..M[5xxx]
LPC
Encode information word
Reset synthesizer Transmit information word
Reset synthesizer. Transmit parity word.

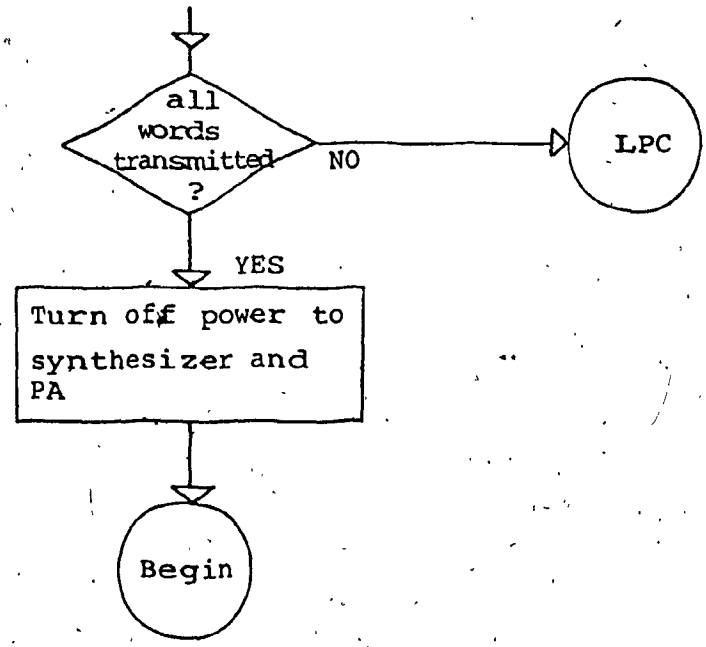
all words transmitted ?
NO
LPC
YES
Turn off power to synthesizer and PA
Begin

REFERENCES

1. Artwick, B.A., Microcomputer Interfacing, Prentice-Hall Inc., Englewood Cliffs, New Jersey, 1980.

2. Gear, W.C., Computer Organization and Programming, McGraw Hill, New York, 1980.

3. Peterson, W.W., and E.J. Weldron Jr., Error Correcting Codes, Cambridge, M.I.T. Press, 1972.

4. Shu Lin, An Introduction to Error Correcting Codes, Prentice-Hall, Englewood Cliffs, New Jersey, 1970.

5. RCA Solid State Division, "User Manual for the CDP 1802 COSMAC Mircoprocessor", 1977.

6. Stafford E., Tavares et al., "Some Rate P/(P+1) quasi-cyclic Codes", IEEE Transactions on Information Theory, Vol. IT-20 No. 1, pp. 133-135, January 1974.

CHAPTER VI

TELEMETRY SYSTEM PERFORMANCE PREDICTION

A., INTRODUCTION

In this chapter we discuss the performance of the underwater acoustic telemetry system. The discussion is divided into two areas. There is the performance analysis of the bottom unit command receiver and a performance analysis of the top unit receiver. In discussing the performance of the bottom unit, detection theory is used to rationalize the detection scheme chosen. The signal-to-noise ratio needed to obtain a specific performance using this detection scheme is calculated. This calculation, together with the environmental study of Chapter II, are used as the basis for recommending the transmit power levels of the top unit for a number of different sea states and communication ranges. A similar approach is adopted in discussing the performance of the top unit. First, a brief description of the operation of the top unit is provided and then the signal-to-noise ratio needed to ensure adequate system performance is examined. Based on these figures, the transmit power levels of the power amplifier in the bottom unit are determined.

B. THE OPTIMUM DETECTION TECHNIQUE

In a tonal communication system with diversity and with or without coding, the demodulated outputs $\{X_i\}$ are added after a transformation which may be determined from the likelihood ratio

$$y_i = L(X_i) = \frac{P_{S+N}(X_i)}{P_N(X_i)} \qquad \text{IV-1}$$

where $P_{S+N}(X_i)$ is the probability density function (pdf) for signal plus noise and $P_N(X_i)$ is the pdf for noise only [1]. In this analysis the statistics $\{X_i\}$ are taken to be the square-law detected outputs of a bank of filters. Idealized Rayleigh fading, with the signal and noise means equal to zero for each frequency slot, is assumed and the signal energies and noise power densities are given as $\{\hat{E}_i\}$ and $\{\hat{N}_i\}$, repectively.

The pdf's of the $\{X_i\}$ are given by,

$$P_{S+N}(X_i) = [(\hat{E}_i+\hat{N}_i)]^{-1} \exp[\frac{X_i}{(\hat{E}_i+\hat{N}_i)}] \; U(X_i) \qquad \text{VI-2}$$

$$P_N(X_i) = [\hat{N}_i]^{-1} \exp[\frac{X_i}{\hat{N}}] \; U(X_i) \qquad \text{VI-3}$$

where $U(\cdot)$ is the unit step function. Substituting VI-2 and VI-3 into VI-1, and taking logarithms on both sides of the result, gives

$$\log(y_i) \triangleq \ell_i = -\log\,[1+R_i] + \left[\frac{R_i}{(1+R_i)}\right]\frac{X_i}{\hat{N}_i} \qquad \text{VI-4}$$

where $R_i = \frac{\hat{E}_i}{\hat{N}_i}$, is the expected signal-to-noise power density ratio for the ith frequency slot (i.e. diveristy channel).

The log-likelihood ratio, ℓ_i, is linear in X_i if the irrelevant logarithmic bias term is ignored. Furthermore, it indicates that the optimum weighting rule of the detected filter outputs, involves the following operations:

(1) Normalization of X_i by the expected noise density $\hat{N}_i$.

(2) Multiplication of the normalized X_i by a function of R_i, whose purpose is to suppress filter outputs with small signal-to-noise ratios.

Evaluation of ℓ_i is difficult because both $\hat{E}_i$ and $\hat{N}_i$ are unknown and must be estimated. Moreover, if the noise $\hat{N}_i$ is very small, ℓ_i can attain high level saturation. This, however, can be avoided by using the minimum value of R_i needed to ensure reliable communication.

The difficulty of realizing the optimum detection scheme, led to a consideration of two sub-optimum schemes both of which involve the omission of the logarithmic

bias term and a modification of the weighting rule as follows:

$$\text{Rule 1. } \ell_{i1} = \frac{X_i}{\hat{N}_i} \qquad \text{VI-5.}$$

$$\text{Rule 2. } \ell_{i2} = \frac{X_i}{\hat{N}} . \qquad \text{VI-6}$$

For Rule 2, the noise power density $\hat{N}_i$ in the 40 Hz band around the center frequencies of the filters, is replaced by a noise power density $\hat{N}$, taken over the entire communication bandwidth of 2048 Hz. It is clear that there are a number of in-band and out-of-band types of interference which can cause $\hat{N}$ to underestimate or overestimate $\hat{N}_i$, resulting in reduced communication performance.

C. INTERFERENCE MODEL

In a frequency-keyed communication system the main concern is that of tonal interference. This type of interference, for example, may result from surface vessel-generated machinery noise or high frequency active sonar transmission systems. The interference model used in this analysis includes the essential features of a variable noise density and it allows for a comparison of the two weighting rules.

It is assumed that in the absence of interference,

the noise power densities are equal with a value N_o. It is also assumed with probability p, that any noise power density level N_i may take on a value so much larger than N_o, that the respective SNR, $R_i = 0$. This larger noise power density level is referred to as N_u. The model then, is described as follows,

$$P\{\hat{N}_i = N_o\} = 1 - p$$

$$i=1,2...D \qquad \text{VI-7}$$

$$P\{\hat{N}_i = N_u\} = p$$

where D is the number of detected filter outputs, or diversity channels. The number of frequency slots I in which interference may be present is binomially distributed with the probability of the number I, given by the expression,

$$P\{I\} = \left[\frac{D!}{I!(D-I)!}\right] p^I (1-p)^{D-I} \qquad \text{VI-8}$$

Equation VI-8 indicates that a knowledge of p, makes it possible to calculate the value of I having the highest probability. The average probability of error, P_e, can then be computed. In computing P_e, it is irrelevant which of the I frequency slots the noise occupies, therefore it is assumed that the first I slots are the ones affected.

Thus, the noise levels in the presence of interference are given as,

$$\hat{N}_i \doteq \begin{cases} N_u & i=1,2\ldots I \\ N_o & i=I+1,I+2,\ldots D \end{cases} \qquad \text{VI-9}$$

The average probability of error, P_e, can be specified in terms of the probability of correct decision P_{CD} and the probability of false alarm P_{FA}, i.e.,

$$P_e = (1-P_{CD})P\{S+N\} + P_{FA}\,P\{N\} \qquad \text{VI-10}$$

where $P\{S+N\}$ and $P\{N\}$ are the a priori probabilities of signal plus noise and noise only, respectively. The command receiver is designed to operate at the points,

$$P_{CD} = 0.99$$
$$P_{FA} = 10^{-8}$$

Since the command receiver receives noise most of the time,

$$P\{N\} = 1 - \varepsilon,\ \varepsilon \ll 1$$

and

$$P\{S+N\} = \varepsilon$$

The P_e according to VI-10, can therefore be approximated

by

$$P_e \simeq P_{FA} = 10^{-8}$$

In terms of the log-likelihood ratio ℓ_i, P_e is expressed as,

$$P_e = P\{\sum_{i=1}^{D} \ell_i \leq \Lambda | S+N\}\ P\{S+N\} + \qquad \text{VI-11}$$

$$P\{\sum_{i=1}^{D} \ell_i > \Lambda | N\}\ P\{N\}$$

where Λ is a threshold level chosen in accord with the previous operating points.

D. PERFORMANCE COMPARISON

The two weighting rules can be compared using VI-11 provided that $P\{\ell_i|S+N\}$ and $P\{\ell_i|N\}$ for the two weighting rules, are known. For the comparison it is assumed that all signal energies are equal, i.e. $E_i=E$, $i=1,2,\ldots D$ and $R_o = E/N_o$. Considering rule 1,

$$P\{\ell_{i1}|N\} = \exp[-\frac{\ell_{i1}}{1}]U(\ell_{i1}) \quad i=1,2\ldots D \qquad \text{VI-12a}$$

$$P\{\ell_{i1}|S+N\} = [1+R_o]^{-1}\exp[-\frac{\ell_{i1}}{(1+R_o)}]U(\ell_{i1}) \quad i=I+1,I+2,\ldots D \qquad \text{VI-12b}$$

In the case of rule 2,

$$P\{\ell_{i2}|N\} = \exp[-\frac{\ell_{i2}}{1}]U(\ell_{i2}) \quad i=1,2,\ldots I \qquad \text{VI-13a}$$

$$P\{\ell_{i2}|S+N\} = [1+R_o]^{-1}\exp[-\frac{\ell_{i2}}{(1+R_o)}\,U(\ell_{i2}) \quad i=I+1,I+2,\ldots D \qquad \text{VI-13b}$$

Using equations VI-11, VI-12, and VI-13, the signal-to-noise ratio needed for effective communication is computed for different interference probabilities, under the two weighting rules assuming $P_e=10^{-8}$ and D=5. The results are tabulated in Table VI-1.

Weighting rule	Probability of of Interference, p		
1	0	.01	.1
	13.6	13.65	14.85
2	13.61	16.05	20.15

Table VI-1 SNR for $P_e=10^{-8}$ and D=5

The Table indicates that for realistic interference probabilities i.e., $p \in [0.01, 0.1]$, rule 1 is better than rule 2 and it can be shown also that for these probabilities, rule 1 is within 1 dB of the optimum performance as specified by VI-4. In the acoustic telemetry system design, rule 1 is used and the SNR needed to ensure reliable

communication is set at R_o=14 dB. This is consistent with the results obtained graphically in Chapter 3, Sec. C. There again R_o was determined to be 14 dB.

E. SIGNAL-TO-NOISE RATIO NEEDED TO INTERROGATE THE BOTTOM UNIT

The signal-to-noise ratio per diversity channel R_o, has to be modified to correct for a frequency loss (L_f) and a time loss (L_t) due to the non-ideal detection schemes of the command receiver. The reader is referred to Chapter III, Section D. In terms of these losses, the required signal-to-noise ratio $(S/N)_{req.}$, is defined as,

$$(S/N)_{req.} = R_o + L_f + L_t$$
$$= 14 + 10 \log\frac{40}{8} + 10\log 2 = 24 \text{ dB} \qquad \text{VI-14}$$

The available signal-to-noise ratio $(S/N)_{avail}$, defined by equation II-4 (Chapter II, Section C) is,

$$(S/N)_{avail} = L_s + (N_{DI})_R - (T_L + L_N) \qquad \text{VI-15}$$

where L_s is the source level, $(N_{DI})_R$ is the directivity index of the receiver, T_L is the transmission loss given in Table II-6, as a function of distance, sea state and operating frequency, and L_N is the band level noise. The band level noise as given in Table II-7 is adjusted

according to equation II-18, for a bandwidth ω = 40 Hz, and the results are given in Table VI-2.

	SEA STATE					
Frequency	0	1	2	3	4	5
7kHz	-42.38	-33.28	-28.08	-24.28	-21.38	-18.98
16 kHz	-48.48	-39.38	-34.18	-30.38	-37.48	-25.078

Table VI-2 Band level noise in 40 Hz frequency band (dB/μbar)

The transmission loss figures of Table II-6 and the band level noise figures of Table VI-2 are combined to form a loss figure defined as (T_L+L_N) and given in Table VI-3.

		SEA STATE					
Range	Freq.	0	1	2	3	4	5
1 km	7 kHz	15.16	25.56	31.06	35.46	38.36	40.96
2 km	7 kHz	22.15	33.55	38.05	42.45	45.35	47.95

Table VI-3 Loss figure (T_L+L_N) for 48 Hz frequency band

Equation VI-15 implies that for effective communication, the source level plus the directivity index of the receiver must exceed the sum of the available signal-to-noise ratio and the loss figure. If the directivity index of the receiver is given as $(N_{DI})_R$= 3 dB and $(S/N)_{req.}$=24 dB, the data of Table VI-3 can be used to determine the source level per tone needed for effective communication at a frequency of 7 kHz, over two ranges r=1 km and r=2 km for six different sea states (SS0-SS5). The source level per tone is given in Table VI-4.

Range in km	Freq. in kHz	SEA STATE					
		0	1	2	3	4	5
1	7	36.16	46.56	52.06	56.46	59.36	61.96
2	7	43.15	54.55	59.05	63.45	66.35	58.95

Table VI-4 Source level, L_s, per tone, in dB

The source level is related to the electrical input power level, w, of the transmitting transducer by the expression,

$$L_s = 10 \log (\beta w) + 71 + (N_{DI})_T \qquad \text{VI-16}$$

where β is the electro-acoustic conversion efficiency of the transmitting transudcer and $(N_{DI})_T$ is its directivity index.

Using β=0.5 and $(N_{DI})_T$ = 3 dB, the input power levels corresponding to the source levels given in Table VI-4, are computed and tabulated in Table VI-5.

Range in km	Freq. in kHz	SEA STATES					
		0	1	2	3	4	5
1	7	.3mw	3.6 mw	12.8 mw	35.2mw	68.7 mw	125 mw
2	7	1.6 mw	22.7 mw	64.0 mw	176.2 mw	343.6 mw	625.2 mw

Table VI-5 Required transmit power levels per tone for top unit to ensure reliable communications

The total transmit power required by the top unit to interrogate the bottom unit can be obtained by modifying the data of Table VI-4 by a factor of 10 log 5 to account for the fact that 5 tones are transmitted instead of 1. If this is done it will be seen that for SS5 at a range of 1 km, the total power required to interrogate the bottom unit is 624 mwatts. Under realistic operating conditions, the shallow water noise magnitude may be 10 dB higher than the values indicated in Table VI-2, due to shipping and industrial noise. In this case the total input power required for a 1 km range and SS5 would be 6.25 watts. For this

reason the top unit is equipped with a variable input power amplifier with the highest setting corresponding to an input power level of 6 watts.

F. TOP UNIT

A brief description of the telemetry system top unit is necessary in order to complete the performance prediction of the system. A block schematic diagram of the top unit is shown in Figure VI-1. The hardware consists of:

(1) A CPU board which contains a 8086 microprocessor, 64 k of RAM, 4k PROM for program memory and a 4.9 MHz clock.

(2) A preprocessor unit consisting of:

(a) A 62 dB variable gain amplifier adjustable in 2 dB steps

(b) A fixed 16 dB user selectable amplifier

(c) A voltage-controlled amplifier with a range of $\pm$ 19 Hz

(d) Two mixers for frequency down conversion to the frequency range $\pm$ 1kHz

(3) Two 12-bit A/D converters

(4) An FFT processor using the TRW TDC 1010J 16x16 bit multiplier with 4 k of memory.

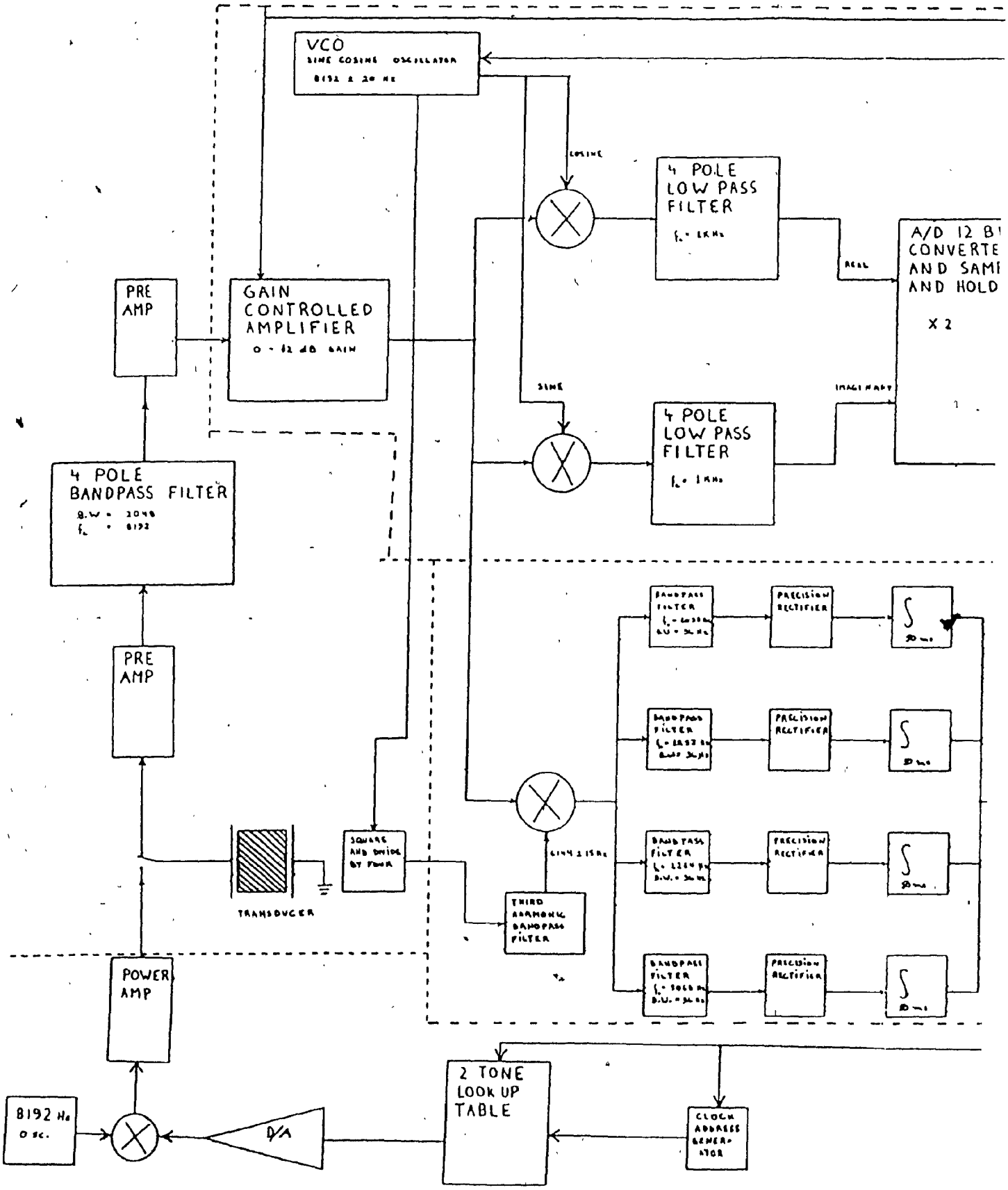
VCO
SINE COSINE OSCILLATOR
8192 ± 20 Hz
COSINE
4 POLE
LOW PASS
FILTER
REAL
A/D 12 B
CONVERTE
AND SAMI
AND HOLD
X 2
PRE
AMP
GAIN
CONTROLLED
AMPLIFIER
0 - 42 dB GAIN
SINE
IMAGINARY
4 POLE
LOW PASS
FILTER
4 POLE
BANDPASS FILTER
PRECISION
RECTIFIER
PRE
AMP
SQUARE
AND DIVIDE
BY FOUR
TRANSDUCER
THIRD
HARMONIC
BANDPASS
FILTER
POWER
AMP
8192 Hz
OSC.
D/A
2 TONE
LOOK UP
TABLE
CLOCK
ADDRESS
GENER-
ATOR

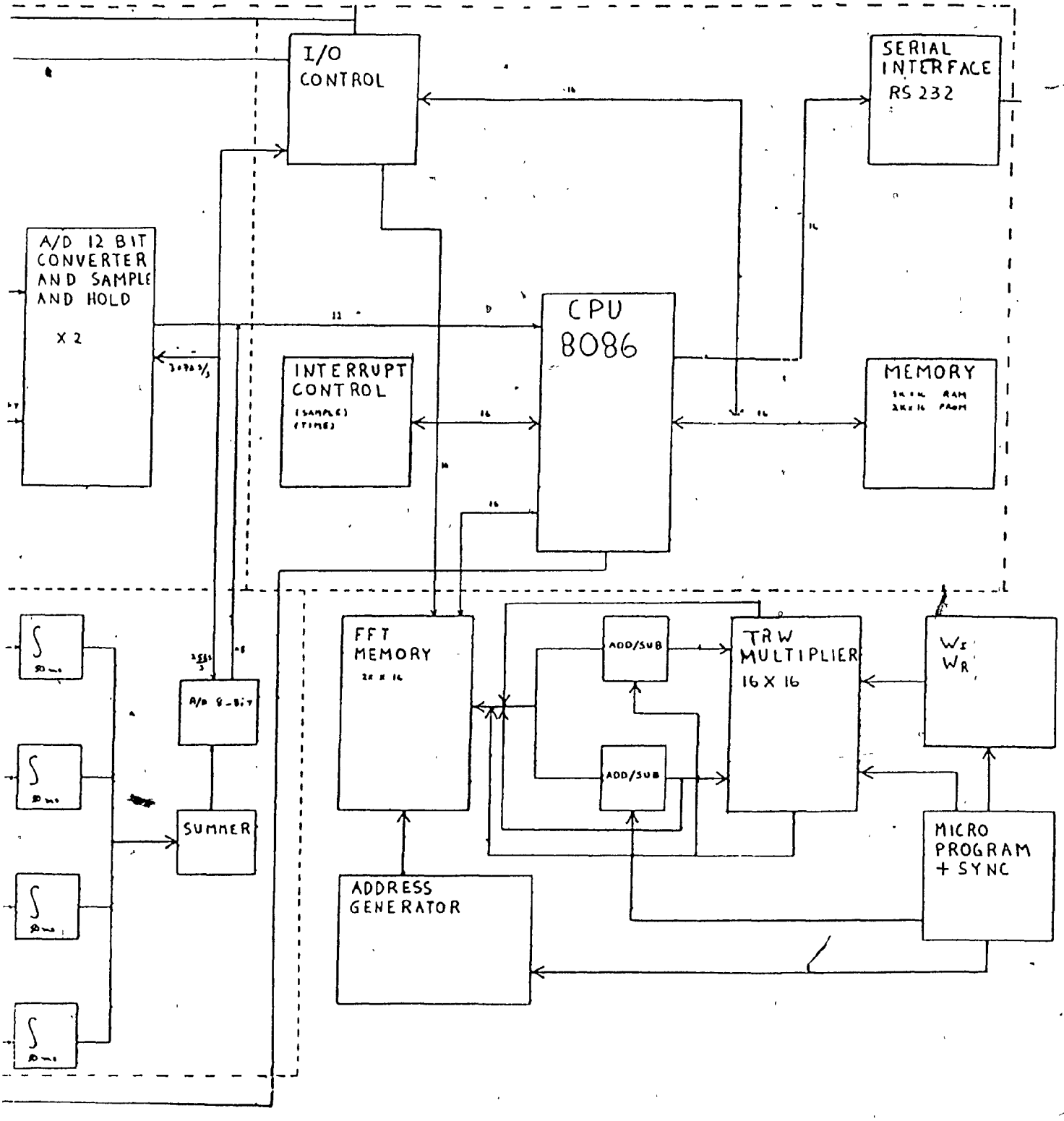

Figure VI-1 Block schematic diagram of top unit

The primary functions of the top unit are:

(1) To interrogate the bottom unit

(2) To estimate the noise and set an appropriate level for the automatic gain control.

(3) To provide time synchronization for the incoming information.

(4) To make a doppler correction

(5) To perform a 512 point complex FFT, i.e., frequency-to-bit conversion

(6) To decode the quasi-cyclic error correcting code.

(7) To provide an interface for the dumping of data.

G. TOP UNIT (S/N)req.

The signal-to-noise ratio required by the top unit to maintain effective communication with the bottom unit, determines the transmit power levels of the bottom unit.

The modulation format selected for use in the bottom unit is MFSK signalling with M=4-ary characters, N=8 characters/band and D=5-fold diversity. If it is specified that the M-ary character error probability be $P_{ec} = \frac{1}{N} \cdot 10^{-4} = 1.25 \times 10^{-5}$, it will be required that the average total received signal energy-to-noise power ratio per M-ary character be $\frac{\overline{E}_{TC}}{N_o}$ = 21 dB. The corresponding

average signal-to-noise power ratio per tone is $\frac{\bar{E}_1}{N_o}$ = 14 dB. This data is obtained from Figure VI-2. [4].

The probability of error per M-ary character is related to the probability of error per bit by the expression,

$$P_{ec} = \frac{2(M-1)}{M} P_{eb} \qquad \text{VI-17}$$

where P_{eb} is the probability of error per bit. Thus, for $P_{ec}=1.25\text{x}10^{-5}$ and $M=4$, P_{eb} is calculated as $8.33\text{x}10^{-6}$. Using these figures and assuming that character errors occur independently, the probability of error per 16 bit message can be computed as $P_{em} \cong 1-\{(1-(\frac{1}{N}\cdot 10^{-4}))\}^N \cong 10^{-4}$, an acceptable figure for the telemetry system application.

The average total received signal energy-to-noise power ratio per message is,

$$\frac{\bar{E}_T}{N_o} = \frac{E_{TC}}{N_o} + 10 \log N = 30 \text{ dB} \qquad \text{VI-18}$$

The addition of coding decreases the signal-to-noise ratio while maintaining the desired communication reliability. This associated decrease in the SNR is called the net coding gain, NCG and for the (32,16) quasi-cyclic code used, is given as NCG$\cong$ 3.6 dB [2]. The NCG is used to adjust the received signal-to-noise ratio thereby giving

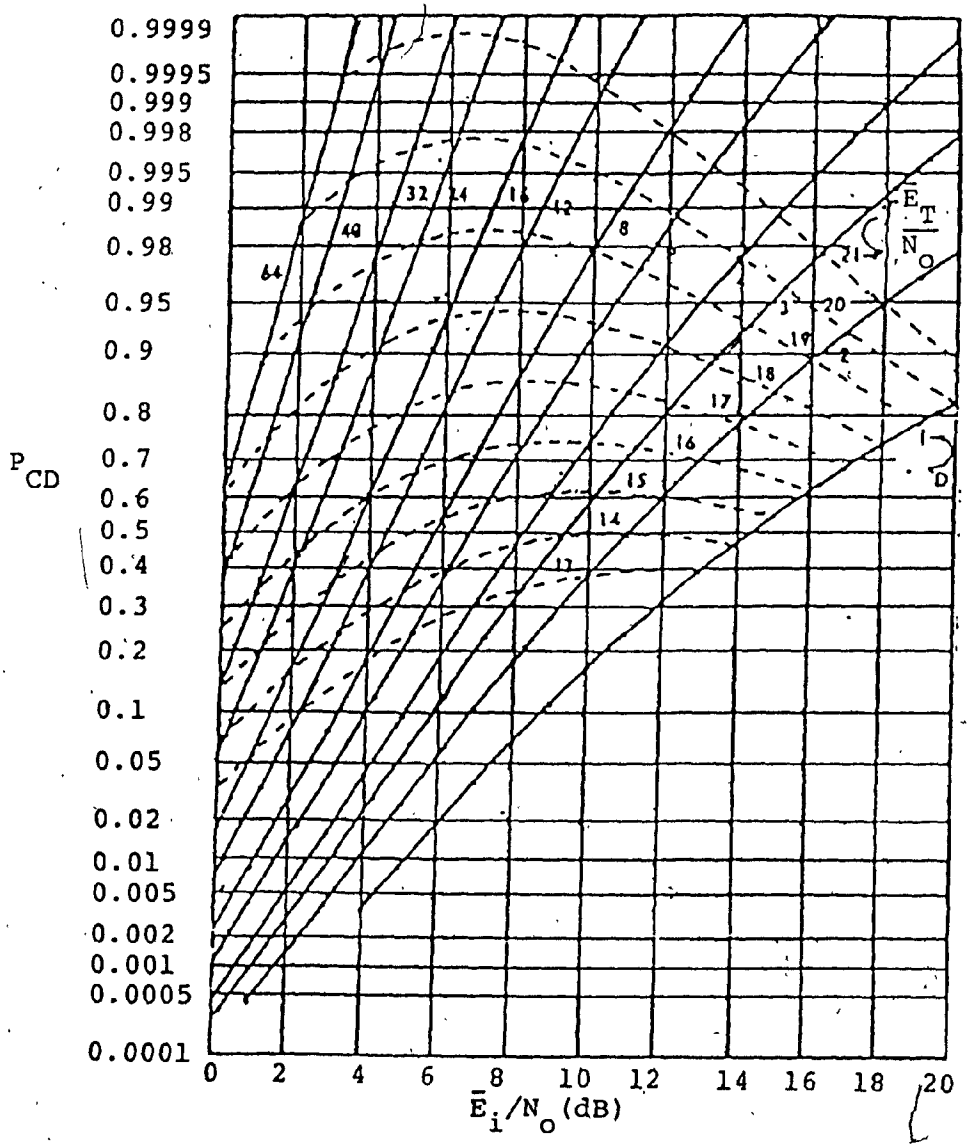

Figure VI-2 Detection Characteristics for $P_{FA}=10^{-8}$, and M=4.

$$\frac{\bar{E}_T}{N_o} = 26.4 \text{ dB} \quad \text{and} \quad \frac{\bar{E}_1}{N_o} = 10.4 \text{ dB} \qquad \text{VI-19}$$

In order to convert $\frac{\bar{E}_1}{N_o}$ and $\frac{\bar{E}_T}{N_o}$ to realistic estimates of signal-to-noise ratios, correction factors for non-ideal top unit processing, frequency uncertainty (L_f) due to doppler shift and time uncertainty (L_t) due to synchronization acquisition, must be taken into account. If these losses are conservatively estimated as 3 dB, 6 dB and 1 dB respectively, the required signal-to-noise ratio per tone would be given as,

$$(S/N)_t = 10.4 + 3 + 6 + 1 = 20.4 \text{ dB} \qquad \text{VI-20a}$$

Since each message is conveyed using 44 tone, the corresponding signal-to-noise ratio per message would be

$$(S/N)_m = 20.4 + 10\log 44 = 36.83 \text{ dB} \qquad \text{VI-20b}$$

The band level noise in a 12 Hz bandwidth (i.e. the width of the FFT bins) is computed by adjusting the data of Table II-7 in accordance with equation 11-18 and the results are given in Table VI-6.

Range in km	Freq. kHz	SEA STATE					
		0	1	2	3	4	5
1	7	-47.61	-38.51	-33.31	-29.51	-26.61	-24.21
2	16	-53.71	-44.61	-39.41	-35.61	-32.81	-30.31

Table VI-6 Band level noise in 12 Hz bandwidth (dB/μbar)

The data of Table II-6 and VI-6 are combined to form the loss figure (T_L+L_N) shown in Table VI-7

Range in Km	Freq. kHz	SEA STATE					
		0	1	2	3	4	5
1	7	9.93	20.33	25.83	30.23	33.13	35.73
2	7	16.92	27.32	38.82	37.22	40.12	42.72

Table VI-7 Loss figures (T_L+L_N) for a 12 Hz bandwidth

Using the required signal-to-noise ratio per tone $(S/N)_t$ as 21.4 dB, the directivity index of the receiver $(N_{DI})_R$ as 3 dB and the loss figure data of Table VI-7, the source level per tone is computed and presented in Table VI-8.

Range km	Freq. kHz	SEA STATE					
		0	1	2	3	4	5
1	7	27.33	37.73	43.23	47.63	50.53	53.13
2	7	34.32	44.72	50.22	54.62	57.52	60.12

Table VI-8 Source level L_s per tone (dB) for bottom unit transmitter

The data of Table VI-8 is substituted into Equation VI-16 and the required bottom unit transmit power per tone is obtained. The results are given in Table VI-9.

Range km	Freq. kHz	SEA STATE					
		0	1	2	3	4	5
1	7	43.06μw	.47mw	1.68mw	4.61mw	8.99mw	16.33mw
2	7	.22mw	2.36mw	8.38mw	23.07mw	44.98mw	81.85mw

Table VI-9 Required transit power per tone for the bottom unit to ensure reliable communication

The total power required by the bottom unit to maintain reliable communication with the top unit can be obtained by adjusting the data of Table VI-8 by a factor 10log44 since each message word is conveyed by 44 tones. If such an adjustment were made it will be observed that for SS5 and a range of 1 km the total power required by the bottom unit to communicate with the top unit is 720 mwatts. This figure will become 7.2 watts if we assume that under realistic conditions the shallow water noise estimates of Table VI-2, are 10 dB higher than indicated. For this reason the bottom unit power amplifier has a variable capability in the range .25 to 6.25 watts.

G. CONCLUSION

Performance predictions were made for the acoustic telemetry system operating in a communication channel modelled to have idealized Rayleigh fading properties. The predictions indicate that reliable two way communication between top and bottom units could be successfully maintained if the output power from both the top and bottom unit amplifiers, can be varied to a maximum of approximately 6 watts.

REFERENCES

1. Wozencraft, J.M., and I.M. Jacobs, Principles of Communication Engineering, John Wiley, New York, 1965.

2. Morgera, S.D., "Optimum Underwater Acoustic Techniques", prepared for Canadian Department of Environment, Oceans and Fisheries, Contract 07SC.KF806-8-E330, 8th February 1979.

3. Morgera, S.D., "A Conceptual Design of an Underwater Acoustic Telemetry System: Phase II study", prepared for DOE, Fisheries and Oceans, February 20th, 1980.

4. Nuttall, A.H., "Operating Characteristics for Detection of a Fading Signal in M Alternative Locations with D-Fold Diversity", NUSC TR4793, 20th August 1974.

CHAPTER VII

CONCLUSION AND RECOMMENDATIONS

A. INTRODUCTION

In this Chapter we review the development of the acoustic telemetry system designed primarily to address the problems of oceanographic data gathering, but flexible enough to have several other potential applications. The Chapter begins with a summary of data obtained from a detailed environmental study and pertinent to the design of the acoustic telemetry system. The features of the telemetry system are then discussed. Finally, recommendations for system improvement and a listing of other potential applications are given.

B. SYSTEM PARAMETERS

Oceanic communication is more of an art rather than an exact science. Even though the principles of communicating in the ocean are well established by the sonar equations, it is difficult to predict the performance of any communication system in such an environment because of the difficulties in precisely estimating such parameters as propagation loss, noise levels, frequency dispersion and time dispersion. Propagation loss estimates, for examples, are affected by the great variability of surface and bottom properties of the ocean with geographical locations, weather conditions and the time of the year. Reliable communication in the ocean

can only be achieved if accurate estimates of these parameters can be obtained. In estimating them, a shallow water environmental model was used and calculations were carried out at two frequencies, 7 and 16 kHz six sea states, SS0-SS5; and three different temperatures, -10°C, 0°C and 10°C.

The results of the environmental study provided the guidelines for the design of the telemetry system. They predicted the following:

1. The worst case transmission loss at a range of 1 km would be 59.95 dB. Such a loss would occur at a temperature of -10°C on a muddy ocean bottom during SS5 weather conditions.
2. The band level noise at 7 kHz during SS5 in the open ocean would be -35 dB.
3. Frequency dispersion (doppler speed, B) would be 4 Hz at a range of 1 km.
4. Time dispersion (multipath spead L) would be 100 ms at a range of1 km.

The dispersion estimates were derived from sound velocity profile studies of six shallow water locations off the Canadian east coast. All six locations are possible candidates for deployment of the acoustic telemetry system. Based on the frequency and time dispersion estimates of 4 Hz and 100 ms respectively, and on practical considerations

from an implementation point of view, the optimum transmit pulse duration (T_p) was set at 125 ms. The receiver frequency resolution was then calculated as $(B+\frac{1}{T_p}) = 12$ Hz and the total received tonal duration was established to be $(T_p+L) = 225$ ms. As a result a 125 ms dead time between transmissions was allowed for multipath decay. Many other system design recommendations were made in accordance with the results of the environmental study. It was decided that the system would transmit at 7 kHz with a bandwidth of 2 kHz, based on the modulation scheme chosen, since for a given transmitter power and directivity index, the signal-to-noise at 7 kHz was better than that at 16 kHz. The 2 kHz transmission band was consequently established around 8192 Hz with 7168 Hz as its lower edge. Data encoding and 5-fold frequency diversity were used to combat fading which could occur because of the dispersive nature of the medium. It was also recommended that the ship on which the top unit is placed should observe a vehicle-current axial velocity of less than 3kts and a horizontal range of approximately 820 yds, while interrogation of the bottom unit is being attempted.

The bottom unit signal processing schemes were also designed in accordance with estimates and recommendations resulting from the environmental study. Bottom unit signal processing is divided into two areas. First, there is the processing of information arriving at the input to the

command receiver for the purpose of identifying interrogation commands. This information is passed through a band of filters spaced a distance of 400 Hz apart, based on the minimum expected multipath spread, in order to ensure statistically independent fading.

The filter outputs are rectified, A/D converted, and combined by a microcomputer to form a detection statistic which is tested against a threshold in order to determine if an interrogation command was issued. If the decision is that an interrogation command was sent, a second type of signal processing, including data encoding and MFSK modulation, ensues. Both the data encoding and modulation schemes are intended to combat fading. MFSK modulation in which M=4 and D=5 was found to be best suited to this design. In this scheme each 16 bit data word is conveyed using 40 tones (8x5) selected from a set of (32x5)=160. Four pilot tones are interleaved between the 5 diversity channels making 44 tones overall. The pilot tones are used by the top unit for doppler and synchronization corrections. The tones are generated digitally using the accumulator-overflow method of frequency synthesis. Quadrature outputs are produced, with all 44 in-phase and quadrature components independently summed to form two composite waveforms. Summation of the tones required that their phases be randomized in order to minimize the peak-to-average ratio of the composite waveforms. This is accomplished by using a quadratic

phase set to initialize the phases of the tones. The tones are created in the range ± 1 kHz and translated to the band 7168 to 9216 Hz through modulation with a 8192 Hz carrier.

The circuity used to implement the design of the bottom unit was built from a mixture of CMOS and special low power-consumption chips. This was in keeping with the stringent power constraint imposed on the bottom unit design because of the fact that it would be located on the ocean floor for reasonably long periods of time.

Finally, theoretical performance predictions were carried out. It was decided that adequate system performance could be achieved if the probability of false alarm P_{FA} and the probability of correct decision P_{CD} for the command receiver were set at 10^{-8} and .99, respectively, and if the bit error rate of the system was fixed at 1.25×10^{-5}. Using these figures and the data obtained from the environmental study, the power levels required to maintain reliable communication between the top and bottom units were calculated. It was found that in order to transmit a 16 bit word during SS5 at a 1 km range the bottom unit needed .72 watts of electrical power to communicate with the top unit while the top unit required .625 watts to communicate with the bottom unit. It is obvious and very likely in a busy shipping environment, that a 10 dB increase in noise power would require that the bottom and top units transmit 7.2 watts and 6.25 watts, respectively, in order to maintain

reliable communication. For this reason, both units are designed with variable gain power amplifiers, adjustable in fixed steps with the highest setting at 6 watts. However it must be emphasized that the power capability of the bottom unit at maximum is only 3 watts because the input to the power amplifier is passed through a triangular window thereby reducing its level by a factor of 0.5. This is done to reduce the sidelobe levels of the transmitted waveforms and to reduce slightly the peak-to-average ratio of the power amplifier input.

C. FIELD TEST DATA

On July 12 and 13 1982, the acoustic telemetry system was taken to the Bedford Institute of Oceanography, Dartmouth, N.S., for field testing. The tests were conducted in the Bedford Basin. One unit was taken aboard the Pheonix while the other was placed on board the Tudlik. Tests were conducted to observe the performance of the system over a number of different ranges with the transducers of the top and bottom units lowered to different depths.

In general the system performed very well inspite of the fact that the test environment was far from ideal. The Basin, unlike the open ocean has closed boundaries making multipath a serious problem. It also has a bottom that is very muddy and therefore highly absorptive. Moreover its

noise level is definitely much higher than that of the open ocean because of the great amount of shipping traffic present and because of the close proximity of the nearby shoreline from which industrial noise emanates. The Bedford Basin is a harsh environment compared to the open ocean. It is felt therefore that the system would perform much better in the environment for which it was designed.

A typical transmission dump of data received by the top unit is shown in Table VII-1. The data transmitted from the bottom unit for the purpose of testing consisted of 64 words; 32 of them were preprogrammed as tidal data words and the other 32 were generated as code words in accordance with the (32,16) quasi-cyclic code: The Table gives the tidal data and the code data as received by the top unit and it shows the tidal data after decoding for error correction has been applied to it. It also provides a summary of important information which can be used to assess the performance of the top unit. For example a knowledge of AGCN, AGC, VCO, errors and time delay values, makes it possible to deduce the SNR, the behaviour of the time and frequency synchronization circuitry, and the number of transmission errors that occurred. A summary of important information relevant to eleven transmission runs is given in Table VII-2. An examination of the results indicates that the system performed excellently. Error free transmission was attained at a range as far as 1500 m with power of

```
ERROR CORRECTED DATA AND CORRECTION WEIGHT

FFFF 0000 FFFF 0000 FFFF 0000 FFFF 0000 FFFF 0000 FFFF 0000 FFFF 0000 FFFF 0000
CCCC 0000 CCCC 0000 CCCC 0000 CCCC 0000 CCCC 0000 CCCC 0000 CCCC 0000 CCCC 0000
0000 0000 0000 0000 0000 0000 0000 0000 0000 0000 0000 0000 0000 0000 0000 0000
AAAA 0000 AAAA 0000 AAAA 0000 AAAA 0000 AAAA 0000 AAAA 0000 AAAA 0000 AAAA 0000

TIDAL DATA AND CODE DATA

FFFF FFFF FFFF FFFF FFFF FFFF FFFF FFFF FFFF FFFF FFFF FFFF FFFF FFFF FFFF FFFF
CCCC 9999 CCCC 9999 CCCC 9999 CCCC 9999 CCCC 9999 CCCC 9999 CCCC 9999 CCCC 9999
0000 0000 0000 0000 0000 0000 0000 0000 0000 0000 0000 0000 0000 0000 0000 0000
AAAA 5555 AAAA 5555 AAAA 5555 AAAA 5555 AAAA 5555 AAAA 5555 AAAA 5555 AAAA 5555

FFT OUTPUT DATA 173 BINS -1032HZ TO +1032HZ 12HZ APART

008E 011A 0059 000E 00A6 0062 0042 0212 02E4 008C 0030 0234 0442 0144 005D 0292
04C7 0168 0059 009F 011D 0096 007A 0132 016A 009E 0006 023F 0465 00C8 00AD 0282
060C 018C 009D 0160 02E3 00FD 007C 008A 014A 00C6 0081 01FC 04A9 0089 0047 0334
0821 014C 0057 020A 0450 0151 00A5 015E 0481 01A7 0096 0254 0426 014C 00F3 0228
0682 018A 0060 015C 0281 00CE 0081 0259 01A4 0082 0107 02EA 0150 008B 0312 0663
0139 006F 0186 0449 0214 04EC 0909 03CF 030C 0104 0065 0231 0457 0107 0087 0383
080F 0229 00AD 02C2 060E 0155 00CE 0362 0419 0080 0299 05EA 0298 0082 020B 04B8
017E 00CE 0390 0799 02A6 00AC 0426 0549 017E 00C0 0177 0209 017E 00C2 0165 0163
0152 00B2 0201 062E 0167 00AA 0290 051E 0170 0084 02BF 0690 0145 00D9 0162 0364
0157 00C7 01A2 028C 005E 0075 0263 0382 000A 00A4 01A0 0270 0186 007A 01C4 0386
00F4 006D 00BF 0110 006B 0063 00BF 0245 006A 0018 00FF 0297 0075

DIVERSITY COMBINED OUTPUT

0704 1269 06E0 02F8 0810 0F34 05A7 033E 0C74 1973 063A 0234 0005 19FC 06D0 06A0
099C 0DFF 05EF 02C0 07EA 0F5B 0612 0382 0004 17E5 060F 035A 0AF8 189F 0652 0297
AGCN AGC  VCO ERRORS TIMEDELAY

0011 0000 0000 0000 0005
```

Table VII-1 Typical transmission data dump. Range of 500m, water depth 25 m bottom unit transducer depth of 40 ft., top unit transducer depth of 50 ft., bottom unit transmit power of 1.5 watts.

TX	SNR (dB)	Bottom unit Transducer depth (m)	Top unit Transducer depth (m)	Range (m)	Bottom Unit Transmit Power Watts	Number of errors	COMMENTS
1	40	6	6	50	.5	0	-
2	36	24	3	100	1.0	0	-
3	26	24	3	100	1.0	6	Destroyer passed by. Burst noise
4	30	15	20	500	3	0	-
5	28	6	6	500	1.5	0	-
6	42	15	20	500	1.0	0	-
7	40	15	20	500	.5	0	-
8	26	6	6	500	3.0	6	Burst error. Maybe due to deep fading.
9	14	6	9	1000	3.0	0	-
10	26	6	6	1000	3.0	2	excessive multipath due to poor geometry of boats with respect to wharf.
11	26	6	9	1500	3.0	0	-

Table VII-2 Summary of results from some transmission runs during field testing in the Bedford Basin

6 watts. In the instances when errors occurred there seemed to be quite plausible explanations. Transmission run number 8 is a special case in point. This was the only transmission in which 1024 data words and their corresponding code words were transmitted. The entire transmission lasted approximately 4 minutes and 6 errors occurred in a burst. These errors may be a result of the fact that a deep fade occurred and the signal energy was not sufficient to overcome it. This is probably a good example of the differences between the fading properties of the real environment and the rather simplistic and ideal Rayleigh model used to simulate it.

D. RECOMMENDATIONS FOR IMPROVED SYSTEM PERFORMANCE

There are a few recommendations that could lead to improvement in the design and operation of the bottom unit. The major concern relates to the power amplifier. The power capability of this amplifier has to be increased so that it becomes possible to obtain 6 watts of undistorted power at its output. This calls for the design of a different power amplifier.

The efficiency of any amplifier used in the bottom unit could be increased also if it were possible to reduce the peak-to-average ratio of the input waveform to it. The use of the quadratic phase set to do this was not as successful as predicted. The theoretical analysis of the effect of

this phase set was based on the fact that the tones are equi-spaced across the transmission band. However, this is not the case in the telemetry system. Very few of the data word pattern exhibit such a regularity. Other phase sets should be tried to observe their effect on the peak-to-average ratio of the input waveform to the power amplifier.

A reduction in the peak-to-average ratio can result also if less tones were transmitted per 16 bit data word. This can occur if the modulation format is modified slightly. The information contained in the tidal data can be conveyed as the differences in the magnitude between successive data words. Since the level of the tide changes slowly with time, these differences would always be small except in cases of adverse weather conditions. It would, therefore be possible to convey the information using an MFSK scheme in which the total number of tones is greatly reduced. The tones would therefore be spread further apart across the transmission band and because there are fewer in number their summation may even out more smoothly. This differential MFSK modulation format would also enhance the reception capability of the top unit and further improve the system communication reliability. Finally, the power supply switching for the command receiver should be studied and a decision made as to whether it should be retained or discarded. The switching was intended to save 50% of the command receiver standby power (i.e. 600μ watts). It does not achieve this.

Power is consumed by the circuitry installed to perform the function and it causes a deterioration of the system reliability. The trade offs should be studied.

E. OTHER APPLICATIONS OF THE TELEMETRY SYSTEM

The flexibility of the acoustic telemetry system makes it a valuable communication system for the collection and telemetering of any type of data that can easily be converted to electrical signals. To accomplish this entails only the redesign of the gauge interface card to meet the specific interface requirements of the new system. For example, if a PH meter were used with an appropriate PH interface card, it would be possible to monitor the acidic contents of lakes and rivers. This could be an initial step in redressing some of the environmental problems created by acid rain. Some other possible applications are:

1. Pollution monitoring in lakes, rivers and water supplies.
2. Water level monitoring in water supplies.
3. Control of underwater submersibles for use in ocean bottom resource mining and oil rig drilling maintenance.
4. Military surveillence. A network of ocean bottom units can be placed in major ocean basins to perform this task. In such a case only one top unit will be necessary to interrogate the entire

network of bottom units.

The telemetry system designed and developed at Concordia University is a big step forward in the area of acoustic telemetry. Its performance indicates that a little extra research and development could lead to the production of a versatile and valuable piece of communication equipment. It is expected that this would take place and that some of the potential applications mentioned will be served by the system in the future.

APPENDIX II-1

```
C                APPENDIX II-1
C
C
      PROGRAM TLOSS(INPUT,OUTPUT)
      DIMENSION RANGE(10)
C
C*****************************************************
C     THIS PROGRAM COMPUTES TRANSMISSION LOSS
C     FIGURES IN DB IN SEA WATER AS A FUNCTION OF
C     RANGE(KM),FREQUENCY(KHZ) AND TEMPERATURE
C     (DEG. CENTIGRADE).
C     THE SALINITY OF SEA WATER IS GIVEN AS 35
C     PARTS PER THOUSAND(PPT)
C     THE RANGE MATRIX CONSISTS OF THE DIFFERENT
C     RANGES FOR WHICH TRANSMISSION LOSS HAS TO
C     BE CALCULATED.
C     N...THE NUMBER OF ENTRIES IN THE RANGE MATRIX.
C*****************************************************
C
      S=35
      A=1.86*10**(-2.)
      B=2.68*10**(-2.)
      PRINT*,"ENTER N"
      READ *,N
      PRINT* "ENTER RANGE MATRIX"
      READ*,(RANGE(I),I=1,N)
      DO 5 L=1,N
      RANGE(L)=RANGE(L)*1.0936
 5    CONTINUE
C     PRINT*,(RANGE(I) I=1 N)
      PRINT 1
 1    FORMAT(4X,"TEMP.",6X,"FREQ.".5X,"RANGE",
     *4X,"TRANS. LOSS")
      DO 10 J=10,30,10
      TT=J-20
      T=6-(1520./(TT+273))
      FT=21.9*10**T
      FT2=FT*FT
      DO 20 K=7,16,9
      F=K
      F2=F*F
      ALFA=A*S*(FT*F2)/(FT2+F2)+B*(F2/FT)
      DO 30 I=1 N
      Z=RANGE(I).
      X=20*ALOG10(Z)
      Y=ALFA*RANGE(I)
      TLP=X+Y+60
      PRINT 2,TT,F,RANGE(I),TLP
 2    FORMAT(2X,4(F7.2,3X))
 30   CONTINUE
 20   CONTINUE
 10   CONTINUE
      STOP
      END
```

TEMP.	FREQ.	RANGE	TRANS. LOSS
-10.00	7.00	1.09	61.74
-10.00	7.00	2.19	68.73
-10.00	16.00	1.09	65.18
-10.00	16.00	2.19	75.60
0.00	7.00	1.09	61.38
0.00	7.00	2.19	68.01
0.00	16.00	1.09	63.77
0.00	16.00	2.19	72.79
10.00	7.00	1.09	61.16
10.00	7.00	2.19	67.57
10.00	16.00	1.09	62.76
10.00	16.00	2.19	70.76

APPENDIX III-1

```
C                APPENDIX III-1
C
C
      PROGRAM DELY(INPUT,OUTPUT)
      REAL NN,X,BB,BW,F,C
      INTEGER RX,R11,R22,RA,RB
C
C*****************************************************
C     THIS PROGRAM GIVES THE COMPONENT VALUES
C     FOR THE DESIGN OF A DELYANNIS BANDPASS
C     FILTER,GIVEN THE REQUIRED GAIN,THE Q-
C     FACTOR AND THE CENTER FREQUENCY.
C     NN...THE NUMBER OF SECOND ORDED SECTIONS.
C     X....THE REQUIRED GAIN.
C     BB...A NUMBER, CONVIENENTLY CHOSEN TO BE
C       ...A PERFECT SQUARE.
C     BW...BANDWIDTH OF THE FILTER.
C     F....THE CENTRE FREQUENCY OF THE FILTER.
C     C....CAPACITANCE IN FARADS.
C*****************************************************
C
      PRINT 5
    5 FORMAT("ENTER NN,X,BB,BW,F,C")
      READ*,NN,X,BB,BW,F,C
      Q=F/BW
      W=2*3.1415927*F
      A=1.0/NN
      X1=X**A
      Q1=Q*(((2**A)-1)**0.5)
      B=SQRT(BB)
      R=1.0/(W*C*B)
      M=(BB*Q1)/((2*Q1)-B)
      RX=(BB*R)
      G=(Q1*(M+1)*B)/M
      R11=(R*G)/X1
      R22=(R*G)/(G-X1)
   10 PRINT 12
   12 FORMAT("ENTER RR")
      READ*,RR
      RA=RR
      RB=RR*M
      RT=RA+RB
      IF(RT.GE.20000 .AND. RT.LE.200000) GO TO 15
      GO TO 10
   15 PRINT 17
   17 FORMAT(5X,"RA",5X,"RB",8X,"RX",5X,"R11",8X,"R22")
      PRINT 20,RA,RB,RX,R11,R22
   20 FORMAT(2X,5(I7,2X))
      STOP
      END
```

APPENDIX IV-1

APPENDIX IV-1
SINE LOOK-UP TABLE IN HEX. FORMAT.

0000	00	02	03	05	06	08	09	0B	0C	0E	10	11	13	14	16	17
0010	19	1A	1C	1D	1F	20	22	23	25	26	28	29	2B	2C	2E	2F
0020	31	32	33	35	36	38	39	3A	3C	3D	3F	40	41	43	44	45
0030	47	48	49	4A	4C	4D	4E	4F	51	52	53	54	55	56	58	59
0040	5A	5B	5C	5D	5E	5F	60	61	62	66	64	65	66	67	68	69
0050	6A	6A	6B	6C	6D	6E	6F	6F	70	71	71	72	73	73	74	75
0060	75	76	76	77	78	78	79	79	7A	7A	7A	7B	7B	7C	7C	7C
0070	7D	7D	7D	7D	7E	7E	7E	7E	7E	7F	7F	7F	7F	7F	7F	7F
0080	7F	7F	7F	7F	7F	7F	7F	7F	7E	7E	7E	7E	7E	7D	7D	7D
0090	7D	7C	7C	7C	7B	7B	7A	7A	7A	79	79	78	78	77	76	76
00A0	75	75	74	73	73	72	71	71	70	6F	6F	6E	6D	6C	6B	6A
00B0	6A	69	68	67	66	65	64	63	62	61	60	5F	5E	5D	5C	5B
00C0	5A	59	58	56	55	54	53	52	51	4F	4E	4D	4C	4A	49	48
00D0	47	45	44	43	41	40	3F	3D	3C	3A	39	38	36	35	33	32
00E0	31	2F	2E	2C	2B	29	28	26	25	23	22	20	1F	1D	1C	1A
00F0	19	17	16	14	13	11	10	0E	0C	0B	09	08	06	05	03	02
0100	FF	FE	FD	FB	FA	F8	F7	F5	F4	F2	F0	EF	ED	EC	EA	E9
0110	E7	E6	E4	E3	E1	E0	DE	DD	DB	DA	D8	D7	D5	D4	D2	D1
0120	CF	CE	CD	CB	CA	C8	C7	C6	C4	C3	C1	C0	BF	BD	BC	BB
0130	B9	B8	B7	B6	B4	B3	B2	B1	AF	AE	AD	AC	AB	AA	A8	A7
0140	A6	A5	A4	A3	A2	A1	A0	9F	9E	9D	9C	9B	9A	99	98	97
0150	96	96	95	94	93	92	91	91	90	8F	8F	8E	8D	8D	8C	8B
0160	8B	8A	8A	89	88	88	87	87	86	86	86	85	85	84	84	84
0170	83	83	83	83	82	82	82	82	82	81	81	81	81	81	81	81
0180	81	81	81	81	81	81	81	81	82	82	82	82	82	83	83	83
0190	83	84	84	84	85	85	86	86	86	87	87	88	88	89	8A	8A
01A0	8B	8B	8C	8D	8D	8E	8F	8F	90	91	91	92	93	94	95	96
01B0	96	97	98	99	9A	9B	9C	9D	9E	9F	A0	A1	A2	A3	A4	A5
01C0	A6	A7	A8	AA	AB	AC	AD	AE	AF	B1	B2	B3	B4	B6	B7	B8
01D0	B9	BB	BC	BD	BF	C0	C1	C3	C4	C6	C7	C8	CA	CB	CD	CE
01E0	CF	D1	D2	D4	D5	D7	D8	DA	DB	DD	DE	E0	E1	E3	E4	E5
01F0	E7	E9	EA	EC	ED	EF	F0	F2	F4	F5	F7	F8	FA	FB	FD	FE

APPENDIX IV-2

APPENDIX IV-2
COSINE LOOK-UP TABLE IN HEX. FORMAT.

0000	81	81	81	81	81	81	81	81	82	82	82	82	82	83	83	83
0010	83	84	84	84	85	85	86	86	86	87	87	88	88	89	8A	8A
0020	8B	8B	8C	8D	8D	8E	8F	8F	90	91	91	92	93	94	95	96
0030	96	97	98	99	9A	9B	9C	9D	9E	9F	A0	A1	A2	A3	A4	A5
0040	A6	A7	A8	AA	AB	AC	AD	AE	AF	B1	B2	B3	B4	B6	B7	B8
0050	B9	BB	BC	BD	BF	C0	C1	C3	C4	C6	C7	C8	CA	CB	CD	CE
0060	CF	D1	D2	D4	D5	D7	D8	DA	DB	DD	DE	E0	E1	E3	E4	E6
0070	E7	E9	EA	EC	ED	EF	F0	F2	F4	F5	F7	F8	FA	FB	FD	FE
0080	00	02	03	05	06	08	09	0B	0C	0E	10	11	13	14	16	17
0090	19	1A	1C	1D	1F	20	22	23	25	26	28	29	2B	2C	2E	2F
00A0	31	32	33	35	36	38	39	3A	3C	3D	3F	40	41	43	44	45
00B0	47	48	49	4A	4C	4D	4E	4F	51	52	53	54	55	56	58	59
00C0	5A	5B	5C	5D	5E	5F	60	61	62	66	64	65	66	67	68	69
00D0	6A	6A	6B	6C	6D	6E	6F	6F	70	71	71	72	73	73	74	75
00E0	75	76	76	77	78	78	79	79	7A	7A	7A	7B	7B	7C	7C	7C
00F0	7D	7D	7D	7D	7E	7E	7E	7E	7E	7F	7F	7F	7F	7F	7F	7F
0100	7F	7F	7F	7F	7F	7F	7F	7F	7E	7E	7E	7E	7E	7D	7D	7D
0110	7D	7C	7C	7C	7B	7B	7A	7A	7A	79	79	78	78	77	76	76
0120	75	75	74	73	73	72	71	71	70	6F	6F	6E	6D	6C	6B	6A
0130	6A	69	68	67	66	65	64	63	62	61	60	5F	5E	5D	5C	5B
0140	5A	59	58	56	55	54	53	52	51	4F	4E	4D	4C	4A	49	48
0150	47	45	44	43	41	40	3F	3D	3C	3A	39	38	36	35	33	32
0160	31	2F	2E	2C	2B	29	28	26	25	23	22	20	1F	1D	1C	1A
0170	19	17	16	14	13	11	10	0E	0C	0B	09	08	06	05	03	02
0180	FF	FE	FD	FB	FA	F8	F7	F5	F4	F2	F0	EF	ED	EC	EA	E9
0190	E7	E6	E4	E3	E1	E0	DE	DD	DB	DA	D8	D7	D5	D4	D2	D1
01A0	CF	CE	CD	CB	CA	C8	C7	C6	C4	C3	C1	C0	BF	BD	BC	BB
01B0	B9	B8	B7	B6	B4	B3	B2	B1	AF	AE	AD	AC	AB	AA	A8	A7
01C0	A6	A5	A4	A3	A2	A1	A0	9F	9E	9D	9C	9B	9A	99	98	97
01D0	96	96	95	94	93	92	91	91	90	8F	8F	8E	8D	8D	8C	8B
01E0	8B	8A	8A	89	88	88	87	87	86	86	86	85	85	84	84	84
01F0	83	83	83	83	82	82	82	82	82	81	81	81	81	81	81	81

APPENDIX IV-3

```
C                APPENDIX IV-3
C
C
      PROGRAM PHIL(INPUT,OUTPUT)
      DIMENSION  L(256),PHI(256),A(256,9) B(256,9)
      DIMENSION D(256,9),LL(256),PPHI(256),MEM(256)
      DIMENSION C(256,9),ML(256)
      INTEGER A,B,C,PHI,PPHI
C
C*****************************************************
C     THIS PROGRAM GENERATES A QUADRATIC PHASE
C     SET CORRESPONDING TO A SET OF FREQUENCIES NL.
C     IT GIVES THE BINARY FORM OF THE PHASES(PHI)
C     AND THE FREQUENCIES(L).THE VALUES OF PHI ARE
C     ROUNDED TO THE NEAREST WHOLE NUMBER.
C     THE PROGRAM CAN PRODUCE 256 VALUES OF BOTH
C     L AND PHI.HOWEVER ONLY 82 VALUES OF L AND
C     82 VALUES OF PHI ARE OF INTEREST  IN THIS
C     DESIGN. THOSE ARE CHOSEN. ANOTHER 82 VALUES
C     ARE CREATED BY NEGATING THESE POSITIVE VALUES.
C     THE VALUE OF N IS GIVEN AS 256.
C     BFREQ....ARE THE BASEBAND FREQUENCIES.
C     MFREQ....ARE THE BASEBAND FREQUENCIES
C     UP-CONVERTED THROUGH MIXING WITH 8192 HZ.
C*****************************************************
      PRINT 1
    1 FORMAT("ENTER N")
      READ*,N
      PRINT 2
    2 FORMAT(2X,"ADDRESS",4X "BINARY L",3X,"BINARY PHI",
     *3X,"BFREQ",4X,"MFREQ")
      PI=180*1.422222
      PI2=360*1.422222
      DO 5 II=1,1025,12
      I=II-1
      K=I/4
      L(K)=K
      RPHI=PI*(K**2)/N
      PHI(K)=AMOD(RPHI,PI2)
      IPHI=AMOD(RPHI,PI2)
      REMAIN=PHI(K)-IPHI
      IF(REMAIN.GE.0.5) GO TO 4
      PHI(K)=IPHI
      GO TO 5
    4 PHI(K)=IPHI+1
    5 CONTINUE
C
C
C*****************************************************
C      EIGHTY TWO VALUES OF POSITIVE L AND PHI ARE
C      CHOSEN FROM THE 256.THE TWO PILOT TONES ARE
C      PLACED AT THE END OF THE REDUCED L AND PHI
C       LISTS.
```

```
C*******************************************************
      DO 20 II=1,257
      I=II*3
      IF(II.GT.85) GO TO 25
      L(II)=L(I)
      PHI(II)=PHI(I)
      GO TO 20
   25 PHI(II)=0
      L(II)=0
   20 CONTINUE
      PHI(86)=PHI(18)
      L(86)=L(18)
C
C
      DO 30 II=84,86
      PHI(II)=PHI(II+1)
      L(II)=L(II+1)
   30 CONTINUE
C
C
C
      DO 35 II=20,85
      PHI(II-3)=PHI(II)
      L(II-3)=L(II)
   35 CONTINUE
C
C
C
C*******************************************************
C     ARRAYS CONTAINING ALL 164 VALUES OF L'S
C     AND PHI'S (I.E. POSITIVE AND NEGATIVE
C     VALUES) ARE CREATED.
C*******************************************************
      DO 50 I=1,82
      IB=83-I
      IP=I+82
      LL(IP)=L(I)
      LL(IB)= -L(I)
      PPHI(IP)=PHI(I)
      PPHI(IB)=-PHI(I)
   50 CONTINUE
C
C
C
C*******************************************************
C      THE FIRST TWO VALUES IN THE L AND PHI LIST
C      ARE PLACED LAST AND THE LIST COMPRESSED SO
C      THAT THE THIRD ENTRY IS NOW FIRST ETC.
C*******************************************************
C
      LL(165)=LL(2)
      LL(166)=LL(1)
      PPHI(165)=PPHI(2)
      PPHI(166)=PPHI(1)
```

```
C
      DO 65 I=1,166
      II=I+2
      LL(I)=LL(II)
      PPHI(I)=PPHI(II)
   65 CONTINUE
C
C
C*****************************************************
C     ALL PHI'S GREATER THAN 180 AND LESS THAN
C     -180 DEGREES ARE COMPLEMENTED(I.E. THEY
C     ARE ADDED TO -360 AND 360 DEGREES
C     RESPECTIVELY).SINCE THE PHI'S ARE TO BE
C     USED TO LOOK-UP A 9-BIT PROM,THEY MUST
C     ALL BE SCALED BY A FACTOR OF 1.42222.
C*****************************************************
C
      DO 70  I=1,164
      IF(PPHI(I).GT.256)  PPHI(I)=PPHI(I)-512
      IF(PPHI(I).LT.( 256)) PPHI(I)=PPHI(I)+512
      IF(IABS(PPHI(I)).EQ.256 )  PPHI(I)=0.0
   70 CONTINUE
C
C
C
C
C
      DO  75  K=1,164
      MEM(K)=K-1
      CALL BINARY(K,MEM,D)
      L(K)=4*LL(K)
      ML(K)=8192+L(K)
      IF(LL(K).LT.0) GO TO 80
      CALL BINARY(K,LL,C)
      GO TO 85
   80 LL(K)= -LL(K)
      CALL BINARY(K,LL,C)
      CALL COMP(K,C)
      LL(K)= -LL(K)
C
C
   85 IF(PPHI(K).LT.0) GO TO 90
      CALL BINARY(K,PPHI,B)
      GO TO 75
   90 PPHI(K)= -PPHI(K)
      CALL BINARY(K,PPHI,B)
      CALL COMP(K,B)
      PPHI(K)= -PPHI(K)
   75 CONTINUE
C
C*****************************************************
C     THE FINISHED ARRAYS OF L AND PHI ARE
C     PRINTED.
C*****************************************************
```

```
      DO 105 I=1,164
      II=I-1
      PRINT 110,(D(I,J) J=1,9),(C(I,J),
     ?J=1,9),(B(I,J),J=1,9),L(I),ML(I)
  110  FORMAT(3(2X,9I1),2(3X,I5))
  105  CONTINUE
      STOP
      END
```

```
C
C
C*************************************************************
C     THIS SUBROUTINE CONVERTS A DECIMAL NUMBER IN
C     THE RANGE 0 TO 256 INTO A 9-BIT BINARY NUMBER.
C*************************************************************
      SUBROUTINE BINARY(K,LL,A)
      DIMENSION A(256,9),B(256,9),C(256,9)
      DIMENSION LL(256),PPHI(256)
      INTEGER A,B,C,PPHI
      DO 9 I=1,9
      A(K,I)=0
    9 CONTINUE
      L=LL(K)
      DO 1  NN=1,9
      N=10-NN
      A(K,N)=MOD(L,2)
      L=L/2
      IF(L.NE.1) GO TO 1
      A(K,N-1)=1
      A(K,1)=0
      GO TO 2
    1 CONTINUE
    2 RETURN
      END
```

```
C
C*************************************************
C     THIS SUBROUTINE GENERATES THE COMPLEMENT
C     OF A 9_BIT BINARY NUMBER.
C*************************************************
C
      SUBROUTINE COMP(K,B)
      DIMENSION B(256,9),C(256,9)
      INTEGER B,C
      DO 2 MM=1,9
      M=10-MM
      IF(B(K,M) NE.0) GO TO 1
      B(K,M)=1
      GO TO 2
    1 B(K,M)=0
    2 CONTINUE
      DO 3 MM=1,9
      M=10-MM
      IF(B(K,M).EQ.0) GO TO 4
      B(K,M)=0
    3 CONTINUE
      GO TO 5
    4 B(K,M)=1
    5 B(K,1)=1
      RETURN
      END
```

ADDRESS	BINARY L	BINARY PHI	BFREQ	MFREQ
000000000	100000111	111010000	-996	7196
000000001	100001010	110011101	-984	7208
000000010	100001101	101011000	-972	7220
000000011	100010000	100000001	-960	7232
000000100	100010011	010011000	-948	7244
000000101	100010110	000011101	-936	7256
000000110	100011001	110010000	-924	7268
000000111	100011100	011110001	-912	7280
000001000	100011111	001000000	-900	7292
000001001	100100010	101111101	-888	7304
000001010	100100101	010101000	-876	7316
000001011	100101000	111000001	-864	7328
000001100	100101011	011001000	-852	7340
000001101	100101110	110111101	-840	7352
000001110	100110001	010100000	-828	7364
000001111	100110100	101110001	-816	7376
000010000	100110111	000110000	-804	7388
000010001	100111010	011011101	-792	7400
000010010	100111101	101111000	-780	7412
000010011	101000000	000000001	-768	7424
000010100	101000011	001111000	-756	7436
000010101	101000110	011011101	-744	7448
000010110	101001001	100110000	-732	7460
000010111	101001100	101110001	-720	7472
000011000	101001111	110100000	-708	7484
000011001	101010010	110111101	-696	7496
000011010	101010101	111001000	-684	7508
000011011	101011000	111000001	-672	7520
000011100	101011011	110101000	-660	7532
000011101	101011110	101111101	-648	7544
000011110	101100001	101000000	-636	7556
000011111	101100100	011110001	-624	7568
000100000	101100111	010010000	-612	7580
000100001	101101010	000011101	-600	7592
000100010	101101101	110011000	-588	7604
000100011	101110000	100000001	-576	7616
000100100	101110011	001011000	-564	7628
000100101	101110110	110011101	-552	7640
000100110	101111001	011010000	-540	7652
000100111	101111100	111110001	-528	7664
000101000	101111111	000000000	-516	7676
000101001	110000010	111111101	-504	7688
000101010	110000101	011101000	-492	7700
000101011	110001000	111000001	-480	7712
000101100	110001011	010001000	-468	7724
000101101	110001110	100111101	-456	7736
000101110	110010001	111100000	-444	7748
000101111	110010100	001110001	-432	7760
000110000	110010111	011110000	-420	7772
000110001	110011010	101011101	-408	7784
000110010	110011101	110111000	-396	7796
000110011	110100000	000000001	-384	7808

000110100	110100011	000111000	-372	7820
000110101	110100110	001011101	-360	7832
000110110	110101001	001110000	-348	7844
000110111	110101100	001110001	-336	7856
000111000	110101111	001100000	-324	7868
000111001	110110010	000111101	-312	7880
000111010	110110101	000001000	-300	7892
000111011	110111000	111000001	-288	7904
000111100	110111011	101101000	-276	7916
000111101	110111110	011111101	-264	7928
000111110	111000001	010000000	-252	7940
000111111	111000100	111110001	-240	7952
001000000	111010000	100000001	-192	8000
001000001	111010011	000011000	-180	8012
001000010	111010110	100011101	-168	8024
001000011	111011001	000010000	-156	8036
001000100	111011100	011110001	-144	8048
001000101	111011111	111000000	-132	8060
001000110	111100010	001111101	-120	8072
001000111	111100101	100101000	-108	8084
001001000	111101000	111000001	-96	8096
001001001	111101011	001001000	-84	8108
001001010	111101110	010111101	-72	8120
001001011	111110001	100100000	-60	8132
001001100	111110100	101110001	-48	8144
001001101	111110111	110110000	-36	8156
001001110	111111010	111011101	-24	8168
001001111	111111101	000000000	-12	8180
001010000	000000011	000000000	12	8204
001010001	000000110	000100011	24	8216
001010010	000001001	001010000	36	8228
001010011	000001100	010001111	48	8240
001010100	000001111	011100000	60	8252
001010101	000010010	101000011	72	8264
001010110	000010101	110111000	84	8276
001010111	000011000	000111111	96	8288
001011000	000011011	011011000	108	8300
001011001	000011110	110000011	120	8312
001011010	000100001	001000000	132	8324
001011011	000100100	100001111	144	8336
001011100	000100111	111110000	156	8348
001011101	000101010	011100011	168	8360
001011110	000101101	111101000	180	8372
001011111	000110000	011111111	192	8384
001100000	000111100	000001111	240	8432
001100001	000111111	110000000	252	8444
001100010	001000010	100000011	264	8456
001100011	001000101	010011000	276	8468
001100100	001001000	000111111	288	8480
001100101	001001011	111111000	300	8492
001100110	001001110	111000011	312	8504
001100111	001010001	110100000	324	8516
001101000	001010100	110001111	336	8528
001101001	001010111	110010000	348	8540

001101010	001011010	110100011	360	8552
001101011	001011101	111001000	372	8564
001101100	001100000	111111111	384	8576
001101101	001100011	001001000	396	8588
001101110	001100110	010100011	408	8600
001101111	001101001	100010000	420	8612
001110000	001101100	110001111	432	8624
001110001	001101111	000100000	444	8636
001110010	001110010	011000011	456	8648
001110011	001110101	101111000	468	8660
001110100	001111000	000111111	480	8672
001110101	001111011	100011000	492	8684
001110110	001111110	000000011	504	8696
001110111	010000001	000000000	516	8708
001111000	010000100	000001111	528	8720
001111001	010000111	100110000	540	8732
001111010	010001010	001100011	552	8744
001111011	010001101	110101000	564	8756
001111100	010010000	011111111	576	8768
001111101	010010011	001101000	588	8780
001111110	010010110	111100011	600	8792
001111111	010011001	101110000	612	8804
010000000	010011100	100001111	624	8816
010000001	010011111	011000000	636	8828
010000010	010100010	010000011	648	8840
010000011	010100101	001011000	660	8852
010000100	010101000	000111111	672	8864
010000101	010101011	000111000	684	8876
010000110	010101110	001000011	696	8888
010000111	010110001	001100000	708	8900
010001000	010110100	010001111	720	8912
010001001	010110111	011010000	732	8924
010001010	010111010	100100011	744	8936
010001011	010111101	110001000	756	8948
010001100	011000000	111111111	768	8960
010001101	011000011	010001000	780	8972
010001110	011000110	100100011	792	8984
010001111	011001001	111010000	804	8996
010010000	011001100	010001111	816	9008
010010001	011001111	101100000	828	9020
010010010	011010010	001000011	840	9032
010010011	011010101	100111000	852	9044
010010100	011011000	000111111	864	9056
010010101	011011011	101011000	876	9068
010010110	011011110	010000011	888	9080
010010111	011100001	111000000	900	9092
010011000	011100100	100001111	912	9104
010011001	011100111	001110000	924	9116
010011010	011101010	111100011	936	9128
010011011	011101101	101101000	948	9140
010011100	011110000	011111111	960	9152
010011101	011110011	010101000	972	9164
010011110	011110110	001100011	984	9176
010011111	011111001	000110000	996	9188

0101 00000	0111 1111 1	0000 0000 0	1020	9212
0101 00001	0001 1011 0	1011 0001 1	216	8408
0101 00010	1000 0000 1	0000 0000 0	-1020	7172
0101 00011	1110 0101 0	0100 1110 1	-216	7976